A Study of Forces on the Body

in Athletic Activities With Particular

Reference to Jumping

A Thesis presented for the degree of

Doctor of Philosophy

in the Department of Physical Education

The University of Leeds

by

A. J. Smith

May, 1972

Abstract

The study is primarily concerned with the analysis of cinematographic records of human movement. Computational techniques for smoothing and differentiation of numerical data are examined and a suitable method is established as a computer programme. The programme accepts displacement data from cine film of a body action and produces inertia force components of the body segments.

The equation of motion is expressed in terms of a summation of segmental forces. The computed results are compared with the total reaction measured on a force platform and are also used to indicate the segmental contributions in the summation.

The analytical procedures are general, but are here applied to simple athletic activities. Discussion of body motion and external force action is followed by estimation of the internal effects in muscles and joints in the lower limbs.

During the course of the work, discussion of segmental models of the human body and of some mechanical principles is undertaken. These sections range beyond the requirements of the central study and offer some broader considerations in movement analysis.

Acknowledgements

The author is indebted to Professors Duncan Dowson and Verna Wright, and to Mr. Graham Adamson, for their respective roles as supervisors of the Engineering, Medical and Physical Education interests in the study.

Messrs Brash, Pegg, Daniels and Ridley, of the Departments of Chemical Engineering and Photography, gave much advice and assistance during the cine filming.

Dr. G.D. Hitchens and Mr. D.D. Andrew, of the Department of Computational Science, readily made available a Fourier Analysis programme developed by the latter in an M.Sc. Dissertation.

Mr. J.S. Mulligan, of the Department of Mechanical Engineering, supervised the installation and testing of the Vanguard Projection Head, which was purchased under a Kodak Award supporting the work.

The force platform was purchased with a Medical Research Council grant from Kistler Limited, whose representative, Mr. W. Munday, gave much assistance in early platform experiments.

Mr. Price, of York County Hospital, kindly arranged access to the archaelogical findings at York Minster.

Dr. B.B. Seedhom, of the Rheumatism Research Unit, discussed and assisted with the anatomical measurements made on the bone rig.

The author wishes to express his thanks to these gentlemen, and to the administrators of the Kodak Award Scheme and the M.R.C. Grants Committee for their support during the work.

GENERAL NOTATION

a	ACCELERATION
d	DIST. OF SEGMENT C.G. FROM YTH
g	GRAVITATIONAL ACCELERATION
h	MOMENT OF MOMENTUM
k	$= d/H$
l	SEGMENT LENGTH
m	SEGMENT MASS
p	$= m/M$
q	$= l/H$ OR DIST. OF SEGMENT C.G. FROM PROXIMAL END
t	TIME
u	VELOCITY (X-COMPT.) OR DISPLACEMENT
v	VELOCITY (Z-COMPT.)
w	DISPLACEMENT
x, y, z	CO-ORDINATES OF SEGMENT C.G.
$\int$	IMPULSE
Δ	'INCREASE IN'
α	ANGULAR ACCEL.
Ω	ANGULAR VELOCITY
λ	ANGULAR VELOCITY OF SEGMENT W.R.T. H-T
ν	FREQUENCY
$\mathcal{W}$	WORK

A	FOURIER COSINE COEFF.
B	FOURIER SINE COEFF.
C	POLYNOMIAL COEFF.
E	ERROR
F	FORCE
G	WHOLE-BODY C.G.
H	STANDING HEIGHT
I	MOMENT OF INERTIA
J	INTEGER FOURIER FREQUENCY
L	DIST. OF G FROM REFERENCE
M	WHOLE-BODY MASS
N	NO. OF FRAMES
P	FORCE
Q	MOMENT OF FORCE OR HEAT FLOW
T	TIME OR KINETIC ENERGY
U	VELOCITY OR INTERNAL ENERGY
V	VELOCITY OR POTENTIAL ENERGY
X, Y, Z	REFERENCE AXES

SUFFICES

i	COUNTING TIME INTERVALS
j	COUNTING SEGMENTS
X, Y, Z	W.R.T. REFERENCE AXES
t, T	AT TIME t, T
TH	TOP OF HEAD
G	WHOLE-BODY C.G.
(rel)	RELATIVE TO MOVING AXES
(inst)	INSTANTANEOUS VALUE
A	ANKLE
K	KNEE
Tib	ALONG TIBIAL AXIS
Norm	NORMAL TO TIBIAL AXIS

ABBREVIATIONS

H-T	HEAD-TRUNK
BUL	BOTH UPPER LEGS
BLL	BOTH LOWER LEGS
BF	BOTH FEET
BUA	BOTH UPPER ARMS
BFA	BOTH FOREARMS
BH	BOTH HANDS
AOH	ARMS OVER HEAD
SFD	SITTING, FOREARMS DOWN

SUPERSCRIPTS

$\bar{Z}$	Z-COORDINATE OF G
$\dot{z}$	$= dz/dt$
$\bar{V}$	$= \dot{\bar{z}}$
$\bar{U}$	$= \dot{\bar{x}}$

Contents

Chapter 1

An Outline of the Contents

The characteristics of walking have been a major interest since the inception of studies in human movement, and in recent years the refinement of experimental techniques in biomedical engineering has led to detailed analysis of the action of the lower limbs and their joints and muscles. This later work has been particularly concerned with improvements in the design of artificial limbs and the development of surgical replacements for the knee and hip joints. Estimates of forces in the leg muscles and joints during normal walking have been made and the quoted maximum values are surprisingly large.

The central theme of the present work is the estimation of forces developed in the body during actions more vigorous than walking. It is to be expected that in athletic activities the forces will often be considerably larger than in normal locomotion, and in some instances they may result in injury.

A common sports injury, the torn semilunar cartilage of the knee joint, appears in many cases to result from violent twisting and compression trapping the cartilage between the mating faces, or condyles, of the femur and tibia. There is, however, a good deal of uncertainty about the intensities and durations of loading which the cartilages will withstand, and it is possible that the tissue will tear under a 'fatigue' effect of repeated compressive impacts. The footballer's knee injury may be the result of a single violent wrench, but similar cartilage trouble in cricketers (the leading leg of a fast bowler) and hill-walkers may be due to the cumulative effect of many moderate impacts. No estimates of the loads imposed on the joints in such situations appear to have been made, and one objective of the present work was to examine an activity involving impact loading at the feet. The landing action from a vertical drop ('drop-landing') was taken as a typical case and a wide range of load intensity was possible by variation in the height of the jump.

To allow uninhibited movement in an athletic performance it was decided that, in experiments, the subject should be free of electrodes, leads and other attachments. The force platform, forming a panel flush with the laboratory floor, and cine photography, a remote recording process, are experimental devices which offer no impediment to body movement. Both techniques have been employed in previous biomedical work and in studies of athletic performance, but the computation of forces from cine data has been attempted in only a few instances. In the present study it was considered important to derive reliable force estimates from cine film and to use the force platform as a check on the computed values. It was intended that the limits of cine analysis would in this way be explored.

The cine record provided detailed displacement data on the body movement and the handling of this information led to the investigation of a range of computational techniques. In essence, the displacement data were to be smoothed and differentiated to give accelerations and inertia forces associate with the moving parts or 'segments' of the body. Experience of the numerical methods gave rise to the formulation of a computer programme for force analysi of the cine data.

The emphasis has necessarily been drawn toward the validation of analytical procedures, but the discussion of measured and computed external forces and of the body action in the drop-landing and the standing long jump offers some points of interest in Physical Education. The subsequent calculation of muscle tensions and joint forces in the lower limbs during the drop-landing raises a number of issues relevant to biomedical engineering.

In addition to the main course of the work outlined above, some other related investigations are presented. Each of these developments evolved naturally in the course of the study. While commencing with tried procedures for the assessment of body movements and forces, it became clear that these procedures themselves needed further appraisal. Thus, in seemingly establish methods important avenues of exploration presented themselves. The Chapters on Segmental Models, Mechanical Principles and Smoothing-Differentiation

contain attempts to probe a little more into current biomechanical ideas. In each case the relevant literature was found to contain 'loose ends' or questionable statements on fundamentals. Reappraisal from first principles was then undertaken and such a formulation suggested developments which clarified the matters in question.

The relations between sections of the work are indicated in Figure 1.1.

In view of the diversity of the topics covered in succeeding Chapters, a general literature review is not appropriate. Instead, each Chapter calling upon published material contains its own literature survey and references.

FIGURE 1.1

RELATIONSHIPS BETWEEN CHAPTERS

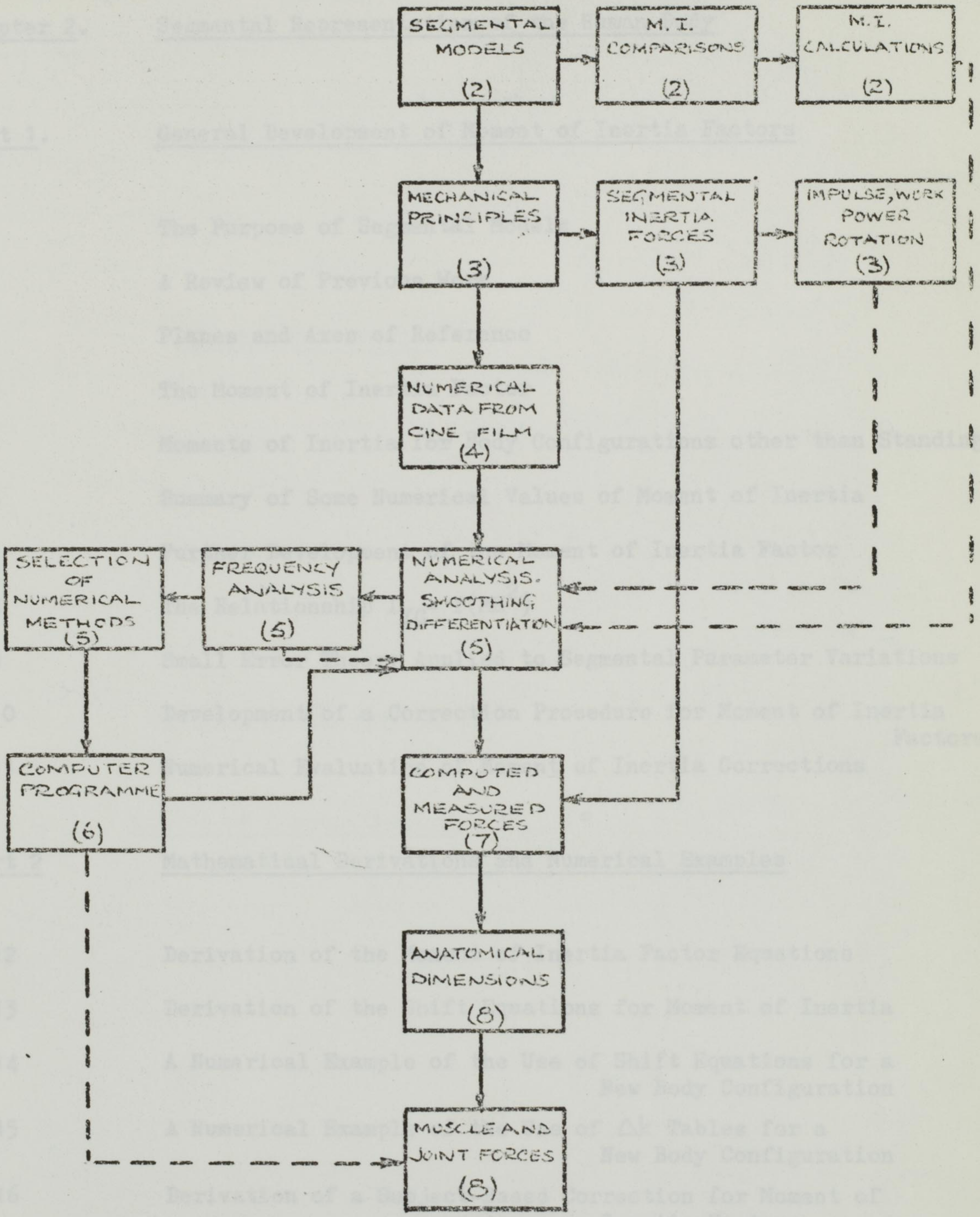

Chapter 2. Segmental Representation of the Human Body

Part 1. General Development of Moment of Inertia Factors

Part 2 Mathematical Derivations and Numerical Examples

Part 3 Discussion

Chapter 2 Part 1

General Development of

Moment of Inertia Factors

2.1 The Purpose of Segmental Models

The study of human movement in mechanical terms requires a knowledge of the dimensions and masses of the various parts of the body. The body parts, or 'segments' are usually defined as the relatively rigid portions lying between the natural joints of the skeleton. For example, the upper leg segment commences at the hip joint and terminates at the knee joint.

Experimental data on segments have been obtained by cutting cadavers at the natural joints, and then measuring and weighing the parts. Simple balancing and oscillation tests have also been conducted, and the linear dimensions, masses, mass centres and moments of inertia of the cadaveric segments are available in the literature.

The term 'segmental model' is generally applied to the conceptual representation of the human body as a set of segmental masses hinged together. Underlying such models are two fundamental assumptions: firstly, that the segments are truly rigid bodies, and secondly, that the joints by which they are connected are simple pivots, either hinge or ball-and-socket.

Clearly, neither assumption is perfectly correct. Muscular contraction and other tissue deformation cause some variation in the shape and mass-distribution of a segment. Again, the joints of the human body are not perfect hinge or ball-and-socket joints; a sliding-rolling contact is often nearer the truth.

Nevertheless, the two assumptions are very reasonable when one is concerned with the overall mechanics of the body. Indeed, it is doubtful whether any attempt at a more elaborate representation of segments or their joints is worthwhile; the cadaveric masses and dimensions upon which models are based cannot be very precise. One may well imagine how difficult it is to cut a cadaver at the hip joint and leave the 'right' amount of tissue attached to the upper leg segment.

The purpose of all segmental models is to depict with reasonable simplicity and accuracy the changes of body mass distribution which occur

as the limbs and trunk are flexed. No pretence is made to represent the actions of muscles and ligaments around a joint. A segmental model is concerned with changes of body configuration and the relative motion between the hinged segments, but not with the means by which these relative motions are brought about. Nonetheless, a segmental model may yield data which is useful in the analysis of muscular and ligamentous action about a joint; a suitable model of the joint itself, with bone dimensions and muscle attachments is also necessary.

2.2 A Review of Previous Work

Almost a century ago Braune and Fischer (1) dissected three cadavers and published the mechanical properties of the segments. For about seventy years thereafter, there seems to have been neither the desire nor the necessity to extend their work. Spurred by the U.S. Astronautics programme, however, Dempster (3) took on the task, using eight bodies and producing a comprehensive set of figures which are the basis of all the modern segmental models.

Williams and Lissner (13) summarise Dempster's work in a convenient form, and Dyson (4) quotes some slightly different values, which also arise from the Astronautics programme. Neither of these texts makes much use of the segmental model as a tool in body mechanics.

Whitsett's report (11) is an example of the way in which a segmental model may be used in a sophisticated mechanical problem in Biomechanics. He develops a 'mean-man' model from Dempster's figures for the segmental masses and lengths. He represents the segments by simple geometrical solids, such as spheres and tapered cylinders, and uses their properties to compute the moments of inertia of the segments and, by summation, of the whole body. Whitsett applies his model to the problem of human manoeuvrability in zero-gravity conditions. Despite the interest of Whitsett's applications, his report is mainly of value in that it presents a carefully constructed segmental model and much more information on mechanical properties than was

previously available.

Santschi, Dubois and Omoto (6) carried out experimental work on 66 living subjects, measuring the mass-centre locations and moments of inertia of each subject in eight different body positions. Their apparatus was a large tubular-steel frame which was swung as a pendulum, with the subject constrained inside it in the required body configuration. The report also records a comprehensive set of anthropometric measurements on each subject.

The work of Santschi provides valuable information on the whole-body mechanical properties of a good range of subjects (aviation employees aged between 21 and 51). It is an unfortunate fact that such whole-body measurements can not be manipulated to yield data on the segments. It is impossible to separate out the mass of a segment unless some assumption be made about the location of its mass-centre. The latter would come from standard values such as those of Dempster, and it is necessary to combine experimental data on a living subject with average values from cadavers.

Santschi's results are most useful norm against which to test segmental models. The natural test is to use a segmental model to predict whole-body mass-centre and moment of inertia values for the configurations used by Santschi in his experiments.

Hanavan (5) carried out such calculations and compared his values with those of Santschi. His segmental models were, however, an advance on previous efforts. He attempted to fit a model to each of the 66 Santschi subjects by incorporating some of the subject's anthropometric dimensions into the segmental model. Using simple geometrical solids, as Whitsett did, to represent the segments, Hanavan determined the dimensions of the solids from the anthropometry of a subject, and thereby constructed a 'tailor-made' model from which the subject's whole-body mechanical properties were computed. These calculated values were compared with the Santschi experimental figures.

The main body of this Chapter is concerned with some extensions to the theory of segmental models which spring from the interrelated works of Whitsett, Santschi and Hanavan.

2.3 Planes and Axes of Reference

Figure 2.1 shows the three planes, frontal, sagittal and transverse, which are commonly used to assist descriptions of body position and movement. The three co-ordinate axes, OXYZ, are chosen as a right-handed set, each being perpendicular to one of the planes.

In this Chapter we regard axis OZ as fixed in the Trunk, parallel to the spine. Where changes in body configuration occur, the limb movements are assumed to be parallel to the sagittal plane.

In this study two other useful axes are introduced. YTH denotes 'Y-axis through the top of the head' and YG denotes 'Y-axis through G' (the whole-body mass-centre). Axis YG moves with the body mass centre in changes of body configuration.

2.4 The Moment of Inertia Factor (M.I.Factor)
(Mathematical derivations are given in Section 2.12)

The first three columns of Table 2.1 list the masses, lengths and mass-centre locations of Whitsett's segments.

Whitsett's USAF mean-man has a stated mass of 163.66 lb, but the sum of the segment masses is only 162.22 lb. The latter figure will be used in this work as the total body mass.

Columns 3, 4 and 5 of Table 2.1 headed p,q and k, are proportions, obtained by dividing columns 1, 2 and 3 by M,H, and H respectively (M = 162.22 lb, H = 69.11 in). These body proportions define the mass distribution of a mean subject irrespective of his actual mass and height. Calculations in terms of these non-dimensional quantities yield information about all subjects who have mean-man proportions. The p,q and k are used to express body moments of inertia about axes YTH and YG.

$$I_{YTH} = MH^2\left[\sum\left(\frac{p_j q_j^2}{12} + p_j k_j^2\right)\right] \quad ; \quad I_{YG} = MH^2\left[\sum\left(\frac{p_j q_j^2}{12} + p_j k_j^2\right) - \left(\sum p_j k_j\right)^2\right]$$

$$\text{or, } I_{YTH} = MH^2 . F_{YTH} \quad ; \quad I_{YG} = MH^2 . F_{YG} \qquad \ldots\ldots(2.4\text{-}1)$$

We shall call the non-dimensional F_{YTH} and F_{YG} the 'moment of inertia factors' for axes YTH and YG. From the column totals in Table 2.1:-

$$F_{YTH} = 0.2450 \quad ; \quad F_{YG} = 0.0564$$

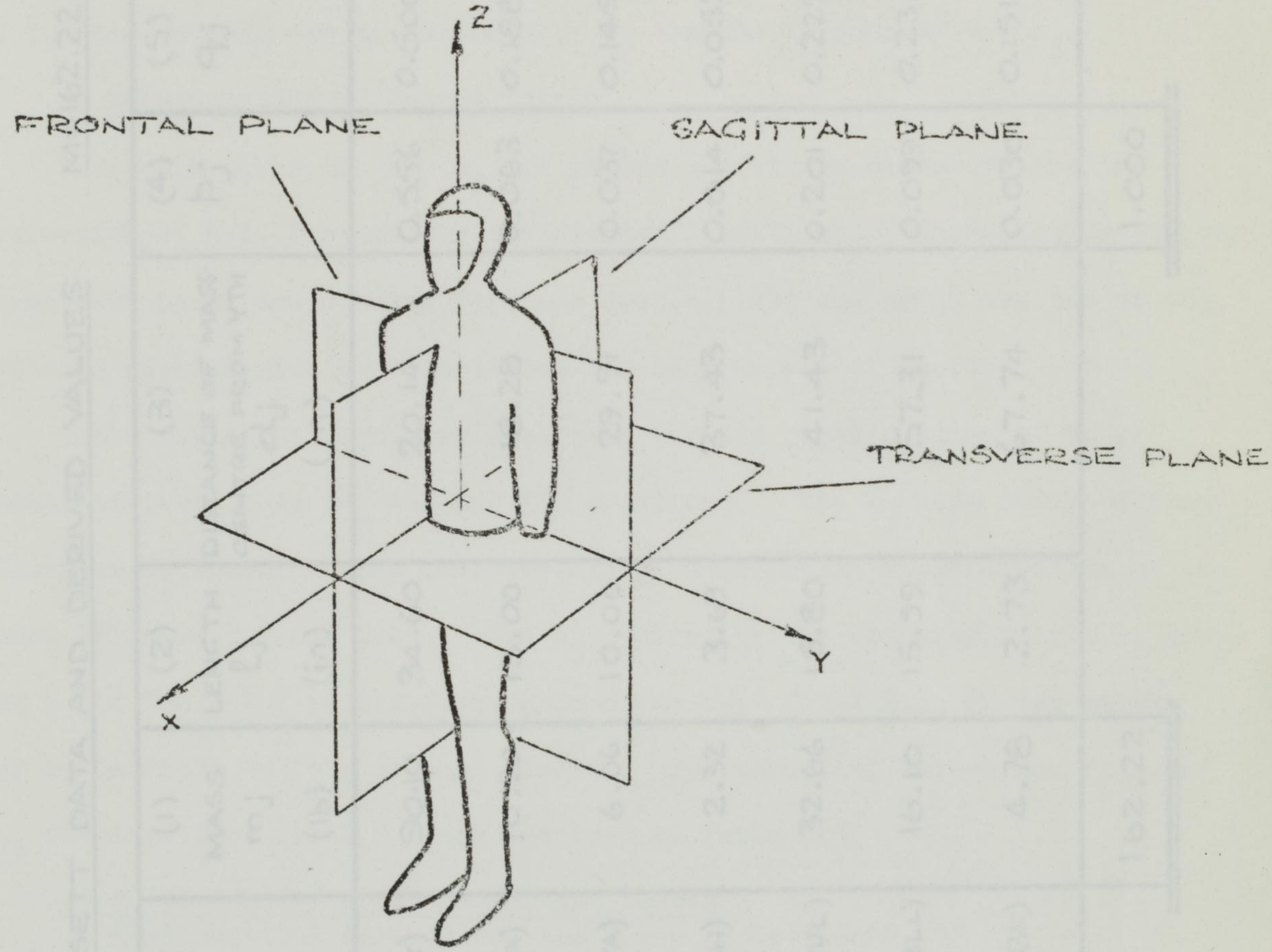

FIGURE 2.1

AXES AND PLANES OF REFERENCE

TABLE 2.1 WHITSETT DATA AND DERIVED VALUES $M = 162.22$ lb, $H = 69.11$ in

SEGMENT NO. j	SEGMENT		(1) MASS m_j (lb)	(2) LENGTH ℓ_j (in)	(3) DISTANCE OF MASS-CENTRE FROM YTH d_j (in)	(4) p_j	(5) q_j	(6) k_j
1	HEAD-TRUNK	(H-T)	90.10	34.60	20.14	0.556	0.500	0.2914
2	UPPER ARMS	(BUA)	10.20	13.00	18.28	0.063	0.188	0.2645
3	FOREARMS	(BFA)	6.06	10.00	29.91	0.037	0.145	0.4328
4	HANDS	(BH)	2.32	3.69	37.43	0.014	0.053	0.5416
5	UPPER LEGS	(BUL)	32.66	15.80	41.43	0.201	0.229	0.5995
6	LOWER LEGS	(BLL)	16.10	15.99	57.31	0.099	0.231	0.8293
7	FEET	(BF)	4.78	2.73	67.74	0.030	0.151	0.9802
COLUMN TOTALS			162.22			1.000		

$\sum \frac{p_j q_j^2}{12} = 0.0132126$

$\sum p_j k_j^2 = 0.2318059$

$\sum p_j k_j = 0.434284$

$\left(\sum p_j k_j\right)^2 = 0.1886027$

2.5 Moments of Inertia for Body Configurations Other than Standing

a) Graphical Determination of Shifts

Shifts in limb position parallel to the sagittal plane may be represented graphically, and the changes in quantities influencing moments of inertia, I_{YTH} and I_{YG}, are easily determined by drawing. Figure 2.2 demonstrates the method. Only columns (3) and (6) of Table 2.1 are affected and the moment of inertia factors are disturbed only by changes in some of the k_j.

b) Recalculation of Column Totals

Table 2.2 gives the new k_j and column summations necessary for the evaluation of M.I. Factors for two new configurations. These body positions, 'arms over head' and sitting forearms down' (AOH and SFD) are two of the Santschi experimental configurations for body moment of inertia.

Table 2.2 gives nondimensional data for the recalculation of body moment of inertia in the AOH and SFD positions. The k_j were obtained from distances d_j measured on a quarter-full-size graphical representation of the model (Figures 2.2 and 2.8). The d_j divided by the standing height H, give the k_j of Table 2.2 to six-figures in order that final M.I. Factor values may be accurate to four decimal places. The numerical values for F_{YTH} and F_{YG} obtained from Table 2.2 are recorded in Table 2.3.

c) Shift Equations for Moment of Inertia

(Mathematical derivations are given in Section 2.13)

An alternative method for obtaining new M.I. Factor values due to limb shifts is based on the effect of a variation Δk_j for the shift of segment j from the reference (standing) position to a new configuration. The Taylor expansion of:-

$$F_{YTH} = \sum\left(\frac{p_j q_j^2}{12} + p_j k_j^2\right) \quad ; \quad F_{YG} = \sum\left(\frac{p_j q_j^2}{12} + p_j k_j^2\right) - \left(\sum p_j k_j\right)^2 \quad \ldots\ldots(2.5\text{-}1)$$

gives

$$\Delta F_{YTH} = p_2 \Delta k_2 (2k_2 + \Delta k_2) \quad ; \quad \Delta F_{YG} = p_2 \Delta k_2 \left[(2k_2 - 2\textstyle\sum p_j k_j) + (1 - p_2)\Delta k_2\right] \quad \ldots\ldots(2.5\text{-}2)$$

The variations ΔF_{YTH} and ΔF_{YG} are expressed here in terms of a shift Δk_2 of segment 2. Alteration of the relevant suffices in equations (2.5-2) allows the shift of any other segment to be represented. The nature of the

FIGURE 2.2

VARIATIONS IN k

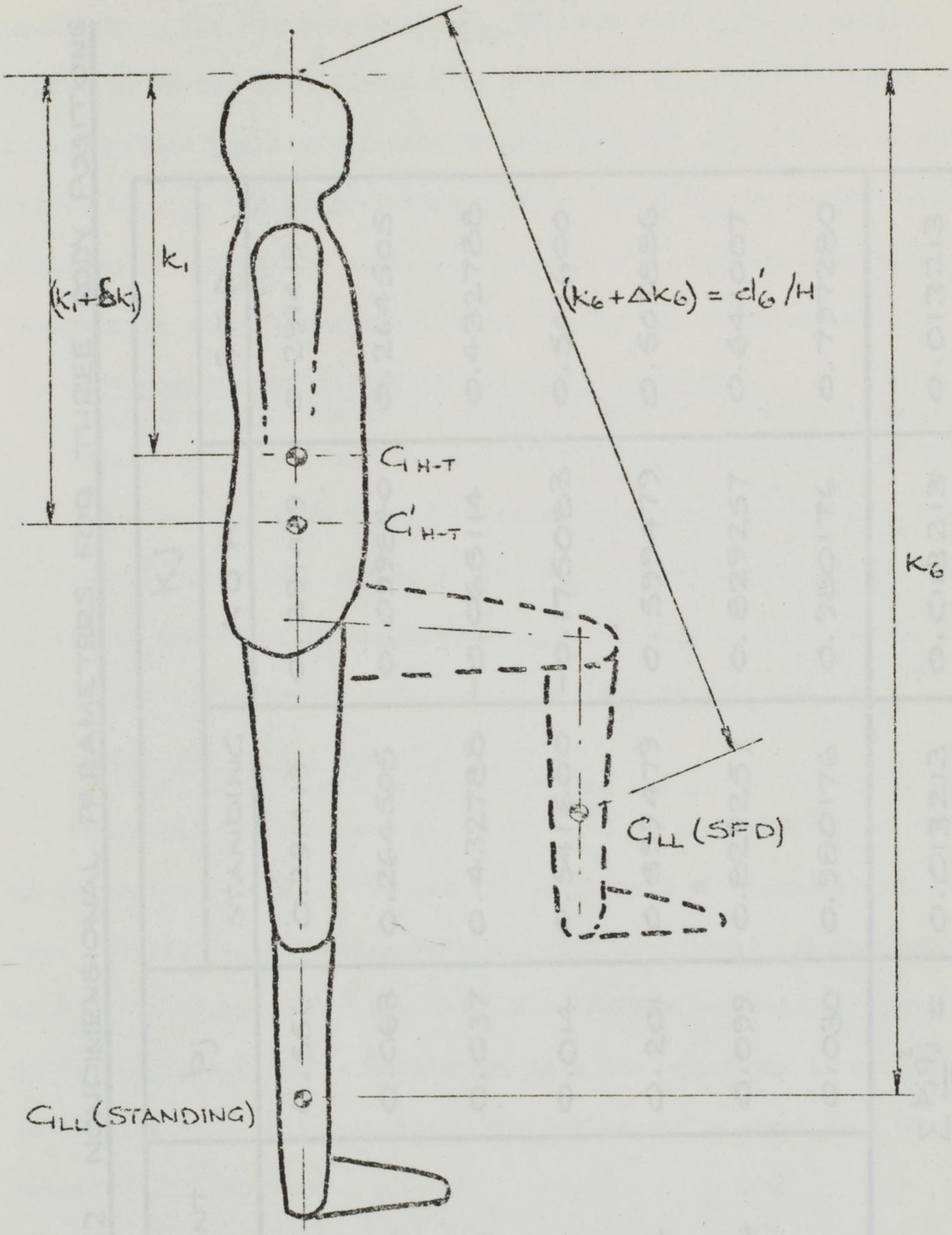

a) GROSS VARIATION Δk_6 FOR CHANGE IN BODY CONFIGURATION FROM STANDING TO SFD.

b) SMALL VARIATION δk_1 FOR CHANGE IN MASS DISTRIBUTION WITHIN H-T.

TABLE 2.2 NONDIMENSIONAL PARAMETERS FOR THREE BODY POSITIONS

SEGMENT NO. J	SEGMENT	p_j	k_j		
			STANDING	AOH	SFD
1	H-T	0.556	0.291419	0.291419	0.291419
2	BUA	0.063	0.264505	0.099840	0.264505
3	BFA	0.037	0.432788	-0.065114	0.432788
4	BH	0.014	0.541600	-0.175083	0.541600
5	BUL	0.201	0.599479	0.599479	0.507886
6	BLL	0.099	0.829257	0.829257	0.641007
7	BF	0.030	0.980176	0.980176	0.797280
		$\sum \frac{p_j q_j^2}{12} =$	0.013213	0.013213	0.013213
		$\sum p_j k_j^2 =$	0.231798	0.217568	0.174258
		$\sum p_j k_j =$	0.434285	0.395455	0.391751
		$(\sum p_j k_j)^2 =$	0.188603	0.156385	0.153469

expression for F_{YTH} permits superposition of segmental shift effects to give total M.I. Factor variation ΔF_{YTH} from its value at the reference (standing) position. The expression for F_{YG} is more difficult to handle. The Taylor expansion of F_{YG} as a function of more than one variable shows that the superposition principle cannot be employed for the effects of several segmental shifts on F_{YG}. A step-by-step process for ΔF_{YG} is proposed, allowing equation (2.5-2) to be used, but requiring a correction at each stage to incorporate the cross-product terms in the Taylor expansion.

d) Numerical Evaluation of the Shift Equation
(Numerical examples are given in Section 2.14)

Equations (2.5-2) may be used directly by substitution of the Δk_j for the shifted segments, with straightforward superposition for F_{YTH} and the additional correction procedure for F_{YG}. Computerisation of the processes is simple and might be employed in a simulation of body motion in which continuous variation of body moment of inertia takes place.

e) Generation and Use of Δk Tables
(The Tables and Numerical Examples are given in Section 2.15)

Equations (2.5-2) have also been used to generate tables for the effects of segmental shifts. The effects of individual segmental shifts are read from the tables, and superposition, with additional corrections in the case of F_{YG}, is employed for the total M.I. Factor variation. This technique is rather faster than substitution into the equations if manual calculation is considered. Alternatively, the tables may be used as a check on the substitution procedure.

Table 2.3

M. I. Factors

Body Configuration	F_{YTH}	F_{YG}
Standing (reference)	0.2450	0.0564
Arms over head (AOH)	0.2308	0.0744
Sitting, Forearms down (SFD)	0.1875	0.0340

Identical results were obtained by Column Total recalculation, substitution into equations (2.5-2) and the Δk Tables.

2.7 Further Development of the Moment of Inertia Factor

The concept of the moment of inertia factor has led me to three ideas which are expanded in subsequent Sections. The full development and exploration of the non-dimensional forms, their extension to three-dimensional body configurations and their use in motion simulation programmes will be of value, but goes beyond the scope of this work. The applications covered in the next three Sections are:-

a) The relationship $I_{YG} = f(MH^2)$, suggested by the form of the equations (2.4-1) and applied to both experimental and segmental estimations of body moment of inertia to facilitate comparison.

b) The examination, by small error theory, of the effects of small variations in the segmental parameters p,q and k upon the total body moment of inertia.

c) The development, from ideas arising out of a) and b) above, of a systematic correction procedure to improve moment of inertia estimates based upon segmental data.

Although F_{YTH} is of simpler form, attention will be mainly on F_{YG}, because the experimental data of Santschi is given in terms of moment of inertia about axis YG.

As a preliminary step, the Santschi results were examined and the values of I_{YG} for the standing position were divided into two sets. Figure 2.3 shows the grouping of the points. The central group of 40 subjects are hereafter termed the 'Main Cluster'. Their moments of inertia fall in a well-defined ellipse and their body masses are not exceptionally high or low. The separation was carried out by inspection and it was expected that the Main Cluster would exhibit less extreme properties than the remainder of the Santschi subjects.

2.8 The Relationship $I_{YG} = f(MH^2)$

The M.I. Factor equation, having the form $I_{YG} = f(MH^2)$ pointed to the plotting of both segmental model and experimental values of moment of inertia

FIGURE 2.3 SANTSCHI SUBJECTS.
MOMENT OF INERTIA AGAINST BODY MASS.
ISOLATION OF MAIN CLUSTER.

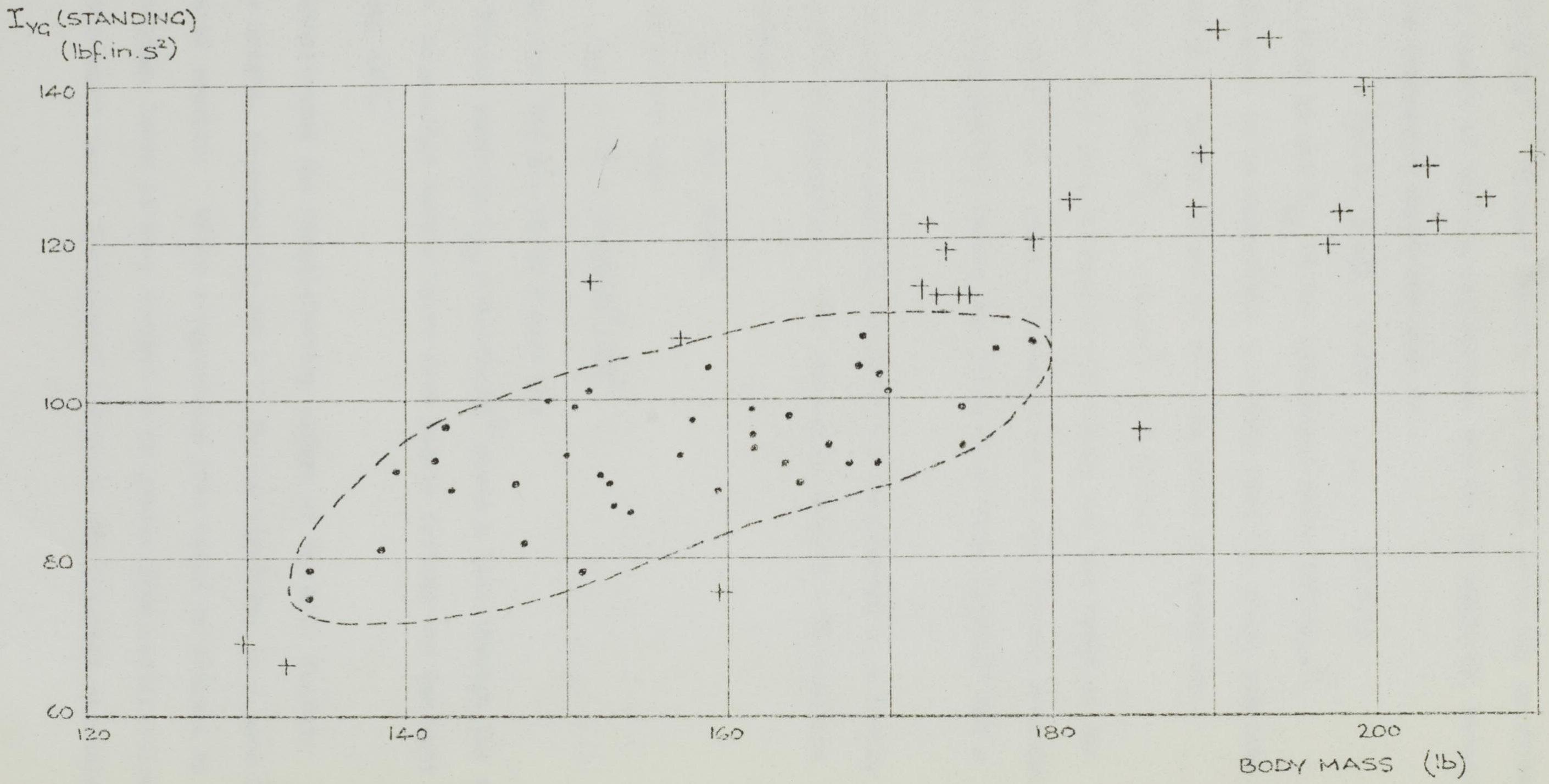

against the quantity MH^2. Neither Santschi nor Hanavan gives any graphical representation of moment of inertia estimations for the 66 subjects, although the former derives regression equations such as -

$$I_{YG} = -212.0 + 3.43H + 0.46M \quad \ldots\ldots\ldots \quad (2.8\text{-}1)$$

with H in inches, M in lb and I_{YG} in the unpleasant units $lbf.in.s^2$. Despite their ugliness, it is convenient to retain them for graph plotting and to convert the M.I. Factor values to the same units as necessary. Conversion is by:- $(lbf.in.s^2) = (lb.in^2 / 12 \times 32.2)$

Figure 2.4 shows four sets of results and brings out the value of the relationship $I_{YG} = f(MH^2)$ as a basis for comparison of the various methods:-

a) Santschi's experimental values are shown as a 'Main Cluster' and a remainder.

b) Santschi's regression equation, (2.8-1), is transformed to a family of lines with H as parameter. For instances, with H = 70 equation (2.8-1) becomes:-

$$I_{YG} = 28 + 0.46M$$

which can be recast as:-

$$I_{YG} = 28 + (0.46/70^2).MH^2$$

This is the line for H = 70 in Figure 2.4

c) The M.I. Factor equation $I_{YG} = 0.0564.MH^2$ gives a line through the orig

d) Hanavan's 'percentile models' give five points fitting the Santschi values very well.

The graph demonstrates the unsatisfactory nature of the M.I. Factor, A line through the origin, representing the M.I. Factor equation, is a poor fit to the experimental results. While a regression line could be derived by least squares fitting, there is more insight to be gained from modifications to the M.I. Factor which have a fundamental link with the physical variables in the problem.

FIGURE 2.4 MOMENT OF INERTIA AGAINST MH^2

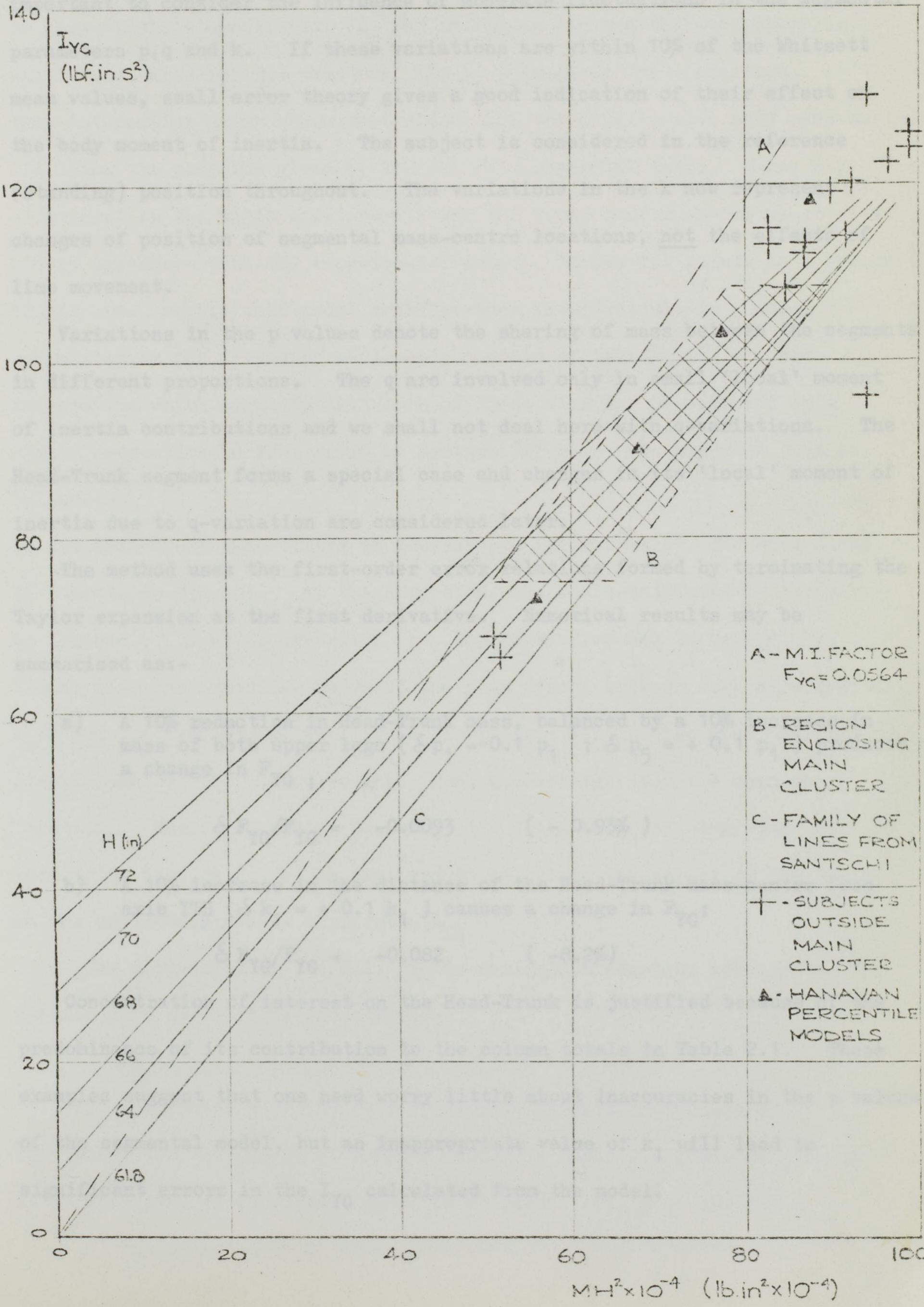

2.9 Small Error Theory Applied to Segmental Parameter Variations

(Mathematical Derivations and Numerical Examples are given in Section 2-13)

The departure of subjects from mean-man body proportions makes it important to consider the influence of moderate fluctuations in the segmental parameters p,q and k. If these variations are within 10% of the Whitsett mean values, small error theory gives a good indication of their effect on the body moment of inertia. The subject is considered in the reference (standing) position throughout. The variations in the k now represent changes of position of segmental mass-centre locations, not the effects of limb movement.

Variations in the p values denote the sharing of mass between the segments in different proportions. The q are involved only in small 'local' moment of inertia contributions and we shall not deal here with q-variations. The Head-Trunk segment forms a special case and changes in its 'local' moment of inertia due to q-variation are considered later.

The method uses the first-order error relations formed by terminating the Taylor expansion at the first derivative. Numerical results may be summarised as:-

a) A 10% reduction in Head-Trunk mass, balanced by a 10% increase in mass of both upper legs ($\delta p_1 = -0.1\ p_1$; $\delta p_5 = +0.1\ p_1$) produces a change in F_{YG} ;

$$\delta F_{YG}/F_{YG} = \quad -0.0093 \qquad (-0.93\%)$$

b) A 10% increase in the distance of the Head-Trunk mass-centre from axis YTH ($\delta k_1 = +0.1\ k_1$) causes a change in F_{YG};

$$\delta F_{YG}/F_{YG} = \quad -0.082 \qquad (-8.2\%)$$

Concentration of interest on the Head-Trunk is justified because of the predominance of its contribution to the column totals in Table 2.1. These examples suggest that one need worry little about inaccuracies in the p values of the segmental model, but an inappropriate value of k_1 will lead to significant errors in the I_{YG} calculated from the model.

2.10 The Development of a Correction Procedure for Moment of Inertia Factors

The Santschi data on 66 subjects includes the distances of the whole-body mass centres from axis YTH. These experimental values, L_z, are plotted as dimensionless quantities, (L_z/H) in Figure 2.5 and the corresponding whole-body value for the mean-man, $(\sum p_j k_j)$ is given for comparison. This informative graph shows that almost all the experimental body mass-centres lie below the position given by the Whitsett segmental data. Thus, any adjustment in the basic model must lower the whole-body mass-centre to give better agreement with the experimental data. Figure 2.4 points to a second requirement, namely that model modifications should result in general reductions in the predicted whole-body moments of inertia, I_{YG}. The calculation which suggests that both of these aims may be achieved by a simple correction is that given in Section 2.9 b). The argument runs as follows:-

If the Head-Trunk mass-centre is lowered (k_1 is increased), the body moment of inertia is reduced. At the same time, the whole-body mass-centre will be lowered ($\sum p_j k_j$ is increased). The correction now to be explored begins with the numerical value of the discrepancy between each experimental L_z/H and the mean-man value. This discrepancy will be ascribed entirely to displacement of the subject's Head-Trunk mass-centre from the mean-man location. Having corrected the subject's k_1 in this way, the equation underlying Section 2.9 b) is employed to calculate the effect of the new k_1 on the whole-body moment of inertia I_{YG}.

The derivation of the M.I. Factor correction equation appears in Section 2.16 where it is shown that:-

$$F_{YG(CORRECTED)} = F_{YG} + 2(k_1 - \Sigma p_j k_j)(L_z/H - \Sigma p_j k_j)$$

To apply this equation as a systematic subject-by-subject model correction for the moment of inertia values in Table 2.1 (standing position) it is necessary to substitute specific numerical data from the Table.

$$F_{YG(CORRECTED)} = 0{\cdot}0564 - 0{\cdot}2857(L_z/H - 0{\cdot}434285)$$

FIGURE 2.5 $\frac{L_z}{H}$ AGAINST MH^2 – SANTSCHI SUBJECTS

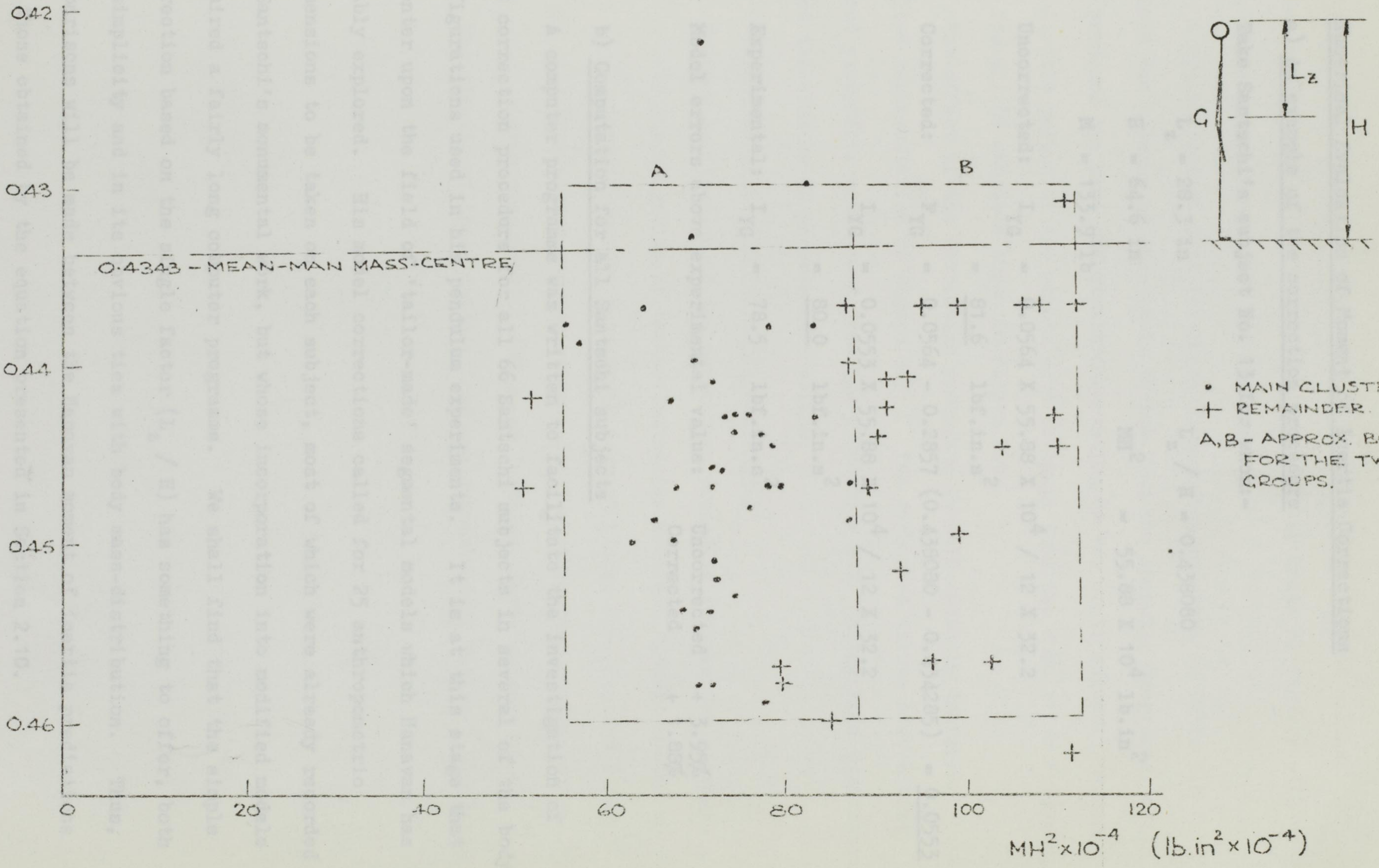

2.11 Numerical Evaluation of Moment of Inertia Corrections

a) An example of the correction procedure

Take Santschi's subject No. 13 for whom:-

L_z = 28.3 in $L_z / H = 0.438080$

H = 64.6 in $MH^2 = 55.88 \times 10^4$ lb.in^2

M = 133.9 lb

Uncorrected: $I_{YG} = 0.0564 \times 55.88 \times 10^4 / 12 \times 32.2$

$= \underline{81.6}$ lbf.in.s^2

Corrected: $F_{YG} = 0.0564 - 0.2857\ (0.438080 - 0.434285) = \underline{0.0553}$

$I_{YG} = 0.0553 \times 55.88 \times 10^4 / 12 \times 32.2$

$= \underline{80.0}$ lbf.in.s^2

Experimental: $I_{YG} = 78.5$ lbf.in.s^2

Model errors above experimental value: Uncorrected + 3.95%
Corrected + 1.88%

b) Computation for all Santschi subjects

A computer programme was written to facilitate the investigation of this correction procedure for all 66 Santschi subjects in several of the body configurations used in his pendulum experiments. It is at this stage that we enter upon the field of 'tailor-made' segmental models which Hanavan has so ably explored. His model corrections called for 25 anthropometric dimensions to be taken on each subject, most of which were already recorded in Santschi's monumental work, but whose incorporation into modified models required a fairly long computer programme. We shall find that the simple correction based on the single factor (L_z / H) has something to offer, both in simplicity and in its obvious ties with body mass-distribution. Thus, comparisons will be made between the Hanavan moment of inertia predictions and those obtained by the equation presented in Section 2.10.

Hanavan assessed his own results by comparing his model values with the Santschi experimental moments of inertia and presented only the median

and interquartile range of the errors between the two sets of values. Similar comparisons between my predictions and the Santschi figures will be made, and errors expressed in the same way.

A typical set of data for these comparisons is given in Table 2.4 The last two columns of this table derive from the computer programme, which also produced the mean and standard deviation of the error column. Median and quartile values of the errors were obtained from the cumulative frequency plot for all 66 subjects shown in Figure 2.6.

The effect of the correction procedure is well shown by the more detailed representation of Figure 2.7 The corrected values are, almost without exception, moved down from the elementary M.I. Factor line predictions toward the cluster of experimental points.

c) Extension of the correction procedure

Further application of the correction procedure follows two lines:-

i) Investigation of the effect of the Whitsett 'local' moment of inertia for the Head-Trunk segment (Table 2.6, Section 2.12)

ii) Predictions and comparisons for two other body configurations, 'arms over head' (AOH) and 'sitting, forearms down' (SFD).

The results of these calculations are summarised in Tables 2.5 (A) and (

TABLE 2.4

M.I. DATA FOR THE 26 SUBJECTS OUTSIDE THE MAIN CLUSTER

SUBJECT NO. (SANTSCHI NUMBERING)	H (in)	M (lb)	L_z (in)	$\frac{L_z}{H}$	$MH^2 \times 10^{-4}$ $(lb\,in^2 \times 10^{-4})$	(A) I_{yG} (SANTSCHI)	(B) I_{yG} (CORRECTED MODEL)	% ERROR IN I_{yG} $\frac{(B-A)}{A} \cdot 100$
11	62.7	132.6	27.7	0.442	52.0	66.6	73.2	+ 9.9
66	63.0	129.8	28.1	0.447	51.4	69.1	70.7	+ 2.4
56	63.4	159.5	28.0	0.442	64.1	75.5	90.1	+ 19.4
10	67.9	197.1	30.2	0.444	90.9	119.0	125.6	+ 5.6
33	68.9	174.9	31.4	0.457	83.0	113.0	108.1	- 4.4
17	69.1	203.8	31.5	0.457	97.1	122.0	126.6	+ 3.8
44	70.7	206.9	32.2	0.457	103.2	125.0	134.8	+ 7.9
54	70.7	174.6	30.9	0.437	87.0	113.0	125.6	+ 11.2
28	70.9	189.3	31.0	0.437	95.3	131.0	136.8	+ 4.5
18	71.2	185.4	31.4	0.441	94.0	95.8	132.5	+ 38.4
6	71.5	203.3	31.8	0.445	104.0	129.0	143.7	+ 11.4
22	71.6	173.1	31.5	0.440	87.4	113.0	125.8	+ 11.4
59	72.0	179.1	32.6	0.452	92.9	120.0	122.9	+ 2.4
1	72.2	173.5	32.2	0.447	90.3	119.0	124.2	+ 4.4
21	72.3	210.4	31.2	0.431	111.0	130.0	162.8	+ 25.2
15	72.6	172.4	32.2	0.443	90.8	122.0	126.5	+ 3.7
8	72.6	188.8	31.7	0.437	99.3	124.0	143.5	+ 15.8
23	73.0	172.2	32.2	0.441	91.8	114.0	129.3	+ 13.5
52	73.2	197.8	32.0	0.437	105.8	123.0	152.5	+ 24.0
2	73.3	203.2	32.5	0.443	109.5	129.0	152.0	+ 17.9
47	73.4	157.1	33.8	0.460	84.7	108.0	107.2	- 0.7
63	73.9	181.2	33.2	0.450	99.0	125.0	133.5	+ 6.8
29	74.1	151.4	33.8	0.456	83.0	115.0	108.0	- 6.1
61	75.3	199.5	32.9	0.437	113.5	139.0	162.9	+ 17.2
50	75.8	190.6	33.8	0.445	109.8	146.0	151.4	+ 3.7
53	76.2	193.6	35.1	0.462	112.0	145.0	142.3	- 1.9

MOMENTS OF INERTIA IN $lbf.in.s^2$

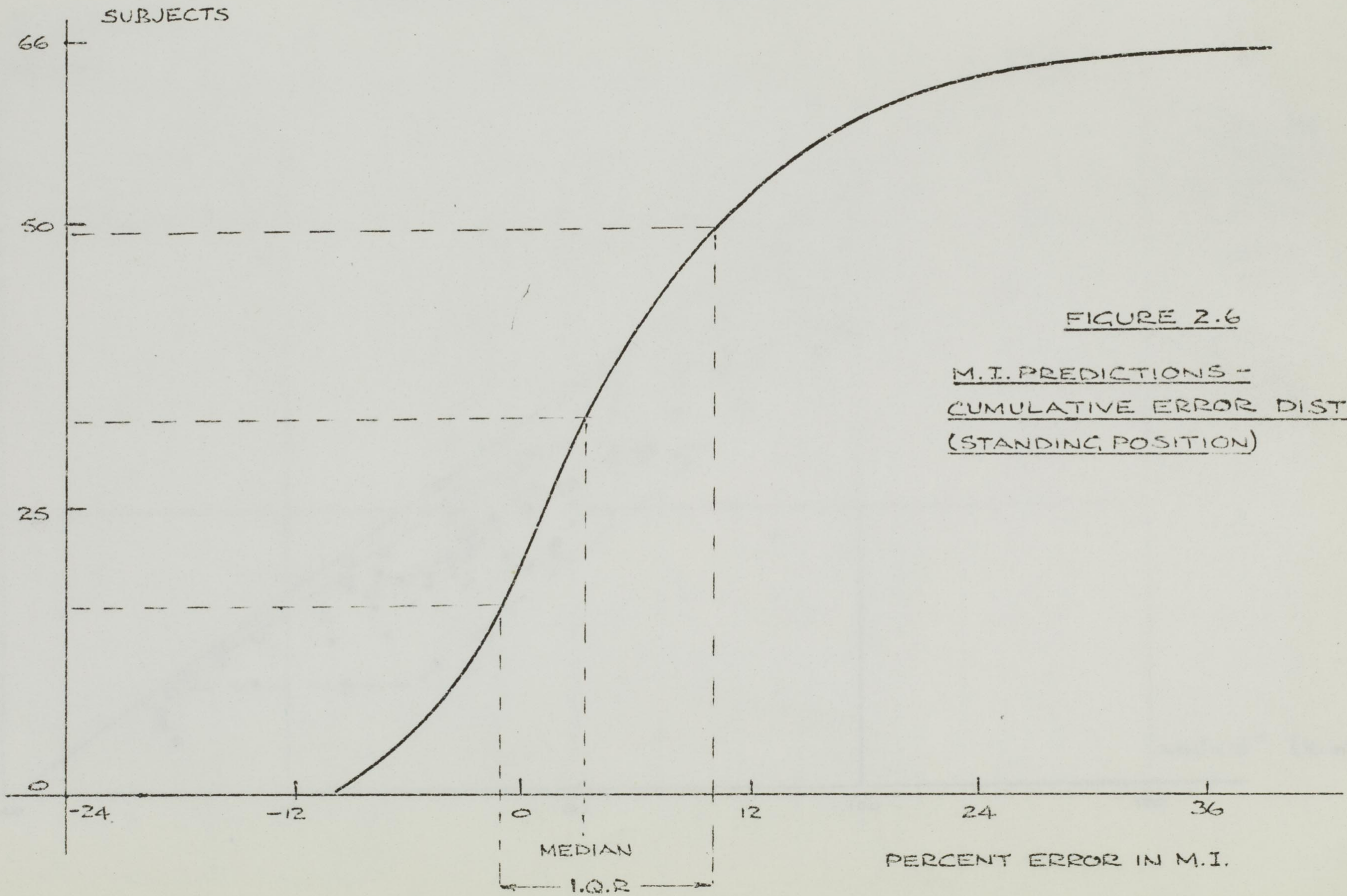

FIGURE 2.6

M.I. PREDICTIONS -

CUMULATIVE ERROR DISTRIBUTION

(STANDING POSITION)

FIGURE 2.7

EFFECT OF L_2/H CORRECTION PROCEDURE

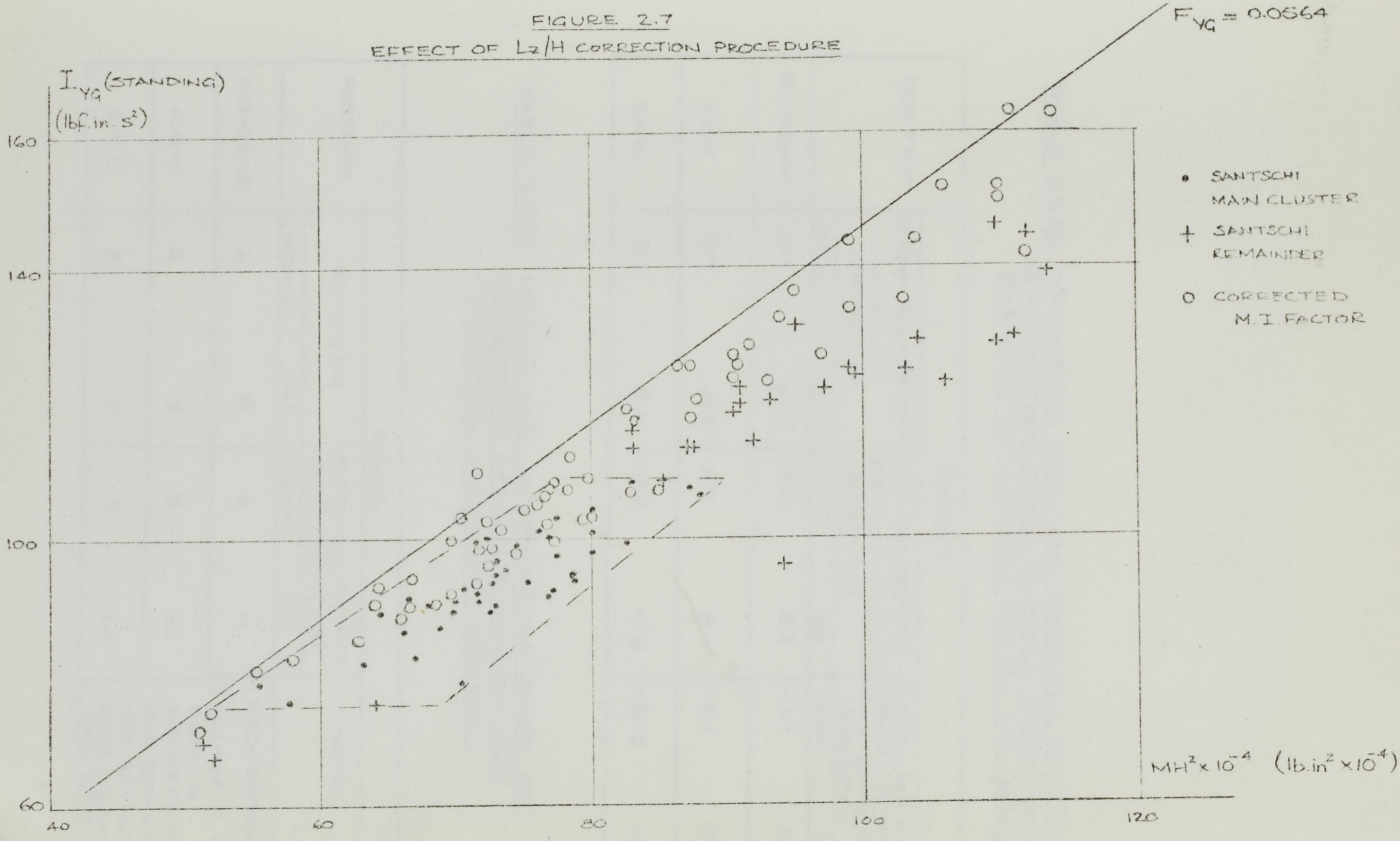

TABLE 2.5(A) ARITHMETIC MEAN AND STANDARD DEVIATION OF PERCENTAGE ERRORS IN MODEL PREDICTIONS COMPARED WITH EXPERIMENTAL M.I. (SANTSCHI)

POSITION	MODEL					
	UNIFORM ROD SEGMENTS NO SUBJECT CORRECTION		UNIFORM ROD SEGMENTS SUBJECT-BASED (L_z/H) CORRECTIONS		UNIFORM ROD H-T REPLACED BY WHITSETT VALUE WITH (L_z/H) CORRECTIONS	
	MEAN	SD	MEAN	SD	MEAN	SD
STANDING	15·1	6·6	8·4	8·7	-3·7	8·1
AOH	13·9	6·3	8·9	8·1	-0·1	7·6
SFD	5·2	8·0	-4·8	11·5	-23·0	10·4

TABLE 2.5(B) MEDIAN AND INTERQUARTILE RANGE OF PERCENTAGE ERRORS IN HANAVAN AND CORRECTED M.I. FACTOR MODELS

POSITION	MODEL				NOTES
	HANAVAN		UNIFORM ROD SEGMENTS (L_z/H) CORRECTIONS		
	MEDIAN	IQR	MEDIAN	IQR	
STANDING	6	8	4	11	1. MEDIAN≃MEAN-4 2. WHIT.SETT H-T MODEL IS SATISFACTORY FOR STANDING AND AOH, BUT GIVES MEDIAN=-23 FOR SFD
AOH	4	7	5	10	
SFD	2	11	-9	16	

Chapter 2 Part 2

Mathematical Derivations

and

Numerical Examples

2.12 Derivation of the Moment of Inertia Factor Equations

For the reference (standing) position of Figure 2.8 the whole-body moment of inertia I_{YTH} is to be evaluated. The moments of inertia of individual segments about their own mass-centres, (the 'local' values), are taken in the form $ml^2/12$. This assumption is justified at the end of this Section.

Moment of Inertia of segment j about YTH

$$= \frac{m_j l_j^2}{12} + m_j d_j^2$$

$$= MH^2\left(\frac{p_j q_j^2}{12} + p_j k_j^2\right)$$

Moment of Inertia of all segments, giving whole-body value,

$$I_{YTH} = MH^2 \sum_j \left(\frac{p_j q_j^2}{12} + p_j k_j^2\right)$$

$$= \underline{MH^2 . F_{YTH}}$$

where $$F_{YTH} = \sum_j \left(\frac{p_j q_j^2}{12} + p_j k_j^2\right)$$

defines the moment of inertia factor for axis YTH.

Similarly, I_{YG} and its corresponding M.I. Factor, F_{YG} are obtained as follows:-

$$I_{YG} = I_{YTH} - \frac{1}{M}\left(\sum_j m_j d_j\right)^2$$

so that $$I_{YG} = MH^2 \sum_j \left(\frac{p_j q_j^2}{12} + p_j k_j^2\right) - MH^2 \left(\sum_j p_j k_j\right)^2$$

and $$F_{YG} = \sum_j \left(\frac{p_j q_j^2}{12} + p_j k_j^2\right) - \left(\sum_j p_j k_j\right)^2$$

Note that $\sum p_j k_j$ gives the location of the whole-body mass-centre from YTH, and that F_{YTH} and F_{YG} are related by the Parallel Axes Theorem.

The assumption of the expression $ml^2/12$ for the 'local' moments of inertia of segments implies that they are regarded as uniform rods. Surprisingly, the simplification is not seriously in error except in the case of the Head-Trunk segment, as the following comparisons indicate:-

FIGURE 2.8

TYPICAL DIMENSIONS FOR MOMENT OF INERTIA

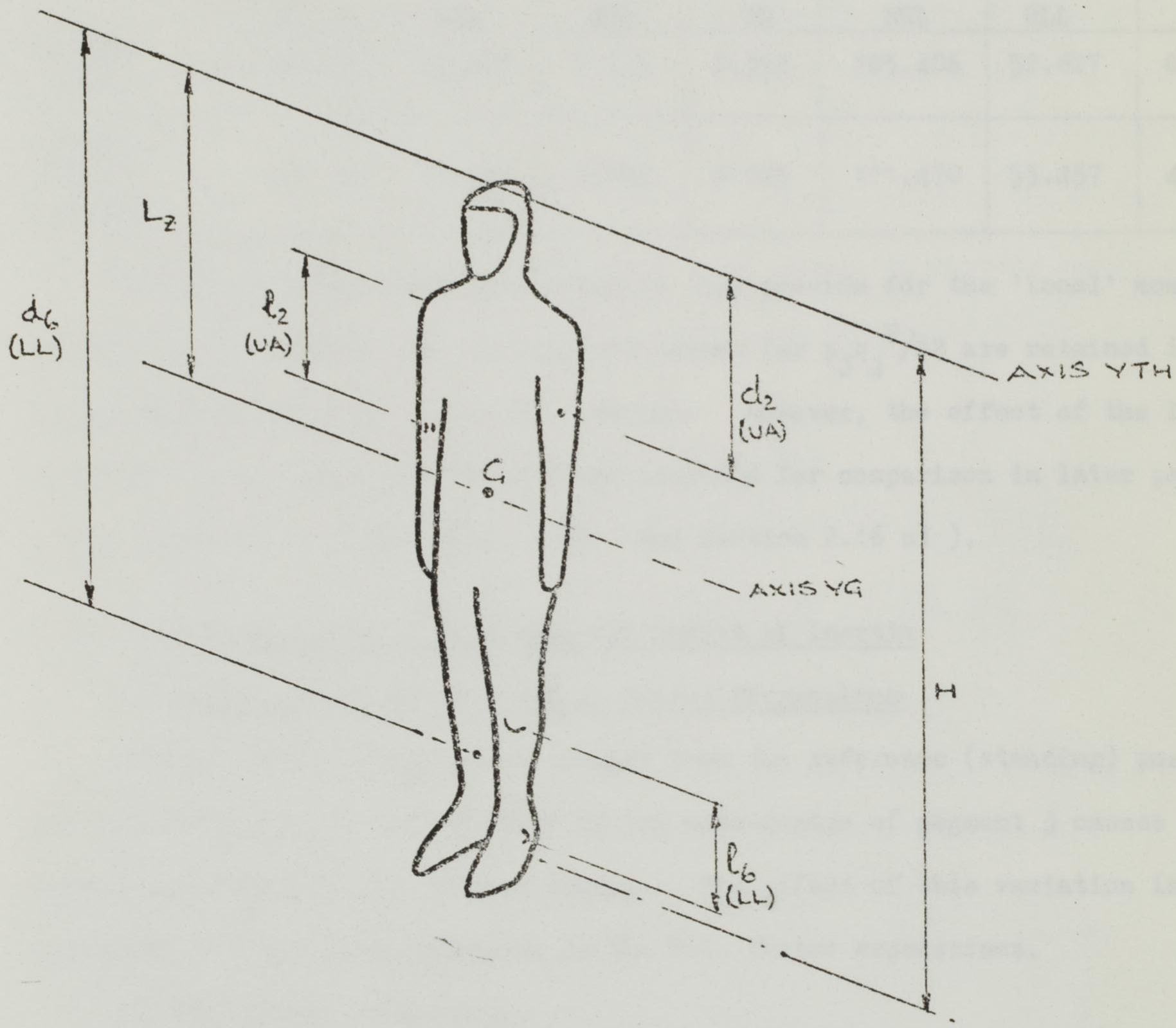

NONDIMENSIONAL FORMS

$q_2 = \ell_2/H = 0.188$

$K_2 = d_2/H = 0.265$

$q_6 = \ell_6/H = 0.231$

$K_6 = d_6/H = 0.829$

Table 2.6 Values of $(p_j q_j^2) \times 10^4$ for uniform rods and Whitsett solids

	SEGMENT						
	H - T	BUA	BFA	BH	BUL	BLL	BF
UNIFORM RODS	1390.000	22.267	7.779	0.393	105.406	52.827	6.840
WHITSETT SOLID SEGMENTS	681.103	22.553	8.044	0.575	111.470	53.437	4.022

Because of the satisfactory estimate they provide for the 'local' moments of inertia of segments, the uniform rod values for $p_j q_j^2/12$ are retained in the general development of the M.I. Factor. However, the effect of the lower Whitsett 'local' value for the H-T was included for comparison in later parts of the treatment. (Section 2.11 c) and Section 2.16 c)).

2.13 Derivation of Shift Equations for Moment of Inertia

a) Taylor Expansion of the M.I. Factor Expressions

When the body configuration changes from the reference (standing) position the variation Δk_j in the location of the mass-centre of segment j causes a modification in both M.I. Factor values. The effect of this variation is expressed by the Taylor expansion of the M.I. Factor expressions.

For the standing position:-

$$F_{YTH} = \sum \frac{p_j q_j^2}{12} + \sum p_j k_j^2$$

Shift Δk_2 in segment 2 only will be considered. In this case:-

$$F_{YTH} = f(k_2)$$

and the Taylor expansion,

$$f(k_2+\Delta k_2) = f(k_2) + \Delta k_2 . f'(k_2) + \frac{\Delta k_2^2}{2!} . f''(k_2) \ldots.$$

provides the result:-

$$F_{YTH} + \Delta F_{YTH} = F_{YTH} + \Delta k_2 . 2p_2 k_2 + \frac{\Delta k_2^2}{2!} . 2p_2$$

Thus,

$$\underline{\Delta F_{YTH} = p_2 . \Delta k_2 (2k_2 + \Delta k_2)}$$

Similarly for

$$F_{YG} = \sum \frac{p_j q_j^2}{12} + \sum p_j k_j^2 - (\sum p_j k_j)^2$$

the expansion gives:-

$$F_{YG} + \Delta F_{YG} = F_{YG} + \Delta k_2 (2p_2 k_2 - 2p_2 \sum p_j k_j) + \frac{\Delta k_2^2}{2} (2p_2 - 2p_2^2)$$

Thus,

$$\Delta F_{YG} = p_2 . \Delta k_2 \left[(2k_2 - 2\sum p_j k_j) + (1-p_2) \Delta k_2 \right]$$

. . . . . (2.13-1)

b) Taylor Expansion for more than one Variable

A change in body configuration will, in most practical cases, involve the shift of more than one segment. While it is tempting to assume that the single-segment effect derived above may be used in some form of superposition principle to obtain the combined effects of several segmental shifts, the validity of such a procedure must be justified. Here, then, we consider the M.I. Factor to be a function of more than one variable so that the Taylor expansion expresses the simultaneous effects of shifts in several segments. For simplicity, the derivation will be carried out for shifts in two segments, Δk_2 and Δk_3.

In general, for F_{YTH} or $F_{YG} = f(k_2, k_3)$

$$f(k_2+\Delta k_2, k_3+\Delta k_3) = f(k_2, k_3) + \Delta k_2 \cdot \frac{\partial f}{\partial k_2} + \Delta k_3 \cdot \frac{\partial f}{\partial k_3}$$
$$+ \frac{\Delta k_2^2}{2} \cdot \frac{\partial^2 f}{\partial k_2^2} + \frac{\Delta k_3^2}{2} \cdot \frac{\partial^2 f}{\partial k_3^2}$$
$$+ \Delta k_2 . \Delta k_3 \cdot \frac{\partial^2 f}{\partial k_2 . \partial k_3}$$
$$+ \text{higher derivatives} \ldots . (2.13\text{-}2)$$

For both F_{YTH} and F_{YG} all derivatives above the second vanish.

In the expansion for F_{YTH}, the cross-product term, $\Delta k_2 . \Delta k_3 . \frac{\partial^2 f}{\partial k_2 . \partial k_3}$ also vanishes, because

$$\frac{\partial f}{\partial k_2} = 2 b_2 k_2 \quad \text{and} \quad \frac{\partial^2 f}{\partial k_2 . \partial k_3} = 0$$

But for F_{YG}, the cross-product term involves:-

$$\frac{\partial^2 f}{\partial k_2 . \partial k_3} = \frac{\partial}{\partial k_3}\left[2 b_2 k_2 - 2 b_2 \Sigma b_j k_j\right] = -2 b_2 b_3 \quad \ldots\ldots\ldots (2.13\text{-}3)$$

The presence of this latter term destroys the validity of the superposition principle for a sequence of segmental shifts Δk_2, Δk_3 influencing F_{YG}. The total variation, given by the terms of the Taylor expansion, cannot be represented by the arithmetic summation of the effects of the individual shifts. In the case of F_{YTH}, however, superposition may be applied, because the cross-product term vanishes identically, and the expansion is a statement of the additive relationship:-

$$f(k_2+\Delta k_2, k_3+\Delta k_3) = f(k_2+\Delta k_2) + f(k_3+\Delta k_3) \quad \ldots . (2.13\text{-}4)$$

which is the underlying meaning of the superposition principle.

c) Small Error Theory. Termination of the Taylor Series

In this treatment the full Taylor expansion is reduced to the simpler first-order form which is adequate for small error variations in k and p; the Taylor series is terminated at the first-derivative terms.

i) Consider first a small variation in p_1 , the mass of segment 1 (H-T).

The overall condition $\sum p_j = 1$ (sum of segment masses = whole body mass) must be kept. Take the case where mass is removed from the H-T, segment 1, and added to BUL, segment 5. No change in k_1 , k_5 or any other p,q or k occurs.

The variation in F_{YG} is now given by:-

$$\delta F_{YG} = \left(\delta p_1 \cdot \frac{\partial}{\partial p_1} + \delta p_5 \cdot \frac{\partial}{\partial p_5}\right)\left(\sum \frac{p_j q_j^2}{12} + \sum p_j k_j^2 - \left[\sum p_j k_j\right]^2\right)$$

$$= \delta p_1\left(\frac{q_1^2}{12} + k_1^2 - 2k_1 \sum p_j k_j\right) + \delta p_5\left(\frac{q_5^2}{12} + k_5^2 - 2k_5 \sum p_j k_j\right)$$

Taking $\delta p_1 = -0.1\ p_1$, which requires $\delta p_5 = +\ 0.1\ p_5$, and using other numerical data from Table 2.1:-

$$\delta F_{YG} = 0.1 \times 0.556 \left(\frac{q_5^2 - q_1^2}{12} + k_5^2 - k_1^2\right) - 2 \times 0.1 \times 0.556 \left([k_5 - k_1] \sum p_j k_j\right)$$

$$= 0.1 \times 0.556 \times 0.2580 \quad - \quad 0.2 \times 0.556 \times 0.3081 \times 0.4343$$

$$= -\ 0.00053$$

$$\text{and} \quad \frac{\delta F_{YG}}{F_{YG}} = \frac{-0.00053}{0.0564} = -\ 0.0093 \qquad (-\ 0.93\%)$$

A 10% shift in mass from segment 1 to segment 5 produces a reduction of only 0.93% in F_{YG} and in the I_{YG} calculated from it.

---

ii) Consider now a small variation in k_1, the mass-centre location for segment 1 (H-T). The first order variation in F_{YG} is given by:-

$$\delta F_{YG} = \frac{\partial}{\partial k_1}\left(\sum \frac{p_j q_j^2}{12} + \sum p_j k_j^2 - \left[\sum p_j k_j\right]^2\right) \delta k_1$$

$$= \left(2 p_1 k_1 - 2 p_1 \sum p_j k_j\right) \delta k_1$$

$$= 2 p_1 k_1 \left(k_1 - \sum p_j k_j\right)$$

Numerical data from Table 2.1, with the assumption $\delta k_1 = 0.1\ k_1$ (a 10% increase in k_1) gives:-

$$\delta F_{YG} = 2 \times 0.556 \times 0.2914\ (-0.142866) = -\ 0.00463$$

$$\text{and} \quad \frac{\delta F_{YG}}{F_{YG}} = -\frac{0.00463}{0.0564} = -0.082 \qquad (-8.2\%)$$

The 10% increase in k_1 causes an 8.2% reduction in F_{YG}, and the same percentage change in the I_{YG} calculated from it.

2.14 A Numerical Example of the Use of the Shift Equations for New Body Configurations

Change in F_{YTH} for a Shift From Standing to A O H position

From Table 2.2 the relevant data is:-

$p_2 = 0.063$ $\quad k_2 = 0.264505$ $\quad \Delta k_2 = -0.164665$

$p_3 = 0.037$ $\quad k_3 = 0.432788$ $\quad \Delta k_3 = -0.497902$

$p_4 = 0.014$ $\quad k_4 = 0.541600$ $\quad \Delta k_4 = -0.716684$

From Section 2.13 a)

$$\Delta F_{YTH} = p_2 . \Delta k_2 (2k_2 + \Delta k_2)$$

By superposition, the total variation

$$\begin{aligned} \Delta F_{YTH} &= -0.003780 \quad (\text{SEGMENT 2 - BUA}) \\ &\quad -0.006773 \quad (\text{SEGMENT 3 - BFA}) \\ &\quad -0.003677 \quad (\text{SEGMENT 4 - BH}) \end{aligned}$$

$$\text{i.e. } \Delta F_{YTH} = -0.014230$$

$$\text{and } F_{YTH}(\text{AOH}) = 0.2450 - 0.014230$$

$$= 0.2308$$

2.15 A Numerical Example of the Use of Δk Tables for a New Body Configuration

Change in F_{YG} for a Shift From Standing to S F D Position

a) From Table 2.2 the relvant data is:-

$p_5 = 0.201$ $\quad k_5 = 0.599479$ $\quad \Delta k_5 = 0.091593$

$p_6 = 0.099$ $\quad k_6 = 0.829257$ $\quad \Delta k_6 = 0.188251$

$p_7 = 0.030$ $\quad k_7 = 0.980176$ $\quad \Delta k_7 = 0.182897$

$$\sum p_j k_j = 0.434285$$

b) Section 2.13 b) shows that superposition cannot be applied in the case of F_{YG} variations due to several segmental shifts. Consideration of equations (2.13-1) to (2.13-4), however, leads to a step-by-step modification of the superposition principle. For shifts in segments 5 and 6, we take

$F_{YG} = f(k_5, k_6)$

Then $f(k_5+\Delta k_5, k_6+\Delta k_6) = f(k_5+\Delta k_5) + f(k_6+\Delta k_6) - 2p_6 . \Delta k_6 . p_5 . \Delta k_5$

from which the change in F_{YG} due to Δk_5 and Δk_6 is:-

$$(\Delta F_{YG})_{5,6} = p_5.\Delta k_5[(2k_5 - 2\Sigma p_j k_j) + (1-p_5)\Delta k_5] + p_6.\Delta k_6[(2k_6 - 2\Sigma p_j k_j) + (1-p_6)\Delta k_6] - 2p_6.\Delta k_6.p_5.\Delta k_5 \quad \ldots\ldots\ldots (2.15\text{-}1)$$

For two segmental shifts the superposition principle is modified only by the inclusion of the final cross-product term. Extending this idea, the <u>further</u> effect on F_{YG} of a shift in segment 7 can be shown to be:-

$$(\Delta F_{YG})_7 = p_7.\Delta k_7[(2k_7 - 2\Sigma p_j k_j) + (1-p_7)\Delta k_7] - 2p_7.\Delta k_7[p_6.\Delta k_6 + p_5.\Delta k_5] \quad (2.15\text{-}2)$$

In the present example, only three shifted segments are involved, but the pattern for more segmental shifts is apparent. These equations appear umwieldy, but the first two terms in (2.15-1) and the first in (2.15-2) are easily obtained from the Δk Table for F_{YG}, Table 2.8. The remaining cross-product terms are simple to compute.

c) As an example of interpolation in Table 2.8 take segment 5 (BUL), for which $\Delta k_5 = -0.091593$

FROM THE TABLE:-

Δk	ΔF_{YG} (BUL)
-0.08	-0.00428
-0.10	-0.00504

BY LINEAR INTERPOLATION:-

$(\Delta F_{YG})_5 = -0.0047205$

d) Calculation of F_{YG} for shifts of segments 5, 6 and 7

<u>Contribution</u>

Segment 5 (BUL) Table 2.8 ;-	- 0.0047205
Segment 6 (BLL) Table 2.8 :-	- 0.0115530
Cross-product term :-	- 0.0006862
Summing $(\Delta F_{YG})_{5,6}$:-	- 0.0169597
Segment 7 (BF) :-	- 0.0050162
Cross-product term :-	- 0.0004065
Summing again $(\Delta F_{YG})_{5,6,7}$:-	- 0.0223824

TABLE 2.7

VARIATIONS IN F_{YTH}

$$(\Delta F_{YTH})_j = b_j . \Delta k_j (2k_j + \Delta k_j) \quad \ldots\ldots (2.5\text{-}2)$$

Δk	ΔF_{YTH}					
	BUA	BFA	BH	BUL	BLL	BF
+0.00	+0.00000	+0.00000	+0.00000	+0.00000	+0.00000	+0.00000
-0.02	-0.00064	-0.00063	-0.00030	-0.00474	-0.00324	-0.00116
-0.04	-0.00123	-0.00122	-0.00058	-0.00932	-0.00641	-0.00230
-0.06	-0.00177	-0.00179	-0.00086	-0.01374	-0.00950	-0.00342
-0.08	-0.00226	-0.00233	-0.00112	-0.01799	-0.01250	-0.00451
-0.10	-0.00270	-0.00283	-0.00138	-0.02209	-0.01543	-0.00553
-0.12	-0.00309	-0.00331	-0.00162	-0.02603	-0.01823	-0.00663
-0.14	-0.00343	-0.00376	-0.00185	-0.02980	-0.02105	-0.00765
-0.16	-0.00372	-0.00418	-0.00207	-0.03341	-0.02374	-0.00864
-0.18	-0.00396	-0.00457	-0.00228	-0.03687	-0.02635	-0.00961
-0.20	-0.00415	-0.00493	-0.00247	-0.04016	-0.02888	-0.01056
-0.22	-0.00428	-0.00526	-0.00266	-0.04329	-0.03133	-0.01149
-0.24	-0.00437	-0.00556	-0.00283	-0.04626	-0.03371	-0.01239
-0.26	-0.00441	-0.00583	-0.00300	-0.04907	-0.03600	-0.01326
-0.28	-0.00439	-0.00607	-0.00315	-0.05172	-0.03821	-0.01412
-0.30	-0.00433	-0.00628	-0.00329	-0.05421	-0.04035	-0.01494
-0.32	-0.00421	-0.00646	-0.00342	-0.05654	-0.04241	-0.01575
-0.34	-0.00405	-0.00661	-0.00354	-0.05870	-0.04438	-0.01653
-0.36	-0.00383	-0.00673	-0.00364	-0.06071	-0.04628	-0.01728
-0.38	-0.00357	-0.00683	-0.00374	-0.06256	-0.04810	-0.01802
-0.40	-0.00325	-0.00689	-0.00383	-0.06424	-0.04984	-0.01872
-0.42	-0.00288	-0.00692	-0.00390	-0.06576	-0.05150	-0.01941
-0.44	-0.00247	-0.00693	-0.00396	-0.06713	-0.05308	-0.02007
-0.46	-0.00200	-0.00690	-0.00401	-0.06833	-0.05458	-0.02071
-0.48	-0.00148	-0.00685	-0.00405	-0.06937	-0.05601	-0.02132
-0.50	-0.00091	-0.00676	-0.00408	-0.07025	-0.05735	-0.02191
-0.52	-0.00029	-0.00665	-0.00410	-0.07097	-0.05862	-0.02247
-0.54	+0.00037	-0.00651	-0.00411	-0.07153	-0.05980	-0.02301
-0.56	+0.00109	-0.00633	-0.00410	-0.07193	-0.06091	-0.02353
-0.58	+0.00186	-0.00613	-0.00409	-0.07216	-0.06193	-0.02402
-0.60	+0.00268	-0.00590	-0.00406	-0.07224	-0.06288	-0.02449
-0.62	+0.00355	-0.00563	-0.00402	-0.07215	-0.06375	-0.02493
-0.64	+0.00448	-0.00534	-0.00397	-0.07191	-0.06454	-0.02535
-0.66	+0.00545	-0.00502	-0.00391	-0.07150	-0.06525	-0.02575
-0.68	+0.00647	-0.00467	-0.00384	-0.07094	-0.06588	-0.02612
-0.70	+0.00754	-0.00429	-0.00376	-0.07021	-0.06643	-0.02647
-0.72	+0.00866	-0.00388	-0.00366	-0.06932	-0.06690	-0.02679

TABLE 2.8

VARIATIONS IN F_{YC}

$$(\Delta F_{YC})_j = b_j \cdot \Delta k_j [(2k_j - 2\Sigma b_j k_j) + (1 - b_j)\Delta k_j] \quad \ldots \quad (2.5\text{-}2)$$

Δk	ΔF_{YC}					
	BUA	BFA	BH	BUL	BLL	BF
+0.00	+0.00000	+0.00000	+0.00000	+0.00000	+0.00000	+0.00000
-0.02	+0.00045	+0.00002	-0.00005	-0.00126	-0.00153	-0.00064
-0.04	+0.00095	+0.00006	-0.00010	-0.00240	-0.00299	-0.00126
-0.06	+0.00150	+0.00013	-0.00013	-0.00341	-0.00437	-0.00186
-0.08	+0.00209	+0.00024	-0.00015	-0.00428	-0.00569	-0.00243
-0.10	+0.00273	+0.00037	-0.00016	-0.00504	-0.00693	-0.00298
-0.12	+0.00342	+0.00053	-0.00016	-0.00566	-0.00810	-0.00351
-0.14	+0.00415	+0.00071	-0.00015	-0.00615	-0.00920	-0.00402
-0.16	+0.00493	+0.00093	-0.00013	-0.00651	-0.01023	-0.00450
-0.18	+0.00576	+0.00117	-0.00009	-0.00675	-0.01119	-0.00495
-0.20	+0.00664	+0.00145	-0.00005	-0.00686	-0.01207	-0.00539
-0.22	+0.00756	+0.00175	+0.00001	-0.00684	-0.01289	-0.00580
-0.24	+0.00853	+0.00208	+0.00007	-0.00669	-0.01363	-0.00618
-0.26	+0.00955	+0.00244	+0.00015	-0.00641	-0.01430	-0.00655
-0.28	+0.01062	+0.00282	+0.00024	-0.00600	-0.01491	-0.00689
-0.30	+0.01173	+0.00324	+0.00034	-0.00547	-0.01544	-0.00721
-0.32	+0.01289	+0.00368	+0.00045	-0.00481	-0.01589	-0.00750
-0.34	+0.01410	+0.00416	+0.00057	-0.00401	-0.01628	-0.00777
-0.36	+0.01535	+0.00466	+0.00071	-0.00309	-0.01660	-0.00802
-0.38	+0.01665	+0.00519	+0.00085	-0.00205	-0.01684	-0.00824
-0.40	+0.01800	+0.00575	+0.00101	-0.00087	-0.01701	-0.00845
-0.42	+0.01940	+0.00633	+0.00117	+0.00044	-0.01711	-0.00862
-0.44	+0.02084	+0.00695	+0.00135	+0.00187	-0.01714	-0.00878
-0.46	+0.02233	+0.00759	+0.00154	+0.00343	-0.01710	-0.00891
-0.48	+0.02387	+0.00826	+0.00174	+0.00513	-0.01699	-0.00902
-0.50	+0.02546	+0.00896	+0.00195	+0.00694	-0.01681	-0.00910
-0.52	+0.02709	+0.00969	+0.00217	+0.00889	-0.01655	-0.00916
-0.54	+0.02877	+0.01045	+0.00240	+0.01097	-0.01622	-0.00920
-0.56	+0.03049	+0.01124	+0.00265	+0.01317	-0.01582	-0.00922
-0.58	+0.03227	+0.01205	+0.00290	+0.01551	-0.01536	-0.00921
-0.60	+0.03409	+0.01289	+0.00317	+0.01797	-0.01481	-0.00918
-0.62	+0.03596	+0.01377	+0.00344	+0.02056	-0.01420	-0.00912
-0.64	+0.03787	+0.01467	+0.00373	+0.02328	-0.01352	-0.00904
-0.66	+0.03983	+0.01559	+0.00403	+0.02613	-0.01276	-0.00894
-0.68	+0.04184	+0.01655	+0.00434	+0.02910	-0.01194	-0.00882
-0.70	+0.04390	+0.01754	+0.00466	+0.03221	-0.01104	-0.00867
-0.72	+0.04601	+0.01855	+0.00499	+0.03544	-0.01007	-0.00850

Original F_{YG} (Standing) = 0.0564

Subtract $(\Delta F_{YG})_{5,6,7}$ = -0.0223824

New F_{YG} (SFD) = 0.0340(176)

Direct substitution into equations (2.15-1) and (2.15-2) leads to an identical result, but with experience the tabular method is somewhat faster for manual calculation. The time of computation for a major six-segment change in configuration, including the graphical construction for Δk values, can be reduced to about five minutes.

2.16 Derivation of the Subject-Based Correction for M.I. Factor

a) For the reference (standing) position

The correction is based on the following :-

(i) The subject's mass-centre location, Lz/H, from axis YTH, is different from that of the mean-man, $\sum p_j k_j$ (Figure 2.5)

(ii) Assume that this difference is caused solely by a discrepancy between the location of the subject's H-T mass-centre and that of the mean-man, (k_1 in Table 2.1)

(iii) Calculate the adjustment in mean-man k_1 to equate the model $\sum p_j k_j$ to the subject's Lz/H

(iv) Insert this adjustment into the formula for F_{YG} to calculate its effect on moment of inertia predictions from the modified model.

The equations are modified as follows:-

(i) Difference between subject and model whole-body mass-centres:-

$$= L_z/H - \sum p_j k_j$$

(ii,iii) Shift Δk_1 which completely accounts for this difference:-

$$= \frac{1}{p_1}\left(L_z/H - \sum p_j k_j\right)$$

(iv) Substitute into:

$$\Delta F_{YG} = 2p_1 . \Delta k_1 (k_1 - \sum p_j k_j)$$

to obtain:-

$$\Delta F_{YG} = 2p_1 . \frac{1}{p_1}\left(L_z/H - \sum p_j k_j\right)\left(k_1 - \sum p_j k_j\right)$$

Numerical values from Table 2.2 give:-

$$\Delta F_{YG} = -0.2857\ (L_z/H - 0.434285)$$

$$\text{and } F_{YG\,(CORRECTED)} = 0.0564 - 0.2857\left(L_z/H - 0.434285\right)$$

This is a corrected value for F_{YG} for the standing position and was

b) Subject-based corrections for other body configurations

All the computational methods and tables presented in this chapter have been derived for situations in which the Head-Trunk remains fixed in the reference position, and the other segments move with respect to the H-T. Thus, k_1, for the H-T remains constant during changes in body configuration and the only change in k_1 is described in the correction procedure above. There is, therefore, no difficulty in applying the subject-based correction to new body configurations. As an example, take the SFD positions:-

The starting value of F_{YG} is taken from Table 2.3:

$$F_{YG}\ (\text{SFD}) = 0.0340$$

The correction, based on the subject's Lz/H, is the same as for the standing position example a) above:

$$\Delta F_{YG} = 0.2857\ (Lz/H - 0.434285)$$

Thus, the corrected F_{YG} becomes:-

$$F_{YG}\ (\text{corrected}) = 0.0340 - 0.2857\ (Lz/H - 0.434285)$$

It is also an easy step to insert F_{YG} starting values based on the Whitsett 'local' value for the H-T segment (Table 2.6). Some of these values are given in Table 2.3. The results of the correction procedure for all 66 Santschi subjects in three body positions have been summarised in Section 2.11 c), Table 2.5.

Chapter 2. Part 3

Discussion

2.17 Discussion of the M.I. Factor Techniques

Comparison has been made in Section 2.11 between Hanavan's results and those obtained by the use of the moment of inertia factor. The values quoted are only a small example of Hanavan's work. He produced model predictions of moment of inertia for seven body configurations with three principal axes of reference, and in all twenty-one of these combinations obtained results of the order of accuracy indicated in Table 2.5 b). He then proposed a condensation of the procedure by setting up five representative models spanning the range of anthropometric data given in the Santschi report. These 'percentile' models, typifying the median, quartiles and 5th and 95th percentiles of Santschi's range of subjects, were used by Hanavan to give a comprehensive set of moment of inertia data for thirty-two body configurations. The points plotted on Figure 2.4 (Section 2.8), indicate the ties between the percentile models and the experimental results. This treatment of segmental models 'tailor-made' to the subjects requires computer programmes running to 58 pages in Hanavan's report.

The work on the M.I. Factor does no more than point the way to a new and possibly fruitful line of investigation into segmental models. The results, as they stand, compare favourably with those of Hanavan. One great advantage is that the calculations for M.I. Factor are essentially very simple. Programming may be desirable to handle the results for a large number of subjects, but the working part of the programme runs to only a few lines.

The purpose has been to explore an idea which may throw some light on the pattern of human moment of inertia, and therefore upon mass-distribution and body form. At the same time some suggestions for speeding up the numerical processes involved in calculating moment of inertia have emerged. Braune and Fischer (2) used non-dimensional coefficients for segmental length, mass and radius of gyration. Further, Whitney (12) has used dimensionless ratios based on Dempster's figures to express segmental moments of inertia, and the concept of 'moment of inertia factor' may have occurred to other workers.

The elements of this Chapter which appear to be novel, but quite natural consequences of the first idea are three in number.

a) The plotting of moment of inertia against MH^2

For both experimental and model results, this form of graph condenses much material into an informative diagram (Figures 2.4 and 2.7). Comparisons are made easy, and the good and bad points of segmental representations are highlighted. It must be emphasised here that prediction of moment of inertia is a stringent test on the accuracy of a model and for this reason the behaviour of the M.I. Factor is worthy of attention. Clearly, there is a fairly high correlation between I and MH^2, and the regions of the graph occupied by experimental results from different subject populations should give some insight into patterns of body mass distribution. Santschi's subjects were factory personnel. Though there is no available data, athletes may well exhibit a significantly different moment of inertia pattern. Subdivision on the basis of specialisation in throwing, jumping or track events might identify characteristics of body build suitable for specific activities. Experimental work in this field could be related to Somatotyping, on which a note is given in the next Section.

b) The investigation of methods for calculation of body moment of inertia

This line has led to the Column Total, Shift Equation and Δk-Table methods for two dimensional body configurations. In each case graphical construction is recommended to establish the individual segmental shifts. The numerical examples in this Chapter may suggest that the methods are unwieldy, but a little practice enables short-cuts to be taken and, by any method, moment of inertia calculations could hardly be reduced to a shorter form. The preliminary graphical work might be avoided by the formation of some additional tables relating a range of segmental positions to the shifts Δk which they represent.

Extension of the procedures would allow the estimation of moments of inertia for three-dimensional segmental shifts. The graphical work would

involve three-dimensional projection methods and the 'local' moment of inertia of segments could be expected to vary.

c) The exploration of a subject-based correction procedure

These proposals were based on the divergences shown up by Figure 2.5. The work is capable of refinement and extension. Other body configurations and axes of reference should be investigated and may point to improvements in the correction technique. The validity of the approach may be further checked by direct measurement of moments of inertia of a larger sample of subjects than are provided by the Santschi report.

The work on M.I. Factor has proceeded alongside the other investigations described in later Chapters. It has not been possible to incorporate the results in subsequent calculations and the Whitsett segmental values have been used for the computation of body forces. Nevertheless, extensions of the work to rotational motion (Chapter 3) and the programming of such equations in a general force-analysis scheme (Chapter 6) will call for a treatment of body moment of inertia variations as the configuration changes. The M.I. Factor developments offer some assistance in this field.

2.18 A Note on Somatotyping

Sheldon's pioneer work, 'The Varieties of Human Physique' (7) proposes the system of Somatotyping as a means of classification of body forms. His procedure is best carried out with standardised photographs of the subject from which essential body dimensions are taken. The subject's mass and height are also needed.

Sheldon provides a set of tables by means of which the measured data may be converted into the three-digit Somatotype rating. The digits represent, in order, the measures of endomorphy, mesomorphy and ectomorphy assessed by Sheldon's scheme. As the procedure is fairly well-known and clearly laid out in Sheldon's book, there is no need to describe it here in detail. Somatotyping was conceived in order to establish links between body form and psychological traits, and it is Sheldon's aim to investigate such

relations. We may, however, expect to find more direct ties between the Somatotype and mechanical properties such as moment of inertia. Both quantities are strongly dependent on the distribution of matter over the body.

Thus it is pertinent to speculate whether Endomorphs, as a group, will exhibit large moment of inertia as compared with the other main groups; or we may expect that one group will tend to have a higher body mass-centre location than the others.

A full consideration of these problems would call for more data than are given in the Santschi report. Although there is correspondence between one or two of Santschi's anthropometric dimensions and those used by Sheldon, it is not possible to follow out the full procedure for Somatotyping. However, it is possible to make a tentative approach via the Ponderal Index, which is one of Sheldon's parameters. Bearing in mind the proviso that Sheldon's subjects were college students and that the Tables apply strictly to a similar age group, only a pointer for more detailed work can be given.

From Sheldon's Table 23, it is clear that subjects with a Ponderal Index $(H/\sqrt[3]{M})$ of 12 or less are rare, and high in endomorphy. The likely Somatotypes in this range are:- 711, 731, 721, 712, 641, 631, 551. For some of these types, Sheldon uses the phrases:- 'huge head ... enormous chest legs enormously inflated .. most massive of all physiques ... ' There are only four Santschi subjects who fall into this category, using the Ponderal Index as criterion. These are subjects 56, 10, 17 and 44. Although all four lie outside the Main Cluster, which suggests some tendency to unusual build, they do not represent the extremes of mass or moment of inertia. Subject 56 is, in fact, below the Main Cluster in Figure 23, and has quite low inertial properties.

The three Santschi subjects who do show exceptionally high moments of inertia are the last three in Table 2.2 of this Chapter, Subjects 61, 50 and 53. Their Ponderal Indices, though, do not indicate extremity in the Somatotyping rating. Table 23 of Sheldon shows their Ponderal Indices,

(12.9; 13.2; 13.2), to correspond to fairly average body builds.

From these sketchy figures there appears to be no simple link between extremes in Somatotyping and in moment of inertia. More detailed work would require photographs of the subjects, accurate Somatotyping and the consideration of several mechanical properties. Relationships are likely to be fairly imprecise but it may be possible to set, say, upper and lower bounds on the moment of inertia associated with a particular Somatotype. In any case, such a study could only throw more light on the variations in body form.

Footnote

Sheldon calls upon the Ponderal Index as a commonly used ratio based on the assumption of constant body density. A remark by Sokoloff (9) throws some doubt on the concept. Sokoloff states that the correlation of M with H^3 is a little lower than that of M with H, for a given male population.

Computation on the 66 Santschi subjects, gave correlation coefficients of 0.593 for M with H^3 and 0.596 for M with H, thus supporting Sokoloff. Certainly the ratio H/M is more easily evaluated, and seems at least as justified as the Ponderal Index $H/\sqrt[3]{M}$ on the evidence of the correlations.

The Ponderal Index springs from the assumption that the subjects to be compared are geometrically similar and that masses are proportional to length cubed (H^3). Some interesting results may be derived for groups of mammals with rough geometrical similarity and considerable differences in size. Thompson (10) and Smith (8) present some convincing arguments. However, the similarity concept seems to have been extended to comparisons between groups of human adults, and the Ponderal Index has been unquestioningly accepted as a valid factor for such comparisons. The evidence above suggests that, in human mass and length comparisons, the Ponderal Index may not deserve its hallowed position and certainly that extensions of the idea to explain athletic abilities in terms of body build must be examined carefully. In such arguments the inherent assumptions of constant density and similarity

2.19 References for Chapter 2

(1) Braune, W.
Fischer, O.
data on body segments summarised in (13)

(2) Braune, W.
Fischer, O.
non-dimensional segmental data quoted by Paul, J.P. 'Forces Transmitted by Joints in the Human Body'
Proc. I. Mech.E. 181 3J Paper 8 (1966)

(3) Dempster, W.T.
data on body segments summarised in (13) (1955)

(4) Dyson, G.H.G.
'The Mechanics of Athletics'
Univ. London Press (1970)

(5) Hanavan, E.F.
'A Mathematical Model of the Human Body'
AMRL-TR-64-102
Wright Patterson Air Force Base, Ohio (1964)

(6) Santschi, W.R.
Dubois, J.
Omoto, C.
'Moments of Inertia and Centres of Gravity of the Living Human Body'
AMRL-TDR-63-36
Wright Patterson Air Force Base, Ohio (1963)

(7) Sheldon, W.
'The Varieties of Human Physique'
Hafner (1970)

(8) Smith, H.M.
'Mathematical Ideas in Biology'
Cambridge Univ. Press (1968)

(9) Sokoloff, L.
'Biology of Degenerative Joint Disease'
Univ. Chicago Press, London (1969)

(10) Thompson, D.A.W.
'On Growth and Form' (ed. Bonner)
Cambridge Univ. Press (1968)

(11) Whitsett, C.E.
'Some Dynamic Response Characteristics of Weightless Man'
AMRL-TDR-63-18
Wright Patterson Air Force Base, Ohio (1963)

(12) Whitney, R.J.
Personal Communication (1969)

(13) Williams, M.
Lissner, H.
'Biomechanics of Human Motion'
Saunders. Philadelphia (1966)

Chapter 3

Mechanical Principles Applied to Human Movement

3.1 Introduction

The purpose of this Chapter is to state some fundamentals of mechanics which are useful in describing and analysing body movement.

There is no point in belabouring well-known principles, but in some published work and in personal discussion it has appeared that certain basic ideas are not well understood. It is surprising how many of the fundamentals discussed in this Chapter have been disputed by persons of some eminence. Professors Offenbacher (13) and Nightingale (11) have on separate occasions criticised the summation statement (3.3-5) below. Their main contention was that the transmission time of forces through the limbs and joints destroys the validity of this equation. The author's reply is contained in Section 3.3 of this Chapter.

Professors Offenbacher (13) and Alexander (2) have disagreed in debate with the author's statements on work and energy set out in Section 3.5. A lecture by Prof. Alexander in 1969 was in fact one of the first stimuli to much subsequent discussion on the study of jumping.

The author's treatment was arrived at over several years' teaching of applied mechanics. In view of the numerous dissensions which arise in the field of biomechanics on what are termed 'elementary principles', the author is constrained to cite here some supporting texts although the developments presented later in this Chapter are not taken from standard works.

a) Work and Potential Energy

Den Hartog (4) in his well-established treatment states:

" ..... the forces that may act on a particle arise from various causes. They can be listed as follows:

1. Gravity forces or weights
2. Spring forces or other elastic forces
3. Normal forces from a wall or other guide
4. Friction forces
5. All other forces such as a pull on a rope, steam pressure on a piston etc.

.... in this article we propose to prove that the work done in overcoming the first two kinds of forces is recoverable and is stored in the form of potential energy; work done by the third kind is zero, while work done by the fourth kind is not recoverable and is said to be 'dissipated' in the form of heat" Later: "gravity forces and spring forces are said to be <u>potential</u> forces while friction forces are <u>dissipative</u> forces" (p.257) and finally "The work done on a particle by the external forces exclusive of the potential and dissipative forces equals the increment of the sum of the kinetic and potential energies plus the work dissipated" (p.259)

Pars (14), from a mathematician's standpoint, also expresses an energy equation as $T + V = \mathcal{W}_2$ (p.446) where $T + V$ is the increase in kinetic and potential energy, and $\mathcal{W}_2$ is the work done by the nonconservative forces acting on the system. If $\mathcal{W}_2 = 0$ the equation reduces to that for a conservative system.

These points clarify that potential energy is used in either conservative or nonconservative systems with no change of meaning. It is also clear that "normal forces from a wall or other guide" do no work on the system on which they act. The latter point is important in Section 3.5 (i) of the present Chapter.

b) <u>Work done by internal forces in a system</u>

Having derived the kinetic energy of a rigid body as $T = \frac{1}{2}mV_G^2 + \frac{1}{2}I_G\omega^2$ Den Hartog (pp.262-3) goes on: "Now we are ready to extend ... from a particle to a large rigid body or to a system of rigid bodies, connected together by hinges or ropes .... The internal forces obey the law of action equals reaction, so that for any internal force acting on a particle 'a' there is an equal and opposite force acting on a neighbouring particle 'b', and if these two forces do not move with respect to one another the work done by one cancels that of the other .... The work done by all external forces on a system of rigid bodies equals the increment in kinetic energy in the system plus the work dissipated in friction in the joints or connections."

These statements support the development shown in Figure 3.5, particularly the third stage dealing with a system of rigid bodies.

c) Transfer of forces to the mass-centre

A great deal of misunderstanding has arisen because of the common practice of 'transferring all forces to the mass-centre'. The process is exemplified by Offenbacher's (12) paper discussed in Section 3.5 (i). Den Hartog (p.135) proves that "a force acting on a rigid body which is given an arbitrary small displacement performs an amount of work that is the same for all locations of the point of application of that force along its own line of action. We note that this statement is true only for small displacements ... We also note that it is true only for rigid bodies, because if the body were deformable, the length A'B' would not have to be the same as AB".

The discussion of Section 3.5 (i) is concerned with misconceptions springing from the transfer of ground force to the mass-centre and the incorrect statements about work which arise therefrom.

d) General Energy Equation

In Figure 3.5 the General Energy Equation is derived from the fundamental concept of energy balance in which all energy entering a system is either stored or emerges from the system in some form. This is merely a matter of accounting, and the underlying principle appears in any text on engineering thermodynamics as: $Q - W = U_2 - U_1$, that is, 'the net heat flow in, minus the net work flow out is equal to the increase in the internal energy of the system'. In Figure 3.5 the concept has been expanded by splitting the internal energy into parts relevant to a mechanical problem, and by regarding the energy into the system as having any form, heat flow included.

e) Kinetic energy of a system

Rutherford (6) provides further evidence of the unity of applied methematics and scund engineering mechanics on fundamental principles. He proves the well-known result " ...the kinetic energy of a system of

particles is equal to the kinetic energy of a mass equal to the total mass of the system placed at and moving with the mass-centre together with the kinetic energy of the system relative to the mass-centre." (p.45)

This statement is at the root of the author's argument in Section 3.5(ii) Use of $\frac{1}{2}m\bar{V}^2$ alone is only a partial expression of the total kinetic energy of a system unless very specific conditions ('A' in Sec.3.5 (ii))are stated and can be shown to apply.

In this Chapter the emphasis is on the 'external' mechanics of human motion, rather than the internal interactions. That is, the equations relating motion of the whole body to forces external to the body are the concern of this review. A later Chapter attempts a description of the muscular and ligamentous action within the lower limbs.

3.2 The Mass Distribution and Mass-Centre of the Body

Various segmental models of the human body have been proposed, and Chapter 2 goes into some detail on the subject. A segmental model divides the body into convenient segments and assigns dimensions, a mass and a mass-centre location to each. Given such information, the mass-centre, G, of the whole body may be estimated from the model for any body configuration. that is, for any arrangement of the segments consistent with the hinge connections between them.

Thus, in Figure 3.1, two fundamental definitions are illustrated:-

$$\sum_j m_j = M \quad \ldots\ldots (3.2\text{-}1) \qquad \text{MASS}$$

$$\sum_j m_j z_j = M\bar{z} \quad \ldots\ldots (3.2\text{-}2) \qquad \text{MASS-CENTRE}$$

Differentiating the second of these:-

$$\sum_j m_j \dot{z}_j = M\dot{\bar{z}} \quad \ldots\ldots (3.2\text{-}3) \qquad \text{MOMENTUM}$$

$$\sum_j m_j \ddot{z}_j = M\ddot{\bar{z}} \quad \ldots\ldots (3.2\text{-}4) \qquad \text{RATE-OF-CHANGE OF MOMENTUM}$$

Equation (3.2-3) expresses the z-momentum of the whole-body either as the sum of the segment momenta, or as the momentum of the whole-body mass moving at the velocity of the mass-centre, G.

FIGURE 3.1

MASS-CENTRE LOCATION

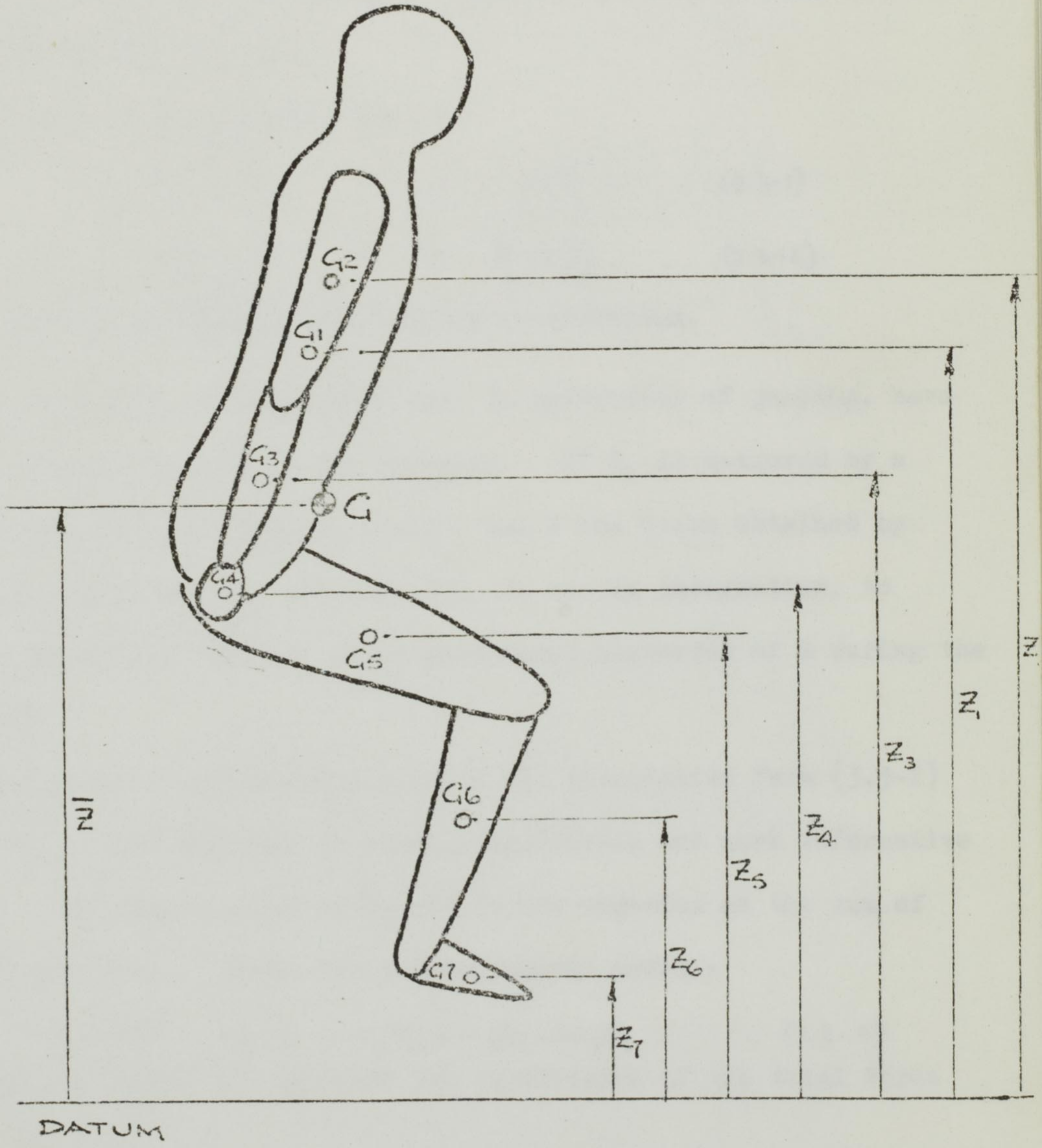

BY DEFINITION:

$$M = m_1 + m_2 + \cdots + m_7 = \sum m_j$$

$$M\bar{Z} = m_1 z_1 + m_2 z_2 + \cdots + m_7 z_7 = \sum m_j z_j$$

Similarly, equation (3.2-4) gives the rate of change of momentum in terms of segmental or whole-body masses and accelerations.

3.3 Newton's Second Law

In the fundamental form:-

$$\left[\begin{array}{c}\text{Sum of external force components} \\ \text{in the z-direction}\end{array}\right] = \left[\begin{array}{c}\text{z-rate-of-change of whole-body} \\ \text{momentum}\end{array}\right]$$

Newton's Second Law may be usefully applied to body movements such as the situation shown in Figure 3.2

In conjunction with equation(3.2-4):-

$$F_z - W = M\ddot{\bar{z}} \quad \ldots\ldots (3.3\text{-}1)$$

$$\text{or } F_z - W = \sum_j m_j \ddot{z}_j \quad \ldots\ldots (3.3\text{-}2)$$

Similar statements apply to the x and y co-ordinates.

A number of studies of human activity, in particular of jumping, have used equation (3.3-1) as a basis for analysis. If F_z is measured by a force platform on which the subject stands, and W and M are obtained by weighing, then (3.3-1) may be used directly, or via an integration, to give the z-acceleration, velocity and displacement histories of G during the take-off period.

No attention seems to have been paid to the alternative form (3.3-2) in such studies. This equation is equally applicable and more informative than (3.3-1). The time history of $(F_z - W)$ is now regarded as the sum of segmental contributions. Thus, for a four-segment model:-

$$F_z - W = m_1\ddot{z}_1 + m_2\ddot{z}_2 + m_3\ddot{z}_3 + m_4\ddot{z}_4 \quad \ldots\ldots (3.3\text{-}5)$$

The graphs in Figure 3.3 indicate the subdivision of the total force curve.

As indicated above, equation (3.3-5) has attracted eminent critics. The main source of doubt seems to be the complex nature of the connections between segments of the human body. It has been argued that, in some way, the time delay in force transmission through such connections makes the equation invalid. This criticism is unfounded. Its proposers may be

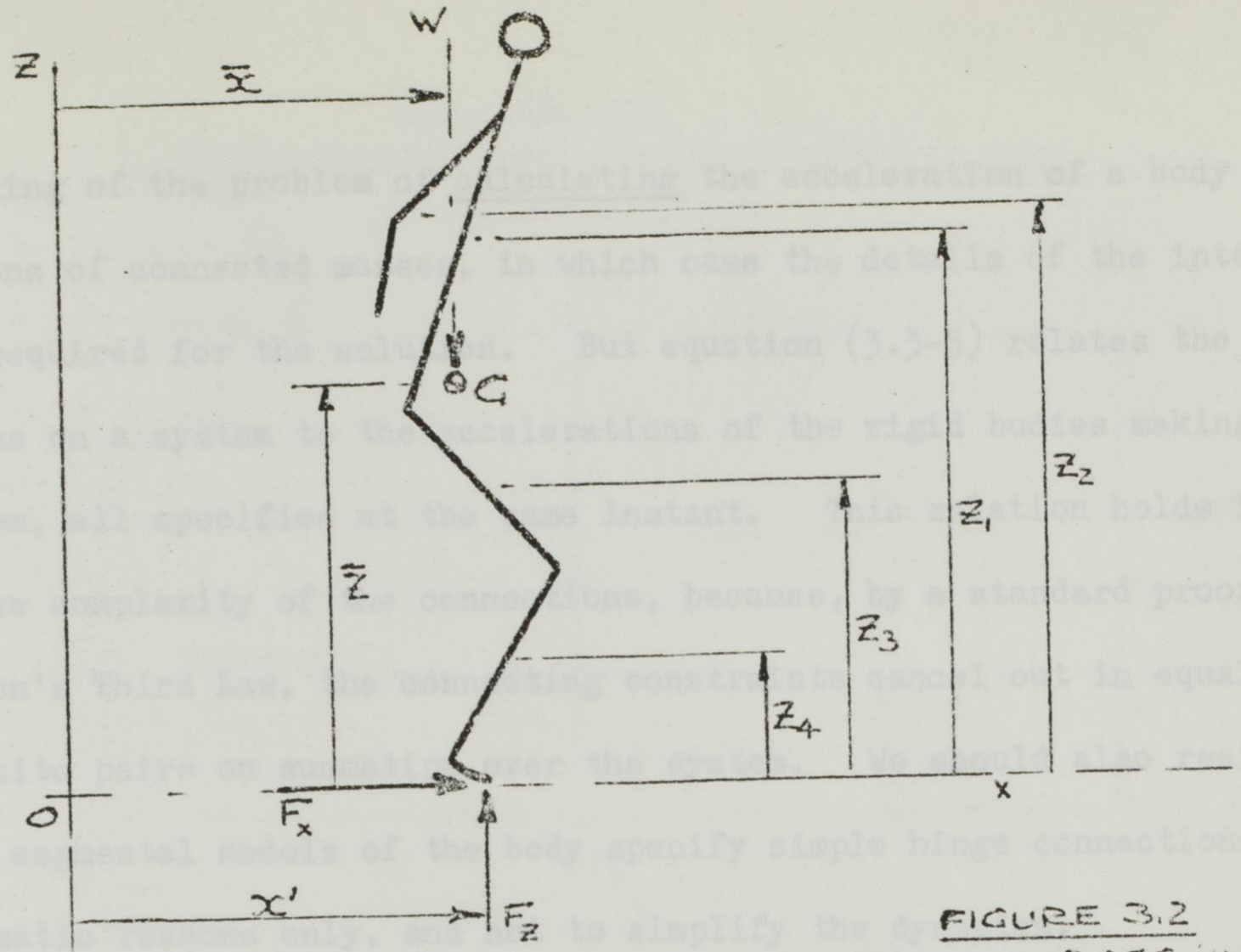

FIGURE 3.2
EXTERNAL FORCES IN A HUMAN ACTION

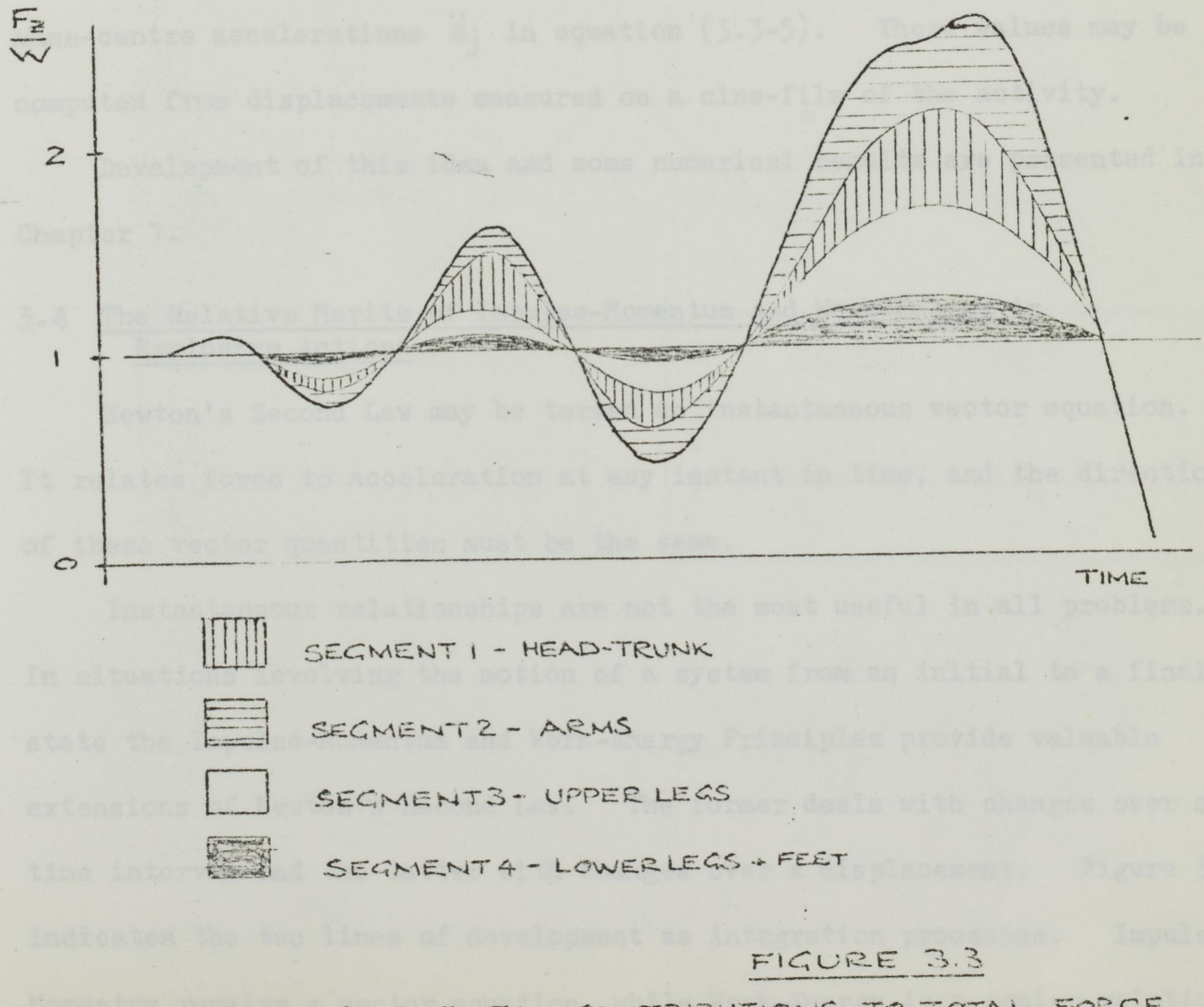

FIGURE 3.3
SEGMENTAL CONTRIBUTIONS TO TOTAL FORCE

thinking of the problem of calculating the acceleration of a body from known motions of connected masses, in which case the details of the inter-connections are required for the solution. But equation (3.3-5) relates the external forces on a system to the accelerations of the rigid bodies making up the system, all specified at the same instant. This relation holds irrespective of the complexity of the connections, because, by a standard proof invoking Newton's Third Law, the connecting constraints cancel out in equal and opposite pairs on summation over the system. We should also reaffirm here that segmental models of the body specify simple hinge connections for kinematic reasons only, and not to simplify the dynamics.

Returning to the use of equation (3.3-5) we find that it leads naturally to consideration of the relative importance of the segmental contributions to the total force curve. One of the unresolved questions about an activity such as jumping is what combination of limb and trunk actions produces a good jump? Some light will be thrown on the problem by using the segment mass-centre accelerations $\ddot{z}_j$ in equation (3.3-5). These values may be computed from displacements measured on a cine-film of the activity.

Development of this idea and some numerical results are presented in Chapter 7.

3.4 The Relative Merits of Impulse-Momentum and Work-Energy in Explosive Actions

Newton's Second Law may be termed an instantaneous vector equation. It relates force to acceleration at any instant in time, and the directions of these vector quantities must be the same.

Instantaneous relationships are not the most useful in all problems. In situations involving the motion of a system from an initial to a final state the Impulse-Momentum and Work-Energy Principles provide valuable extensions of Newton's Second Law. The former deals with changes over a time interval and the latter with changes over a displacement. Figure 3.4 indicates the two lines of development as integration processes. Impulse-Momentum remains a vector equation, while Work-Energy is a scalar relationship.

FIGURE 3.4

DEVELOPMENT OF NEWTON'S SECOND LAW

PARTICLE MOTION

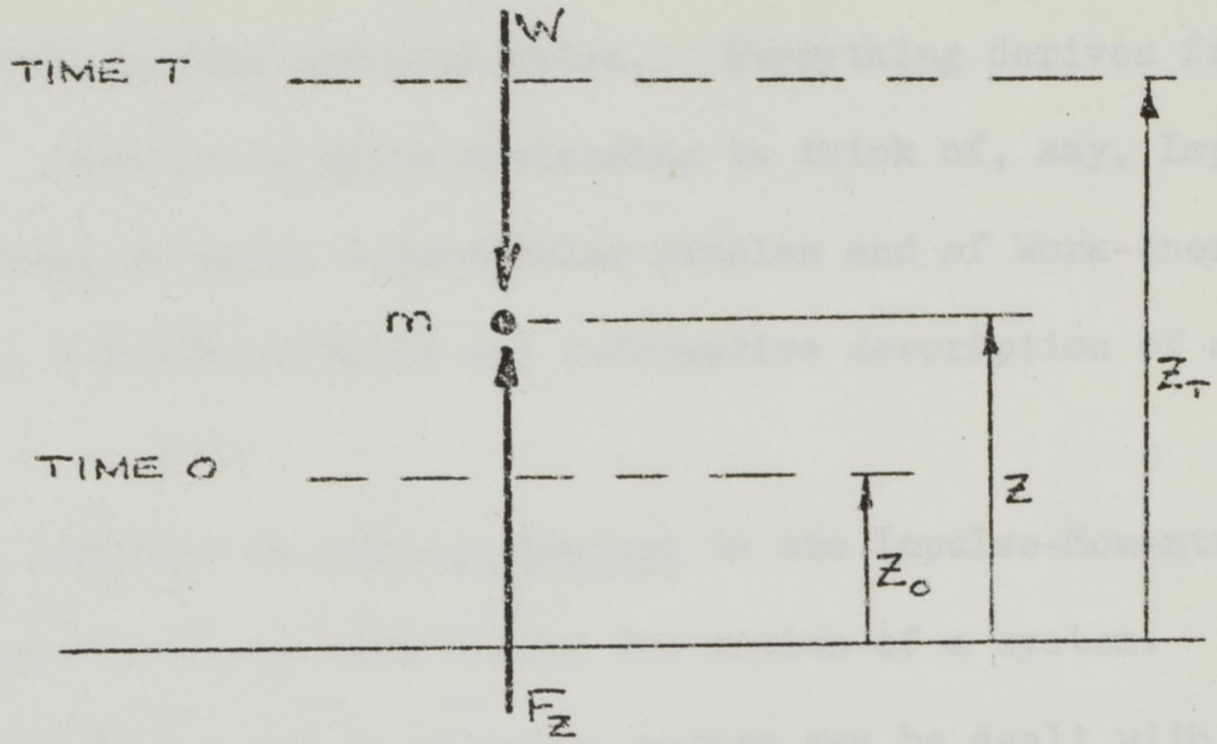

NEWTON II

$$F_z - W = m\frac{dv}{dt} = mv\frac{dv}{dz}$$

INTEGRATION OVER DISPLACEMENT $(Z_T - Z_o)$

INTEGRATION OVER TIME INTERVAL O-T

IMPULSE-MOMENTUM

$$\int_0^T (F_z - W)\,dt = m(V_T - V_o)$$

WORK-ENERGY

$$\int_{Z_o}^{Z_T} F_z\,dz = W(Z_T - Z_o) + \frac{1}{2}m(V_T^2 - V_o^2)$$

Figures 3.5 and 3.6 show the extensions of these two principles to more general forms. The Power equation is part of the Work-Energy development, dealing in energy-rates and work-rates. Everything derives from Newton's Second Law. Thus it is quite misleading to think of, say, Impulse-Momentum as the right way to solve a particular problem and of Work-Energy as incorrect. Each approach provides a valid and informative description of any dynamic situation.

It may, however, be more convenient to use Impulse-Momentum rather than Work-Energy or Power, in considering the motion of a system. In particular, human activity of a rapid 'explosive' nature may be dealt with more easily in terms of the Impulse-Momentum Principle. Since the advent of the force-platform it has become easy to record rapidly varying forces at the feet, and to obtain a force-time curve during an activity. Integration of the curve is a direct appeal to the Impulse-Momentum relation and useful results come from its application. In contrast, measurement of energy changes in short-term human actions is a very difficult problem in instrumentation. Exercise physiologists are at present unable to deal with such transients and are restricted to relatively steady-flow energy measurements.

There is, therefore, a strong case for preferring Impulse-Momentum to Energy or Power in the investigation of an explosive action, such as jumping. This preference rests upon the reliability and availability of instrumentation for the Impulse approach. Adamson and Whitney (1) express a similar preference, but their case is based on theoretical arguments, rather than on problems of instrumentation.

Their comparison between the engine test and the firing of a cannon shot brings out the difference between the steady-flow energy equation and a process involving rapid energy release. But this contrast does not constitute an argument against the use of power, the instantaneous energy-rate or work-rate, in unsteady-state problems. They point out also that the product F x V, for instantaneous power, does not take account of the events preceding that instant and giving rise to the instantaneous velocity V.

There is, however, no need for the prior course of either F or V to be known. Much the same point may be made in the case of Newton's Second Law. The instantaneous force is expressed in terms of instantaneous acceleration, irrespective of the previous acceleration history. Power is, by definition, an instantaneous rate-of-change quantity, and a power equation for the explosive action of the jump may be written:-

Rate at which useful energy is released by muscle action (Power output)	=	Rate of change of kinetic and potential energy of the performer	+	Rate of energy loss to surroundings

There is no theoretical objection to this use of power in the description of explosive action. That is not to say that an average power over the period of the action might not be more appropriate than a statement about the maximum instantaneous value. This is, I think, Adamson and Whitney's real criticism of the paper by Davies and Rennie (3). I would question the latter more on their handling of fundamentals than on the appropriateness of their point of view, and some comments are offered in the next Section.

Practical application of the power equation above requires the estimation of the middle term from cine analysis of the activity, for this is the only practical way in which all the segmental linear and angular velocieities may be obtained. It may also be necessary to assume that the energy loss term is negligible, in the absence of physiological techniques for short-duration energy measurements.

3.5 Some Misconceptions in the Use of the Work-Energy Principle

Some authors have presented work-energy analyses of jumping which appear not to call upon the measurement of physiological energy changes in the activity. I believe their approach, despite an attractive simplicity, to embody some snags of a fundamental nature. The following discussion is concerned with theoretical consistency and no longer with the problems of measurement discussed in the previous Section.

FIGURE 3.5

DEVELOPMENT OF THE ENERGY EQUATION

PARTICLE

$$\int_{Z_o}^{Z_T} F_z\,dz = W[z_T - z_o] + \frac{1}{2} m [V_T^2 - V_o^2]$$

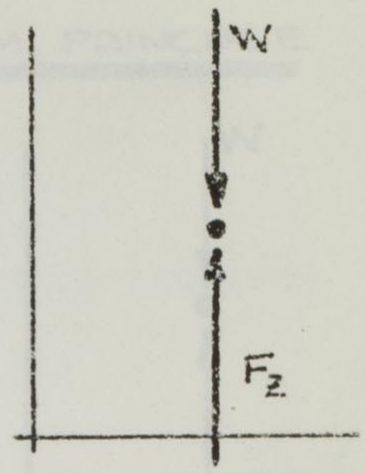

SINGLE RIGID BODY

$$\int_{Z_o}^{\bar{Z}_T} F_z\,dz + \int_{X_o}^{X_T} F_x\,dx = W[\bar{Z}_T - \bar{Z}_o] + \frac{1}{2} m[\bar{U}_T^2 - \bar{U}_o^2] + \frac{1}{2} m[\bar{V}_T^2 - \bar{V}_o^2] + \frac{1}{2} I_c[\omega_T^2 - \omega_o^2]$$

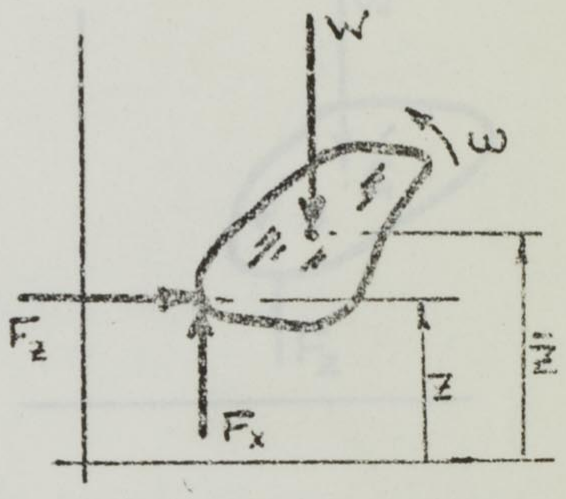

SYSTEM OF SEVERAL RIGID BODIES
SEVERAL EXTERNAL FORCES

FORCE INTEGRALS (FOR WORK-DOING FORCES ONLY)

CHANGES OF SYSTEM POTENTIAL AND KINETIC ENERGY

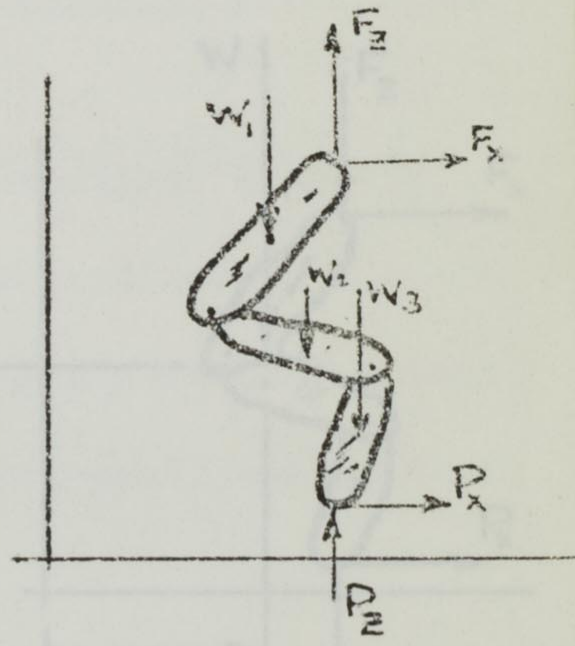

GENERAL ENERGY EQUATION

ANY SYSTEM. ALL FORMS OF ENERGY

$$\text{NET}\left(\begin{matrix}\text{WORK} \\ \text{INTO SYSTEM}\end{matrix} + \text{ENERGY}\right) = \Delta\left(\begin{matrix}\text{SYSTEM} \\ \text{POTENTIAL} \\ \text{ENERGY}\end{matrix}\right) + \Delta\left(\begin{matrix}\text{SYSTEM} \\ \text{KINETIC} \\ \text{ENERGY}\end{matrix}\right) + \Delta\left(\begin{matrix}\text{OTHER} \\ \text{SYSTEM} \\ \text{ENERGIES}\end{matrix}\right)$$

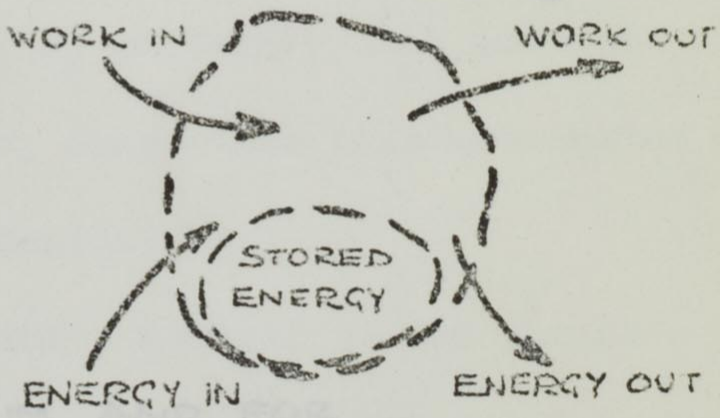

POWER EQUATION

$$\left(\begin{matrix}\text{NET} \\ \text{WORK-RATE} \\ \text{PLUS} \\ \text{ENERGY-RATE} \\ \text{INTO} \\ \text{SYSTEM}\end{matrix}\right) = \frac{d}{dt}\left(\text{SYSTEM P.E.}\right) + \frac{d}{dt}\left(\text{SYSTEM K.E.}\right) + \frac{d}{dt}\left(\begin{matrix}\text{OTHER} \\ \text{SYSTEM}\end{matrix}\right)$$

FIGURE 3.6

DEVELOPMENT OF THE IMPULSE-MOMENTUM PRINCIPLE

PARTICLE

$$\int_0^T (F_z - W)\,dt = m(V_T - V_o)$$

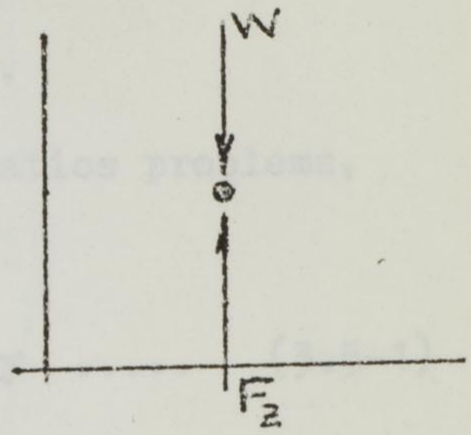

SINGLE RIGID BODY

$$\int_0^T (F_z - W)\,dt = m(\bar{V}_T - \bar{V}_o)$$

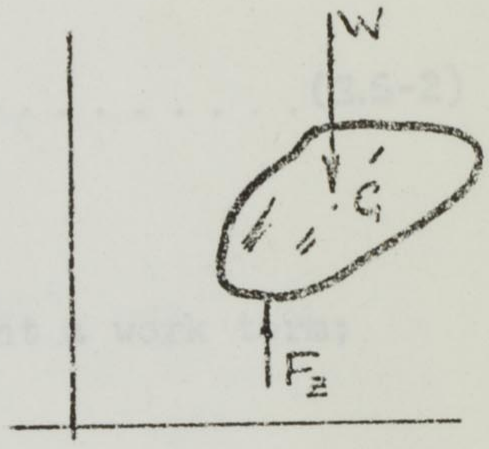

SYSTEM OF SEVERAL RIGID BODIES
SEVERAL EXTERNAL FORCES

$$\int_0^T (P_z - F_z - W)\,dt = M(\bar{V}_T - \bar{V}_o) \uparrow$$

$$\int_0^T (P_x + F_x)\,dt = M(\bar{U}_T - \bar{U}_o) \rightarrow$$

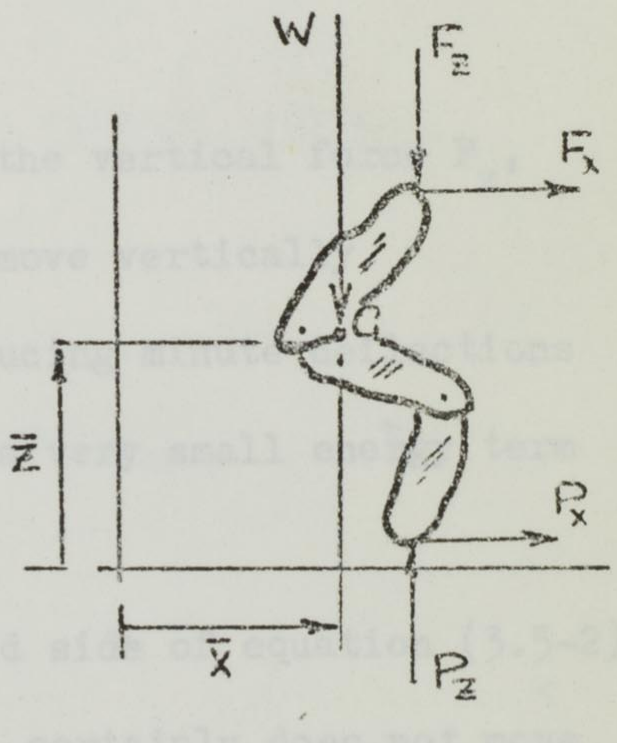

EQUATIONS FOR MOMENT OF MOMENTUM AND FOR MORE GENERAL NON-RIGID SYSTEMS ARE OMITTED FOR SIMPLICITY.

The essence of the problem is shown in Figure 3.7

At time 0 a man is crouched, stationary and prepared to jump.

At time T he is just losing contact with the ground.

Recalling solutions to many standard applied mathematics problems, one may be led to use:-

Work Done = increase in kinetic and potential energy ..... (3.5-1)

and the text quoted below interpret this statement as:-

$$\int_{\bar{z}_0}^{\bar{z}_T} F_z \cdot d\bar{z} = \tfrac{1}{2} M \bar{V}_T^2 + W(\bar{z}_T - \bar{z}_0) \quad \ldots\ldots\ldots\ldots (3.5\text{-}2)$$

(i) The Work Term

The left-hand side of (3.5-2) purports to represent a work term; but the work done by a force is properly defined as:-

"the force multiplied by the distance moved by its point of application in the direction of the force"

It is obvious that the point of application of the vertical force F_z, (the toes, in contact with a rigid floor), does not move vertically.

There is no need to confuse the issue by introducing minute deflections of a nearly-rigid floor, which would represent only a very small energy term in equation (3.5-2)

On the accepted definition of work the left-hand side of equation (3.5-2) is not a work term. The point of application of F_z certainly does not move through the distance $(z_T - z_0)$. I have, however, found this point advocated and defended in published work and personal discussion.

As to the published material, Hopper (7) commits himself to the phrase:- "work done by the ground reaction" in analysing a high jump, and indicates the area under a ground-force vs. distance curve. Davies and Rennie (3) make statements about the power produced in jumping, which use the form $F_z \times \bar{V}$ (force X velocity of body mass-centre). So they too multiply the ground force F by the motion of a dissociated point. Finally, Offenbacher (12) derives an 'energy equation' for the vertical jump, arriving at the result:-

$Mg.H = \int_{\bar{z}_0}^{\bar{z}_T} (F_z - Mg) d\bar{z}$, where H is the elevation of the mass-centre.

FIGURE 3.7

POWER OUTPUT IN JUMPING

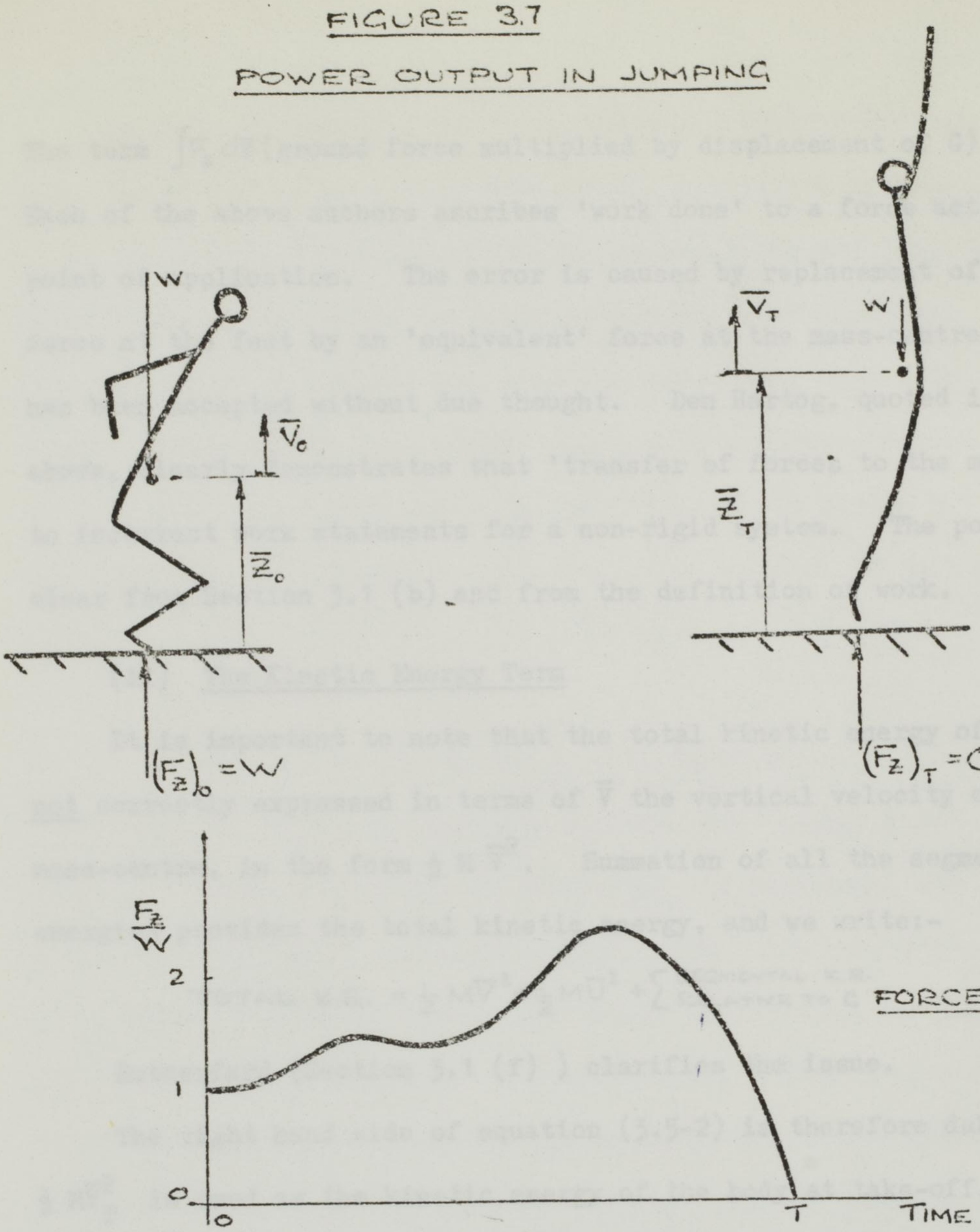

The term $\int F_z d\bar{z}$ (ground force multiplied by displacement of G) again appears. Each of the above authors ascribes 'work done' to a force acting at a fixed point of application. The error is caused by replacement of the ground force at the feet by an 'equivalent' force at the mass-centre. 'Equivalence' has been accepted without due thought. Den Hartog, quoted in Section 3.1(d) above, clearly demonstrates that 'transfer of forces to the mass-centre' leads to incorrect work statements for a non-rigid system. The point is also clear from Section 3.1 (b) and from the definition of work.

(ii) The Kinetic Energy Term

It is important to note that the total kinetic energy of the body is not correctly expressed in terms of $\bar{V}$ the vertical velocity of the whole-body mass-centre, in the form $\frac{1}{2} M \bar{V}^2$. Summation of all the segmental kinetic energies provides the total kinetic energy, and we write:-

$$\text{TOTAL K.E.} = \tfrac{1}{2} M\bar{V}^2 + \tfrac{1}{2} M\bar{U}^2 + \sum \text{SEGMENTAL K.E. RELATIVE TO G}$$

Rutherford (Section 3.1 (f)) clarifies the issue.

The right hand side of equation (3.5-2) is therefore dubious, in that $\frac{1}{2} M\bar{V}_T^2$ is used as the kinetic energy of the body at take-off. This expression is correct only if the following assumptions hold:-

1. The jumper's body is rigid, that is, limbs and trunk remain locked in a fixed configuration through the take-off.
2. There is no horizontal velocity of the body mass-centre.
3. There is no angular motion of the trunk or limbs.

} A

The quoted texts make no mention of these assumptions, although statements are implicitly based on them. It is possible that the simplifications so introduced do not seriously impair the analysis, but some justification of the assumptions should be given. Failure to mention the above conditions 'A' in basic jumping studies is unfortunate. The approximate expression of kinetic energy in equation (3.5-2) may be carried unquestioningly into the analysis of more complicated activities, with misleading consequences.

The main contention here is that the Work-Energy approach may be properly stated without introducing such restrictive assumptions. There is no need to rule out complex bodily movements in the jump, nor to exclude general translational and rotational velocities of the body. There is also no reason to confuse the issue by associating work with non-working forces. The proper form of the Work-Energy equation (Figure 3.5) leads to the following equation for the problem shown in Figure 3.7 (The derivative of this equation gives the power relation of Section 3.4):-

$$\left[\begin{array}{l}\text{WORK DONE BY}\\ \text{EXTERNAL FORCES}\\ \text{(GROUND FORCE)}\end{array}\right] = \left[\begin{array}{l}\text{INCREASE}\\ \text{IN P.E.}\end{array}\right] + \left[\begin{array}{l}\text{INCREASE IN K.E.}\\ \text{(SUM OVER SEGMENTS)}\end{array}\right] + \left[\begin{array}{l}\text{USEFUL ENERGY}\\ \text{RELEASED IN}\\ \text{MUSCLE ACTION}\end{array}\right]$$

$$0 = W(\bar{Z}_T - \bar{Z}_0) + \Delta\left(\sum_{SEGS}\left(\tfrac{1}{2}mU^2 + \tfrac{1}{2}mV^2 + \tfrac{1}{2}I_G\omega^2\right)\right) + \left[\begin{array}{l}\text{USEFUL ENERGY}\\ \text{RELEASED IN}\\ \text{MUSCLE ACTION}\end{array}\right]$$

As discussed in the previous Section, the 'energy loss' term is omitted. We have no means of estimating its magnitude, and assume it to be fairly small in an explosive action. The same assumption is made implicity by both Offenbacher, and Davies and Rennie, but they make no mention of the omission and its significance. Practical use of the above equation requires the estimation of potential and kinetic energy changes from cine-film to give an assessment of the muscular energy release in the action.

(iii) The Derivation of an Equation Involving a Ground-Force - Displacement Integral

Earlier in this Section we have seen the inconsistency in using in an energy equation. It is, however, a fact that the equation (3.5-2) can give sensible numerical results in a very simple representation of body motion, and it is important to recognise that what looks like an energy equation is, in fact, something fundamentally different, with a physical significance which should be clearly understood.

Referring to Figure 3.2 and equation (3.3-1), an application of Newton's Second Law, we may quite properly regard the right hand side as:-

$$M\ddot{\bar{z}} = M\dot{\bar{z}}\frac{d\dot{\bar{z}}}{dz}$$

Separation and integration produces:-

$$\int_{\bar{z}_o}^{\bar{z}_T} F_{\bar{z}}\, d\bar{z} = \int_{z_o}^{\bar{z}_T} W\, d\bar{z} + \int_{\bar{v}_o}^{\bar{v}_T} M\dot{\bar{z}}\, d\dot{\bar{z}} \quad \ldots\ldots\ldots (3.5\text{-}5)$$

And this result appears to be identical with the so-called energy-equation (3.5-2). There are, however, important distinctions to be made.

a) Equation (3.5-5) is not, and makes no claim to be, a work-energy equation for the body. It is the integral of the z-component equation of motion and, by the very selection of a specific component direction, other forces and motions are eliminated. A true work-energy equation is a scalar relationship in which prior selection of a particular set of component forces and velocities plays no part. The source of equation (3.5-2) is now clear and its incorrectness as an 'energy' equation is apparent.

b) The first term in (3.3-5) must not be regarded as a work term, despite the fact that it has a similar form. The definition of work does not allow that physical significance be associated with the left hand side of (3.5-5).

Similarly, the last term in (3.5-5) is not an expression of the body's kinetic energy, for Section 3.5 (ii) has shown that the total kinetic energy involves other terms representing horizontal velocity of the mass-centre and all segmental motions relative to the mass-centre.

The aim of this discussion is not to create unnecessary complexity. There are subtelties in the application of quite elementary principles which have not only been ignored by recognised authors, but also accepted unquestioningly by the uncritical reader. We must first get a clear understanding of the principles we propose to employ; secondly, derive meaningful relationships for the particular problem to be studied; and thirdly, make quite clear all assumptions and simplifications brought into the analysis.

3.6 Equations for Plane Rotational Motion of a Segmental Model

a) Theoretical development

In Section 3.3 Newton's Second Law is applied to translational motion of a segmental model, and equation(3.3-5) enables the contribution of each segment to be represented. For plane motion, equation (3.3-5), with the corresponding x-component equation, completely describes the translation of the system. A third equation, for plane rotational motion of the system, is also available, and a concise statement is:-

$$\left[\begin{array}{l}\text{Sum of external force-moments}\\ \text{about system mass-centre G}\end{array}\right] = \left[\begin{array}{l}\text{Rate-of-change of moment}\\ \text{of momentum of system}\\ \text{about system mass-centre G}\end{array}\right]$$

or $$\Sigma Q_G = \dot{h}_G \qquad \ldots\ldots(3.6\text{-}1)$$

The left-hand side of this equation is not difficult to evaluate. In Figure 3.2, for example:-

$$\Sigma Q_G = F_x.\bar{z} + F_z(x'-\bar{x}) \qquad \ldots\ldots(3.6\text{-}2)$$

The right-hand side is a little less straightforward, especially if its physical significance is to be brought out. A three-dimensional equation has been employed by McCrank and Seger (9) in a complicated analysis of spatial rotations in astronautics. Miller (10) has used a much more clearly expressed three-dimensional form in her studies of springboard diving. Both versions, of course, encompass plane, or two-dimensional motion as a special case, but it is not easy to use them to gain insight into the plane motion problem. Other workers, such as Kane and Scher (8) and Hatze (6), advocate a Lagrangian approach, powerful and elegant, but liable to obscure the very real ties between segmental-model and single-rigid-body equations of motion.

There is much to be said for casting the right hand side of equation (3.6-1) into a form involving whole-body moment of inertia about G, bearing in mind that this quantity is likely to be a variable in most human motions. In so doing, we keep ties with the mechanics of a single

rigid body, for which equation (3.6-1) takes the simple form:-

$$\Sigma Q_q = I_q . \alpha \qquad \ldots\ldots (3.6\text{-}3)$$

Whitsett (18) derives rotational equation of motion for a two-segment model, but is concerned only with moment of momentum and not its rate-of-change. He also leaves the physical significance of the terms unexplained. Groesberg (5) provides an equation for a general system of particles in three dimensions. Both of these treatments have provided stimulus to the work set out below. However, the derivation which follows does not appear elsewhere, as far as I know. The lack of a proper treatment of rotational motion has hampered studies of body rotation in diving and gymnastics.

Figure 3.8(a) shows two sets of reference axes for the moving segmental model. Axes zGx have their origin at, and move with, the system mass-centre G; they also rotate with the angular velocity of the major segment, the Head-Trunk (H-T). Axes $\eta G \xi$ are an inertial set whose origin coincides with G at the instant shown.

Figure 3.8(b) gives the basis for the co-ordinate relationships derived below. Gj represents a typical segment mass-centre; for illustration take that of the arms.

From Figure 3.8(b):-

$$\eta_j = z_j \cos\theta + x_j \sin\theta \quad ; \quad \xi_j = x_j \cos\theta - z_j \sin\theta$$

Differentiating:-

$$\dot{\eta}_j = \dot{z}_j \cos\theta - z_j \sin\theta . \dot{\theta} + \dot{x}_j \sin\theta + x_j \cos\theta . \dot{\theta} \quad ; \quad \dot{\xi}_j = \dot{x}_j \cos\theta - x_j \sin\theta . \dot{\theta} - \dot{z}_j \sin\theta - z_j \cos\theta . \dot{\theta}$$

Now take the special situation $\theta = 0$ to simplify. Further, write $\dot{\theta} = \Omega$, the angular velocity of the H-T segment.

Thus:-

$$\eta_j = z_j \quad ; \quad \xi_j = x_j$$

$$\dot{\eta}_j = \dot{z}_j + x_j \Omega$$

$$\dot{\xi}_j = \dot{x}_j - z_j \Omega$$

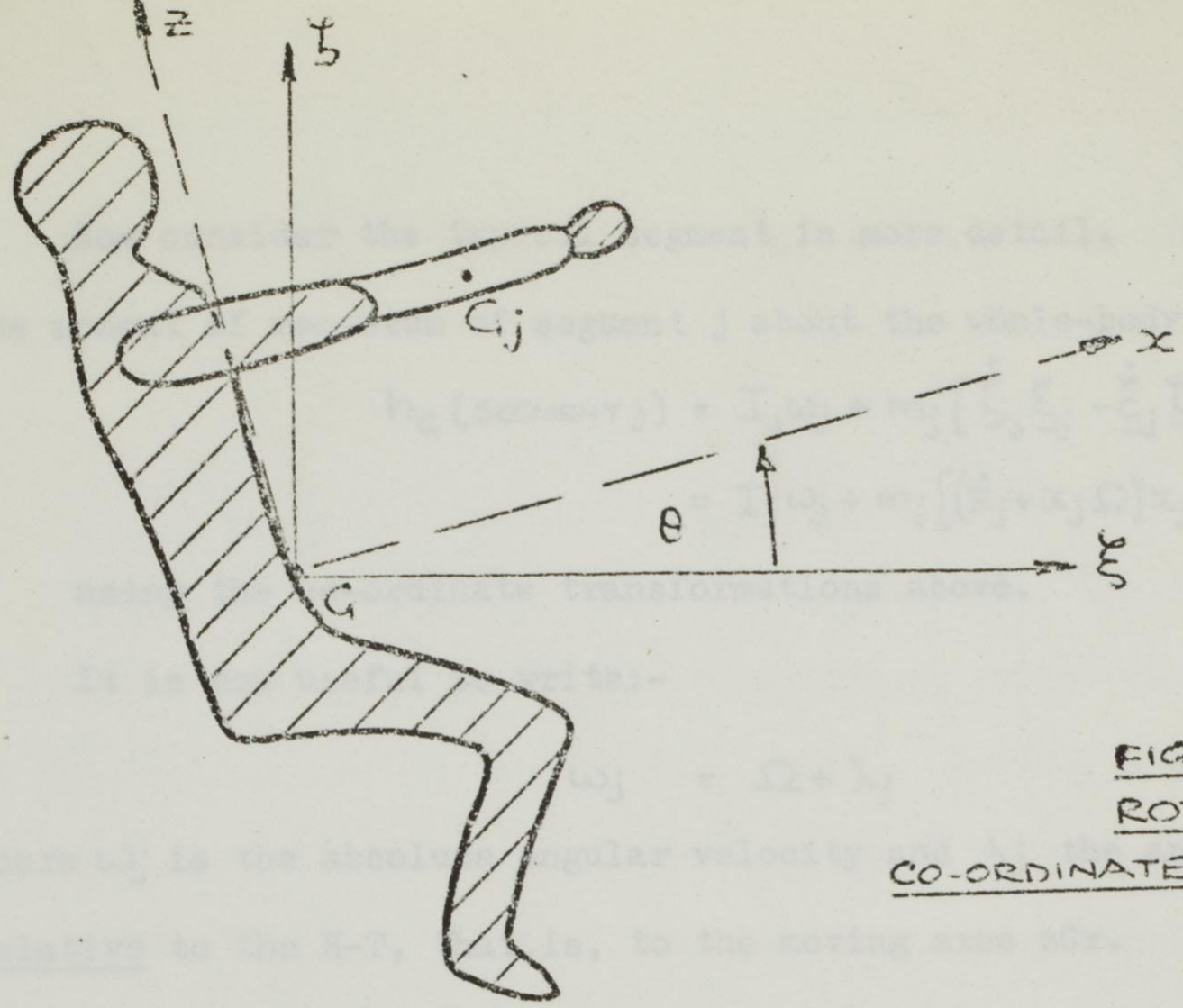

FIGURE 3.8
ROTATIONAL MOTION
CO-ORDINATES OF TYPICAL SEGMENT

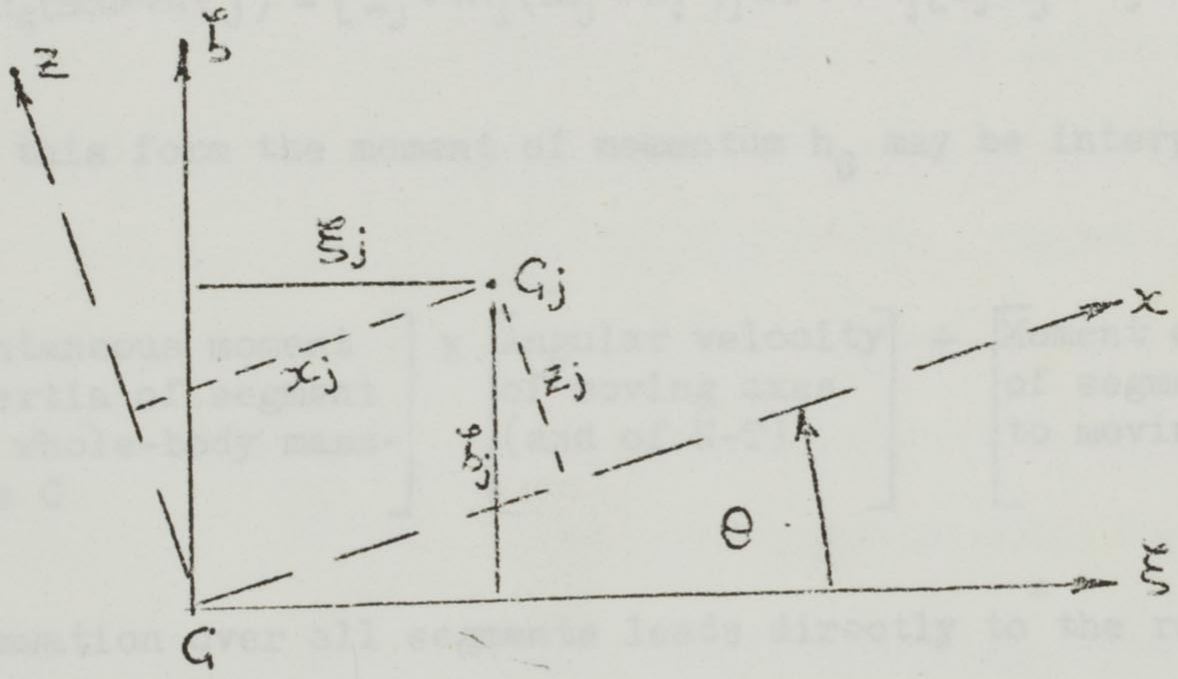

FIGURE 3.9
MOMENT OF MOMENTUM OF TYPICAL SEGMENT

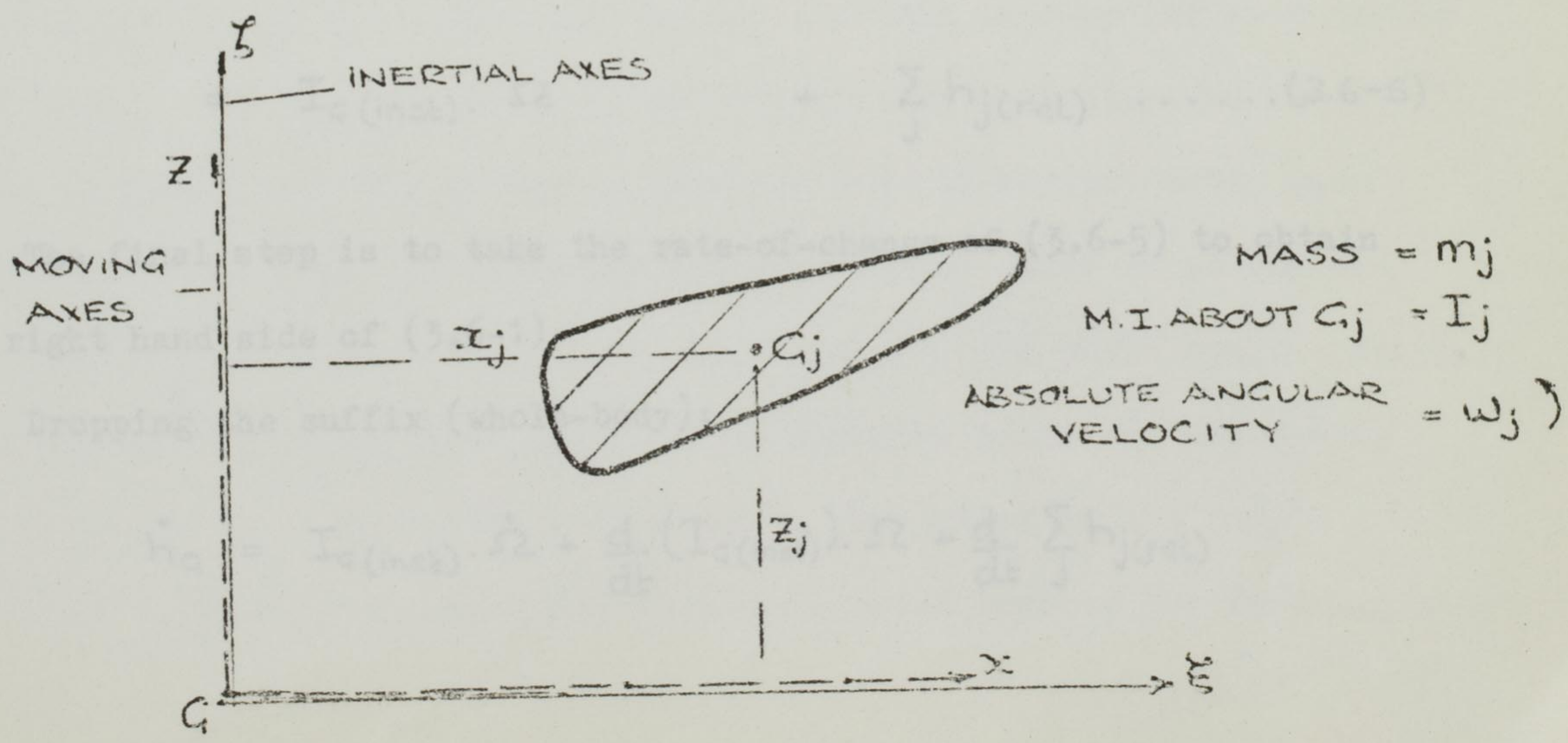

Now consider the typical segment in more detail. From Figure 3.9 the moment of momentum of segment j about the whole-body mass-centre G is:-

$$h_G(\text{SEGMENT } j) = I_j\omega_j + m_j\left[\dot{\zeta}_j\xi_j - \dot{\xi}_j\zeta_j\right]$$

$$= I_j\omega_j + m_j\left[(\dot{\xi}_j + x_j\Omega)x_j - (\dot{x}_j - z_j\Omega)z_j\right]$$

using the co-ordinate transformations above.

It is now useful to write:-

$$\omega_j = \Omega + \lambda_j$$

where ω_j is the absolute angular velocity and λ_j the angular velocity relative to the H-T, that is, to the moving axes zGx.

With a little rearrangement:-

$$h_G(\text{SEGMENT } j) = \left[I_j + m_j(x_j^2 + z_j^2)\right]\Omega + m_j\left[\dot{z}_j x_j - \dot{x}_j z_j\right] + I_j\lambda_j \quad \ldots\ldots (3.6\text{-}4)$$

In this form the moment of momentum h_G may be interpreted as:

[Instantaneous moment of inertia of segment about whole-body mass-centre G] × [Angular velocity of moving axes (and of H-T)] + [Moment of momentum of segment relative to moving axes]

Summation over all segments leads directly to the result:-

$$\underset{(\text{whole-body})}{h_G} = \left[\begin{array}{l}\text{Instantaneous moment of inertia of whole body about G}\end{array}\right] \times \left[\begin{array}{l}\text{Angular velocity of H-T}\end{array}\right] + \sum_j \left[\begin{array}{l}\text{Moments of momentum of all segments relative to moving axes}\end{array}\right]$$

$$= I_{G(\text{inst})}\cdot\Omega + \sum_j h_{j(\text{rel})} \quad \ldots\ldots (3.6\text{-}5)$$

The final step is to take the rate-of-change of (3.6-5) to obtain the right hand side of (3.6-1)

Dropping the suffix (whole-body):

$$\dot{h}_G = I_{G(\text{inst})}\cdot\dot{\Omega} + \frac{d}{dt}\left(I_{G(\text{inst})}\right)\cdot\Omega + \frac{d}{dt}\sum_j h_{j(\text{rel})}$$

So that equation(3.6-1), the rotational equation of motion for general plane motion of the segmental model is fully expressed as:-

$$\Sigma Q_G = \dot{h}_G = I_{G(inst)} \cdot \dot{\Omega} + \frac{d}{dt}\left(I_{G(inst)}\right) \cdot \Omega + \sum_j \dot{h}_{j(rel)} \quad \ldots\ldots (3.6\text{-}6)$$

It is instructive to compare this result with the rigid-body equation (3.6-3). Clearly, a rotational situation in which the body configuration is variable must be dealt with by (3.6-6). If, for a period, the body configuration is kept fixed by the performer, then the simpler equation (3.6-3) will apply. Further, in numerical evaluation for a real situation, some simplification may be possible if certain terms in (3.6-6) turn out to be negligible. However, the real purpose of the derivation of (3.6-6) is to throw light on the nature of the rotational motion. It will help to explain two-dimensional turns and somersaults of divers and trampolinists while in the air, in a way that the rigid-body treatment can never do. The concept of'rate-of-change of moment of inertia' is not generally used in mechanics, although I cannot claim originality in this respect, for the idea is employed by Groesberg and may appear in other specialised texts.

There is a widespread misconception that a specific 'axis of rotation' may be defined for aerial motion. The general segmental motion discussed above can not be considered to possess such an axis. Whether the performer is in the air or in contact with the ground, it is meaningless to speak of 'the axis of rotation' unless the body is behaving as a single rigid body. For a rigid body we may construct an instantaneous centre by the usual geometrical technique, but for a multi-segment model each segment possesses its own instantaneous centre, and there is no way of combining them into a single rotational centre for the whole body. The fact that we take moments of force and of momentum about the whole-body mass-centre G, does not imply that G can be thought of as the body's rotational centre. We use G as a reference point because the fundamental

equation (3.6-1) comes out in its simplest form.

b) Physical significance of the equations

In a general description of the motion of the body through the air, the discussion is often confined to a plane-motion situation. Such non-twisting dives and somersaults are accomplished when opposite limbs move together, and the body configuration remains at all times symmetrical about the sagittal plane. The conservation of moment of momentum (angular momentum) usually forms the basis of discussion, and the constant value of the product $I_q \times \omega$ is correctly explained by an increase in spin velocity ω when the body attitude shifts to one of smaller moment of inertia. This form of explanation may be termed a 'quasi-rigid-body' view of the motion. It is implied that the configuration of the body is held rigid for at least a short time so the rigid-body equation applies. Nothing can really be said on such an elementary basis about the flowing of the configuration through a sequence of forms, a situation in which a continuous rate-of-change of the moment of inertia takes place. Further, the quasi-rigid view is powerless to explain the angular displacement effects of limb motions on a body possessing no moment of momentum.

Equations (3.6-5) and (3.6-6) are useful for the explanation of the aerial manoeuvres of a non-rigid human body in plane motion.

The equation:-

$$0 = I_{q(inst)} \cdot \Omega + \sum_j h_{j(rel)} \quad \ldots\ldots (3.6\text{-}5)$$

applies to a freely-falling body with zero moment of momentum. If the arms rotate about the shoulder, the term Σh_j immediately has a value and, to satisfy the equation, the term $I_q \cdot \Omega$ must take the same value but with the opposite sign. Thus, a positive rotation of the arms results in a negative rotation of the trunk, although at no time during or after the action does the whole-body system possess other than zero moment of momentum. The general form of (3.6-5) may, of course, be applied to

motions in which the moment of momentum is a constant other than zero.

The more elaborate equation (3.6-5) may be used to clarify the torque-free aerial motion during the execution of a body configuration change. In the statement

$$0 = I_{c(inst)} \cdot \dot{\Omega} + \frac{d}{dt}\left(I_{c(inst)}\right) \cdot \Omega + \sum \dot{h}_{j\,(rel)} \qquad \ldots\ldots (3.6\text{-}6)$$

the signs of $\sum \dot{h}_j$ and $\frac{d}{dt}(I_c)$ may be assessed for some maneouvres without recourse to numerical evaluation. It becomes clear that the term $\sum \dot{h}_j$ expressing rate-of-change of relative moment of momentum, will become large if a vigorous arm or leg flexion is made in flight. Coupled with sketches of the body form, which show whether $\frac{d}{dt}(I_c)$ is positive or negative, one may come to some conclusion about the trunk angular acceleration, expressed by the first term on the right. Numerical evaluation of terms will give much more information, but has not yet been attempted.

Verbal descriptions of aerial movement sometimes appeal to the concept of 'transfer of angular momentum', particularly in considering three-dimensional problems like the twisting of a cat to land on its feet. It is suggested that 'transfer of angular momentum' should not be too freely used before a proper understanding of the two-dimensional case has been achieved. The simpler equation, (3.6-5) gives a precise meaning to the idea of transfer of moment of momentum, in that balance of the equation is maintained by a gain in the first term and a matching loss in the second, or vice-versa. The left hand side remains constant (generally non-zero). It may further be emphasised that the vector nature of the equation implies constancy in both the magnitude of total moment of momentum and the direction of the axis about which moments are taken.

The above equations also throw light on the manoeuvres of astronauts under zero-gravity and the behaviour of a performer on a frictionless turntable, which is sometimes used in laboratory demonstrations of rotation.

3.7 Plagenhoef's Approach to Motion Analysis

a) Introduction

Plagenhoef's recent book (15), is an important contribution to biomechanical literature. He presents a novel formulation of the equations of motion for a segmental model, a computer programme based on these equations and cine analyses of a wide range of sports activities. The emphasis is on a method of cine analysis which requires only the angular displacements of the segments as input variables. Using standard segmental masses and lengths, the computations lead to values of total force and force-moment at every joint of the model, and these numerical results are combined with spatial motion patterns drawn directly from the film.

Plagenhoef and his colleagues produce many illuminating examples of biomechanical analysis and relate the work to practical coaching and performance. There is no comparable published work in the field and it is therefore likely that the book will be widely adopted as a student text and as a source of ideas in biomechanics projects.

Some comments on this work are given because there are aspects which can be tackled in ways other than those proposed by Plagenhoef. Comparisons may lead to more discerning use of his techniques.

b) Plagenhoef's Use of Coriolis Force

In developing general equations of motion Plagenhoef begins his Chapter 5 with a two-segment motion. As an example, consider motion of the upper arm and forearm with the shoulder as a fixed joint. Although they are hinged at the elbow, the two segments have, in general, independent angular motions. It may be convenient to consider the angular motion of the forearm relative to the upper arm, rather than to measure it against a fixed frame of reference, and Plagenhoef here states:-

"Coriolis was the first to recognise a force that exists when a segment is rotating about an axis that itself is rotating" (p.49)

His subsequent developments give segmental inertia forces in terms of

Coriolis accelerations, and there is no question as to the soundness of the theoretical or numerical results. But it is important to note that introduction of a Coriolis force into the segmental mechanism analysis is not essential. Figure 3.10 compares the Plagenhoef derivation with an approach which is common in mechanism analysis.

Plagenhoef has a particular interest in using relative angular velocities between adjacent segments in his later interpretations. In restricting himself to the Coriolis formulation, he gives the impression that it is essential to the mechanics of relative segmental motion. The non-Coriolis approach may, however, be expressed quite conveniently in terms of relative angular motions.

The main contention here is that the Coriolis concept is quite difficult for the student to grasp. Plagenhoef uses it in a rather unusual way for an analysis which does not, in fact, require it.

c) Plagenhoef's Requirement for a Fixed Starting Point

The example of Figure 3.10 has the shoulder joint fixed. Angular displacements θ_1, θ_2 of the arm segments are the only time-dependent variables required for complete determination of accelerations through the mechanism. In some practical situations a fixed point exists; frequently, for instance, the feet are in contact with a rigid floor. Plagenhoef starts his analysis from this fixed point and works progressively toward the other end of the system. Nevertheless, he recognises that there are many cases in which the fixed point is not easily determined:- "A mid-air joint-moment analysis can be done only by determining the joint which is moving the least and analysing the other body motions relative to this most stable joint (usually the hip ... If all the body parts are moving a great deal, only the axis of rotation, the path of the total body centre of gravity, the path of the joint centres or the body segment positions relative to the floor may be determined." (p.120).

FIGURE 3.10

COMPARISON OF DYNAMIC EQUATIONS IN CORIOLIS AND NON-CORIOLIS FORMULATIONS. 2-SEGMENT MODEL

PLAGENHOEF (CORIOLIS)

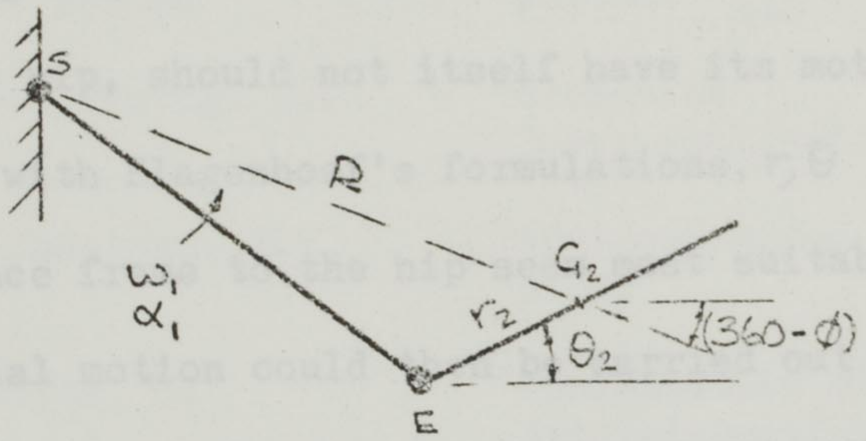

NON-CORIOLIS

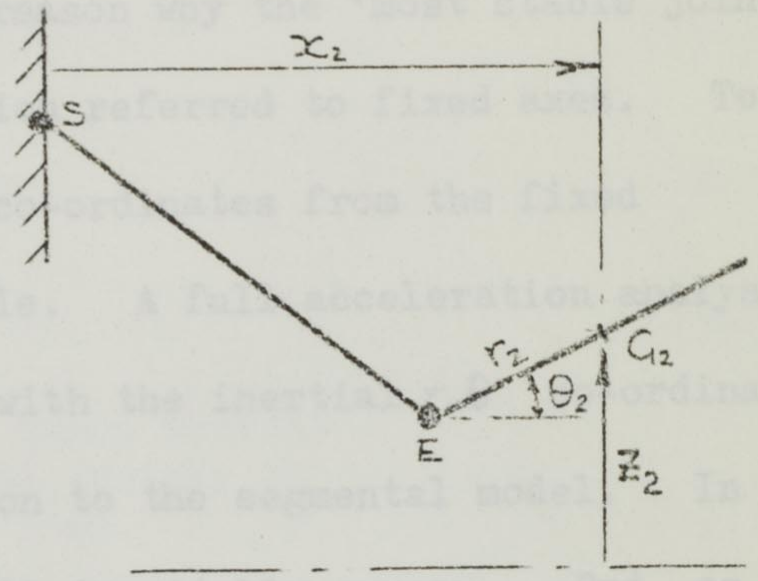

TOTAL MOMENT AT E

$$M_E = -W_2 r_2 \cos(360-\theta_2) - m_2 R \omega_1^2 \sin(\theta_2-\phi).r_2 - m_2 R \alpha_1 \cos(\theta_2-\phi).r_2 - m_2 k_2^2 \alpha_2$$

$$M_E = -W_2 r_2 \cos\theta_2 + m_2 \ddot{x}_2 \sin\theta_2 . r_2 - m_2 \ddot{z}_2 \cos\theta_2 . r_2 - m_2 k_2^2 \alpha_2$$

W_2 – WEIGHT OF SEGMENT 2

m_2 – MASS " " "

k_2 – RADIUS OF GYRATION OF SEGMENT 2

Plagenhoef is faced with the need for a fixed starting point by virtue of his formulation in terms only of the segmental angles. However, to work from 'the joint which is moving the least' is dubious, because what he really seeks is a point having zero acceleration. Small displacement ("moving the least") does not necessarily mean near-zero acceleration. The insistence on a fixed starting point brings problems when aerial motion or swimming are to be analysed. There is no reason why the 'most stable joint' say the hip, should not itself have its motion referred to fixed axes. To accord with Plagenhoef's formulations, r,θ co-ordinates from the fixed reference frame to the hip seem most suitable. A full acceleration analysis of aerial motion could then be carried out with the inertial r,θ co-ordinates of the hip behaving very much as an extension to the segmental model. In this r,θ formulation a Coriolis reference will inevitably appear. But, as shown in the previous section, it is not necessary to use a Coriolis form in the analysis of the body segments themselves. Plagenhoef's programme would require a short additional subroutine to accommodate the acceleration of the hip-joint, but there is no need to regard mid-air joint-moment analysis as an intractable problem, even when "all the body parts are moving a great deal".

3.8 References for Chapter 3

(1) Adamson, G.T.
Whitney, R.J.
"Critical Appraisal of Jumping as a Measure of Human Power"
Medicine and Sport. Vol. 6
Biomechanics II, 208-211
Karger. Basle. (1971)

(2) Alexander, R.M.
Professor of Zoology, University of Leeds - Personal communication (1970)

(3) Davies, C.T.M.
R. Rennie
"Human Power Output"
Nature. 217 770-1 (1968)

(4) Den Hartog, J.P.
"Mechanics"
Dover Publications (1948)

(5) Groesberg, S.W.
"Advanced Mechanics"
Wiley (1967)

(6) Hatze, H.
"Optimisation of Human Motions"
3rd International Seminar in Biomechanics. Rome. (1971)

(7) Hopper, B.J.
"Explosive Action"
Athletics Coach. June. (1966)

(8) Kane, T.R.
Scher, M.P.
"Human Self-Rotation by means of Limb Movements"
J. Biomechanics. 3. 1. 39-49 (1970)

(9) McCrank, J.M.
Seger, D.R.
"Torque-free Rotational Dynamics of a Variable-Configuration Body"
GAW/Mech 64-19
Wright Patterson Air Force Base. Ohio (1964)

(10) Miller, D.I.
"Computer Simulation in Springboard Diving"
3rd International Seminar in Biomechanics
Rome (1971)

(11) Nightingale, J.M.
Professor of Automatic Control
University of Southampton
Conference discussion on ref.(17)
(not yet published) (1971)

(12) Offenbacher, E.L.
"Physics and the Vertical Jump"
Amer. J. Physics. 38. 7. 829-836 (1970)

(13) Offenbacher, E.L.
Professor of Physics
Temple University, Philadelphia
Personal ccmmunication (1970)

(14) Pars, L.A.
"Introduction to Dynamics"
Cambridge Univ. Press (1953)

(15) Plagenhoef, S.
"Patterns of Human Motion"
Prentice Hall (1971)

(16) Rutherford, D.E.
"Vector Methods"
Oliver and Boyd (1957)

(17) Smith, A.J.
Dowson, D.
Adamson, G.T.
Wright, V.
"Comparison of Predictions of a Segmental Analysis and Experimental Observations in Selected Athletic Activities"
I. Mech. E. Conference on Human Locomotor Engineering (1971)

(18) Whitsett, C.E.
"Some Dynamic Response Characteristics of Weightless Man"
AMRL-TDR-63-18
Wright Patterson Air Force Base, Ohio (1963)

Chapter 4

Experimental Methods for Cine and Force Platform Measurements

4.1 Introduction

At the outset it was intended that the experimental procedure should hamper the subject's performance as little as possible. Athletic activities of a complex nature, such as vaults and somersaults, were envisaged in later investigations, and the use of apparatus connected directly to the subject was ruled out. Even in the simpler action of jumping through moderate distances freedom of movement was deemed important, for major arm and leg flexions occur at fairly high speed.

While it is possible for the experimenter to cope with a moving bundle of leads from electromyographic electrodes during a vertical jump, the subject cannot feel free, physically or psychologically, to carry out the jumping action in an uninhibited fashion. Thus, in the present studies, the subject was given as much liberty as possible. Accelerometry, e.m.g. and other contact methods of measurement were avoided. In addition to their effects on the subject there are also technical problems with accelerometers placed on the skin during violent limb movement. Errors may arise due to rapid oscillation and stretching of the tissue on which the sensors are attached. The only constraints imposed on the subject were the need to operate within the camera's field of view and, at times, the necessity to take off or land with both feet on the force platform. No special instructions to perform a 'maximal' jump or 'the softest possible landing' were given. Rather, the overall aim was to record an unrestricted movement and to use the data to give some understanding of the motion which had occurred.

The development of cine analysis of sports activities may be seen in the long term as the only method of data recording which can go on unknown to the performer and therefore allow a completely natural skilled action. Ideally, even the force platform may eventually be eliminated during field measurements, for the contact forces at the feet may, in principle, be computed from cine data. Fieldwork in filming sports situations implies that the subject is not specially marked at the body joints and that the

surroundings may not be ideal for photography. It may be difficult to obtain accurate camer-to-subject distances in such situations and, in all, measurements taken from the film will be liable to several kinds of error.

In view of these problems in the application of cine methods, the experimental methods described herein do not aim for extreme precision. For example, it is of little value to locate body joint (hinge point) markers with high accuracy when the skeletal 'hinge' itself does not possess a fixed axis, and when the skin may shift appreciably over the joint during activity. In the present study this, and all other sources of error are treated together as 'noise' contaminating the information, since separation of the individual components is virtually impossible. Useful results may still be obtained in these circumstances. A detailed discussion of the errors is given in Section 4.10.

4.2 Cameras

Two 16mm cine cameras were used for filming the jumping activities analysed in this work. A third, higher quality camera was available at a later stage although analysis of results obtained with the latter has not been carried out. All three cameras are, however, described because their relative merits are important in future development of the work.

a) The Bolex H.16 RX (25mm. f1.4 lens)

The Bolex is a spring-driven camera with nominal frame rates of 8, 16, 24, 32 and 64 frames per second. A nominal rate of 64 was selected for the jumping experiments, but calibration of the camera gave the correct value as 68.5 per second. One disadvantage of the Bolex is the absence of built-in indication of the frame-rate applying at the time of filming. Discussion with photographic technicians and a representative of Dawe Instruments Limited led to the idea of using direct stroboscopic timing of the camera shutter. The lens system was removed and a short length of film was run at the desired nominal rate. Adjustment of the stroboscope frequency gave a stationary image of the shutter and an accurate measure of its rate of

b) The Fastair 1-B (13 mm. f2.3 lens)

The Fastair was originally made by Photosonics Inc., California as an electrically driven high altitude camera running at a fixed rate of 1000 frames per second. In the laboratory, the camera speed was controlled with a Variac unit, allowing wide variation of running speed but only approximate presetting of the frame rate on the basis of the voltage at the Variac output. The camera was, however, provided with a timing light operated at mains frequency by the power supply and producing streak marks at the edge of the exposed film. Thus, the frame rate was accurately known only after the film was processed.

The camera design requires steady running of the film past the lens. The traditional stop-start gating of frames is replaced by a rotating triangular prism driven in synchronisation with the film. This arrangement causes the image received by each frame to move downward at the speed of the film and produce an unblurred picture.

c) The Mitchell HS-16 F4 (16mm. f1-8 lens)

The Mitchell provides a wide range of frame rates within which most types of human motion may be satisfactorily filmed. There are 10 rates from 4 to 500 frames per second, and the stated accuracy is $\pm$ 1% or $\pm$ 1 frame (the greater). In addition, a mains frequency timing light is provided as a posterior check on the running speed, permanently recorded on the film.

d) Comparisons

Motion recording using the rotating prism principle of the Fastair camera may be somewhat distorted by the vertical 'panning' action of the image received by the film. An instantaneous record of the body position would be more accurately produced on a given frame by exposure with the frame held stationary. Low speed cameras, such as the Bolex, succeed in holding each frame in the gate by friction as the shutter opens, but frictional positioning cannot be used successfully much beyond 64 frames per second because the momentum of the running spools is liable to drag the film when

it should be stationary. The Mitchell camera has a pin-register mechanism which, during exposure, locks each frame in position by pins engaging in the sprocket holes. This system is superior to the Bolex and Fastair devices and operates at all frame rates up to 500 per second.

4.3 The Kistler Force Platform and Amplifiers

a) The Platform. Type 9261

The essential features of the force platform are shown in Figures 4.1 and 4.2. The base and the working surface are both cast in aluminium alloy with integral reinforcing ribs. Each of the four piezo-electric load washers, sandwiched between the base and top castings is mounted on a steel stud. In assembly the four studs are screwed into blind tapped holes on the underside of the top casting, the load washers are push-fitted on the studs, and the base is finally clamped in position by nuts at the lower ends of the studs. The platform is supplied in the assembled state and sealed, with a slight precompression on the load washers.

The platform was mounted in a concrete well in the laboratory floor. In preparing the mounting the four cylindrical steel pads specified by the manufacturers were bolted through their undersides to a $\frac{1}{4}$ in. thick steel plate and the assembly was grouted into the floor of the well. The upper surfaces of the mounting pads were finally hand-finished so that their surfaces were horizontal and coplanar within the manufacturers specification. When positioned in the well, the working surface of the platform was flush with the laboratory floor. The platform was lightly clamped on its mounting pads by nuts on four $\frac{1}{4}$ in. diameter studs, welded to the base and locating in the stud holes and slots in the platform base.

The load washers within the platform are capable of force measurement along three mutually perpendicular axes, one in compression and two in shear. Internal connections between them provide appropriate summations of the X, Y and Z load washer force readings. In the piezo-crystal the application

FIGURE 4.1

KISTLER FORCE PLATFORM

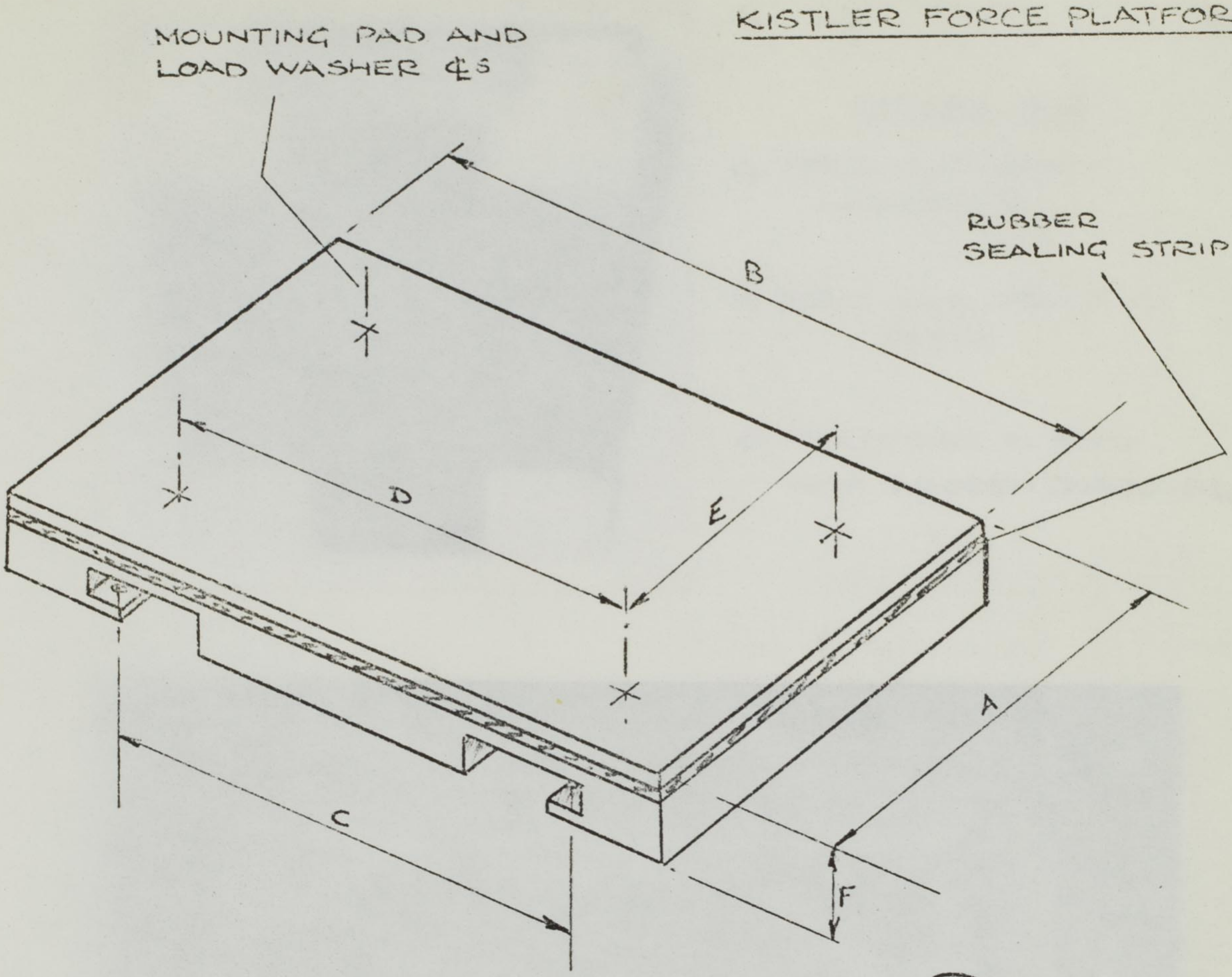

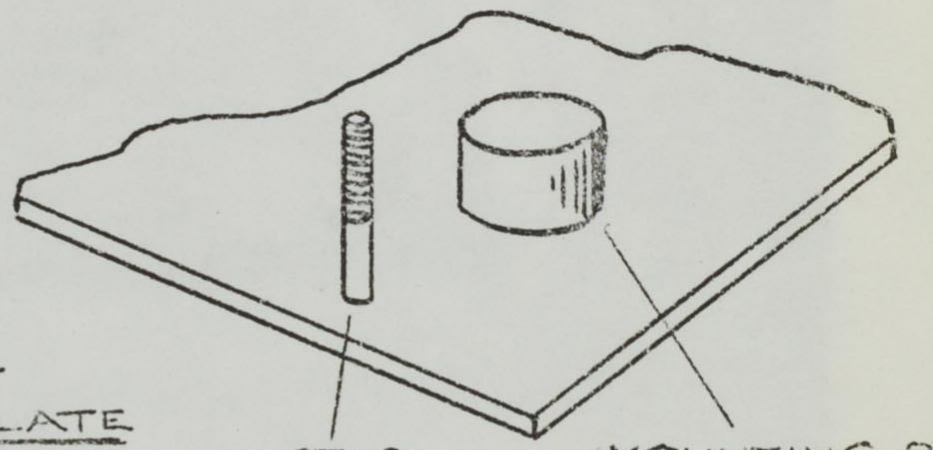

DETAIL OF
MOUNTING PLATE
(¼ in MILD STEEL)

MAJOR DIMENSIONS

DIMENSION	A	B	C	D	E	F
MANUFACTURER'S SPECIFICATION mm	400	600	368	440	264	—
APPROXIMATE EQUIVALENT	1'4"	2'0"	1'2½"	1'6"	1'0"	1·3"

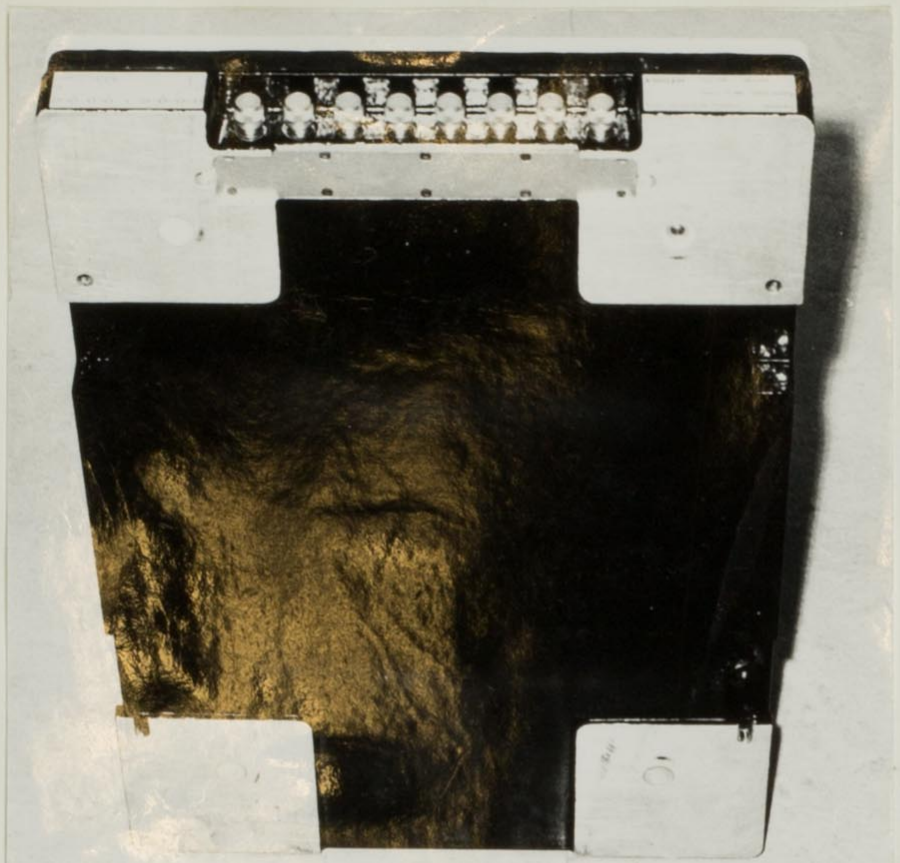

FIGURE 4·2

a) FORCE PLATFORM – UNDERSIDE

b) WELL AND MOUNTING PLATE

c) PLATFORM IN SITU WITH WOODEN SURROUND

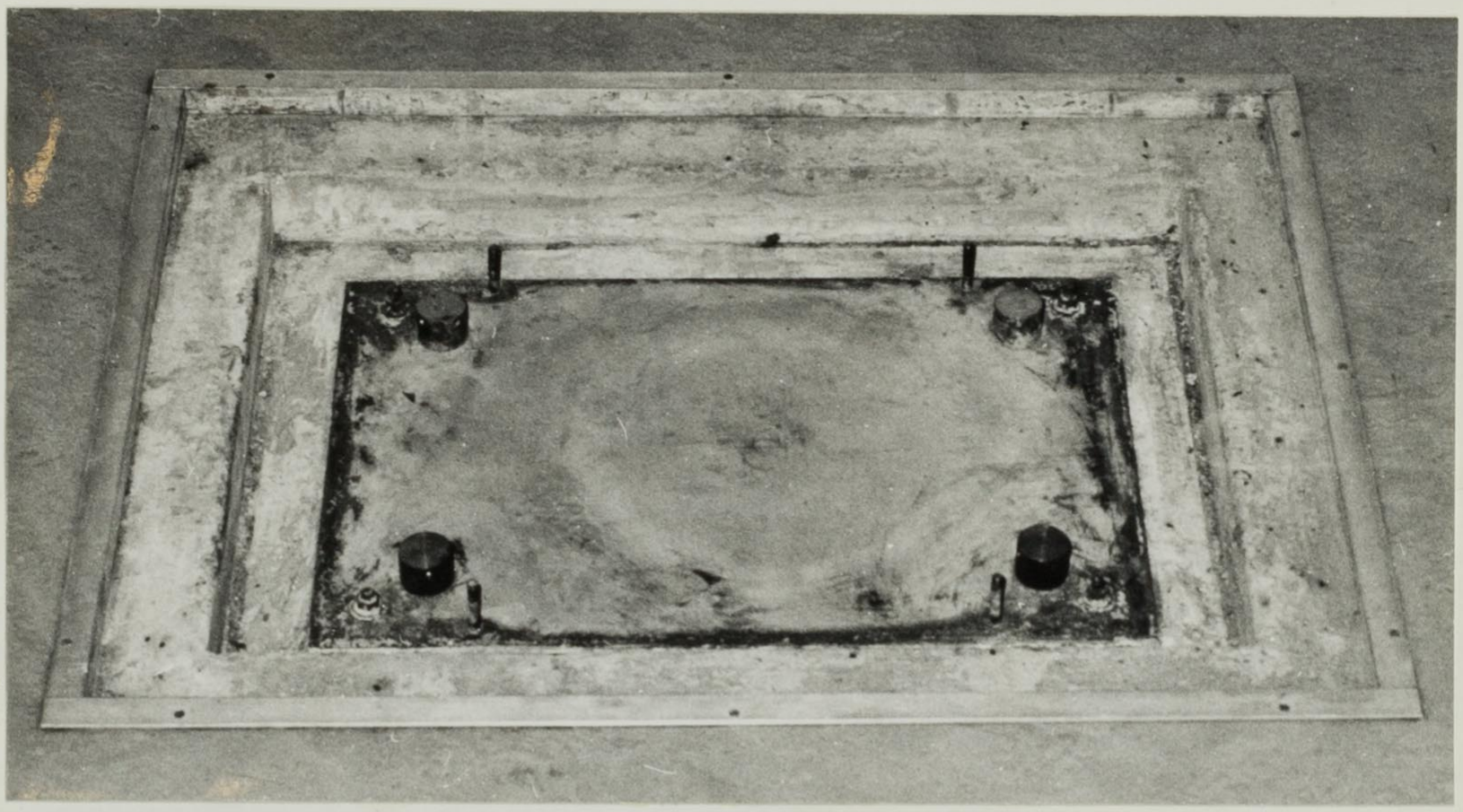

FIGURE 4·2

d) CHARGE AMPLIFIER CONTROLS

e) VANGUARD - P.C.D. FILM ANALYSER

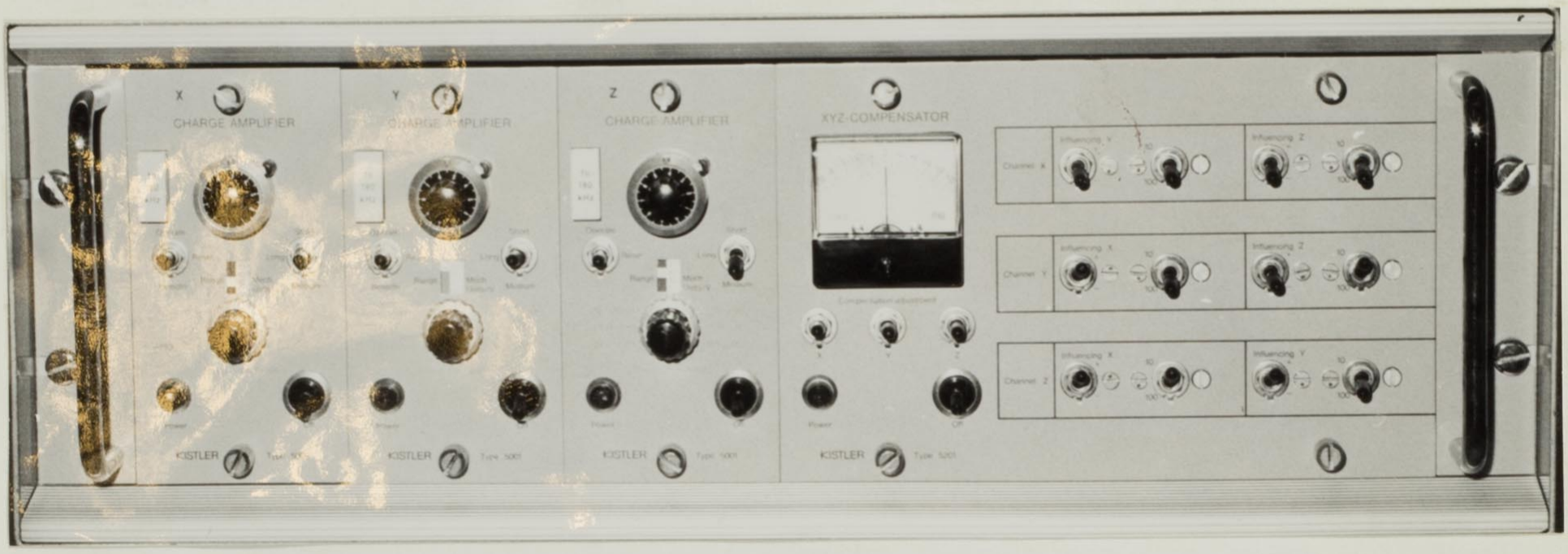

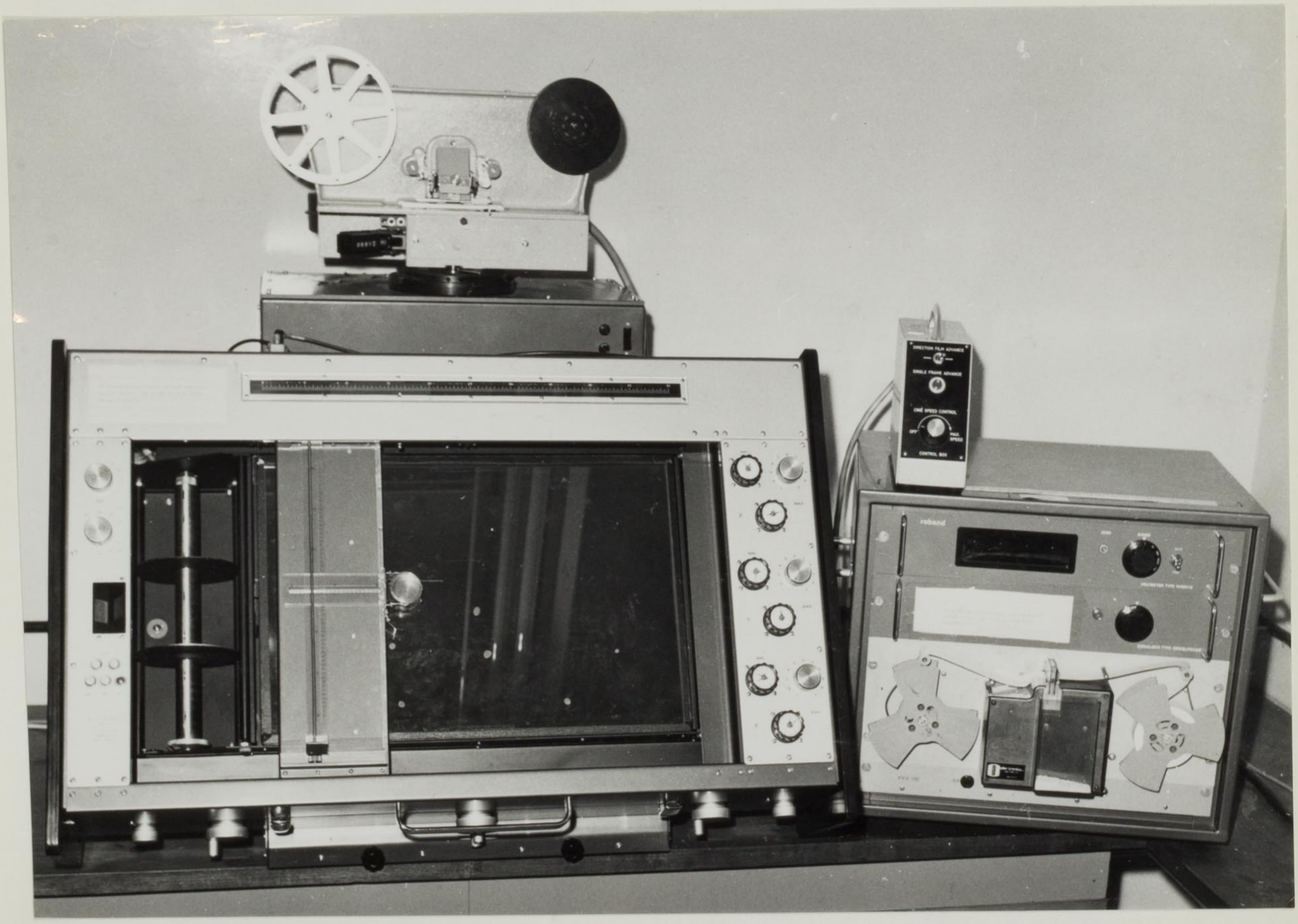

of force produces a static charge, and a group of charges is summed in the Kistler system by being led to capacitor storage within a charge-amplifier.

b) The Charge Amplifiers. Type 9801 (Figure 4.2d)

A separate charge amplifier for each axis of force measurement allows simultaneous handling of the three components. The measurement of couples by the present system does not appear possible although the manufacturers are investigating the problem.

The output of each charge amplifier is a voltage proportional to the total force applied to the platform along its associated reference axis. Cross-sensitivity between the force axes has been kept to a low level. A force applied along the Z-axis gives unwanted input to the X and Y charge amplifiers but the manufacturers quote these cross-effects as only 0.2% and 0.4% of the Z-force. All the cross sensitivities are below 1%. The charge amplifier unit is provided with a separate facility which allows measurement and compensation of the cross-sensitivities, but in practice the effects are so small as to be negligible. The amplifiers have, therefore, been used in the present work without compensation.

Static calibration curves are provided by Kistler and may be summarised as follows:-

AXIS	Z	X	Y
RANGE, kp	0-500	0-250	0-250
CALIBRATION CHARGE/FORCE pC/kp	34.3	75.2	75.5
LINEARITY ERROR %	0.4	0.3	0.4

1 kp = 1 kgf = 2.205 lbf

The charge amplifier range switch is graduated to represent the combined effect of platform and amplifier. Twelve steps giving force-sensitivities between 0.001 and 5 kp/mV are provided.

Amplifier linearity error is less than 0.05%

Vertical (Z) force measurements form the centre of interest in the present work and these forces have generally been nondimensionalised in the form F/W. Thus, use of the scaling values given above for direct measurement of force has been avoided. The main assumption in the use of the system has been the assumption of linear response characteristics in dynamic as well as static operation.

Each amplifier may be operated at one of three time-constant settings:-

SHORT	MEDIUM	LONG	T.C.
0.01-50	1-5000	1000-100,000	Seconds

The long time-constant is recommended for static calibration. The medium setting is most suitable for the measurement of force variations over periods of about 1 to 100 seconds, which cover many types of athletic activity.

4.4 The Southern Instruments Ultraviolet Oscillograph Series 10-100

The u.v. oscillograph was coupled directly to the charge amplifier output. Galvanometers with a natural frequency of 2200 Hz and a sensitivity of 6.23 mV/mm were used in all force measurements. These characteristics, in conjunction with the range of charge amplifier settings, gave reasonable force-sensitivity for the activities investigated.

Output from the oscillograph was recorded on Kodak Linagraph direct print paper, 120 mm wide, and fixed photographically, either by spraying with a yellow filter solution, or by processing in a suitable developer. Both materials are supplied by Kodak.

The oscillograph was provided with range-switches for the selection of paper speeds and timing line frequencies. Galvanometers not coupled to the charge amplifier system were used to mark zero-force and body-weight lines on the recorder paper during the period of activity.

4.5 The Experimental Area

The need for rapid assembly and dismantling of equipment in temporarily

occupied laboratory space imposed simplicity on the arrangements. The essential requirements for filming were:-

a) a backcloth, for which large rolls of photographic black paper, or preferably rough black curtain material were employed. (Smooth-surfaced cotton and man-made fibre materials have a considerable reflective sheen under intense lighting and may give poor contrast in the final picture.)

b) a distance scale in the plane of movement, provided either by a marked vertical bar or a subdivided white chalk line running across the floor at right angles to the camera's axis of view.

c) a vertical reference line, provided by a plumbline of white cord hanging well behind the region of movement.

d) mains power supplies.

In cases where the vertical bar distance scale might impede movement, floor markings were preferred. In some experiments a scale was filmed for a few seconds and then removed completely from the working area.

4.6 Preparation of the Subject

A black felt-pen was used to mark the estimated joint centres at the ankle, knee, hip shoulder elbow and wrist. The subject wore briefs tied up sufficiently at the side to reveal the hip joint marker. He was also allowed indoor training shoes for comfort in jumping on hard surfaces. Joint centres were satisfactorily located by observing the skin region which remained stationary during simple limb flexions.

4.7 Two Experimental Activities

a) The drop-landing

In a downward jump on to a firm surface, the lower limbs act as a shock absorbing mechanism against impact loading applied at the feet. To provide some information on a simple, non-injurious impact situation the subject was asked to hang from a horizontal bar above the surface of the force platform. He was filmed with a Bolex camera as he allowed himself to drop and made a comfortable landing on both feet. The foot thrust measured by the platform

is reproduced in Figure 4.3 and corresponding body positions are shown.

b) The Standing Long Jump

This activity provided a contrast to the drop landing in that the forces imposed on the body are caused by voluntary muscular action rather than external impact. As an experimental activity it has two virtues; the motion up to take-off occurs in a limited area and the body action is symmetrical about the sagittal plane.

The take-off and early aerial stages of a standing long jump were filmed at 224 frames per second with a Fastair camera.

4.8 Reading of Data from the Processed Film

The film was processed only to the negative stage and was adequate in this form for the reading of displacement data.

The Fastair film was first viewed by means of an Aldis slide projector with a 16mm film strip attachment. Hand feeding of short lengths was satisfactory and the full width of the film was projected on the screen, including timing marks at the edge. Counting of the 50 Hz marks against the frames gave an accurate measure of the frame rate. Opportunity was also taken to mark every tenth frame from the start of the activity to assist subsequent analysis. The Bolex film frames were also numbered but timing marks were not available and an independent camera calibration was relied on for the frame rate.

Measurement of body displacements in both activities was made by projecting the film frame-by-frame on a white paper screen firmly taped to a smooth wall. A Specto Analysing Projector was employed, and on each projected frame dividers were used to pick off the vertical displacement co-ordinates of the body hinge points. For the longer distances a large adjustable beam compass was made and fitted with needle points. This device allowed rapid measurement of distances between 12 and 23 in. while the shorter lengths were covered by ordinary drawing office dividers. Each displacement was measured from a fixed horizontal datum in the picture and verticality was

FIGURE 4.3 DROP-LANDING FORCE PLATFORM RECORD

DROP HEIGHT 42 in.
FRAME RATE 68·5 s^{-1}

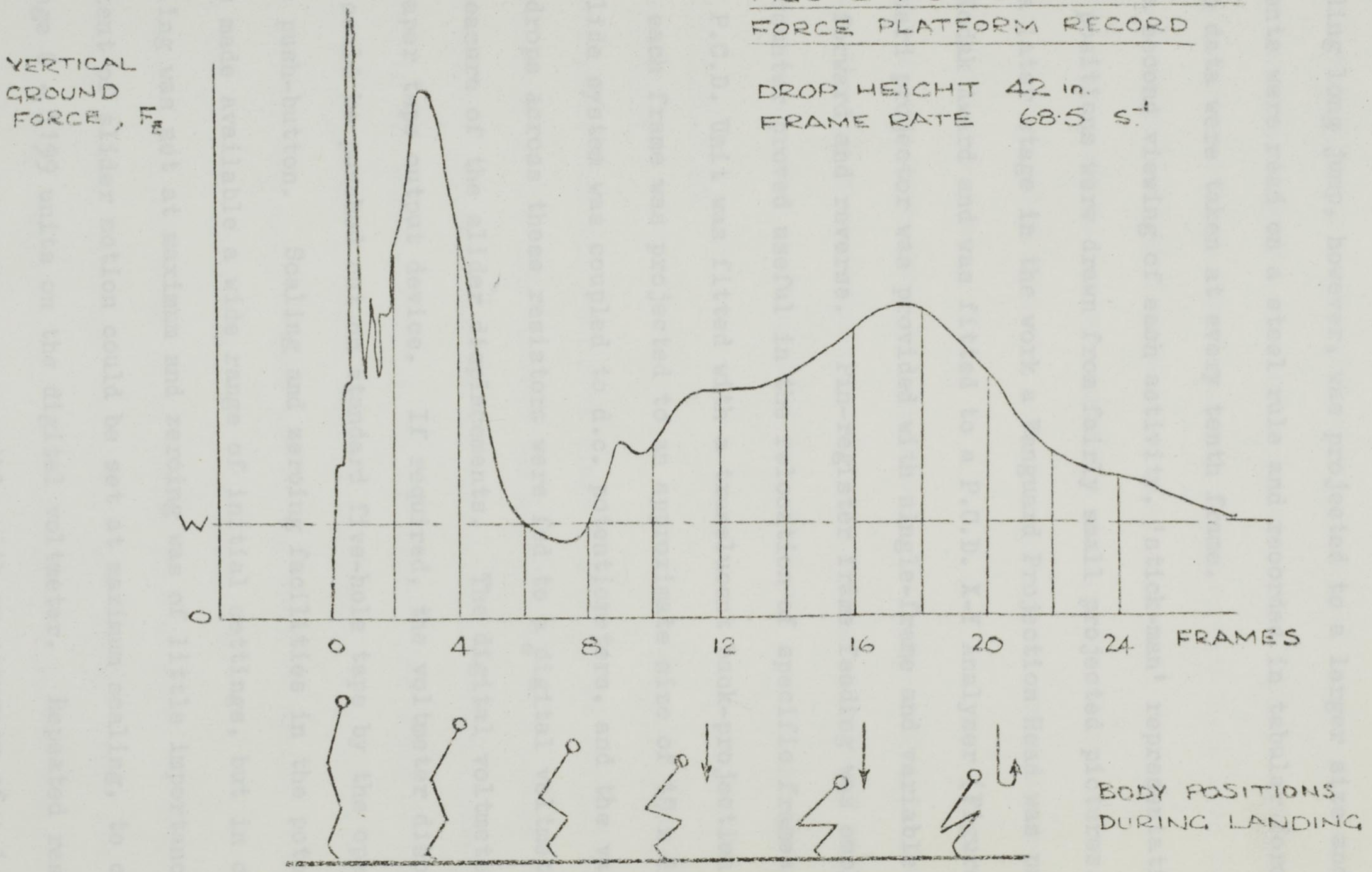

BODY POSITIONS DURING LANDING

checked against the plumbline behind the subject.

In the case of the drop-landing, the scale of projection was small enough for divider settings to be transferred directly to graph paper. The standing long jump, however, was projected to a larger size and the divider measurements were read on a steel rule and recorded in tabular form. The long jump data were taken at every tenth frame.

On a second viewing of each activity, 'stick-man' representations of the body positions were drawn from fairly small projected pictures.

At a later stage in the work a Vanguard Projection Head was purchased under a Kodak Award and was fitted to a P.C.D. X-Y Analyser (Figure 4.2e). The Vanguard projector was provided with single-frame and variable speed control, forward and reverse. Pin-register frame feeding was employed, and a frame counter proved useful in the relocation of specific frames.

The P.C.D. Unit was fitted with a translucent back-projection screen on which each frame was projected to an approximate size of 18 x 24 in. An X-Y slide system was coupled to d.c. potentiometers, and the variable voltage drops across these resistors were fed to a digital voltmeter as a direct measure of the slider displacements. The digital voltmeter was built into a paper tape output device. If required, the voltmeter displacement reading could be punched out on standard five-hole tape by the operation of a single push-button. Scaling and zeroing facilities in the potentiometer circuits made available a wide range of initial settings, but in cine analysis the scaling was set at maximum and zeroing was of little importance. The full extent of slider motion could be set at maximum scaling, to correspond to a range 0 - 1199 units on the digital voltmeter. Repeated resetting of the slider to the same point was possible with an accuracy of $\pm$ 1 unit.

The Vanguard P.C.D. Unit was used to read vertical displacement data for the two activities and to produce data tape for direct input into the computer programme of Chapter 6. Part of the long jump was analysed at 1-frame intervals in addition to the 10-frame spacing employed in the overall

analysis. The finer spacing was taken to provide data for the detailed investigation of smoothing and differentiation procedures (Chapter 5).

4.9 Displacement Measurements

Figure 4.4 shows typical vertical displacement curves for hinge-points during the drop-landing, the ordinates being plotted directly as measured from the projected film. These curves, together with data from Table 2.1 (Chapter 2) and additional information on hinge points from the same source (Whitsett), were used to derive segmental mass-centre displacements. The procedure, later written into the computer programme, is explained in Chapter 6, Section 6.3 a).

Smooth curves were drawn by eye through the mass-centre displacement points, and the smoothed ordinates were read off and tabulated in preparation for computation. The standing long jump film was treated in the same manner.

4.10 Sources of Error

a) 'Parallax'

Displacement data are read from hinge points on the initial assumption that the markers on the body nearest the camera move in a common vertical 'plane of motion' perpendicular to the camera axis. This assumption is invalidated in two ways. Firstly, to the camera, the edges of the plane of motion are at a greater distance than is the central area of the plane; secondly, if the body markers move out of the plane of motion, toward or away from the camera, distances are again distorted.

The term 'parallax' seems to be widely used to refer to both of these camera viewing errors, although 'obliquity' and 'depth' error are suggested as more informative descriptions. The obliquity error in the drop-landing, calculated by trigonometry on the camera-subject distance, was found in the present work to be somewhat less than the variation of segment lengths between hinge-points. The depth error cannot be properly estimated without information in a third dimension, usually by means of a second camera. In view of these points 'parallax' correction was not employed in the calculations.

ORDINATE ON PROJECTED PICTURE

FIGURE 4.4
VERTICAL ORDINATES - DROP-LANDING

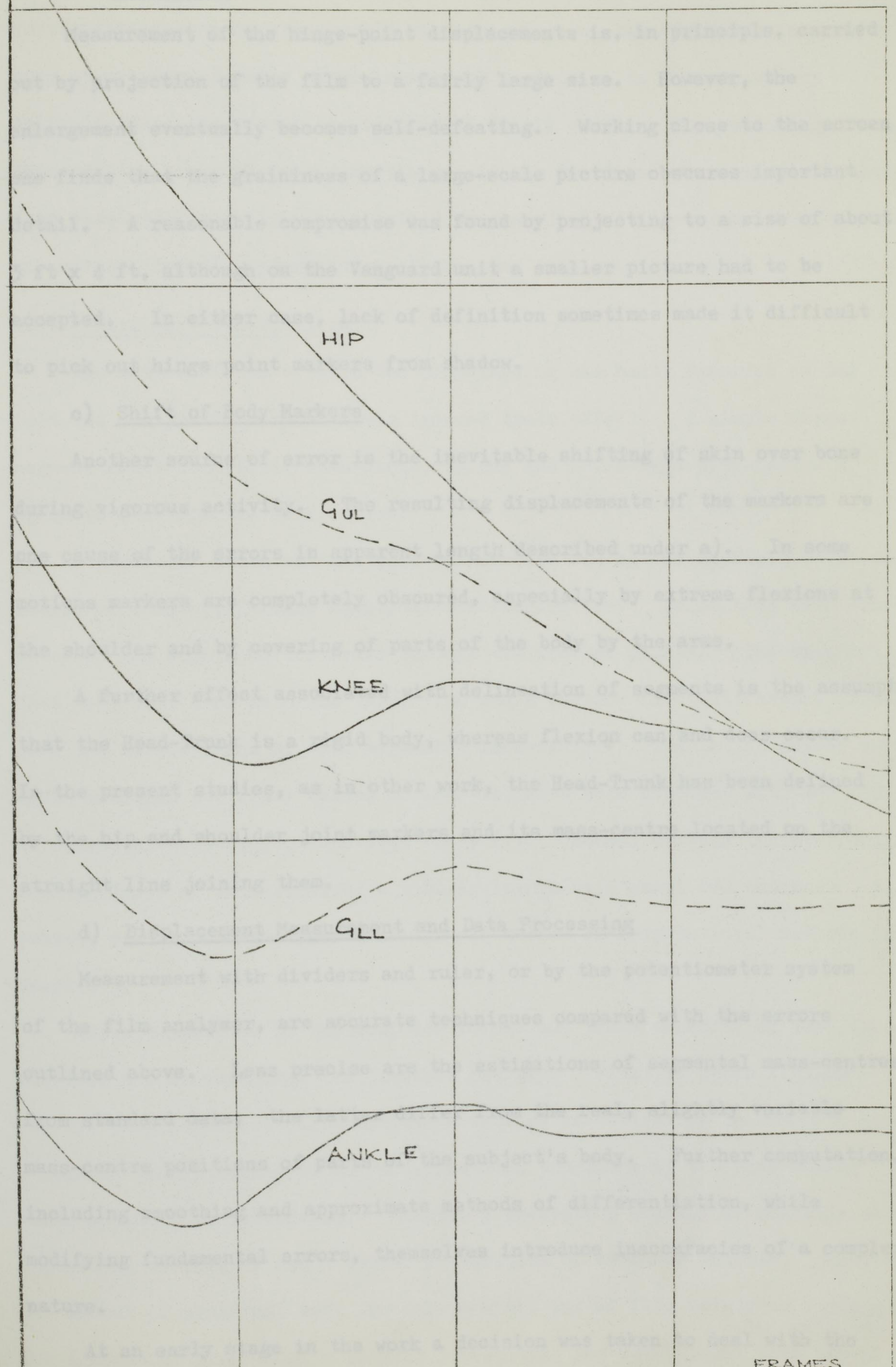

b) Definition

Measurement of the hinge-point displacements is, in principle, carried out by projection of the film to a fairly large size. However, the enlargement eventually becomes self-defeating. Working close to the screen one finds that the graininess of a large-scale picture obscures important detail. A reasonable compromise was found by projecting to a size of about 3 ft x 4 ft, although on the Vanguard unit a smaller picture had to be accepted. In either case, lack of definition sometimes made it difficult to pick out hinge point markers from shadow.

c) Shift of Body Markers

Another source of error is the inevitable shifting of skin over bone during vigorous activity. The resulting displacements of the markers are one cause of the errors in apparent length described under a). In some motions markers are completely obscured, especially by extreme flexions at the shoulder and by covering of parts of the body by the arms.

A further effect associated with delineation of segments is the assumption that the Head-Trunk is a rigid body, whereas flexion can and does occur. In the present studies, as in other work, the Head-Trunk has been defined by the hip and shoulder joint markers and its mass-centre located on the straight line joining them.

d) Displacement Measurement and Data Processing

Measurement with dividers and ruler, or by the potentiometer system of the film analyser, are accurate techniques compared with the errors outlined above. Less precise are the estimations of segmental mass-centres from standard data; the latter differ from the real, slightly variable mass-centre positions of parts of the subject's body. Further computation, including smoothing and approximate methods of differentiation, while modifying fundamental errors, themselves introduce inaccuracies of a complex nature.

At an early stage in the work a decision was taken to deal with the

data under the combined influence of all sources of error, and to develop computational methods which would be successful in such circumstances. The only error which permits simple numerical correction is that caused by obliquity, and its effect has been found fairly small. The remaining inaccuracies are much less tangible and it was found in preliminary calculation that meaningful results were obtained by regarding all the error sources as an overall 'noise' contamination of the cine data.

4.11 Preliminary Calculations

The motion of the arms in the drop-landing was badly recorded on the film and the preliminary analysis ignored their effect. A simple three-segment model comprising Head-Trunk, Thighs and Lower-legs-plus-feet was taken to describe the body action.

A series of force calculations was carried out by the application of two stages of first-difference numerical differentiation. Velocities were first obtained and smooth curves drawn through the plotted points. The smoothed data were read back into the tabulation and a further first-difference process gave the acceleration of each segmental mass-centre. The latter points were again smoothed and final values of inertia force were produced with the aid of segmental mass-proportions from Table 2.1. Manual calculation over only twenty frames of film required a tabular layout with about 600 entries. A summary of the results appears in the discussion of computational methods in Chapter 5.

While comparison of the computed forces and those measured by the force platform was encouraging, two problems emerged. Firstly, curve fitting 'by eye' and numerical differentiation require investigation in order to give a clearer understanding of the modifications undergone by the data during these approximate procedures. Chapter 5 presents a summary of possible data-processing techniques and a closer examination of selected methods. Secondly, the amount of numerical work for only a short run of film points to the need for a computer programme. Chapter 5 indicates the development from manual

computation to techniques suitable for the computer, and in Chapter 6 the computer programme is explained in detail.

Chapter 5

Smoothing and Differentiation of Displacement Data

5.1 Introduction

Measurements on cine film of a human activity provide sets of displacement time data. If a displacement-time graph is plotted, the points should lie along a fairly well defined curve, but there will be some scatter of points about a 'smooth' curve passing among them. The process of fitting a smooth curve to slightly erratic data points may be carried out in several ways. Whichever method is employed, it is difficult to specify the 'right' curve for the data. Indeed, the choice of a 'best' curve, despite refined computational techniques for curve fitting, remains a somewhat arbitrary procedure. The purpose of this discussion is to consider some of the available techniques and their applicability to the analysis of cine data on human movement.

5.2 Smoothing Techniques

a) Curve Fitting by Eye

A curve may be quickly fitted to data points on a graph by sketching a reasonable line passing near to or through the points. Human judgement of the 'best' curve is, for many purposes, satisfactory, but no-one would argue that the process is repeatable nor that it will produce the same results when applied by different people. Moreover, it is impossible to describe mathematically the decision processes by which the curve is determined. It is therefore difficult to specify exactly what has been done to the data by this form of curve-fitting and smoothing. If the modifications to the data points caused by the fitting of a 'best' curve are to be examined, and if the term 'best' is to be given a less subjective meaning, more exact methods are necessary and the problem has been approached in several ways.

b) Polynomial Curve Fitting

The simplest example of polynomial fitting is the regression line. It is assumed that a straight line, or polynomial of the first order, will give a satisfactory fit and the two coefficients necessary to specify the line are determined by the least squares principle, using all the data points.

When a higher order polynomial is judged to be a suitable representation of the data, several coefficients must be determined. For n data points, the polynomial fitted cannot be of order greater than (n-1). The curve of order (n-1) fits the data points exactly.

If smoothing is to be introduced, the polynomial fitted will be of order $m < n-1$. Rather than choose a specific value of m as the most suitable order for the fitted function, it has been proposed that the whole range of polynomials (m=1 (1) n-1) be fitted and some criterion be found to select the 'best' fit. For example, the criterion may be based on the mean square of the residuals, where 'residual' refers to the difference between a data point and the corresponding ordinate on the fitted curve (Cook (2)).

In practice orthogonal polynomials are preferred to ordinary power functions because the equations for the coefficients generated by the least squares principle are less likely to be an ill-conditioned set.

c) Periodic Functions

The periodic functions, sine and cosine, form one of the many sets of orthogonal functions. Fourier showed that periodic functions may be used in the same way as orthogonal polynomials for fitting a curve to experimental data. Fourier Analysis introduces the concept of frequency structure of a data record. If the fitted function is expressed by sinusoidal terms of increasing frequency, it is usually found that the high frequency terms represent a 'ripple' superimposed on the more slowly varying curve of the low frequency components. This effect suggests that the error fluctuation of data points about the smooth curve is described by the higher frequency terms of the fitted periodic function.

Just as reduction in the order of a fitted polynomial is a means of applying smoothing to the data points, so truncation of the Fourier series by the omission of the high frequency terms tends to remove the smaller fluctuations, or 'noise' in the data. The remaining low frequency terms are then supposed to represent the 'true' course of the curve.

Lanczos (4) advocates this form of Fourier smoothing. It is necessary to take the Fourier analysis to the maximum number of terms. As with polynomial fitting, this number is determined by the number of data points available. The Fourier coefficients should decrease in magnitude toward the higher frequency end of the series and all those above a critical 'cutoff' frequency may be removed as noise. Lanczos shows how the Fourier series may be expressed purely in terms of sines so that discontinuities at the ends of the data set are avoided. Judgement of the 'cutoff' frequency is somewhat subjective and truncation above this level assumes that all the high frequency terms represent noise. Nevertheless, the technique yields valuable insight into the composition of the data and is closely related to the more sophisticated methods of spectral density analysis which have been developed in the electronic and vibration fields. Fourier smoothing is considered in more detail in Sections 5.5 and 5.6.

d) Moving Averages

For any group of adjacent data points, a smoothed value for the mid-point of the group is obtained by taking the arithmetic mean of the group. The larger the group, the more severe the smoothing effect. Hamming (3) demonstrates the effect of a three-point moving-average in terms of the frequency structure of the data; the procedure effectively removes the upper half of the frequency range represented by the Fourier analysis of the data. Moving averages on more than three points have an even more severe smoothing effect.

5.3 Differentiation Techniques

The estimation of velocity from displacement-time data is a process sensitive to errors in the data points. Calculation of the second derivative, for acceleration, is still more difficult. The differentiation formulae of classical numerical analysis, based on successive differences, are of little value because errors propagate uncontrollably through the difference table. Lanczos (4) demonstrates the effect clearly. Many numerical analysts

regard the computation of derivatives as a dubious procedure, but some practical methods have proved fairly successful.

a) First Central Differences

Human judgement of the 'best' fit curve may be extended to differentiation by judging the tangent to the curve, a fairly inaccurate method. Alternatively, the smoothed data provided by the 'best' fit may be used in the elementary first difference formula:-

$$\dot{z}_{n+\frac{1}{2}} = \frac{z_{n+1} - z_n}{\Delta t}$$

which uses the chord to estimate the gradient of the tangent. The resulting graph of derivative values should itself be smoothed before final values of or second derivatives are taken. Despite its apparent crudity, this procedure may, with experience, be relatively accurate, but human judgement is necessary at the smoothing stage.

b) Local Polynomial Differentiation

Lanczos proposes a development of polynomial curve fitting for the calculation of derivatives. Given a set of data points, he takes a small subset of r adjacent points and fits a polynomial of order $s<r$ to them. The first or second derivative at the midpoint is given by appropriate algebraic differentiation of the polynomial. The process is repeated by moving the subset along the data points. The least squares polynomial provides 'local' smoothing of the data prior to differentiation and the derivative formulae are expressed directly in terms of the data point values. Lanczos combines this treatment with Fourier smoothing by truncation.

c) Overall Polynomial Differentiation

If overall smoothing is carried out by a polynomial fit to all the data points, it is possible to obtain derivatives by algebraic differentiation of the polynomial expression. Plagenhoef (7) proposes this approach, suggesting polynomials of order 4 to 9 for human motion analysis. The procedure appears to give good results. However, it is worth noting that while a polynomial is reduced in order by differentiation, velocity and

acceleration curves from displacement data often exhibit a progressive increase in the number of their maxima and minima suggestive of an increase in polynomial order. Plagenhoef does not give an analytical justification of his procedure. Certainly its counterpart for periodic functions is not satisfactory. Lanczos points out that term-by-term differentiation of the Fourier series will always lead to large errors.

d) Interpolation Prior to Differentiation

Wallach and Saibel (8) use a novel technique. Having fitted a cubic to a group of five data points, they interpolate to create 49 new values between each adjacent pair of original data points. This closely spaced smoothed data is fitted, in sequential sets of 101 points, with a new cubic, and derivatives are obtained algebraically from the cubic expression.

e) Check Integration

Felkel, quoted by Paul (5), suggests integration of the curves produced by numerical differentiation, but there appear to be no practical studies incorporating this kind of check, desirable though it is.

5.4 Summary of Smoothing and Differentiation Techniques

a) Smoothing

Method		Comments
Curve fitting 'by eye'	For	Rapid and informative if the general smoothed form is known 'a priori'. Highlights bad data points for re-measurement.
	Against	Heavily subjective. Non-repeatable Cannot be computerised.
Polynomial curve fitting-ordinary power series or orthogonal functions (Cook)	For	Computational procedures and programmes available.
	Against	Selection of suitable polynomial order is partly subjective.
Periodic functions. Fourier fitting and truncation (Lanczos)	For	Brings out the frequency structure of data. Computer programmes available.
	Against	Truncation smoothing by omission of high frequency terms may remove both 'noise' and real data. Choice of 'cutoff' frequency partly subjective.
Moving averages	For	Simple manual calculation. Easily programmed.
	Against	May oversmooth with wide data spacing.

b) Differentiation

Tangent drawn 'by eye'	For	Rapid
	Against	Unreliable and unrepeatable
First Central Differences	For	Rapid. Often satisfactory if preceded and followed by smoothing.
	Against	Poor when displacement curve is significantly curvilinear between data points.
Higher Difference formulae of Numerical analysis	For	Nothing
	Against	Errors spread wildly through the difference table
Local polynomial differentiation. A subset of 4 to 9 adjacent points contributes to the value of the derivative at their midpoint. Fitted polynomial usually of order 2 or 3. (Lanczos)	For	Local least squares smoothing of the subset, governed by the number of subset points and the order of polynomial fitted. Easily computerised in terms of data point values.
	Against	Choice of number of points and polynomial order subjective A danger of oversmoothing derivative values.
Overall Polynomial differentiation (Plagenhoef)	For	Programmes available
	Against	Subjective choice of polynomial order. Decrease in polynomial order seems at variance with increasing maxima/minima of derivative curves.
Polynomial fitting with interpolation. Algebraic differentiation. (Wallach and Saibel)	For	Interpolation reduces data spacing and oversmoothing is less likely in the differentiation.
	Against	Considerable increase in the data to be handled.
Fourier smoothing combined with local polynomial differentiation	For	Advantages of the individual techniques.
	Against	A semi-computerised process with human intervention.

5.5 Fourier Smoothing - Basic Concepts

a) Sampling frequency

Cine film provides a sampled-data record of motion. Basically, the sampling frequency is the rate at which the cine frames are exposed, that is, the frame speed, provided that the user takes data from every frame. In this discussion, however, sampling frequency denotes the rate at which data is actually taken for analysis. For example, film taken at 500 frames per second may have data read from only every fifth frame, so that the data sampling frequency is 100 items per second.

b) Aliasing or folding

The well-known cinema illusion of stage coach wheels revolving backwards is an example of aliasing in sampled data. The essential point is that sampling of a periodic function at a sampling frequency ν_s leads to a two-valued solution for the frequency of the measured function. Two functions, having frequencies $\frac{1}{2}\nu_s \pm \nu_o$, cannot be distinguished from each other by means of the sampled data record. Thus, information relating to periodic functions between $\frac{1}{2}\nu_s$ and ν_s is confused with that pertaining to functions between 0 and $\frac{1}{2}\nu_s$. The information is folded back on itself at $\frac{1}{2}\nu_s$, the folding frequency, and the duality so created is termed aliasing. The phenomenon is fundamentally mathematical and is not confined to visual illusions.

c) Fourier Analysis

Since any displacement-time record may be analysed by Fourier methods into periodic functions, the effects of aliasing on non-periodic sampled data from cine film may be investigated. Lanczos describes a method in which any section of a sampled-data record may be analysed into a Fourier series consisting only of sine terms. The data must first be prepared by subtracting a linear trend. This process ensures continuity in the function and in its first derivative at the ends of the range, and transforms the data into an odd function.

The Fourier coefficients are evaluated in terms of the data-point values For N data points, at most N unknown coefficients may be found, of which only half are sine coefficients. Thus, there will be only N/2 sine frequencies in the odd-function expansion of the N data points. This halving effect is another expression of the folding frequency.

Provided that the cine data behave as Lanczos indicates in his numerical examples, it will be possible to fix a 'cut-off' frequency, ν_c somewhere below the folding frequency $\frac{1}{2}\nu_s$. Frequencies between ν_c and $\frac{1}{2}\nu_s$ are then discarded as 'noise', and those below ν_c are interpreted to be the 'real' information provided by the data record. Figure 5.1 illustrates the relationships between the frequencies. Clearly, it is possible to raise the folding frequency by increasing the sampling frequency ν_s . There is, however, little point in this step if the 'cut-off' frequency ν_c is fairly well established at a low value. Any increase in folding frequency merely adds noise terms to the Fourier expansion and the extra data handled provides no real benefit.

The applicability of Fourier smoothing is best shown by numerical examples, which follow.

5.6 Fourier Smoothing - Application

a) Data

Cine film of a standing long jump was taken in side view at 224 frames per second to provide data on a vigorous voluntary activity. A fuller discussion of the jump action appears in Chapter 7 but for this analysis attention is confined to the violent arm-swing prior to take-off. The vertical displacement co-ordinates of the elbow joint were, for purposes of comparison, obtained in two ways, by direct projection and measurement on a rigid screen, and by the Vanguard-P.C.D. film analyser. Typical curves at two different sampling frequencies are shown in Figure 5.2. The film analyser operated at two different scale factors for these sets of data.

FIGURE 5.1

FREQUENCY RELATIONSHIPS IN FOURIER SMOOTHING

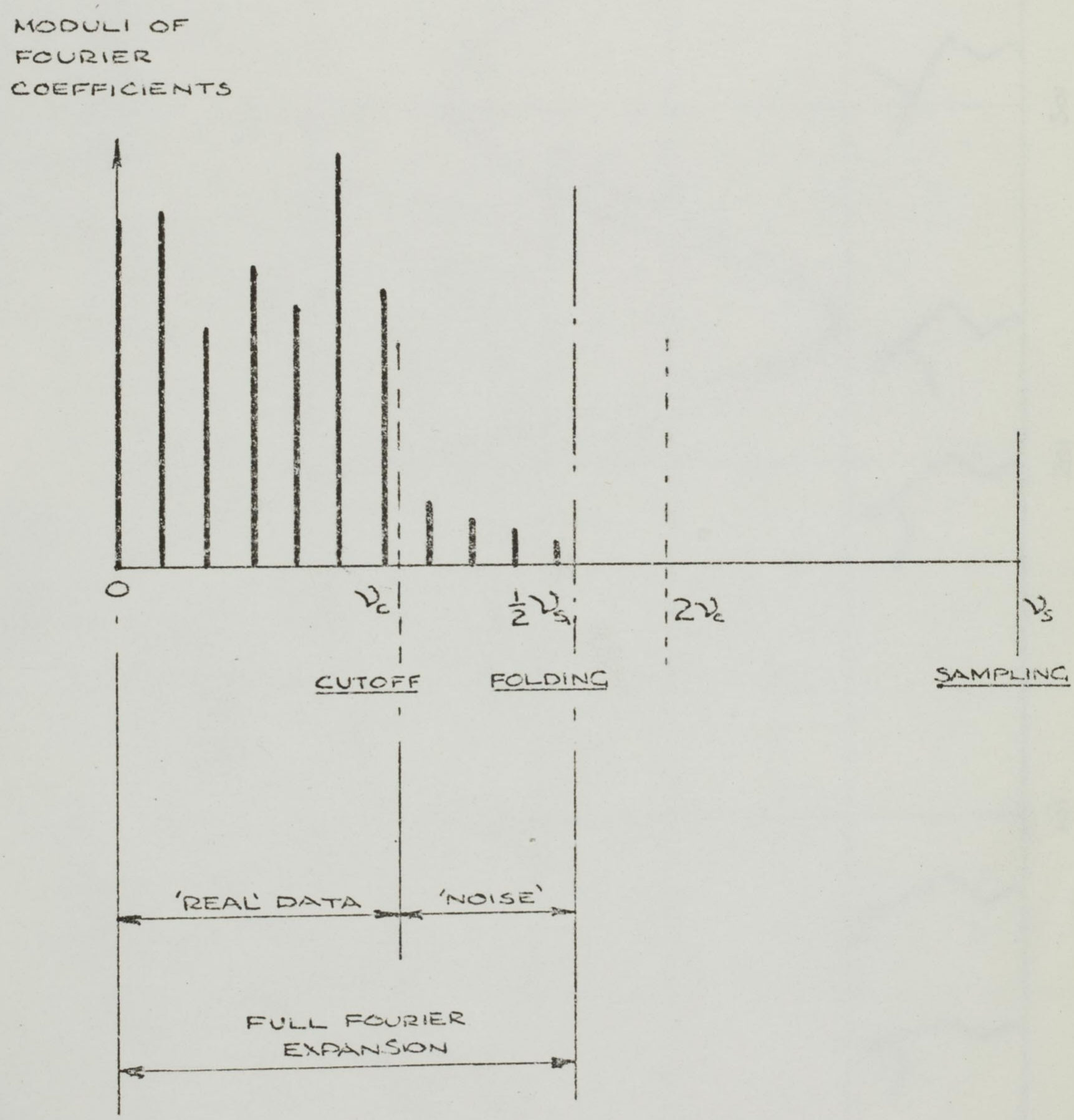

FIGURE 5.2

STANDING LONG JUMP

VERTICAL DISPLACEMENT OF ELBOW JOINT

FRAME RATE 224 /SECOND

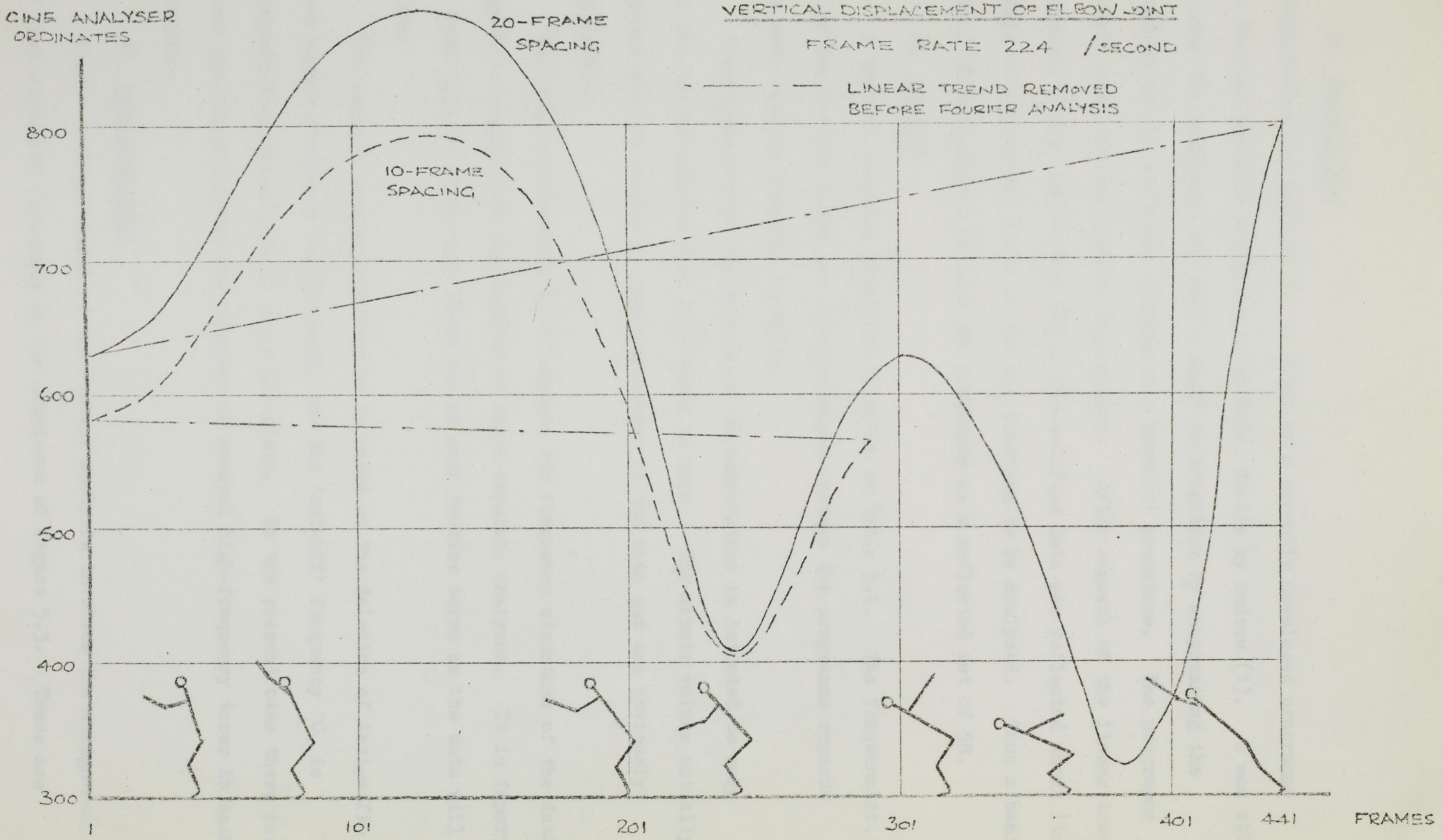

b) Computation

Computation was carried out by means of a recently developed programme for Fourier analysis presented as an M.Sc. Thesis by Andrew (1). I was able to copy the programme and made a small modification by suppressing the printing out of residuals related to a best-fit procedure. The programme accepts a set of equi-spaced data points. After removal of the linear trend (Sections 5.5.c) and Figure 5.2), the modified data was reflected about its origin to obtain one cycle of the odd function to be analysed. Thus a basic set of 30 data points entered the programme as a reflected set of 58.

c) Results

A typical computer print-out is given in Table 5.1. The frequencies, J, of the Fourier terms are integer-valued because the programme regards the data spacing interval as unity.

Transformation of the data prior to computation is intended to make all the cosine coefficients A(J) equal to zero. The minute values actually printed out are caused by rounding errors in the data and are obviously negligible.

The sine coefficients B (J) express the frequency structure of the data. Figure 5.3 summarises the results of three separate analyses. It is important to note that in every case there are as many Fourier terms as the data will allow.

The Lanczos smoothing procedure is based on the deletion of insignificant higher-frequency coefficients, and the 'cut-off' frequency ν_c is determined by inspection of the B (J) plots. In the present case there seems clear justification for the omission of several high-frequency terms in each analysis.

d) Interpretation

Proper interpretation of the Fourier analysis involves the assignment of real values of frequency to the abscissae of Figure 5.3. These are

TABLE 5.1

TYPICAL OUTPUT FROM FOURIER PROGRAMME

STANDING LONG JUMP DATA AT 20-FRAME SPACING

VALUE OF A[(Q+1)/2] IS +1.3858966884₀-12

J	A[J]	B[J]
+0	-2.6609216418₀-10	+0.0000000000
+1	-7.0957910447₀ -9	-1.9898778210₀ +0
+2	+5.9427249999₀ -8	+8.2050821715₀ +0
+3	-7.7443906949₀ -9	-7.2193181086₀ -1
+4	-4.8657966545₀-11	-4.1350511887₀ -3
+5	+8.7300404197₀ -8	+4.8593179195₀ +0
+6	+7.7222163479₀ -8	+3.5811478844₀ +0
+7	+2.4258735634₀ -8	+9.6499968886₀ -1
+8	-1.2578051870₀ -8	-4.3794645512₀ -1
+9	+1.8724503683₀ -8	+5.7988685360₀ -1
+10	+2.3685320879₀ -8	+6.6037248322₀ -1
+11	+2.4507330853₀ -8	+6.2148131333₀ -1
+12	+1.4766512669₀ -9	+3.4361526627₀ -2
+13	-8.6845483609₀ -9	-1.8642724112₀ -1
+14	-1.0074429502₀ -8	-2.0075295733₀ -1
+15	-5.3000154107₀ -9	-9.8631782904₀ -2
+16	+1.0094178530₀ -8	+1.7623040320₀ -1
+17	+1.0956899219₀ -8	+1.8017130222₀ -1
+18	+6.8719687295₀ -9	+1.0673925511₀ -1
+19	-9.6846460587₀ -9	-1.4252991884₀ -1
+20	-6.0619121151₀ -9	-8.5149271333₀ -2

PROGRAM ENDS
RUN TIME 17 SECS

FIGURE 5.3 (SEE FIGURE 5.1)

FOURIER ANALYSIS OF DISPLACEMENT DATA. ELBOW JOINT ORDINATES STANDING LONG JUMP.

$\dagger$ — NEGATIVE COEFFICIENT

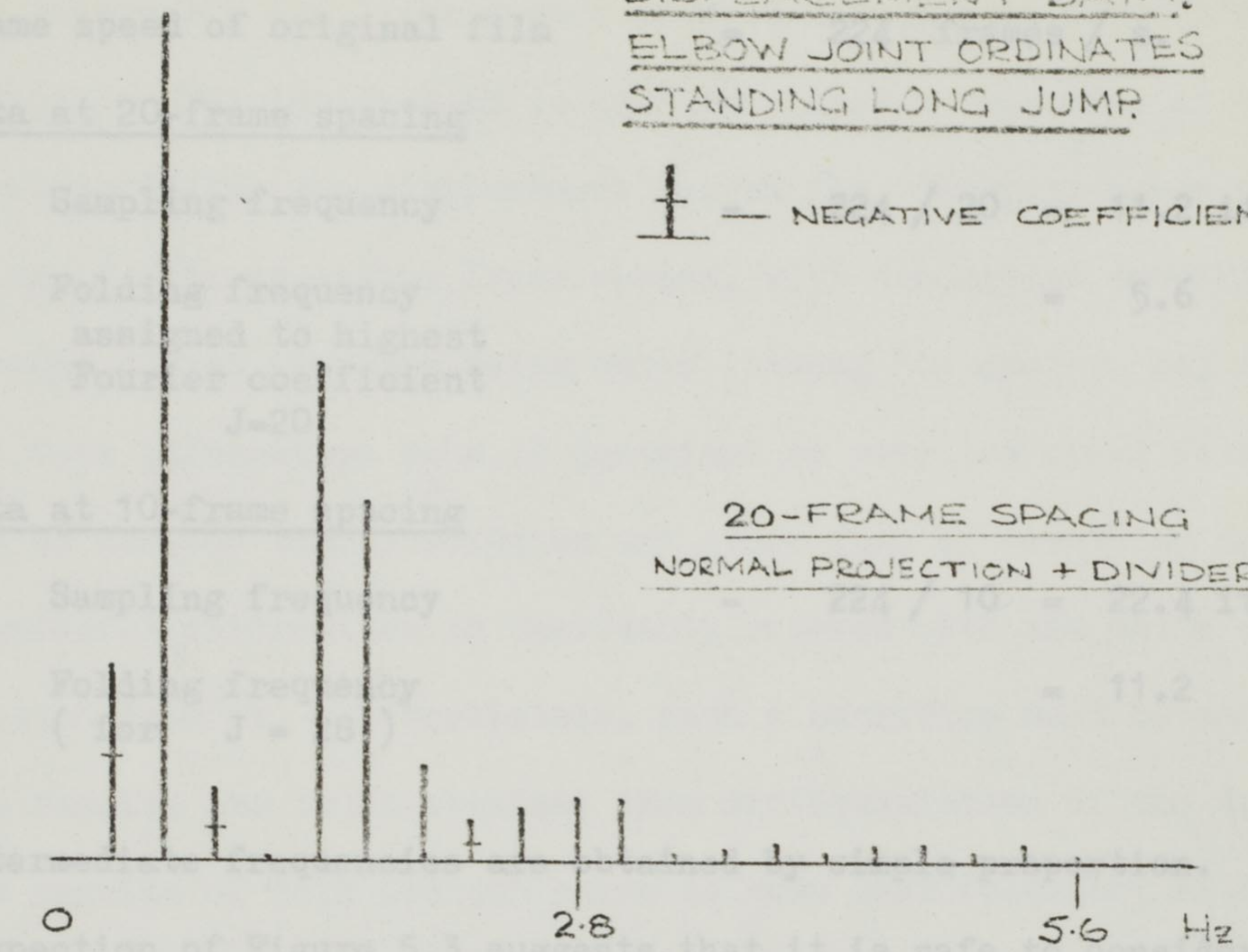

obtained as follows:-

Frame speed of original film = 224 frames / s.

Data at 20-frame spacing

Sampling frequency - 224 / 20 = 11.2 item / s.

Folding frequency assigned to highest Fourier coefficient J=20 = 5.6 "

Data at 10-frame spacing

Sampling frequency - 224 / 10 = 22.4 item / s.

Folding frequency (for J = 28) = 11.2 "

Intermediate frequencies are obtained by simple proportion.

Inspection of Figure 5.3 suggests that it is safe to consider Fourier terms above the frequency 5 per second as noise. Their magnitudes are relatively very small and their signs oscillate fairly randomly between positive and negative. The cutoff frequency ν_c may therefore be set at 5 per second, and this implies that the folding frequency $\frac{1}{2}\nu_s$ of the sampled data could be as low as 5. Thus the sampling frequency may be reduced to 10 per second without any loss of real information. This latter is approximately equal to the sampling frequency of the 20-frame data and about half that of the 10-frame data. The latter are rich in noise frequencies and the consequences of this contamination will become unpleasant when derivatives of the displacement curves are computed. (Section 5.11.g)). The Fourier treatment therefore indicates that the motion would be adequately recorded on film running at only 10 frames per second. Indeed, if an even bolder cutoff frequency, around 3, were allowed, the corresponding frame speed would be 6 per second. Such a low cutoff frequency is not unreasonable in the light of Figure 5.3 although it may be considered undesirably close to the limit of the 'real' information band.

e) Discussion of Fourier smoothing

The remarkably low frame speeds derived here may at first sight seem unacceptable. The implication is that very sparse recording of data is sufficient to define the displacement curves for voluntary human motion. The taking of film at higher frame speeds, with subsequent smoothing of the displacement curves (perhaps using curve fitting 'by eye'), may finally yield no more information than is contained on very low speed film. It must not be assumed that Fourier or any other form of smoothing is perfect. Some meaningful information is inevitably removed with the noise and cannot be separated from it. Nevertheless, such a sacrifice must be made if sensible results are to be obtained from differentiation of the data.

The results of this Section serve to show that frequency analysis of biomechanical data will repay further investigation. There appears to be no published work in the field which takes account of the frequency structure of cine information, but the approach will probably become increasingly important and displace intuitive choice of frame speed and of the degree of smoothing to be employed in data analysis.

Extension of the work requires a study of translational and rotational displacements of all body segments, and particularly of the extremities of the limbs, which generally have the highest velocities and accelerations. It will also be informative to analyse body motions influenced by external impact. These should not be classified as voluntary movements, though they may still be non-injurious. Kicking and landing from a downward jump are typical examples in which very high rates-of-change of force are suffered by the body. Later sections of this work demonstrate that accelerations in such cases are much larger than can be produced by voluntary muscular action. Thus, the impact situation may contain important high frequency terms which cannot be regarded as noise.

5.7 Differentiation - Basic Concepts

a) Magnification of errors

Figure 5.4 demonstrates why the errors in derivative estimates are generally much higher than those in the displacement ordinates. If ordinates z_1 and z_2 are subject to error $\pm \delta$, the estimates of gradient in the interval Δt may lie between the extremes AD and BC. To express the order of magnitude of first-derivative errors, consider:-

'True' gradient	=	$(z_2 - z_1)/\Delta t$
AD gradient	=	$(z_2 + \delta - [z_1 - \delta])/\Delta t$
		$(z_2 - z_1)/\Delta t + 2\delta/\Delta t$
Proportional error in AD gradient	=	$2\delta/(z_2 - z_1)$
Proportional error in z - ordinates	=	δ/z_1

The gradient error is much larger than that of the z-ordinates themselves because of the factor 2 in the numerator and the small difference $(z_2 - z_1)$ in the denominator.

b) The effect of data spacing

If the error band is constant for all displacement ordinates there appears to be some advantage in increasing the data spacing to reduce errors in derivative estimates. The effect is shown in Figure 5.5, where the range of gradients AF and BE is somewhat less than that of AD and BC. If, however, the spacing is increased to $n\Delta t$, the derivative estimated over such a large increment is only a crude mean value of the rates-of-change of the true displacement curve, and only a small number of derivative values will be obtained.

FIGURE 5.4

MAGNIFICATION OF ERRORS

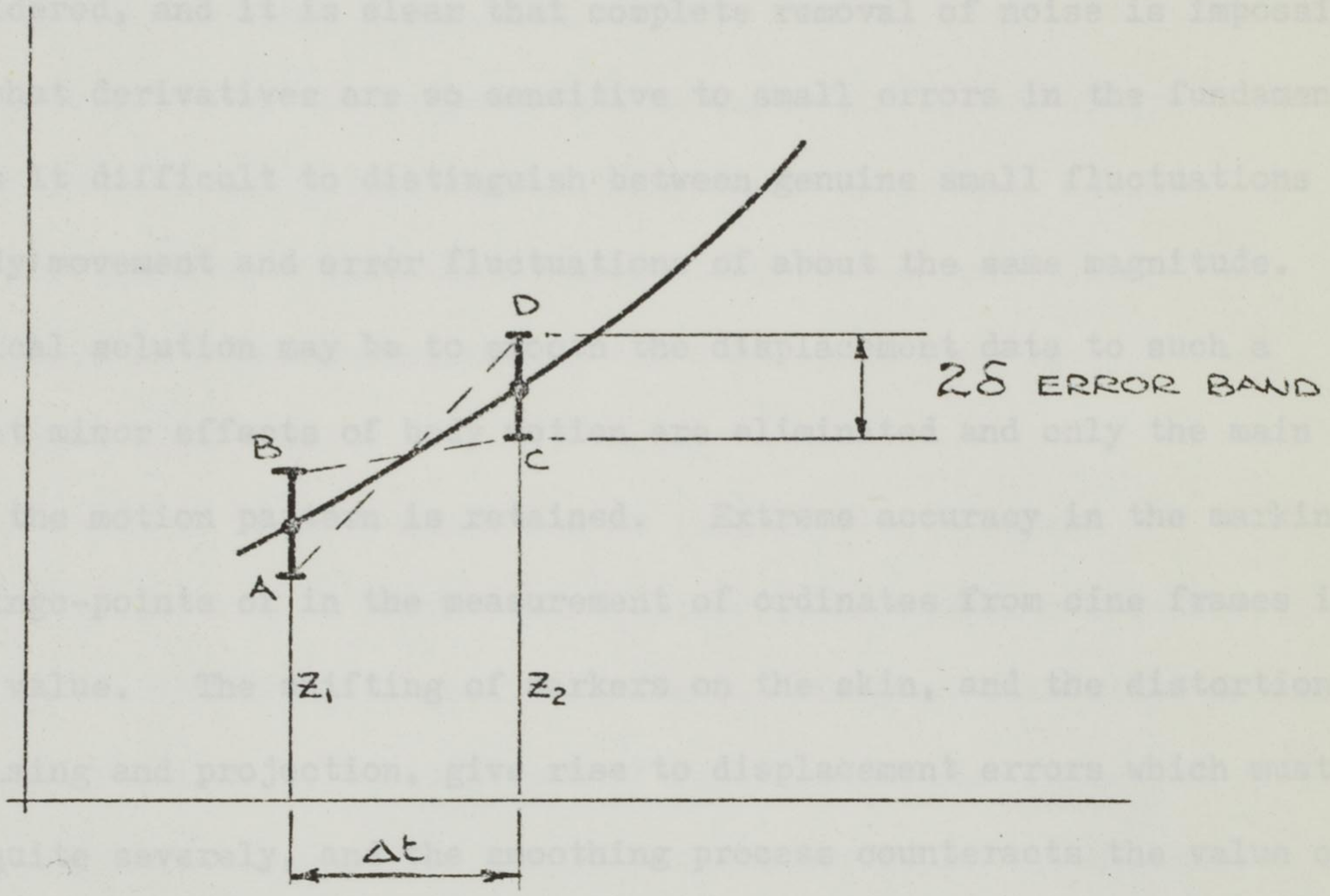

FIGURE 5.5

EFFECT OF DATA SPACING

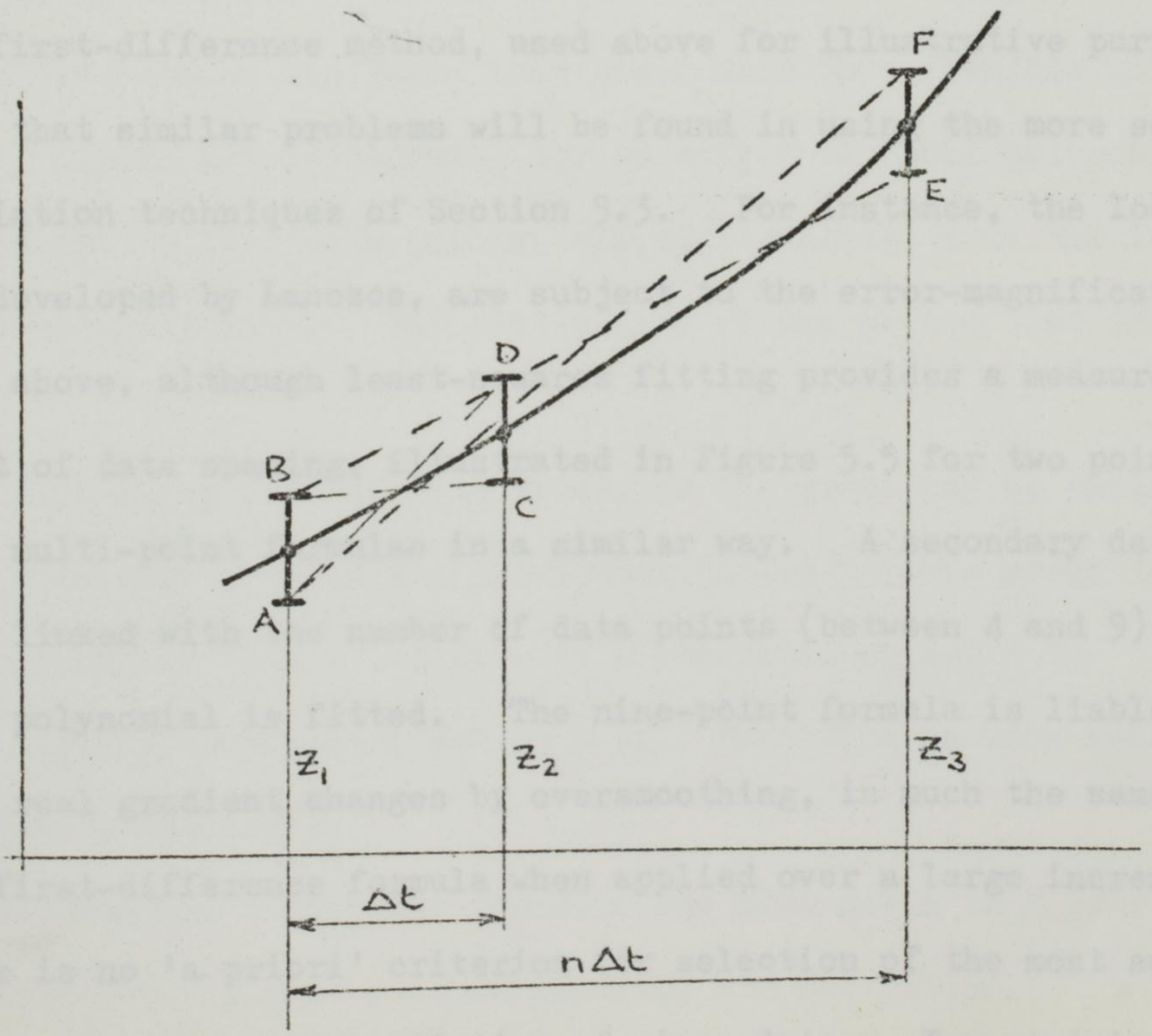

c) A practical approach to the differentiation problem

The obvious answer is to reduce the ordinate error δ by some smoothing process. Initial smoothing of displacements by Fourier methods has already been considered, and it is clear that complete removal of noise is impossible. The fact that derivatives are so sensitive to small errors in the fundamental data makes it difficult to distinguish between genuine small fluctuations due to body movement and error fluctuations of about the same magnitude. The practical solution may be to smooth the displacement data to such a degree that minor effects of body motion are eliminated and only the main course of the motion pattern is retained. Extreme accuracy in the marking of body hinge-points or in the measurement of ordinates from cine frames is of little value. The shifting of markers on the skin, and the distortions due to filming and projection, give rise to displacement errors which must be smoothed quite severely, and the smoothing process counteracts the value of high experimental accuracy. For this reason good quality film of athletic events on track and field may yield as much information as that taken with refined laboratory preparations.

The first-difference method, used above for illustrative purposes, indicates that similar problems will be found in using the more sophisticated differentiation techniques of Section 5.3. For instance, the local polynomial methods, developed by Lanczos, are subject to the error-magnification effects indicated above, although least-squares fitting provides a measure of smoothing. The effect of data spacing, illustrated in Figure 5.5 for two points, will influence multi-point formulae in a similar way. A secondary data spacing effect is linked with the number of data points (between 4 and 9) to which the local polynomial is fitted. The nine-point formula is liable to eliminate real gradient changes by oversmoothing, in much the same way as does the first-difference formula when applied over a large increment.

There is no 'a priori' criterion for selection of the most suitable local polynomial for differentiation of given data. Two empirical tests

are proposed to check the validity of differentiation processes:-

(i) Apply several different derivative formulae to a typical data set and compare results, especially those for the sensitive second derivative.

(ii) Select one or two formulae on the basis of (i) and apply them to acceleration calculations for a whole-body motion performed on a force-platform. Compare the resultant force with the corresponding curve obtained from the force-platform.

On the basis of these comparisons it is possible to select differentiation procedures which take a middle path between oversensitivity to noise and oversmoothing of real variations. Only at this stage should one apply the formulae to calculations of acceleration and force for individual segments necessary in a more detailed study of the motion.

5.8 Lanczos' Local Polynomial Differentiation

a) Principles

The Lanczos technique is chosen in preference to other methods listed in Section 5.4 because his basic idea gives rise to a flexible group of formulae. Figure 5.6 illustrates the principle of local polynomial least-squares fitting to five data points, and differentiation of the function for the mid-point derivative. The flexibility of the method lies in two factors:-

(i) The number, r, of data points in the group may be varied.

(ii) The order, s, of the polynomial fitted to this group is variable (s = 1....r-1); a quadratic or cubic is usually employed (s=2 or 3). Smoothing is more severe with smaller s.

Seven-point and nine-point formulae are also given on Figure 5.6. Special forms for the end-point derivatives are not quoted.

FIGURE 5.6

LOCAL POLYNOMIAL DIFFERENTIATION

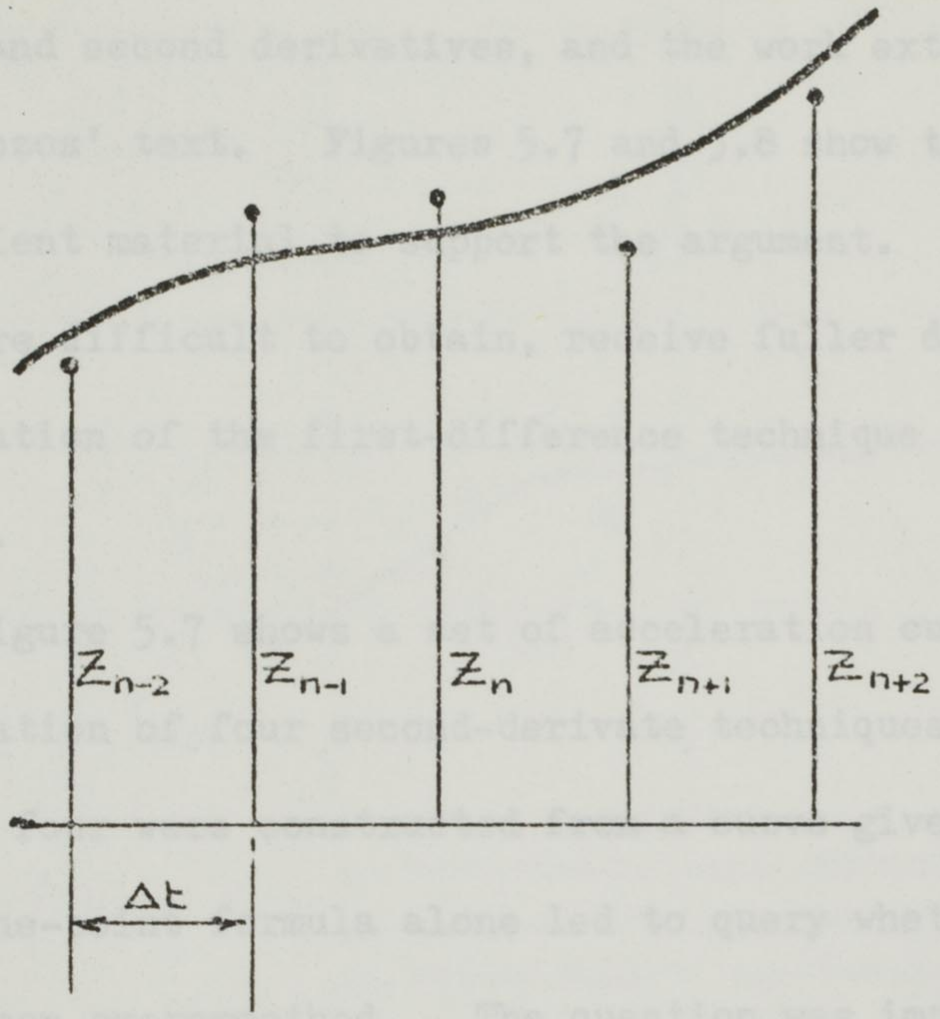

THIRD ORDER FITTED POLYNOMIAL ON FIVE POINTS

$$Z = C_0 + C_1 t + C_2 t^2 + C_3 t^3$$

COEFFICIENTS C EVALUATED BY LEAST SQUARES

SECOND DERIVATIVE:-

$$\ddot{Z} = 2C_2 + 6C_3 t$$

$$= 2C_2 \quad \text{AT } t = 0$$

STANDARD FORMS

i. FIVE-POINT, THIRD ORDER, SECOND DERIVATIVE

$$a_n = \frac{2Z_{n-2} - Z_{n-1} - 2Z_n - Z_{n+1} + 2Z_{n+2}}{7(\Delta t)^2}$$

SECOND ORDER, SECOND DERIVATIVE:

2. SEVEN-POINT

$$a_n = \frac{9Z_{n-3} + 6Z_{n-2} - 5Z_{n-1} - 20Z_n - 5Z_{n+1} + 6Z_{n+2} + 9Z_{n+3}}{100\,(\Delta t)^2}$$

3. NINE-POINT

$$a_n = \frac{4Z_{n-4} + 4Z_{n-3} + Z_{n-2} - 4Z_{n-1} - 10Z_n - 4Z_{n+1} + Z_{n+2} + 4Z_{n+3} + 4Z_{n+4}}{100\,(\Delta t)^2}$$

b) Comparisons between formulae

A number of comparisons have been made between the available formulae for first and second derivatives, and the work extended to cases not covered in Lanczos' text. Figures 5.7 and 5.8 show typical results and give sufficient material to support the argument. The second derivatives, being the more difficult to obtain, receive fuller discussion and results of double application of the first-difference technique are presented as an independent method.

Figure 5.7 shows a set of acceleration curves obtained by the application of four second-derivate techniques. The displacement data common to all four were constructed from a curve given by Paul (6). His use of the nine-point formula alone led to query whether the accelerations might have been oversmoothed. The question was important because the accelerations were used in calculations of forces in joints during walking. The curves of Figure 4.7 suggest that the nine-point formula applies rather severe smoothing, while the five-point, with no initial smoothing of data, leads to erratic results. Intuitively, the compromises offered by the other two curves are more satisfactory.

Figure 5.8 gives results of four second-derivative processes applied to vertical displacement data on the shin mass-centre during the drop-landing of Chapter 4. The data were smoothed 'by eye' prior to differentiation. Again, the first-difference and five-point formulae agree acceptably while the seven and nine-point methods appear to oversmooth the acceleration peaks.

A number of comparisons of this kind led to the adoption of three methods for general application to cine analysis of human movement.

(i) First differences with smoothing 'by eye' for velocity and acceleration calculations on a desk calculator.

(ii) The five-point, second order, first-derivative form for velocity:

$$V_n = \frac{-2Z_{n-2} - Z_{n-1} + Z_{n+1} + 2Z_{n+2}}{10.\Delta t}$$

FIGURE 5.7 COMPARISONS BETWEEN DIFFERENTIATION PROCEDURES

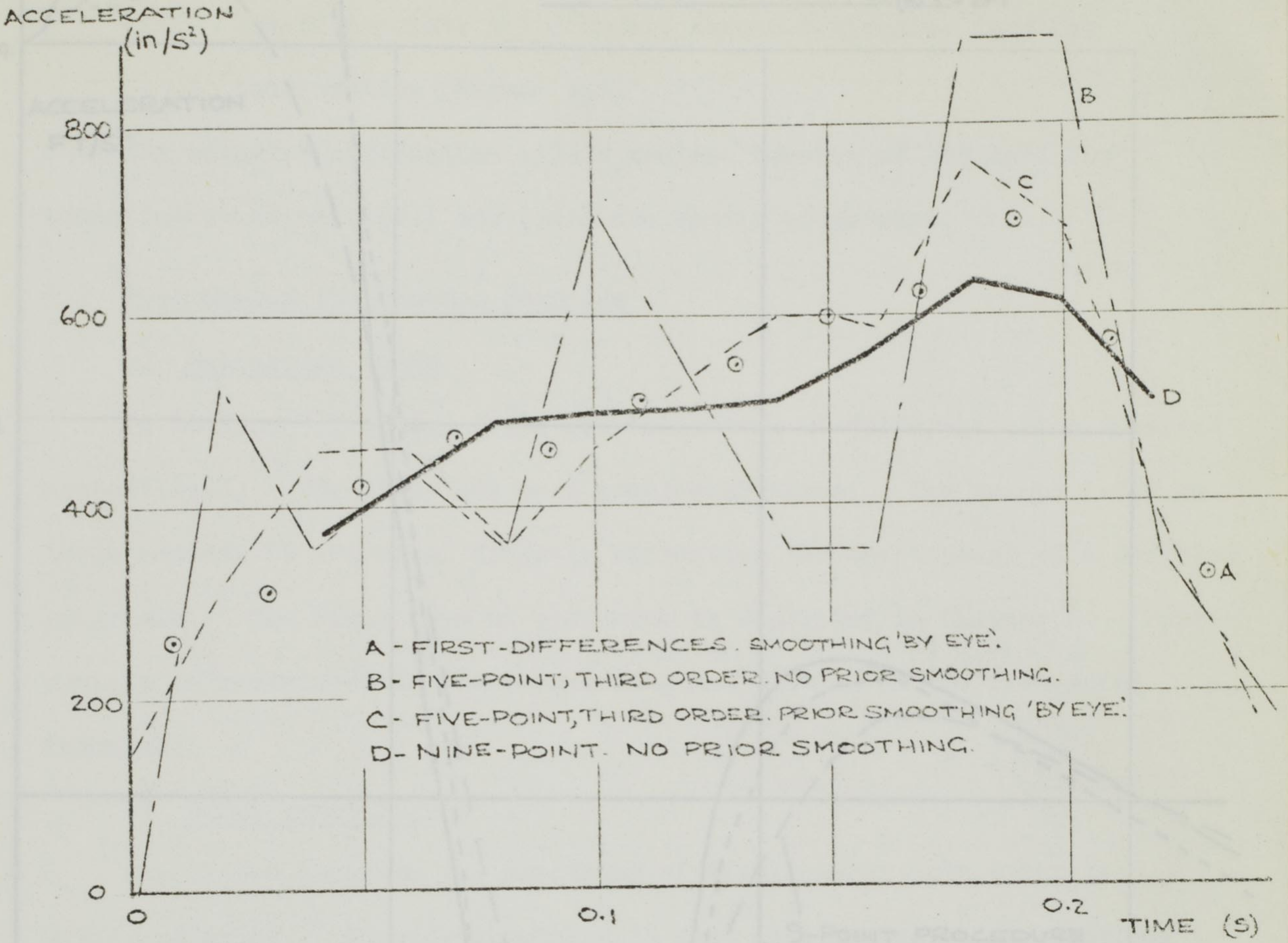

DISPLACEMENT DATA FOR DIFFERENTIATION

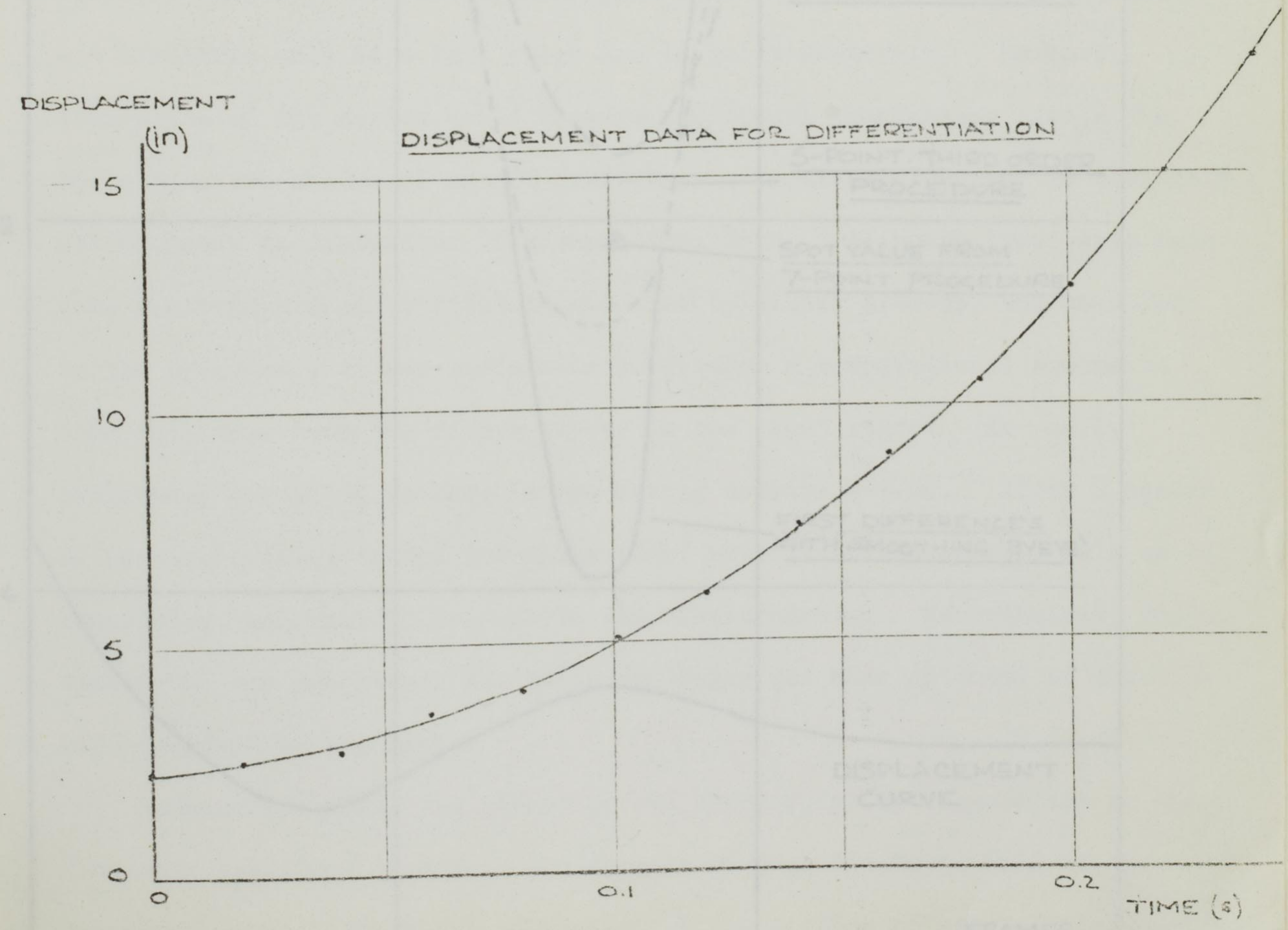

FIGURE 5.8

ACCELERATION OF $G_{(BLL+BF)}$

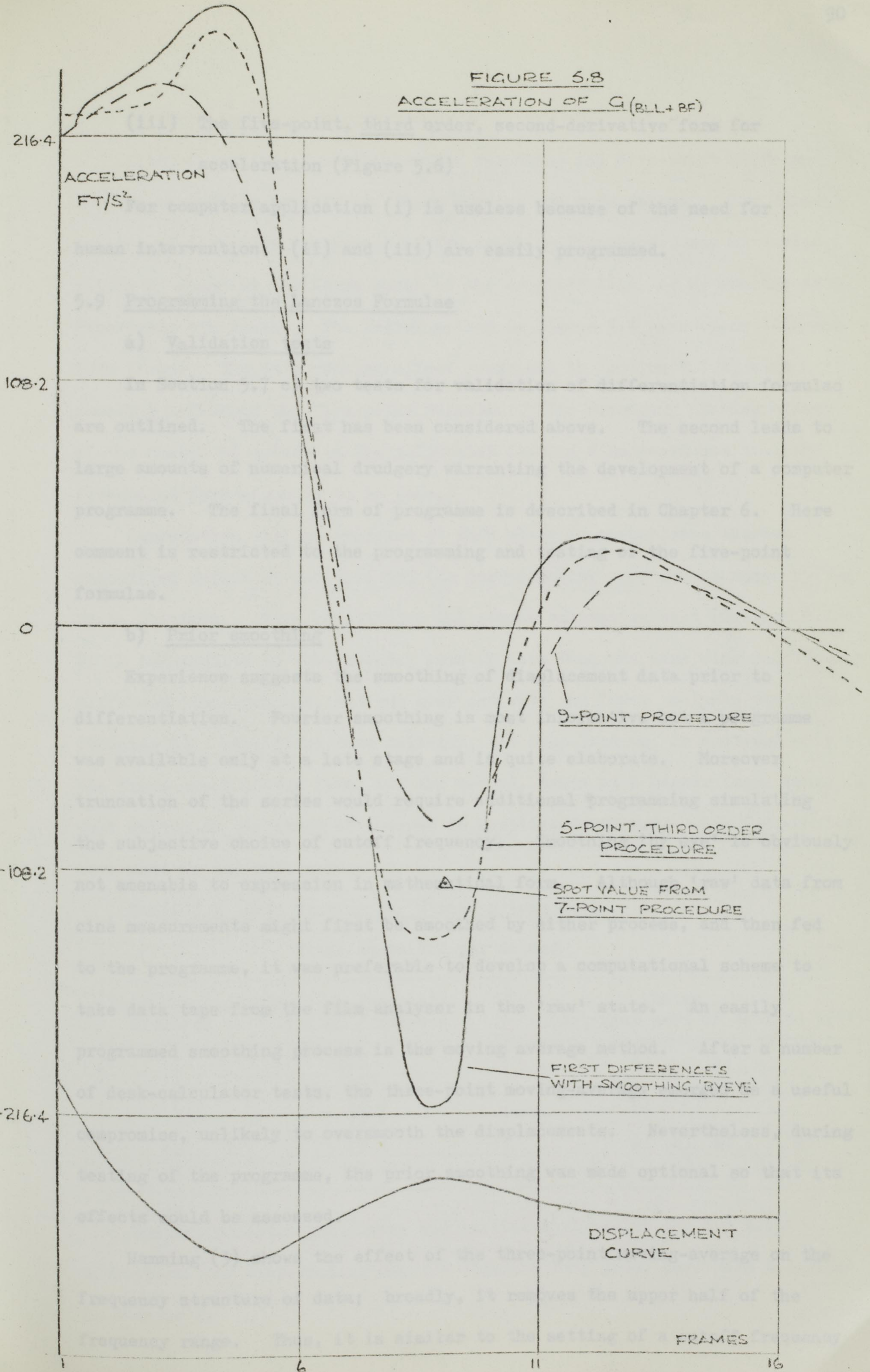

(iii) The five-point, third order, second-derivative form for acceleration (Figure 5.6)

For computer application (i) is useless because of the need for human intervention; (ii) and (iii) are easily programmed.

5.9 Programming the Lanczos Formulae

a) Validation tests

In Section 5.7 c) two tests for validation of differentiation formulae are outlined. The first has been considered above. The second leads to large amounts of numerical drudgery warranting the development of a computer programme. The final form of programme is described in Chapter 6. Here comment is restricted to the programming and testing of the five-point formulae.

b) Prior smoothing

Experience suggests the smoothing of displacement data prior to differentiation. Fourier smoothing is most informative but a programme was available only at a late stage and is quite elaborate. Moreover truncation of the series would require additional programming simulating the subjective choice of cutoff frequency. Smoothing 'by eye' is obviously not amenable to expression in mathematical form. Although 'raw' data from cine measurements might first be smoothed by either process, and then fed to the programme, it was preferable to develop a computational scheme to take data tape from the film analyser in the 'raw' state. An easily programmed smoothing process is the moving average method. After a number of desk-calculator tests, the three-point moving-average emerged as a useful compromise, unlikely to oversmooth the displacements. Nevertheless, during testing of the programme, the prior smoothing was made optional so that its effects could be assessed.

Hamming (3) shows the effect of the three-point moving-average on the frequency structure of data; broadly, it removes the upper half of the frequency range. Thus, it is similar to the setting of a cutoff frequency

c) Data input to the programme

After selection of moving-average smoothing and five-point differentiation as working procedures, there remains one more option. The time-spacing of data (the reciprocal of the sampling frequency), may be varied, either by changing the frame speed of the original film, or by reading data from every nth frame. The latter method in Figure 5.2 uses every 10th and 20th frame. The data spacing effect described in Section 5.7 b) will somewhat influence the five-point formula. (The secondary spacing effect of the number of points in the polynomial formula disappears now that the five-point form alone is to be used.)

Computation will be employed at this stage in comparisons between calculated thrust at the feet and the corresponding reaction measured by the force platform. This constitutes the second validation test (Section 5.7 c)) It is informative to take several sets of data from the same cine record with different time-spacings, and run each set with the force analysis programme (Chapter 6). The first test activity, the drop-landing, is analysed only at the frame speed of the film, but the second, taken at a higher frame speed is well suited to the study of changes in sampling frequency. Six frequencies were used in the test runs:-

Table 5.2 Data Spacing for Standing Long Jump

Frame speed 224 per second

Data spacing (frames)	Sampling frequency (item / second)	Notes (relevant part of Section 5.11)
1	224	b) c) e)
4	56	e)
5	44.8	c)
6	37.3	
10	22.4	c) d) e) g)
20	11.2	b) d) f) g) h)

The experimental procedures and initial analyses of the two test activities, the drop-landing and the standing long jump, have been described in Chapter 4.

5.10 Force Comparisons for the Drop-Landing

The experimental procedure and the results of a preliminary desk-calculator study are presented in Chapter 4. Figure 5.9 adds force computations from the programme of Chapter 6. Some general points concerning the comparisons should be borne in mind:-

a) Only screen measurements of displacement are used. Analyser readings were taken, but gave dubious results via the programme. Considerable noise appeared in the results and they are not presented here.

b) Vertical force components only are used. (Chapter 4)

c) Arm motion is not included. (Chapter 4)

d) The initial peak recorded by the force platform cannot be computed from film data. (Chapter 4)

e) Synchronisation of the force platform record with computed curves is based on general agreement of maxima and minima. (Chapter 4)

f) The end values (frames 1, 2 and 18, 19) are less reliably computed than the central group. In the five-point formula, two synthetic displacement points are created by extrapolation at the ends of the range to allow some estimate of end-point accelerations.

In assessing the effectiveness of the computation, two points may be made:-

(i) Oversmoothing of the force peak at frame 5 occurs in both computational methods, but fairly good agreement is achieved over the more moderate rates-of-change later in the motion. This result suggests that, around frames 2-6, a finer data spacing in the displacements would have been valuable. However, as I have shown with Fourier smoothing, and will reinforce in the next Section, the additional information provided by the higher sampling frequency is useless if it is inextricably mixed with noise at the higher frequencies.

FIGURE 5.9 DROP-LANDING

TOTAL VERTICAL FORCE

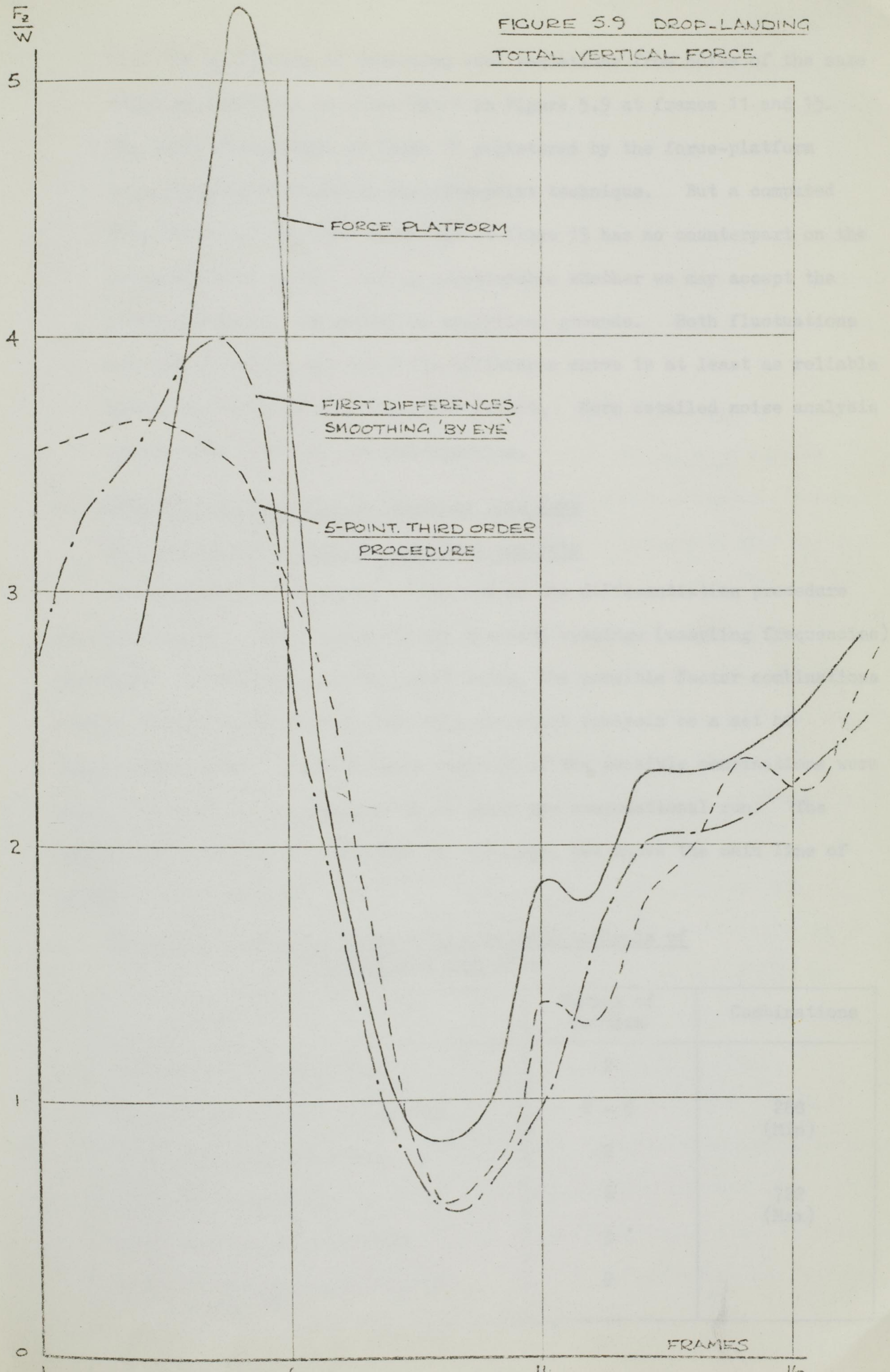

(ii) The difficulty of isolating real variations from noise of the same order of magnitude is illustrated in Figure 5.9 at frames 11 and 15. The small fluctuation at frame 11 registered by the force-platform is apparently detected by the five-point technique. But a computed fluctuation of the same magnitude at frame 15 has no counterpart on the force platform curve. It is questionable whether we may accept the first and ignore the second on analytical grounds. Both fluctuations are due to noise, and the first-difference curve is at least as reliable as the more capricious five-point result. More detailed noise analysis would throw light on the discrepancies.

5.11 Force Comparisons for the Standing Long Jump

a) Factors affecting the numerical analysis

The influence of a number of factors on the differentiation procedure was considered. Table 5.2 gives the six data spacings (sampling frequencies) employed. With other factors listed below, the possible factor combinations number several hundred, each requiring numerical analysis on a set of displacement data. In fact, only about 30 of the possible combinations were taken, but each factor appeared in at least one computational run. The summary in this Section condenses the findings, but shows the main line of argument as it emerged.

Table 5.3 Factors affecting the numerical analysis of Standing Long Jump data

Factor	Number of Factors	Combinations
Velocity and acceleration	2	
Typical segments and whole-body	2 - 5	288 (Min)
Screen and Analyser data	2	
Sampling frequencies	6	722 (Max)
Zero, one and two smoothings	3	
First-difference and five-point formulae	2	

The basic cine data are presented in Chapter 4. A four-segment model forms the basis of the vertical force analysis. The remainder of this Section gives comments on the sequence of graphs in Figures 5.10 and 5.16.

b) Figure 5.10 Smoothing of analyser displacements

One run of 3-pt m.a. smoothing on film analyser ordinates is applied at 1-frame spacing. The smoothing is insufficient. It appears that the three points at 20-frame spacing may be adequate to define the smooth displacement curve.

c) Figure 5.11 Segment velocities at three data spacings

The erratic nature of velocities obtained for the smoothed 1-frame displacements of Figure 5.10 is contrasted with the more acceptable 5-frame and 10-frame results. The latter two, however, differ appreciably and will lead to widely differing acceleration curves.

d) Figure 5.12 Body mass-centre velocities at two data spacings

These velocities are obtained by the summation of segmental momenta. 3-pt m.a. smoothing is applied to all displacements at entry to the programme. The curves illustrate the further smoothing introduced by the wider data spacing. Both curves are of reasonable form but we have no criterion for choosing between them at this stage.

The marked smoothing effect of 20-frame spacing has already been observed, but even at this spacing there remain some fluctuations in the fundamental displacement curves of Chapter 4 which appear to justify the blanket use of 3-pt m.a. smoothing at entry to the force analysis programme.

e) Figure 5.13 Segment accelerations at three data spacings

The 1-frame acceleration curve puts in its place the vague idea that increasingly fine data spacing provides increasingly more accurate information. The effects of very heavy smoothing on 1-frame data are achieved with much less effort and, in future runs, with considerable saving in film, by reducing the sampling frequency well below 224 per second. The 5-frame and 10-frame curves are more acceptable, although there are still considerable acceleration

FIGURE 5.10. DISPLACEMENT OF MASS-CENTRE OF LOWER LEG PLUS FOOT.
1-FRAME SPACING.

—— DIRECT READING.

--- AFTER 3 PT. MOVING-AVERAGE SMOOTHING.

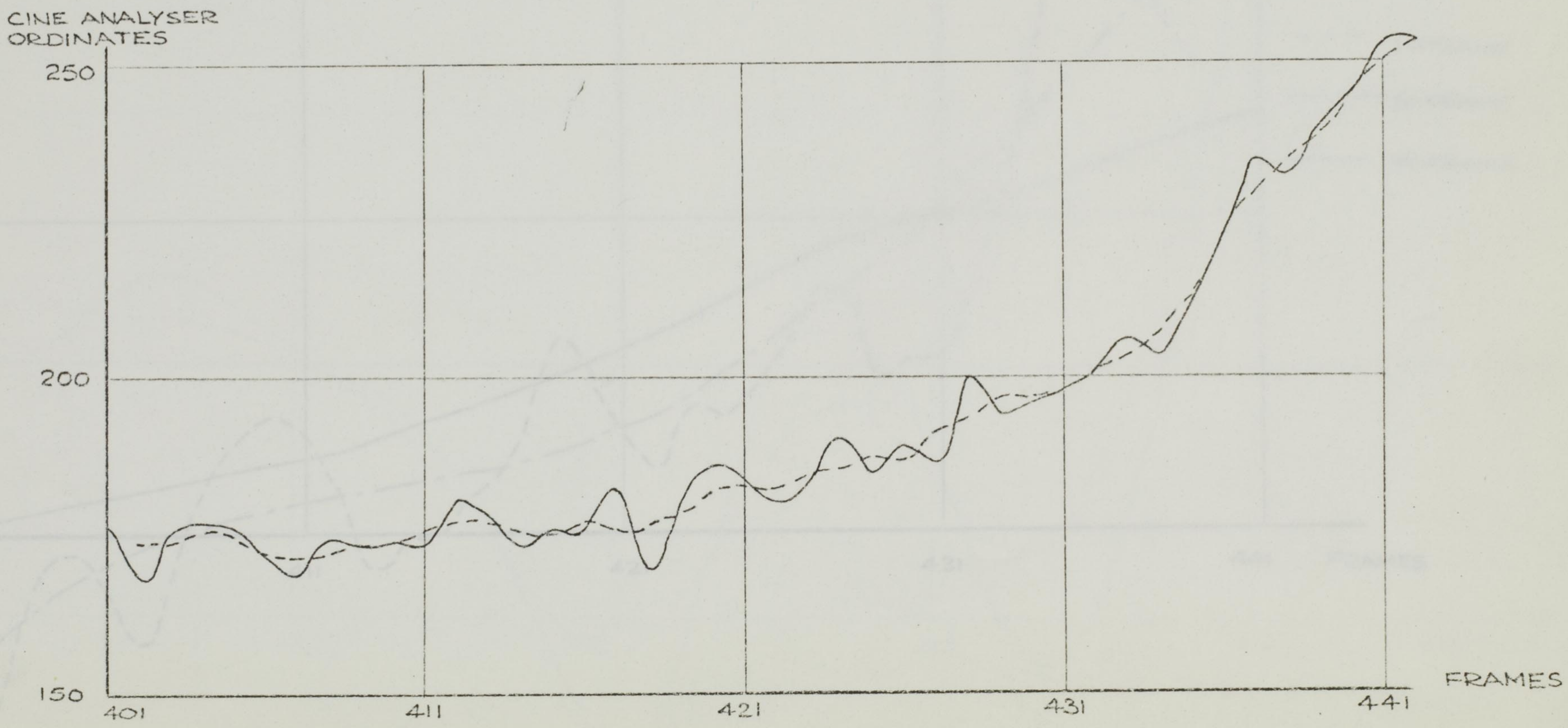

FIGURE 5.11
VELOCITY OF G (BLL+BF)
AT THREE DATA-SPACINGS
(BASED ON 1-FRAME DATA SMOOTHED BY 3-PT MOVING AVERAGE)

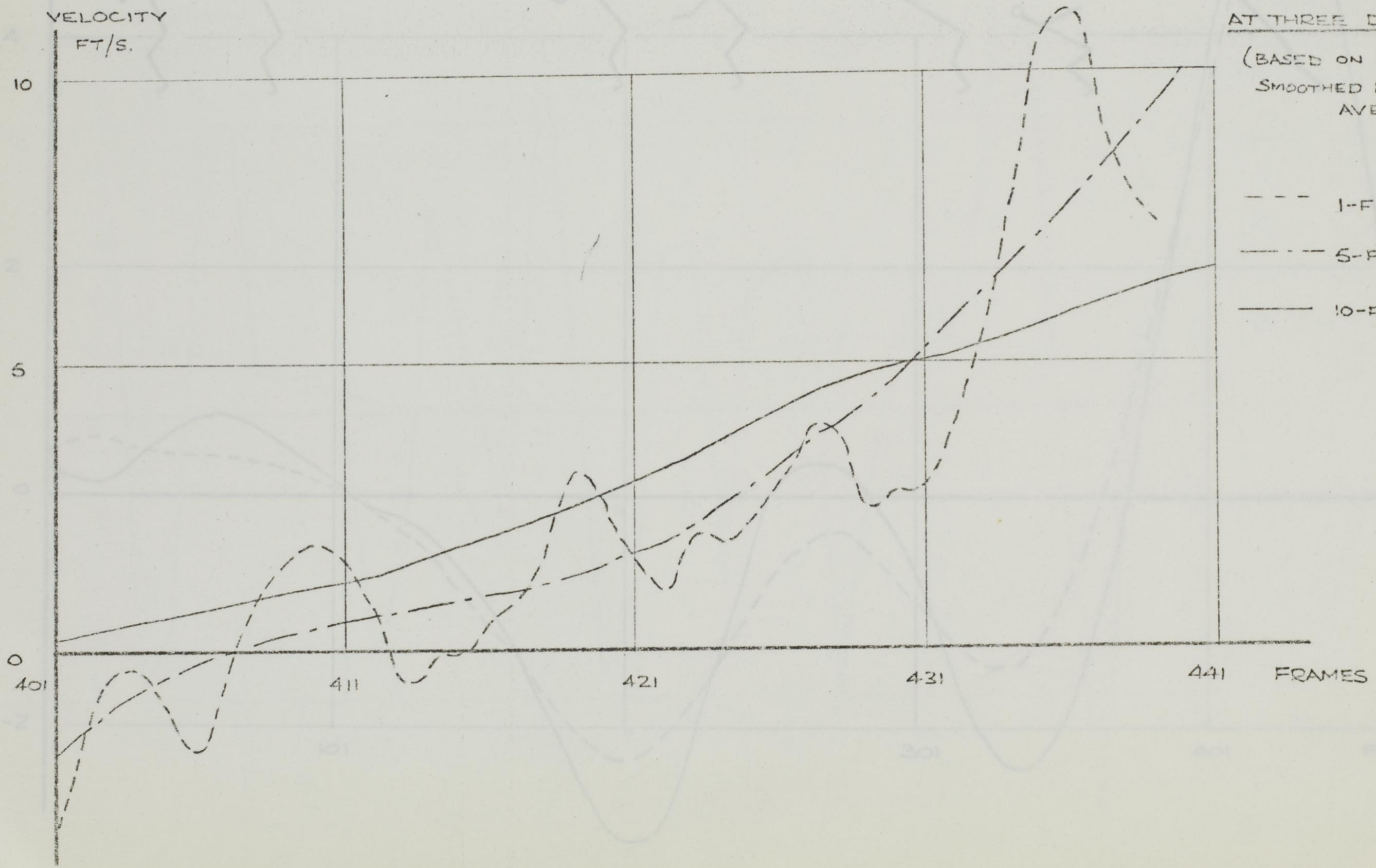

FIGURE 5.12 STANDING LONG JUMP
VELOCITY OF WHOLE-BODY MASS-CENTRE

——— 10-FRAME DATA
– – – 20-FRAME DATA

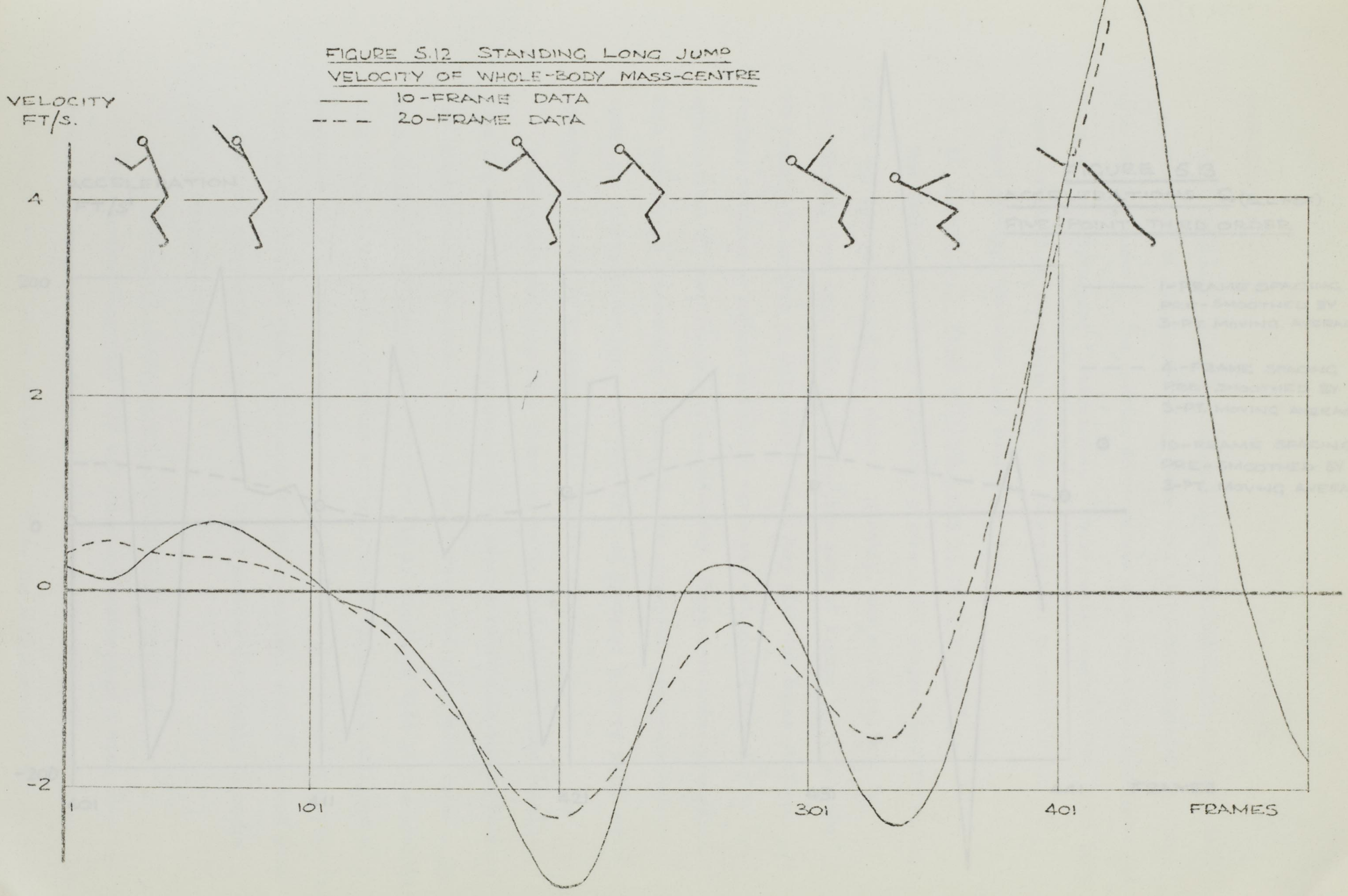

FIGURE 5.13

ACCELERATIONS G (BLL+BF)

FIVE-POINT. THIRD ORDER

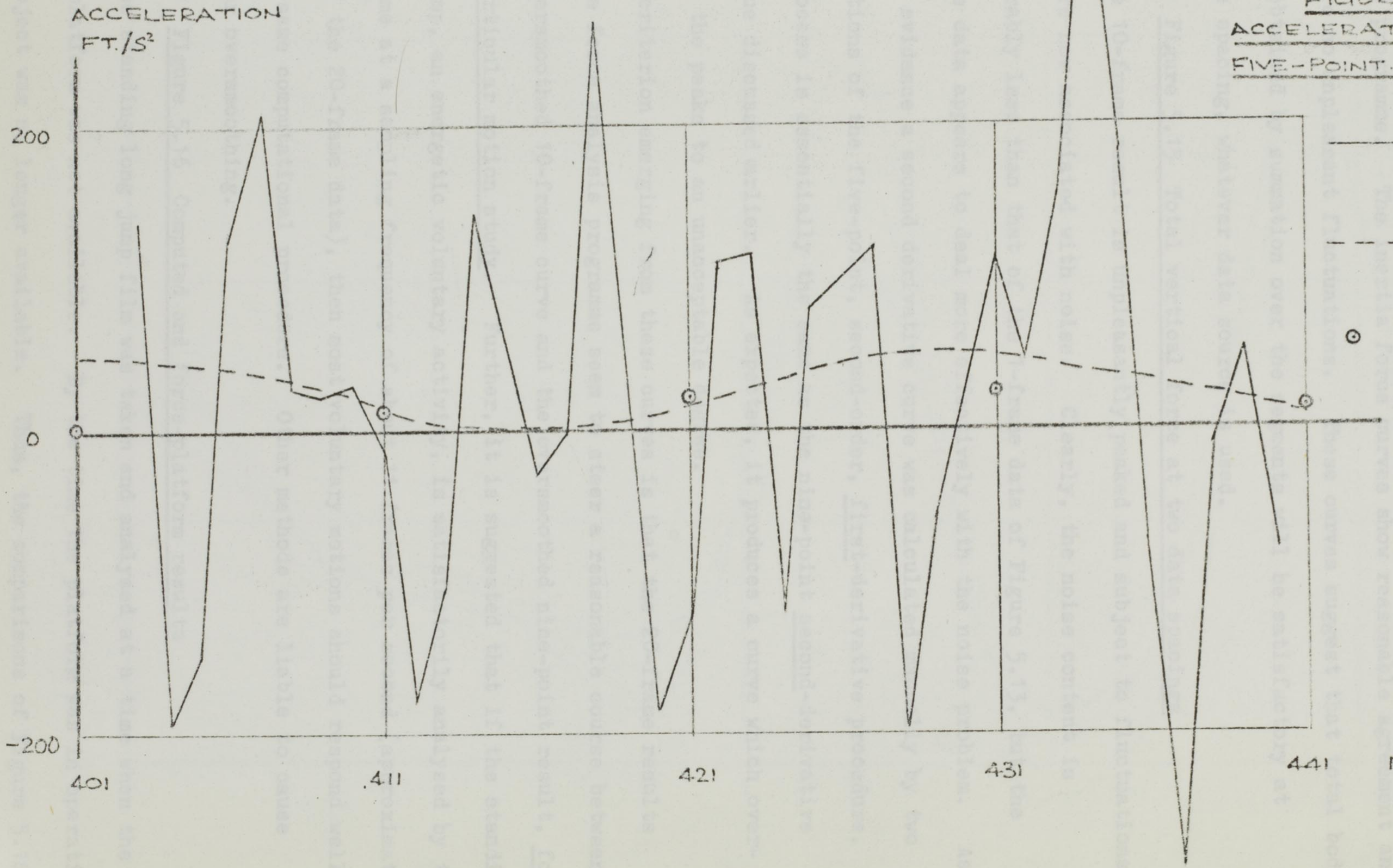

variations in the former.

f) Figure 5.14 Segment inertia forces from screen and analyser data

Both sets of displacement data were read at 20-frame spacing and run with the programme. The inertia force curves show reasonable agreement and there are no unpleasant fluctuations. These curves suggest that total body forces obtained by summation over the segments will be satisfactory at 20-frame spacing, whatever data source is used.

g) Figure 5.15 Total vertical force at two data spacings

The 10-frame result is unpleasantly peaked and subject to fluctuations which are now associated with noise. Clearly, the noise content is considerably less than that of the 1-frame data of Figure 5.13, but the 20-frame data appears to deal more effectively with the noise problem. As further evidence a second derivative curve was calculated manually by two applications of the five-point, second-order, first-derivative procedure. This process is essentially the same as the nine-point second-derivative technique discussed earlier. As expected, it produces a curve which oversmooths the peaks to an unacceptable degree.

A criterion emerging from these curves is that the 20-frame results from the force analysis programme seem to steer a reasonable course between the undersmoothed 10-frame curve and the oversmoothed nine-point result, for this particular motion study. Further, it is suggested that if the standing long jump, an energetic voluntary activity, is satisfactorily analysed by the programme at a sampling frequency of about 11 frames per second (approximately that of the 20-frame data), then most voluntary motions should respond well to the same computational procedure. Other methods are liable to cause under or oversmoothing.

h) Figure 5.16 Computed and force-platform results

The standing long jump film was taken and analysed at a time when the force-platform was not available. By the time the platform was in operation, the subject was no longer available. Thus, the comparisons of Figure 5.16

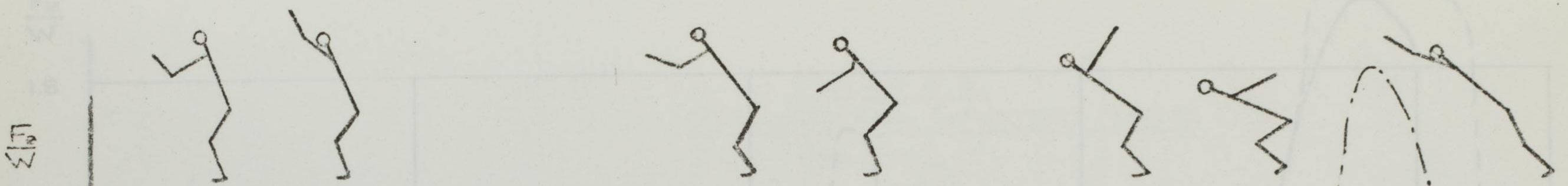

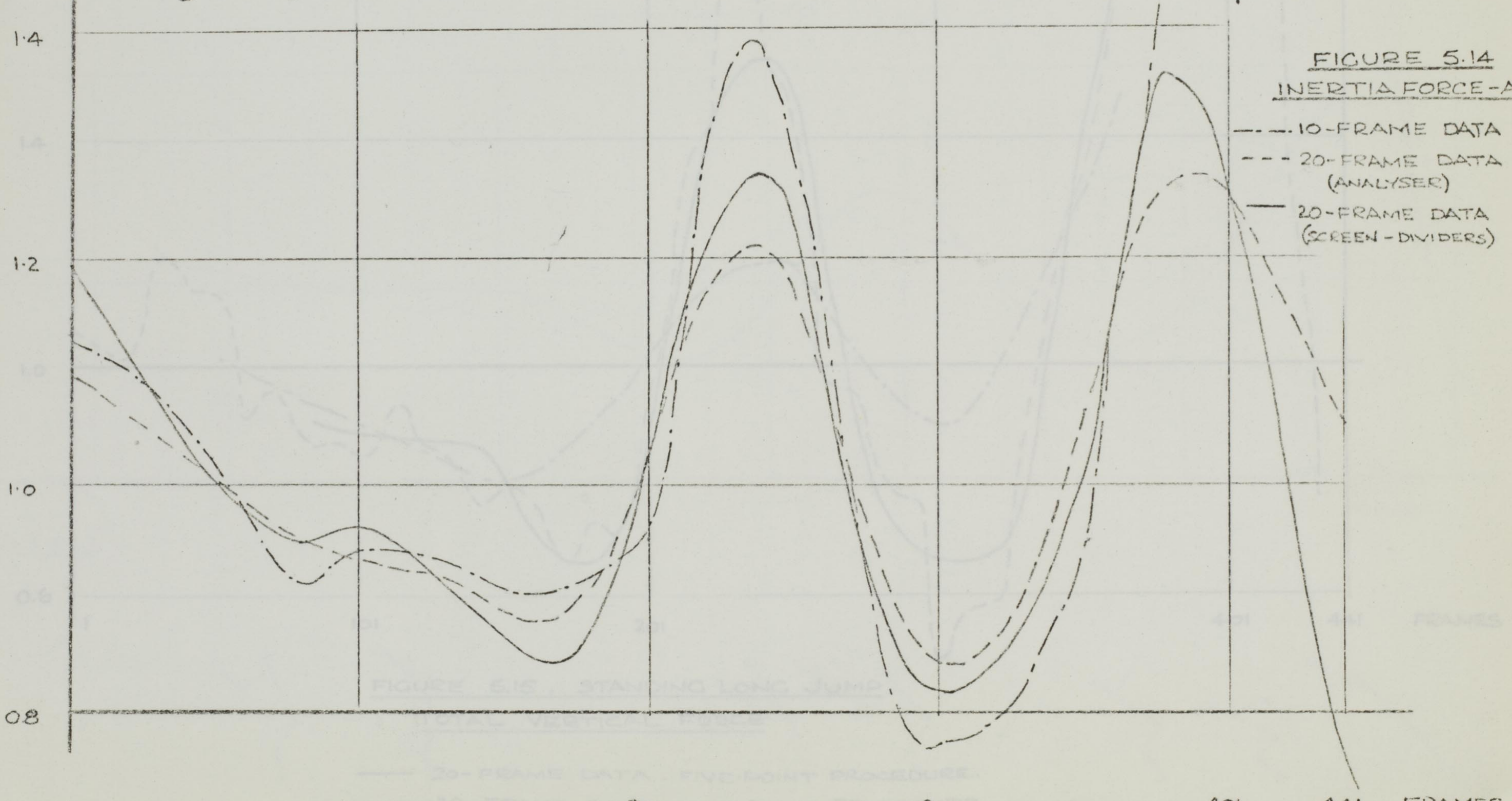

FIGURE 5.14
INERTIA FORCE-ARM

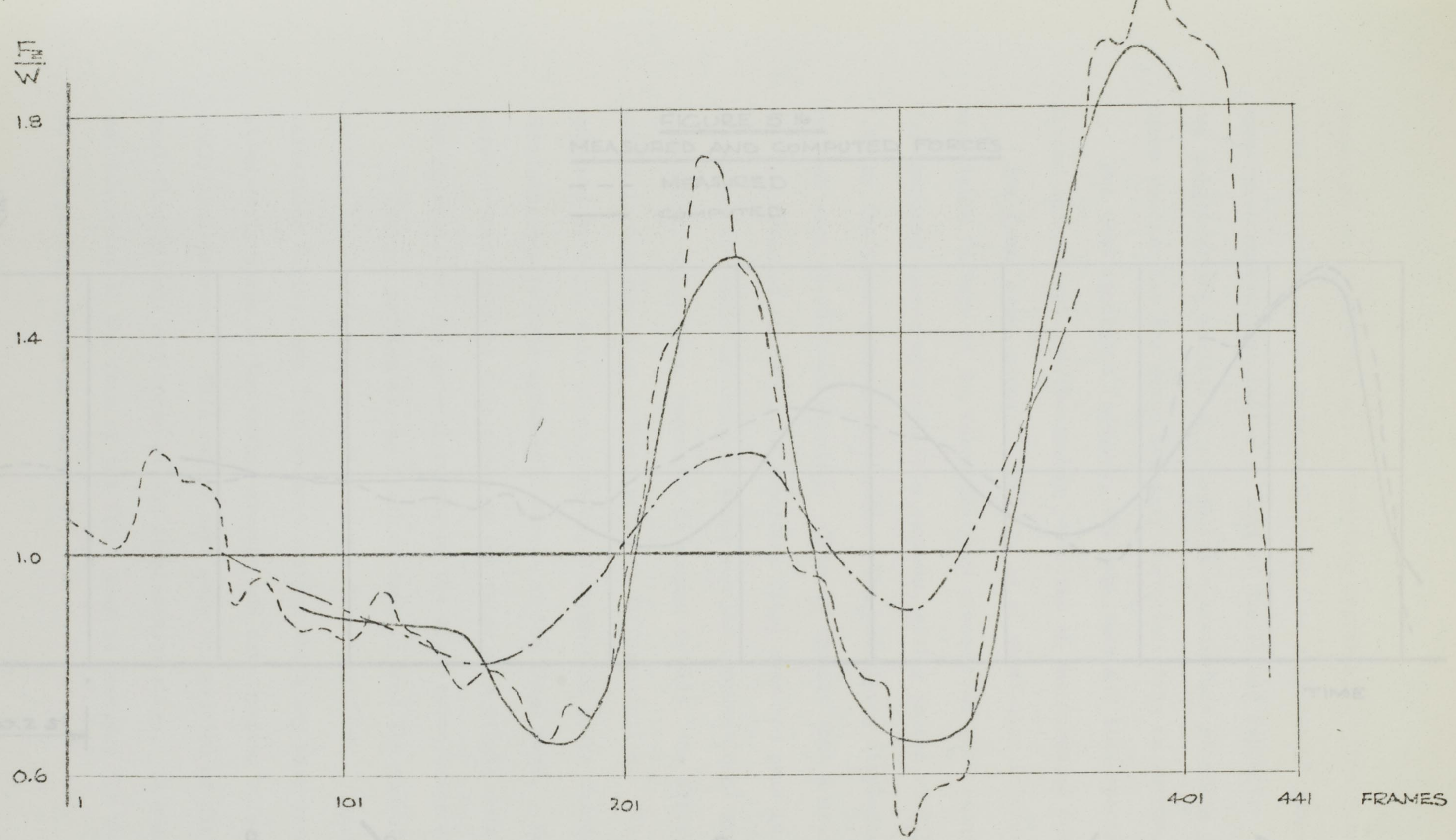

FIGURE 5.15 . STANDING LONG JUMP

TOTAL VERTICAL FORCE

—— 20-FRAME DATA . FIVE-POINT PROCEDURE.

—·—· 20-FRAME DATA . NINE-POINT PROCEDURE.

- - - - 10-FRAME DATA . FIVE-POINT PROCEDURE.

FIGURE 5.16

MEASURED AND COMPUTED FORCES

– – – MEASURED

——— COMPUTED

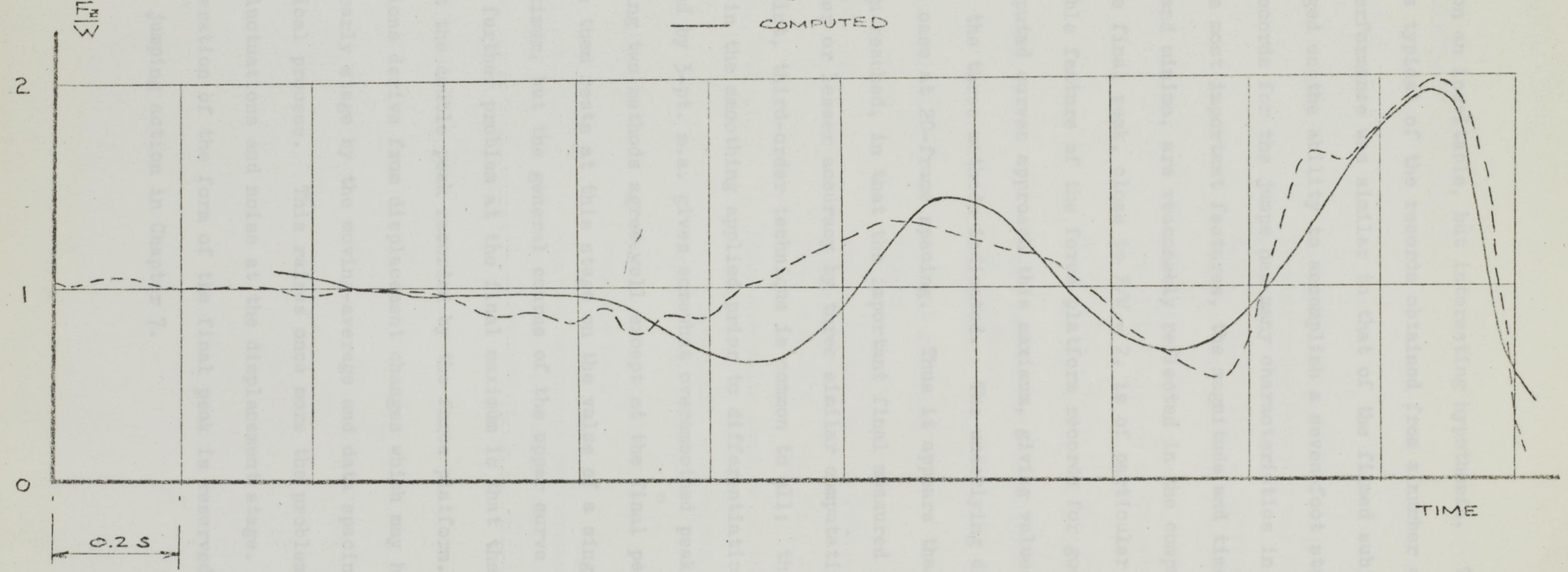

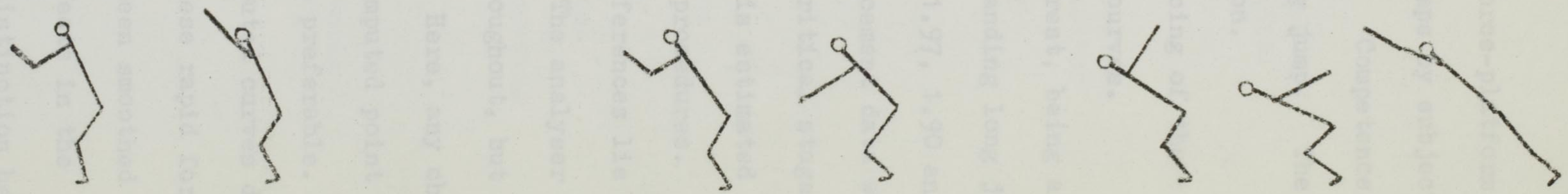

depend on an inevitable, but interesting hypothesis. The force-platform curve is typical of the records obtained from a number of jumps by subjects whose performance was similar to that of the filmed subject. Competence was judged on the ability to accomplish a seven-foot standing jump. The force records for the jumps had many characteristics in common.

The most important features, the magnitude and time-spacing of the maxima and minima, are reasonably reflected in the computed curves.

The final peak, close to F/W = 2, is of particular interest, being a repeatable feature of the force platform records for good standing long jumps. The computed curves approach this maximum, giving values of 1.97, 1.90 and 1.82 by the three methods indicated. The underlying displacement data was in each case at 20-frame spacing. Thus it appears that a critical stage has been reached, in that the important final measured peak is estimated to a greater or lesser accuracy by three similar computational procedures. The five-point, third-order technique is common to all; the differences lie solely in the smoothing applied prior to differentiation. The analyser data smoothed by 3-pt. m.a. gives somewhat oversmoothed peaks throughout, but the remaining two methods agree well except at the final peak. Here, any choice between them rests at this stage on the value of a single computed point at the maximum, but the general course of the upper curve seems preferable.

A further problem at the final maximum is that the computed curves do not exhibit the double peak recorded by the force platform. These rapid force variations derive from displacement changes which may have been smoothed out at an early stage by the moving-average and data spacing effects in the analytical process. This raises once more the problem of distinction between real fluctuations and noise at the displacement stage. A more detailed consideration of the form of the final peak is reserved for the discussion of the jumping action in Chapter 7.

5.12 References for Chapter 5

(1) Andrew, D.D., 'An investigation of methods of Curve Fitting using Periodic and Exponential functions' M.Sc. Dissertation in Electronic Computation, University of Leeds (1971)

(2) Cook, J.B., 'Development of a procedure incorporating a modified version of Forsythe's method for polynomial curve fitting' 4A Project. Dept. of Computational Science, University of Leeds (1971)

(3) Hamming, R.W. 'Numerical Methods for Scientists and Engineers' McGraw Hill (1962)

(4) Lanczos, C., 'Applied Analysis' Pitman (1967)

(5) Paul, J.P., 'Forces Transmitted by Joints in the Human Body' Proc. 1 Mech.E. 181 Pt.3 J Paper 8 (1966)

(6) Paul, J.P., 'Bioengineering studies of the forces transmitted by joints'(ii) in 'Biomechanics and Related Engineering Topics' ed. Kenedi (1965)

(7) Plagenhoef, S., 'Patterns of Human Motion' Prentice Hall (1971)

(8) Wallach, J., Saibel, E., 'Control mechanism performance criteria for an above-knee prosthesis' J. Biomechanics 3. 1. 87-97 (1970)

Chapter 6

A Computer Programme for Force Analysis

6.1 Introduction

In essence the programme uses the equations:-

$$F_z - W = M\ddot{\bar{z}} = m_1\ddot{z}_1 + m_2\ddot{z}_2 + m_3\ddot{z}_3 + \ldots\ldots \qquad (3.3\text{-}1), (3.3\text{-}2)$$

set out in Chapter 3.

As input, z-displacement data for the body hinge points are read from cine film frame-by-frame. Scaling constants and segmental parameters are also required.

The programme first computes segmental mass-centres. Each is then put through a 3-point moving-average smoothing routine. These smoothed values are retained for later computation, but are also used to calculate the values of whole-body mass-centre displacement on the basis of equation (3.2-2).

The segmental mass-centre ordinates are next differentiated for velocity and acceleration values by local polynomial differentiation. (Chapter 5). Summation of the resulting inertia forces provides numerical evaluation of:-

$$m_1\ddot{z}_1 + m_2\ddot{z}_2 + m_3\ddot{z}_3 + \cdots\cdots \qquad (A)$$

As an independent check the whole-body mass-centre ordinates are also taken through the differentiation procedures to give:-

$$M\ddot{\bar{z}} \qquad (B)$$

Comparison between (A) and (B) is easily made on the printed output and provides both a computational check and a validation of the summation principle on which the programme is based.

A secondary summation check may be made on the basis of momentum (equation (3.2-3))

A block diagram of the programme is given in Figure 6.1 and the full ALGOL text in Section 6.7.

Figure 6.1 Single Component Force Analysis

Programme Block Diagram

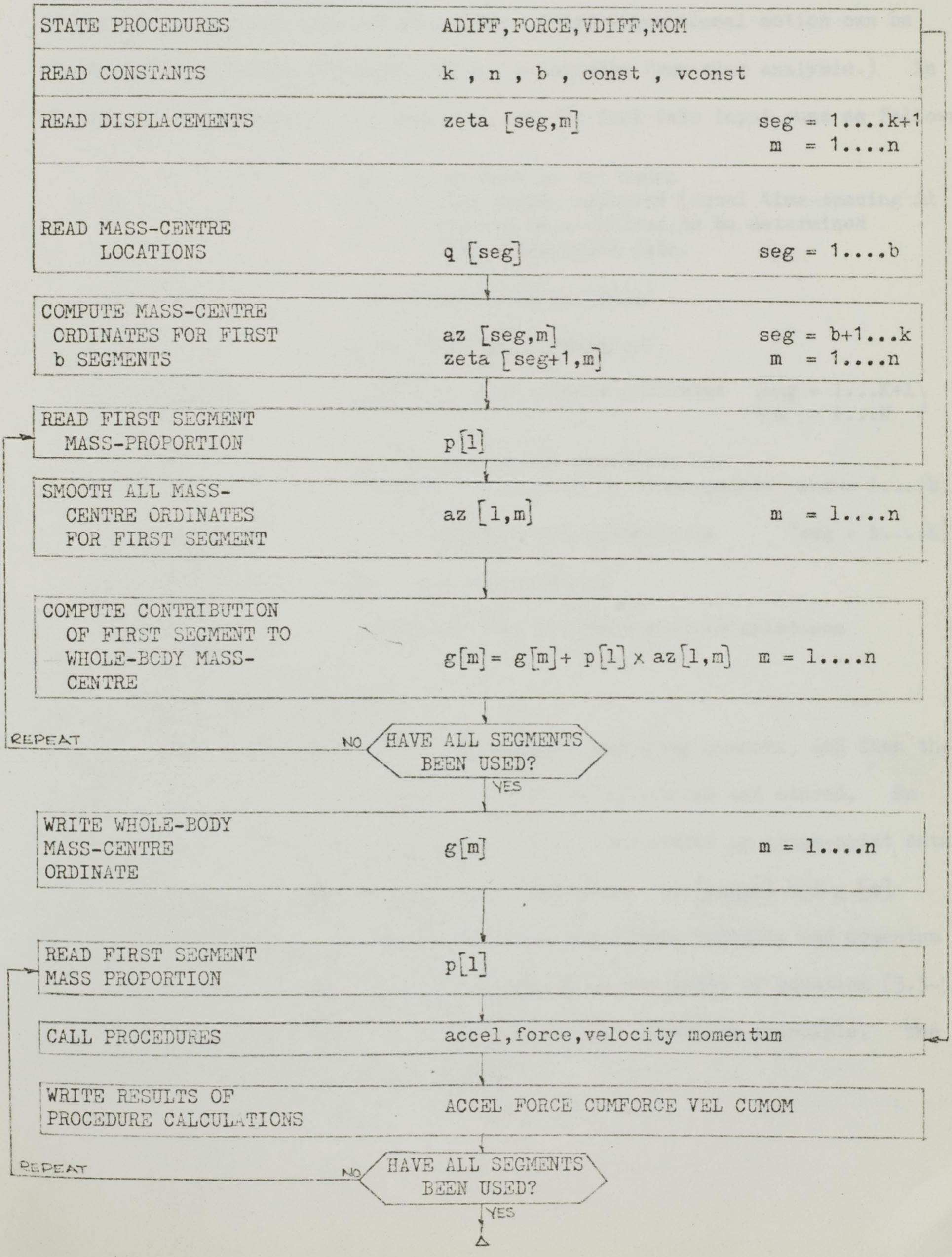

6.2 Data Input

The programme deals with displacement data for all segments in a segmental representation of human motion. For plane motion the data may be read from cine film in two distinct sets, for the z- and the x-component displacements. The programme handles one set at a time. (Three-dimensional motion can be handled if the y-axis displacements are obtainable from cine analysis.) In addition, some constants are required, and the full data input runs as follows:

K	no. of segments in the model
N	no. of cine frames employed (equal time-spacing Δt)
b	no. of segment mass-centres to be determined from hinge-point data.
const	cine-film linear scale/Δt^2
vconst	cine-film linear scale/Δt
zeta [seg,m]	matrix of displacement ordinates (seg = 1...K+1; m = 1...N)
q [seg]	set of mass-centre locations for segments determined by hinge-points (seg = 1....b)
p [seg]	set of segment mass-proportions (seg = 1....K)
p [seg]	the above set repeated
1.0	unity mass for the whole-body calculations

6.3 Computational Equations

The displacement data is taken through a smoothing process, and then the co-ordinates of the whole-body mass-centre are calculated and stored. En route, the mass-centres of segments initially represented by hinge-point data are also determined. These mass-centre ordinates az [seg,m] and g [m] go through procedures for acceleration, inertia force, velocity and momentum computation. Cumulative force is calculated on the basis of equation (3.3-5). Cumulative momentum (cumom) is based on a similar summation principle. The working equations are indicated below:-

a) Segment Mass-Centre from Hinge Points

Take the lower-leg-foot segment as an example. Given the value of q [1], locating the mass-centre of the combined segment the programme uses the equation:-

$$az[1,m] = zeta[2,m] - q[1]\left(zeta[2,m] - zeta[1,m]\right)$$

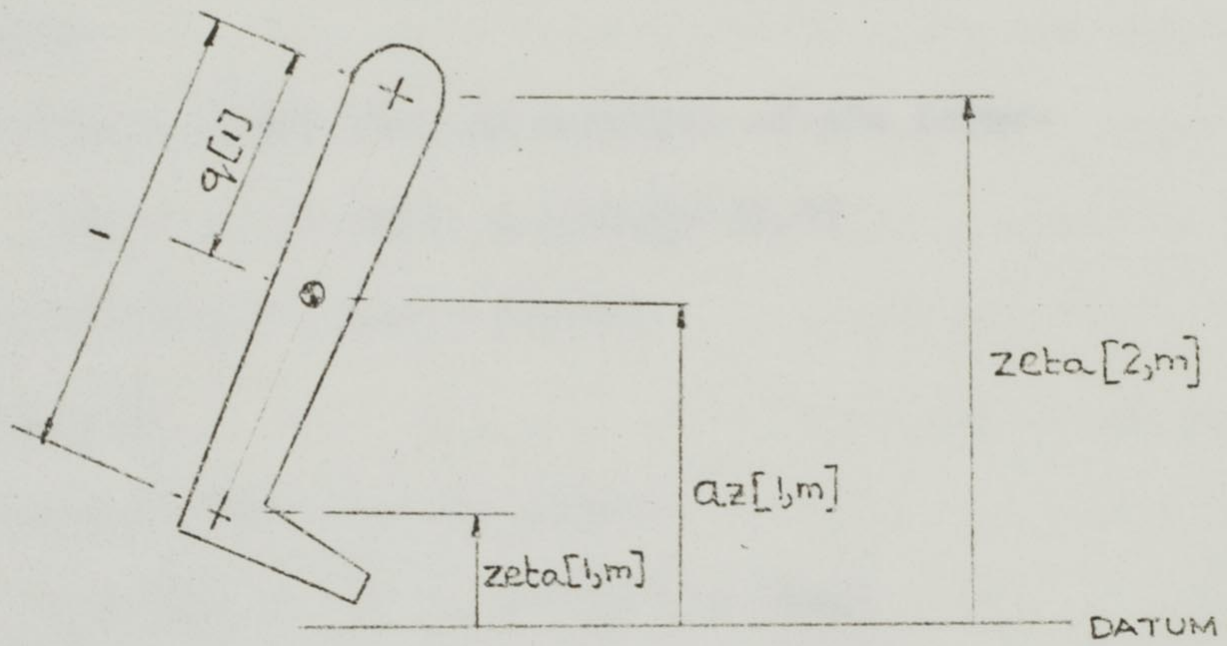

b) Smoothing

The displacements are put through a three-point moving average process in the form:-

$$sm[seg,m] = \frac{az[seg-1,m] + az[seg,m] + az[seg+1,m]}{3}$$

The end points are left as :-

$$sm[seg,1] = az[seg,1]$$

$$sm[seg,N] = az[seg,N]$$

c) Whole-Body Mass-Centre

Given the values p [seg] (seg = 1.....K), the z-co-ordinates of the whole-body mass-centre are obtained by summation over all K segments:-

seg = 1

g [m] = g [m] + p [seg] x az [seg,m]

seg = seg + 1

repeat until seg = K

d) Velocity

The procedure VDIFF uses the 5-point second order least squares technique given by Lanczos:-

$$v_3 = (-2w_1 - w_2 + w_4 + 2w_5)/10$$

There are special forms for end point values.

e) Acceleration

The procedure ADIFF uses the 5-point third-order least squares form given by Lanczos:-

$$a_3 = (2w_1 - w_2 - 2w_3 - w_4 + 2w_5)/7$$

f) f) Force

The procedure FORCE uses an equation of the form:-

$$F/W = a \times \text{const} \times p[\text{seg}]/ 32.17$$

to give nondimensional inertia forces.

g) Momentum

The procedure MOM uses the form:-

$$\text{momentum} = v \times \text{vconst} \times p[\text{seg}]$$

to give momenta in the units:- mass-proportion x velocity $(ft/s^2.)$

Both FORCE and MOM also incorporate summation processes over the segments to produce CUMFORCE and CUMOM in the units indicated above.

6.4 Flexibility of the Programme

(i) Normal data input presupposes that the displacements zeta [seg,m] will be given in the following form:-

Frame	Hinge 1	Hinge 2	Mass-centre K-1	Mass-centre K
1	Zeta [1,1]	Zeta [2,1]	Zeta [K,1]	Zeta [K+1,1]
N	Zeta [n,1]			Zeta [K+1,n]

This (N x (K+1)) matrix is reduced to an (NxK) matrix by the evaluation of the mass-centres of the first b segments. It is essential that the hinge-points follow one another in sequence through the body. The usual order would be: Ankle, Knee, Hip, Shoulder, Elbow, Wrist. Segments whose mass-centres are read in directly are added in order at the end of each row of the matrix. Other types of data input or special output requirements may be accommodated as follows:-

(ii) Input consisting entirely of hinge points

Output in terms of mass-centres:-

Set b = K and provide q [seg] for seg = 1....K

(iii) Input consisting entirely of mass-centres.

Output in terms of mass-centres:-

Set b = 1 and q [1] = 0 . No other q's are required.

Also provide a first column in the matrix to represent a dummy hinge point. This column may consist entirely of 1's; the zeta values themselves are quite arbitrary.

This technique is also suitable when only hinge points are considered.

6.5 Typical Programme Output

A sample of the programme output is given in Figure 6.2. The comparisons between segmental sums and whole-body quantities are indicated by the connected boxes. The first comparison is between CUMOM for all segments and VEL for the whole-body mass-centre. The second is between CUMFORCE for all segments and FORCE for the whole body. These form checks on the nondimensional momentum and inertia-force relationships:

$$\sum_j \frac{m_j}{M} \cdot \dot{z}_j = \dot{\bar{z}}$$

$$\sum_j \frac{m_j}{M} \cdot \ddot{z}_j = \ddot{\bar{z}}$$

6.6 Extension of the Programme

The programme, as it stands, accepts a single component set of displacements and numerical results are illustrated for the z-components. Data tape from the PCD-Vanguard film analyser may be used directly as input if only z-components are read. However, the analyser is able to read x-z displacement pairs for each hinge point. Such a data tape may be used if the programme is preceded by a simple sorting routine which splits the matrix of x-z pairs into separate x and z displacement matrices. Two

FIGURE 6.2

TYPICAL FORCE ANALYSIS PROGRAMME OUTPUT

ACCEL	FORCE	CUMFORCE	VEL	CUMM	
+120.416	+0.483	+0.483	-1.739	-0.224	
+79.112	+0.317	+0.317	-0.093	-0.013	
+37.807	+0.152	+0.152	+0.543	+0.070	
+2.950	+0.012	+0.012	+1.101	+0.142	FIRST
+34.779	+0.139	+0.139	+1.618	+0.209	SEGMENT
+94.782	+0.380	+0.380	+3.240	+0.418	
+119.478	+0.479	+0.479	+5.240	+0.676	
+71.882	+0.288	+0.288	+7.799	+1.006	
+24.286	+0.097	+0.097	+10.107	+1.304	
+8.441					
-1.662					
-0.326					

INTERMEDIATE SEGMENTS

ACCEL	FORCE	CUMFORCE	VEL	CUMM	
+316.017	+1.120	+4.489	+22.750	+4.870	
+186.017	+0.659	+2.301	+25.039	+6.518	
+56.017	+0.199	+1.113	+18.786	+5.279	FINAL
-50.800	-0.130	+0.061	+19.031	+5.382	SEGMENT
-67.095	-0.238	+1.010	+17.860	+6.283	
-72.918	-0.258	+1.289	+16.344	+7.093	
-121.784	-0.432	-0.327	+13.810	+7.076	
-244.877	-0.868	-4.200	+10.702	+6.453	
-367.970	-1.304	-8.073	+6.682	+4.922	
+10.600					
+15.960					
+9.742					

ACCEL	FORCE	CUMFORCE	VEL	CUMM	
+144.976	+4.507	+3.995	+4.373	+9.742	
+90.268	+2.306	+5.607	+6.521	+13.039	
+35.560	+1.105	+2.219	+5.282	+10.560	WHOLE-
+1.758	+0.055	+0.116	+5.333	+11.765	BODY
+32.225	+1.020	+2.034	+6.283	+12.566	MASS-
+41.226	+1.282	+2.570	+7.092	+14.195	CENTRE
-10.551	-0.328	-0.655	+7.077	+14.153	
-134.328	-4.176	-8.375	+6.454	+12.907	
-259.105	-8.023	-16.096	+4.928	+9.849	

successive runs of the programme will produce the x and z inertia forces.

A second, more elaborate extension would incorporate the equations for rotational motion developed in Chapter 3. Programming of the expressions for moment of momentum and its rate-of-change has not yet been attempted. Variation of body moment of inertia must be incorporated and the M.I. Factor results in Chapter 2 will be useful in this context. Input to the equation will be in the form of segmental angles and it will probably be more convenient to compute these from hinge point ordinates than to attempt direct measurement of angles from the film. An outline of these extensions is shown in Figure 6.3.

The rotational motion section of the extended programme has several uses:-

a) As an independent check on the x and z forces computed by the existing translational motion programme. This check is useful when external forces such as ground reaction are to be computed.

b) As a source of the internal moments at the body joints. These values are important in the estimation of muscle and joint-force actions during motion.

c) As a description of complex aerial motion where the only external force is gravity, and the translational equations provide trivial results.

In its provision of joint moments the outline scheme of Figure 6.3 stands as an alternative to Plagenhoef's programme (Chapter 3). It uses a fundamentally different set of working equations, with no Coriolis components and with linear rather than angular displacements as input. One advantage over Plagenhoef's approach is that no appeal to a quasi-fixed starting point within the body needs to be made. The displacements are measured quite naturally with respect to a fixed x-z reference system on the film analyser or by direct methods with dividers and ruler.

FIGURE 6.3

PROGRAMME DEVELOPMENT

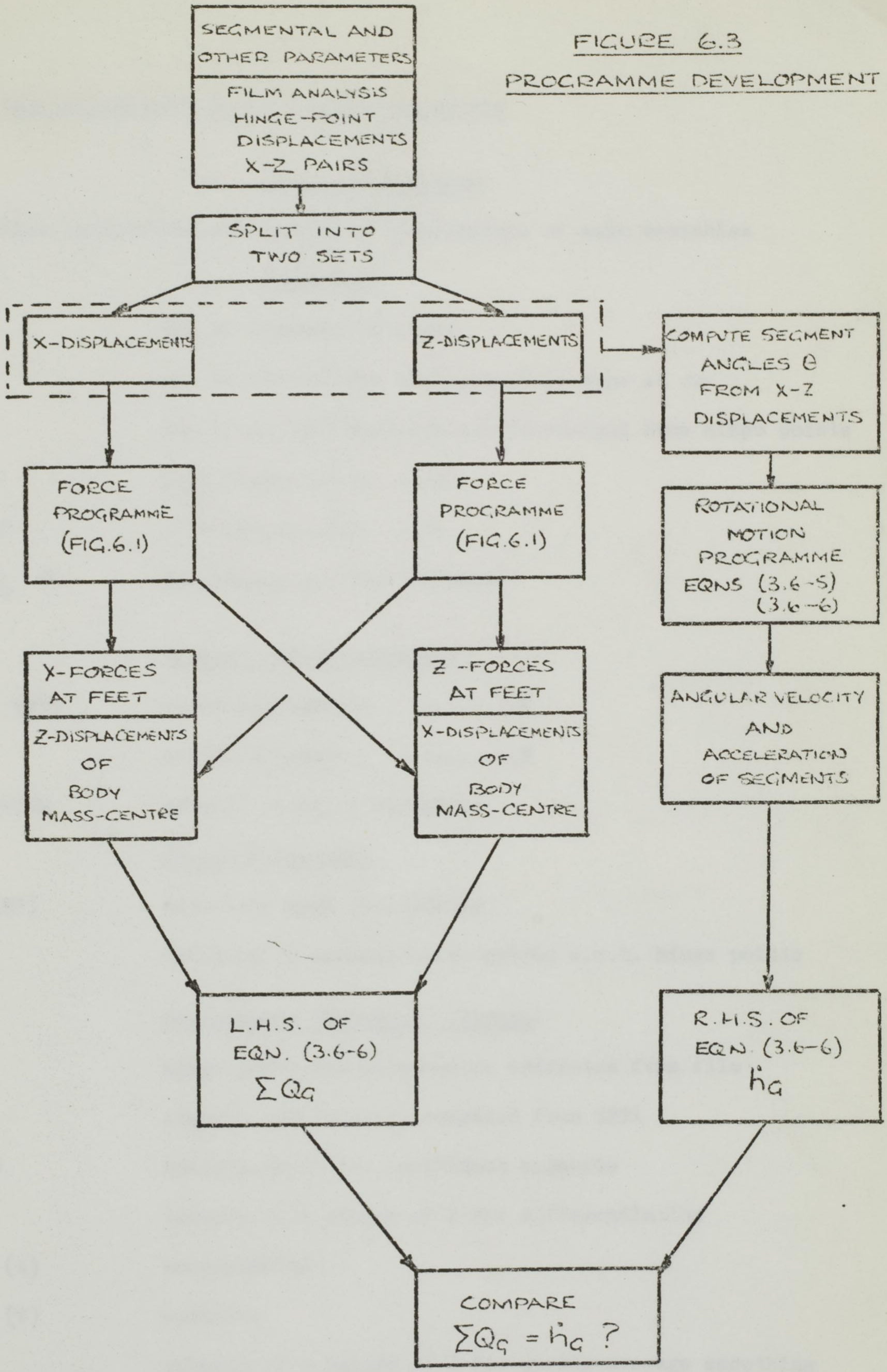

NOTE: EQN. (3.6-6):-

$$\Sigma Q_G = F_x \bar{z} + F_z (x' - \bar{x}) = \frac{d}{dt}\left[I_{G(inst)} . \Omega + \sum_j h_{j(rel)} \right] = \dot{h}_G$$

6.7 Single-Component Force Analysis Programme

a) Programme Notation

Variables in brackets are procedure counterparts of main variables

Constants

K	no. of segments in model
N	no. of cine frames equi-spaced in time at Δt
B	no. of segment mass-centres determined from hinge points
CONST	film linear scale $/ \Delta t^2$
VCONST	film linear scale $/ \Delta t$
F_1 F_2 F	specifying printout formats

Integer valued variables

SEG (NS)	counting segments 1.....K
M	counting frames 1.....N
R,S,TWICE	general counting variables

Preset Parameters

P (MP)	segmental mass proportions
Q	location of segment mass-centres w.r.t. hinge points

Subscripted Variables (Arrays)

ZETA	hinge-point and mass-centre ordinates from film
AZ	segment mass-centres computed from ZETA
Z , Y	subsets of AZ for individual segments
U	subsets of 5 points of Y for differentiation
ACC (A)	acceleration
VEL (V)	velocity
SM	subsets of 3 points of Z for moving-average smoothing
G	whole-body mass-centre co-ordinates
F (FS)	inertia force
SUM (SIGMA)	cumulative inertia force
TM (TOT)	cumulative momentum

b) PROGRAMME TEXT

. . .

```
CO. BELEOVR←
BELEOVRØ2APU **OK
C↑FE
```

```
←
!COMMENT A PROGRAM FOR SINGLE-COMPONENT FORCE ANALYSIS OF
         A SEGMENTAL MODEL;

!BEGIN !INTEGER K,N,M,SEG,B,R,F1,F2,F3,TWICE;
      !REAL P,CONST,VCONST;
!COMMENT PROCEDURE ADIFF USES 5-POINT 3RD ORDER LEAST SQUARES
          PARABOLA FOR ACCELERATION;
 !PROCEDURE ADIFF(Y,NS,A);
      !VALUE Y,NS;
        !REAL !ARRAY Y,A;
        !INTEGER NS;

!BEGIN   !INTEGER K,S;
        !REAL !ARRAY U[1:5];
        !FOR K:=1 !STEP 1 !UNTIL 5 !DO U[K]:=Y[K];
        A[1]:=(9*U[1]-15*U[2]-2*U[3]+13*U[4]-5*U[5])/7;
        A[2]:=(5.5*U[1]-8*U[2]-2*U[3]+6*U[4]-1.5*U[5])/7;
WRITE(30,FORMAT('+NDDD.DDDC'),A[1]);
        S:=5;
     L1:A[S-2]:=(2*U[1]-U[2]-2*U[3]-U[4]+2*U[5])/7;
        !IF S=NS !THEN !GOTO L2;
        !FOR K:=2 !STEP 1 !UNTIL 5 !DO U[K-1]:=U[K];
       S:=S+1;
        U[5]:=Y[S];
        !GOTO L1;
     L2:A[NS-1]:=(5.5*U[5]-8*U[4]-2*U[3]+6*U[2]-1.5*U[1])/7;
        A[NS]:=(9*U[5]-15*U[4]-2*U[3]+13*U[2]-5*U[1])/7;
!END;


!COMMENT PROCEDURE FORCE EVALUATES SEGMENTAL INERTIA FORCES;
     !PROCEDURE FORCE(A,C,MP,NS,FS,SIGMA);
        !VALUE A,C,MP,NS;
       !REAL !ARRAY A,FS,SIGMA;
       !REAL C,MP;
       !INTEGER NS;
!BEGIN !INTEGER K;
        !FOR K:=1 !STEP 1 !UNTIL NS !DO
!BEGIN FS[K]:=A[K]*C*MP/32.17;
       SIGMA[K]:=SIGMA[K]+FS[K];
!END;
!END;
```

```
!COMMENT PROCEDURE VDIFF USES 5-POINT 2ND ORDER LEAST SQUARES
          PARABOLA FOR VELOCITY;
 !PROCEDURE VDIFF(Y,NS,V,CV);
         !VALUE Y,NS,CV;
          !REAL !ARRAY Y,V;
         !REAL CV;
       !INTEGER NS;
!BEGIN  !INTEGER R,S;
       !REAL !ARRAY U[1:5];
       !FOR R:=1 !STEP 1!UNTIL 5!DO U[R]:=Y[R];
      V[1]:=(-21*U[1]+13*U[2]+17*U[4]-9*U[5])/20;
      V[2]:=(-11*U[1]+3*U[2]+7*U[4]+U[5])/20;
WRITE(30,FORMAT('+NDDD.DDDC'),V[1]);
       S:=5;
   L3:V[S-2]:=(-2*U[1]-U[2]+U[4]+2*U[5])/10;
       !IF S=NS !THEN !GOTO L4;
       !FOR R:=2 !STEP 1 !UNTIL 5 !DO U[R-1]:=U[R];
       S:=S+1;
       U[5]:=Y[S];
       !GOTO L3;
L4:V[NS-1]:=(11*U[5]-3*U[4]-7*U[3]-U[2])/20;
 V[NS]:=(21*U[5]-13*U[4]-17*U[3]+9*U[2])/20;
!END;
!COMMENT PROCEDURE MOM EVALUATES SEGMENTAL MOMENTA;
       !PROCEDURE MOM(V,CV,MP,NS,TOT);
           !VALUE V,CV,MP,NS;
           !REAL !ARRAY V,TOT;
           !REAL CV,MP;
           !INTEGER NS;
!BEGIN  !INTEGER K;
         !FOR K:=1 !STEP 1 !UNTIL NS !DO
                                TOT[K]:=(V[K]*CV*MP)+TOT[K];
WRITE(30,FORMAT('+NDDD.DDDC'),TOT[1]);
!END;

       OPEN(20);
       K:=READ(20);
        N:=READ(20);
        B:=READ(20);
      CONST:=READ(20);
       VCONST:=READ(20);

      F1:=FORMAT('+NDDD.DD;');
       F2:=FORMAT('2S+NDDD.DD;');
       F3:=FORMAT('2S+NDDD.DD;C');
!BEGIN  !REAL !ARRAY AZ[1:K+1,1:N], ZETA[1:K+1,1:N],
                     G[1:B],G[1:N+1],Z[1:N],SM[1:3];
       !FOR M:=1 !STEP 1 !UNTIL N !DO
       !FOR SEG:=1 !STEP 1 !UNTIL K+1 !DO
!BEGIN G[M]:=0;
        ZETA[SEG,M]:= READ(20);

!END;
```

```
!COMMENT THIS SECTION CALCULATES SEGMENT MASS-CENTRES
         FROM HINGE-POINTS;
 !FOR SEG:=1 !STEP 1 !UNTIL B !DO
       G[SEG]:=READ(20);
     !FOR M:=1 !STEP 1 !UNTIL N !DO
       !FOR SEG:=1 !STEP 1 !UNTIL B !DO
      AZ[SEG,M]:=ZETA[SEG+1,M]-G[SEG]*(ZETA[SEG+1,M]-ZETA[SEG,M
      !IF B=K !THEN !GOTO MISS;
      !IF B=K+1 !THEN !GOTO MISS;
     !FOR M:=1 !STEP 1 !UNTIL N !DO
      !FOR SEG:=B+1 !STEP 1 !UNTIL K !DO
      AZ[SEG,M]:=ZETA[SEG+1,M];
   MISS: ;
      SEG:=1;
       OPEN(30);
      WRITE(30,FORMAT('ND;C'),K+1);
       WRITE(30,FORMAT('NDD;C'),N);
       WRITE(30,FORMAT('NDDD.DDDDD;C'),CONST);
       WRITE(30,FORMAT('NDD.DDDDD;C'),VCONST);


START: P:=READ(20);
       !FOR M:=1 !STEP 1 !UNTIL N !DO
 Z[M]:= AZ[SEG,M];
      R:=1;
       TWICE:=0;
      !GOTO W7;
    W1: WRITE(30,F1,Z[R]);
       WRITE(30,F2,Z[R+1]);
       WRITE(30,F2,Z[R+2]);
       WRITE(30,F2,Z[R+3]);
       WRITE(30,F3,Z[R+4]);
       R:=R+5;
      !IF N-R!>4 !THEN !GOTO W1;
       !IF N-R=0 !THEN !GOTO W5;
     !IF N-R=1 !THEN !GOTO W4;
     !IF N-R=2 !THEN !GOTO W3;
     !IF N-R=3 !THEN !GOTO W2;
   W2: WRITE(30,F1,Z[N-3]);
   W3: WRITE(30,F2,Z[N-2]);
   W4: WRITE(30,F2,Z[N-1]);
   W5: WRITE(30,F3,Z[N]);
    WRITE(30,FORMAT('ND.DDD;C'),P);
     W7: ;
     !IF TWICE = 1 !THEN !GOTO W6;
     R:=1;
     TWICE:=1;
```

```
!COMMENT THIS SECTION APPLIES 3-POINT MOVING AVERAGE
          SMOOTHING TO DISPLACEMENTS;
     SM[1]:= Z[1];
    AZ[SEG,1]:=Z[1];
  POT:SM[2]:=Z[R+1];
     SM[3]:= Z[R+2];
     Z[R+1] := (SM[1]+SM[2]+SM[3])/3;
    AZ[SEG,R+1]:=Z[R+1];
     R:=R+1;
     !IF R=N-1 !THEN !GOTO HOP;
     SM[1]:= SM[2];
     !GOTO POT;
  HOP:;
     R:=1;
!COMMENT THIS LINE CALCULATES WHOLE-BODY MASS-CENTRE;
  W6:!FOR M:=1 !STEP 1 !UNTIL N !DO
       G[M]:= G[M]+P*Z[M];
     SEG:=SEG+1;

     !IF SEG!= K+1 !THEN !GOTO START;

   G[N+1]:=1;
     !FOR M:=1 !STEP 1 !UNTIL N !DO
!BEGIN WRITE(30,FORMAT('+NDDDD.D;C'),G[M]);
     AZ[K+1,M]:=G[M];
!END;
    WRITE TEXT(30,'1.0;'C'');

    SEG:=1;
!BEGIN !REAL !ARRAY ACC,VEL,F,SUM,TM[1:N];
     !FOR M:=1 !STEP 1 !UNTIL N !DO
!BEGIN SUM[M]:=0;
     TM[M]:=0;
!END;
  LOOP: P:=READ(20);
     !FOR M:=1 !STEP 1 !UNTIL N !DO Z[M]:=AZ[SEG,M];
  ADIFF(Z,N,ACC);
    FORCE(ACC,CONST,P,N,F,SUM);
    VDIFF(Z,N,VEL,VCONST);
     MOM (VEL,VCONST,P,N,TM);
   OPEN(30);
  WRITE TEXT(30,''2C'ACCEL '9S'FORCE '6S'CUMFORCE '5S'VEL '9S'
                                   CUMOM '2C'');
    !FOR M:=1 !STEP 1 !UNTIL N !DO
!BEGIN
     WRITE(30,FORMAT('+NDDD.DDD'),ACC[M]*CONST);
     WRITE(30,FORMAT('3S+NDD.DDD'),F[M]);
     WRITE(30,FORMAT('3S+NDD.DDD'),SUM[M]);
     WRITE(30,FORMAT('3S+NDD.DDD'),VEL[M]*VCONST);
     WRITE(30,FORMAT('6S+NDD.DDDC'),TM[M]);
!END;
    SEG:=SEG+1;
    !IF SEG!=K+2 !THEN !GOTO LOOP;

!END;
     CLOSE(30);
!END;
     CLOSE(20);
!END;
```

```
4;
23;
3;
0.8548;
0.07632;
0096; 0305; 0487; 0891; 0629;
0103; 0303; 0491; 0901; 0647;
0096; 0296; 0482; 0899; 0698;
0097; 0299; 0481; 0901; 0770;
0098; 0297; 0482; 0899; 0830;
0098; 0296; 0481; 0902; 0866;
0095; 0296; 0477; 0901; 0880;
0096; 0291; 0474; 0889; 0878;
0096; 0292; 0467; 0873; 0843;
0098; 0295; 0466; 0845; 0776;
0098; 0294; 0443; 0777; 0640;
0095; 0293; 0431; 0695; 0481;
0090; 0285; 0426; 0616; 0402;
0102; 0296; 0443; 0575; 0482;
0102; 0297; 0451; 0541; 0587;
0105; 0294; 0448; 0508; 0627;
0111; 0294; 0437; 0466; 0599;
0120; 0283; 0413; 0413; 0528;
0124; 0262; 0390; 0387; 0428;
0132; 0251; 0386; 0437; 0324;
0133; 0236; 0399; 0551; 0374;
0135; 0241; 0433; 0668; 0612;
0193; 0328; 0475; 0813; 0797;

0.5845;
0.4329;
0.5823;

0.129;
0.201;
0.556;
0.114;
0.129;
0.201;
0.556;
0.114;
1.0; **OK
```

Chapter 7

External Forces and Body Action in Jumping

7.1 Introduction

In previous chapters the emphasis has been on the investigation of experimental and computational methods applicable to a general study of human motion. The techniques have been developed and tested on two simple jumping activities, the drop-landing and the standing long jump. The primary aim has been to determine limits to which cine analysis can be taken. It has become clear that, with unavoidable inaccuracies in filming, film measurement and computation, values of velocity, and especially of acceleration and force, are subject to some distortion. Nevertheless, meaningful results have been derived with careful handling of the 'noise' contaminating the data.

The validity of results computed from cine film has been assessed by comparing calculated forces with measured values of foot thrust from the force platform. The comparisons are encouraging, but shortcomings of the cine analysis techniques are clearly highlighted. The fact that computed force values leave something to be desired should not, however, lead one to discard cine analysis in favour of the force platform. Cine film of a human activity contains much more information than can be measured by a force platform. In particular, there is on film, a wealth of information about the co-ordinated movements of body segments in a skilled action. Only from this source can we expect to gain data on the relative importance of arm, leg and trunk movements in a complex activity. Thus, despite the presence of several types of error and their unfortunate interference with computed results, the analysis of cine film has a great deal to offer.

The force platform provides a valuable check on certain computed results, but it gives acceleration, velocity and displacement data only for the whole-body mass-centre, and can not be ussed to investigate the effects of individual segments in a complex movement.

In this Chapter we discuss the results obtained by cine analysis and force platform measurement for the drop-landing and standing long jump. The discussion centres around the successes and failures of the experimental

techniques and deals with extensions of the methods applicable to a wide range of movement studies.

7.2 The Drop-Landing - Cine and Force Platform Comparisons

a) The Drop-Landing as an impact load activity

The drop-landing is described in Chapter 4, Section 4.7 and the computational analysis is summarised in Chapter 5, Section 5.10. Before dropping from the horizontal bar in this test, the subject's toes were 42 inches above the force platform as he hung in a fully extended position. Although this would be only a moderate height for a normal downward jump from a bench to the floor, a drop-landing height of 42 inches provided problems for a competent athlete. His view of the floor from the hanging position was restricted and it was difficult to judge the timing of the landing. The recorded vertical foot thrust given in Figure 7.1 represents a rather hard landing. The first impact of the balls of the feet is severe and was a little painful. Drop-landings from heights greater than 42 inches would have been dangerous without a good deal of practice. Indeed, it is unlikely that any subject will be willing to perform a drop-landing from 5 feet, although he may be quite at home with a normal downward jump from that height.

The drop-landing was selected as an activity involving impact loading on the body, and by allowing the subject to drop from a height which he deemed safe, it was hoped that the impact effects would not be injurious. In view of the very high force recorded on impact, however, it is open to question whether such landings are desirable. The subject felt only momentary discomfort under the balls of the feet, but the transmission of the shock load through the ankle and knee joints may have had undesirable effects. In Chapter 8 the effect of the drop-landing on the joints and muscles of the leg is considered and surprisingly large forces are calculated.

The severity of the impact could have been lessened by covering the force platform with matting, and the effects of different forms of surface covering would provide an interesting study. However, in the present work direct

FIGURE 7.1 DROP-LANDING FORCE PLATFORM RECORD

DROP HEIGHT 42 in.
FRAME RATE 68·5 s^{-1}

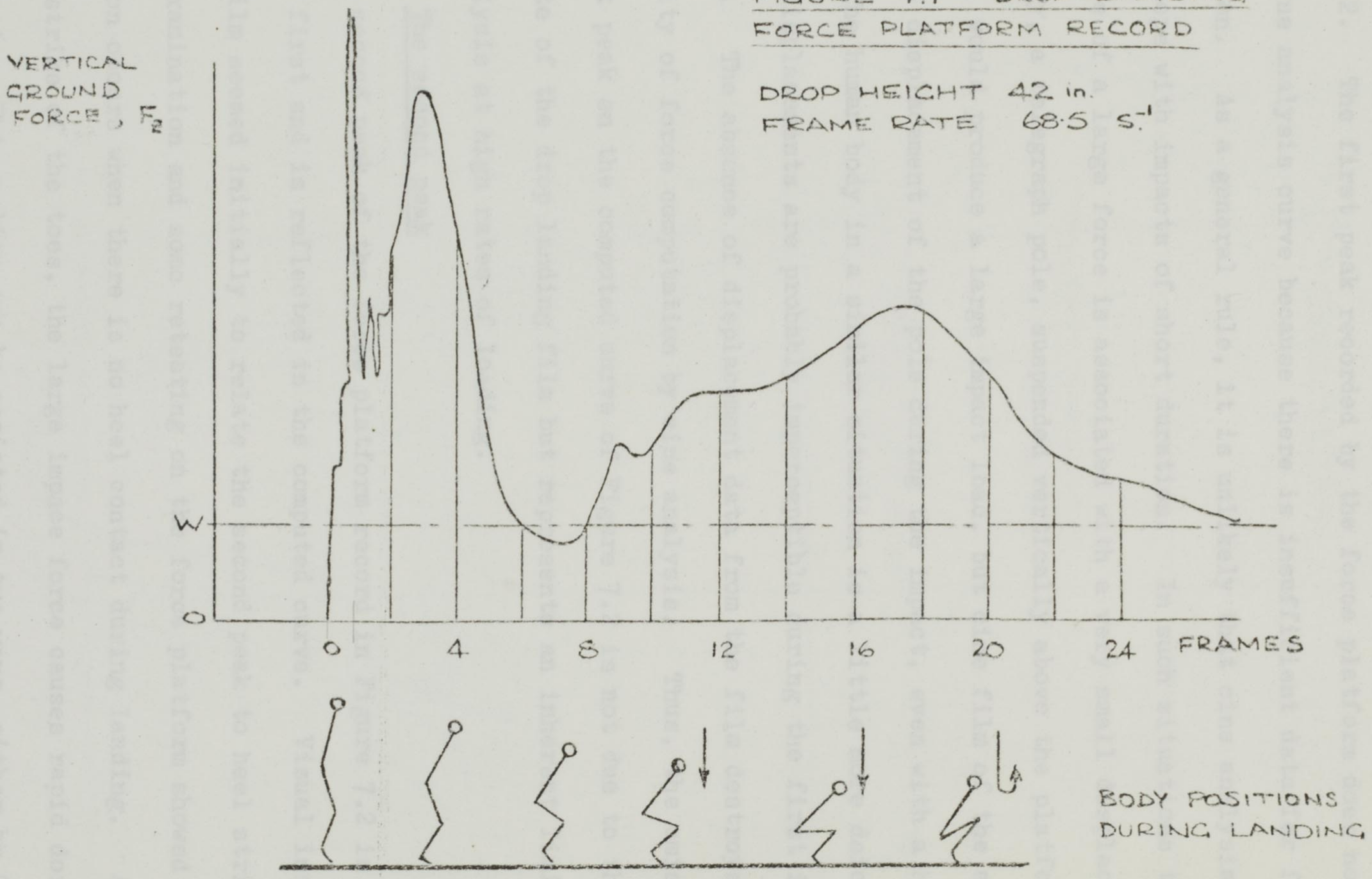

BODY POSITIONS DURING LANDING

landing on the platform was selected as a typical impact situation for analysis.

b) The Initial impact

Cine analysis of the activity produced the force curve shown in Figure 7.2. The first peak recorded by the force platform does not appear on the cine analysis curve because there is insufficient data for force computation. As a general rule, it is unlikely that cine analysis will be able to cope with impacts of short duration. In such situations the occurrence of a large force is associated with a very small displacement. As an analogy, a telegraph pole, suspended vertically above the platform and then released, would produce a large impact load, but cine film of the event would detect no displacement of the pole during the impact, even with a high frame rate. The human body in a similar situation is a little more deformable, but its displacements are probably imperceptible during the first impact of the toes. The absence of displacement data from the film destroys any possibility of force computation by cine analysis. Thus, the omission of the first peak on the computed curve of Figure 7.2 is not due to the slow frame rate of the drop landing film but represents an inherent limitation of cine analysis at high rates of loading.

c) The second peak

The second peak of the force platform record in Figure 7.2 is much lower than the first and is reflected in the computed curve. Visual inspection of the film seemed initially to relate the second peak to heel strike, but closer examination and some retesting on the force platform showed that the phenomenon occurs when there is no heel contact during landing. After the initial strike of the toes, the large impace force causes rapid dorsi flexion of the foot. This motion can be resisted in two ways, either by Gastrocnemius acting on the Achilles tendon or by the heel being forced down on the platform. If heel strike does not occur, activation of Gastrocnemius must begin shortly after the first impact. Details of the Gastrocnemius tensions appear in Chapter 8 as part of the internal force calculations for the ankle and knee

FIGURE 7.2 DROP-LANDING

TOTAL VERTICAL FORCE

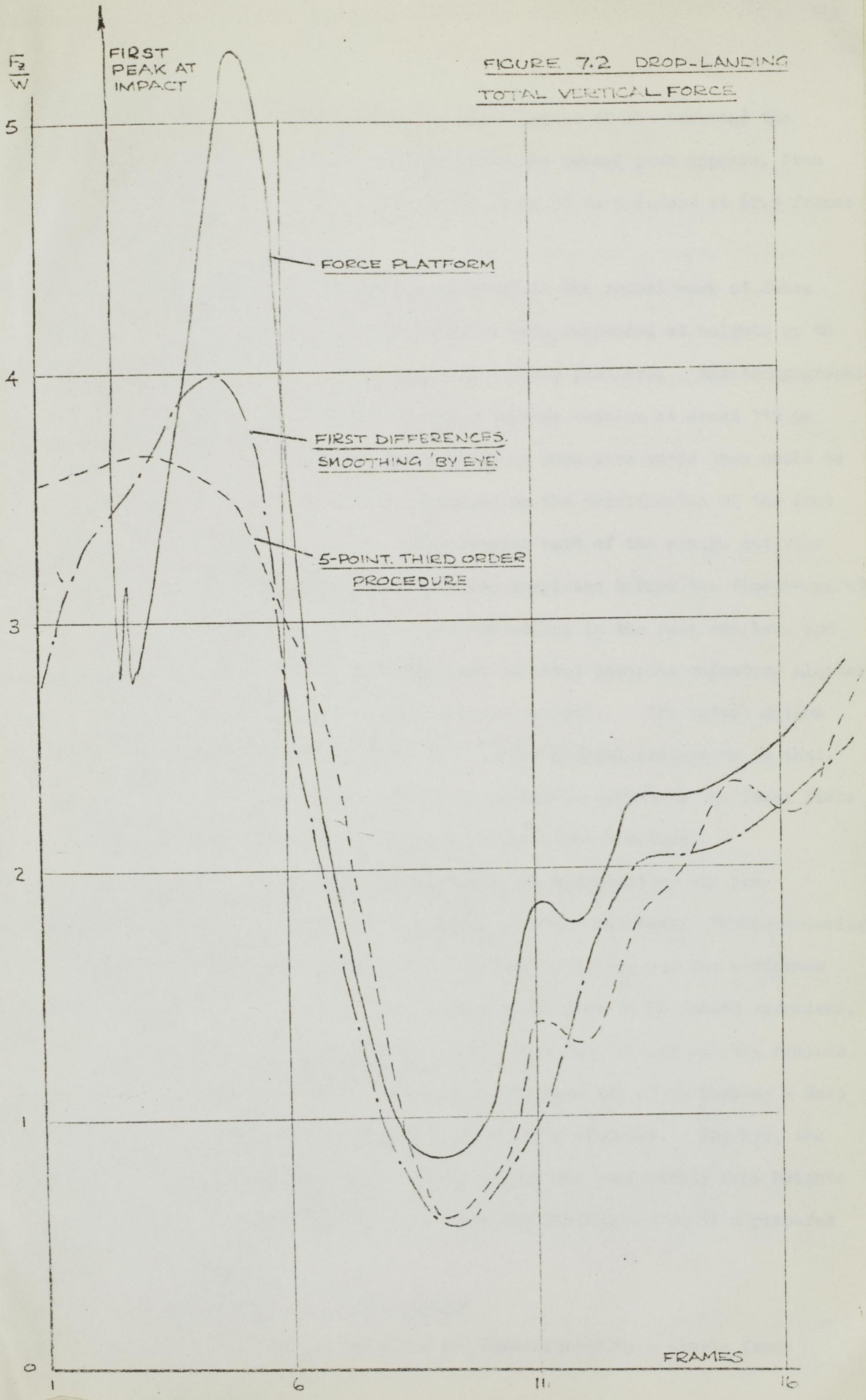

joints. The time interval between the first impact of the toes and the maximum Gastrocnemius tension associated with the second peak appears, from Figure 8.5 of Chapter 8, to be about 60 to 75 ms (4 to 5 frames at 68.5 frames per second).

This result bears an interesting relation to the recent work of Jones and Watt (3). In their experiments subjects were suspended at heights up to 7 inches and dropped without warning on to a force platform. Electromyographic records of Gastrocnemius activity showed a maximum tension at about 119 ms after the touch-down. This muscle activity is much more rapid than could be explained by stretch reflex action triggered by the dorsiflexion of the foot on landing. The authors state:- "The largest part of the e.m.g. activity associated with the landing deceleration was completed before the time required to generate a functionally effective stretch reflex in the same muscles, and certainly before the time taken to make the quickest possible voluntary plantar flexion effort to a light tap on the Achilles tendon". The latter action was found to take a mean time of 163 ms. Their general conclusion is that, even in unexpected falls, 'preprogramming' of muscle action in the lower limbs must override the relatively slow action of the stretch reflex.

The results of the present study, where the drop-landing was pre-meditated, appear to support the statements of Jones and Watt. 'Preprogramming' of landing action is a concept readily accepted by anyone who has performed downward jumps from various heights. As the distance to be jumped increases, one tends to spend more time looking at the floor and 'sizing up' the demands of the jump. The importance of landing on the toes and of performing a deep squat may be rehearsed mentally before the jump is executed. Further, the fact that one can gradually learn to land softly and comfortably from heights of 6 feet or more underlines the point that the landing action is a prepared sequence of body movements.

d) Adaptation of the landing action

Improvement in landing technique was demonstrated by a simple force

platform experiment in the present studies. Using a drop height of only 1 ft. the author was able to land extremely badly and then progressively improve the landing to a very soft deep-squat action. The force platform results are shown in Figure 7.3 and it is clear that the severity of the impact is considerably reduced by a good jumping action. A 'cat-like' landing, producing relatively small forces, appears to have two important characteristics. Firstly, just before contact knee flexion is commenced snd the relative velocity between toes and floor is reduced; by this means the first impact is kept small. Secondly, the knee flexion is carried through to its maximum extent (deep-squat) and to retain balance on the feet a correspondingly large flexion at the hip must occur. The combined effect of these flexions is to spread the deceleration of the body over a long time interval and thereby to reduce the magnitude of the foot thrust. There is no doubt that similar improvements in landing technique could reduce the large impact force associated with the 42 inch drop-landing, and a study of the learning process with cine film and force platform would be informative.

7.3 The Drop-landing - Momentum Considerations

The total vertical momentum of the body in any motion may be calculated as the summation of the momenta of the segments, in accordance with equation (3.2-3). In Figure 7.4 the curve of total momentum is obtained in this way. The time-derivative of this curve gives the total vertical force on the body, by the general form of Newton's Second Law:-

Force = Rate-of-change of momentum

Alternatively, the total force is expressed by the summation of segmental inertia forces, obtained from individual segmental accelerations (Section 3.2, Chapter 3). It is interesting to compare the total vertical forces obtained by these two methods, and Figure 7.4 shows a satisfactory agreement between the two sets of values.

The relationship between force and rate-of-change of momentum is seldom illustrated by the motion of systems of rigid bodies, the usual applications

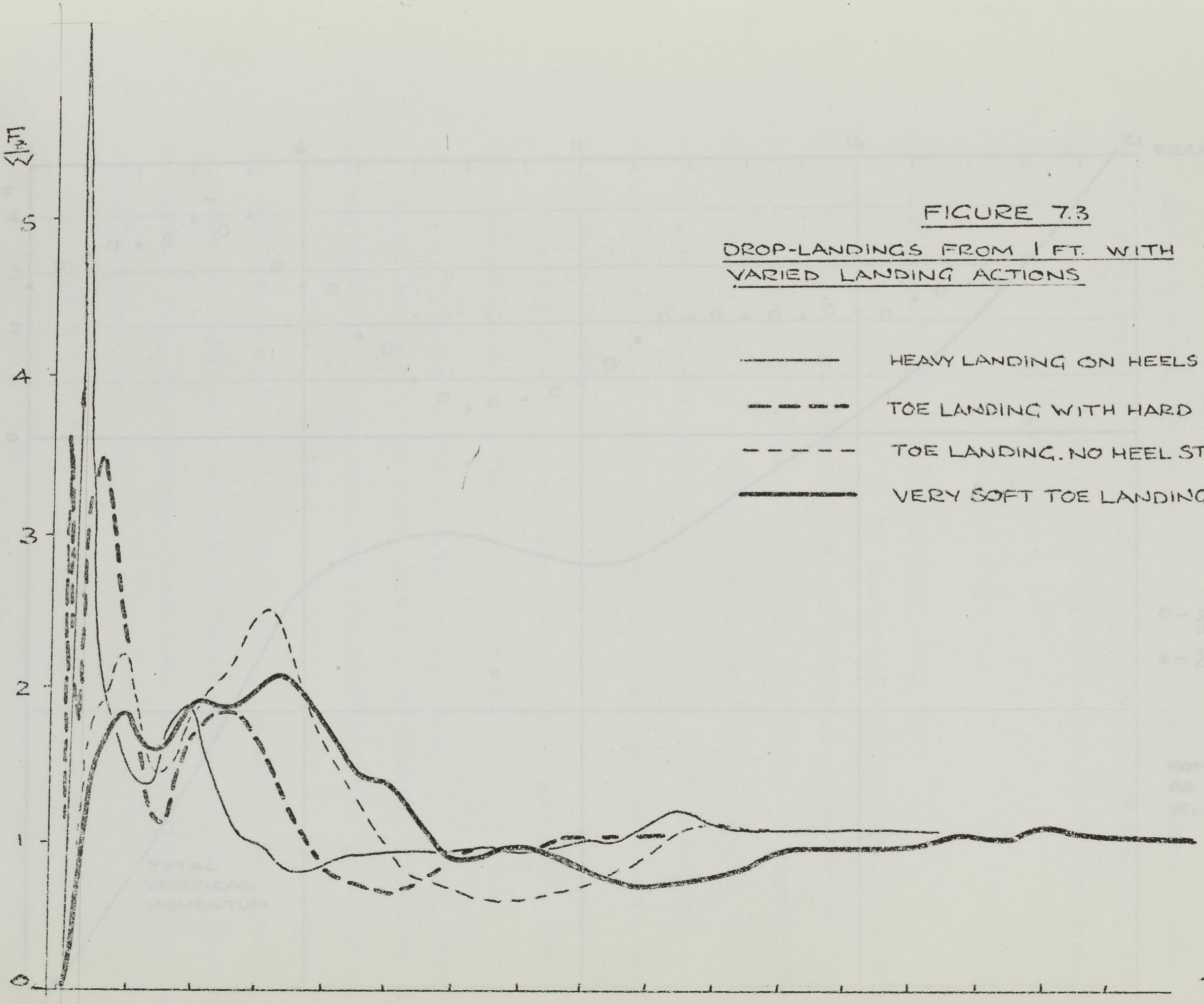

FIGURE 7.3

DROP-LANDINGS FROM 1 FT. WITH VARIED LANDING ACTIONS

——— HEAVY LANDING ON HEELS

– – – – TOE LANDING WITH HARD HEEL-STRIKE

– – – – – TOE LANDING. NO HEEL STRIKE

——— VERY SOFT TOE LANDING. NO HEEL STRIKE

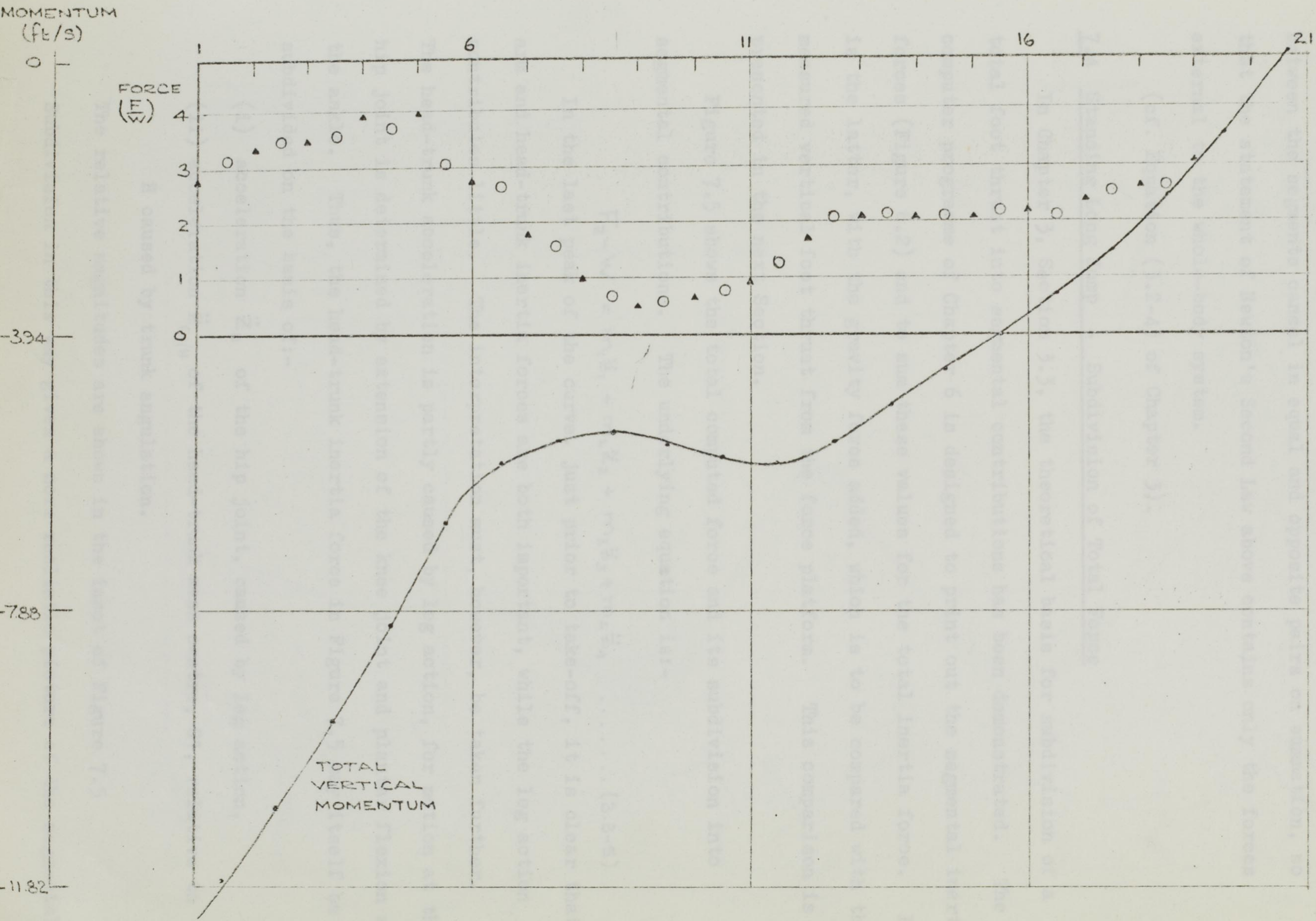

FIGURE 7.4

DROP-LANDING

TOTAL VERTICAL MOMENTUM

(+↑)

AND FORCES

COMPUTED BY

TWO METHODS

O - $\frac{d}{dt}$(TOTAL MOMENTUM)

▲ - $\sum$ SEGMENTAL INERTIA FORCES

MOMENTUM EXPRESSED AS UNITY BODY-MASS X VELOCITY OF MASS-CENTRE

being in fluid mechanics. Here the system is an interconnected set of rigid bodies.

The analysis also brings out the point that internal forces acting between the segments cancel in equal and opposite pairs on summation, so that the statement of Newton's Second Law above contains only the forces external to the whole-body system.

(cf. Equation (3.2-4) of Chapter 3).

7.4 Standing Long Jump - Subdivision of Total Force

In Chapter 3, Section 3.3, the theoretical basis for subdivision of a total foot thrust into segmental contributions has been demonstrated. The computer programme of Chapter 6 is designed to print out the segmental inertia forces (Figure 6.2) and to sum these values for the total inertia force. It is the latter, with the gravity force added, which is to be compared with the measured vertical foot thrust from the force platform. This comparison is presented in the next Section.

Figure 7.5 shows the total computed force and its subdivision into segmental contributions. The underlying equation is:-

$$F_z - W = m_1\ddot{z}_1 + m_2\ddot{z}_2 + m_3\ddot{z}_3 + m_4\ddot{z}_4 \quad \ldots\ldots (3.3\text{-}5)$$

In the last peak of the curve, just prior to take-off, it is clear that the arm and head-trunk inertia forces are both important, while the leg action contributes little. The interpretation must, however, be taken further. The head-trunk acceleration is partly caused by leg action, for motion at the hip joint is determined by extension of the knee joint and plantar flexion at the ankle. Thus, the head-trunk inertia force in Figure 7.5 may itself be subdivided on the basis of:-

(i) acceleration $\ddot{z}_H$ of the hip joint, caused by leg action.

(ii) acceleration $\ddot{z}_{G1/H}$ of the head-trunk mass centre, G1, relative to H caused by trunk angulation.

The relative magnitudes are shown in the inset of Figure 7.5

Subdivision in this way gives a more realistic picture of the segmental

FIGURE 7.5
STANDING LONG JUMP
SUBDIVISION OF TOTAL FORCE

ARMS
HEAD-TRUNK
WHOLE LEG + FOOT (OR UPPER LEG ALONE)
LOWER LEG + FOOT

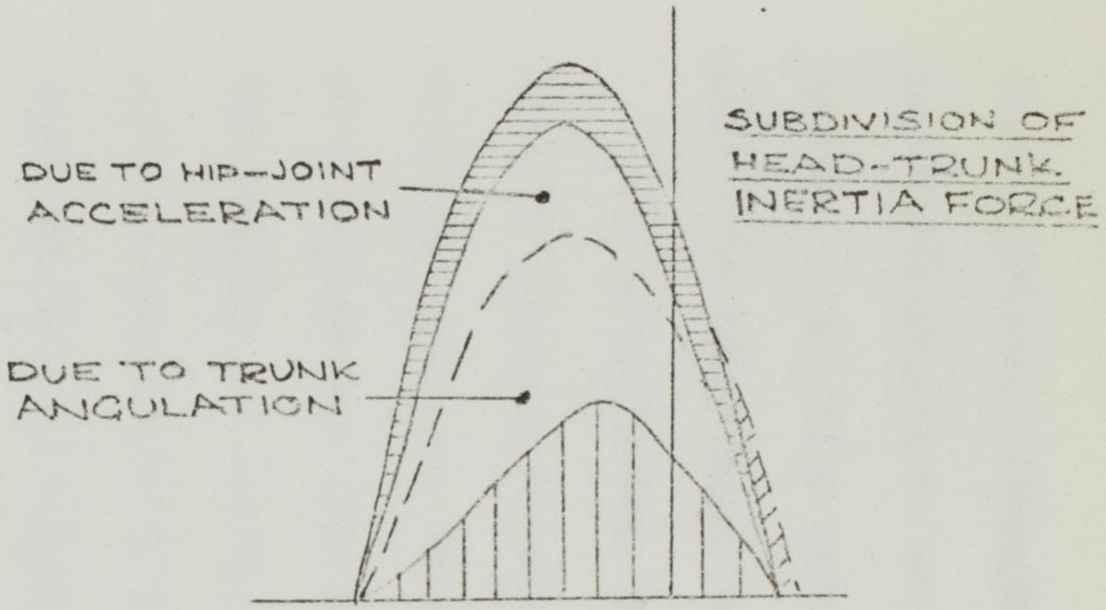

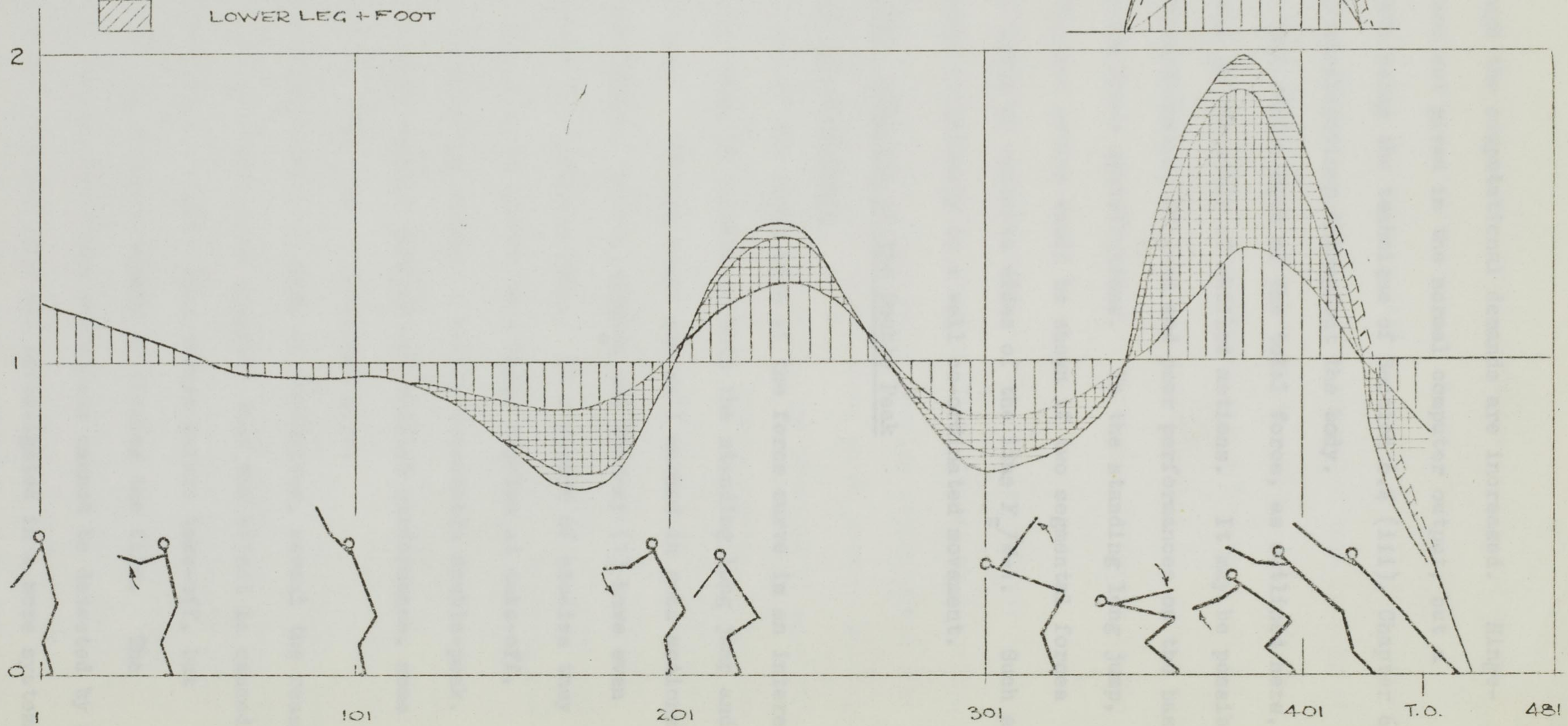

contributions, although the computational demands are increased. Hinge-point accelerations are not given in the normal computer output, but a re-run on the cine data using the technique of Section 6.4 (iii), Chapter 6, will give hinge-point accelerations throughout the body.

It is suggested that subdivision of the total force, as outlined here, will be a useful method in the study of skilled actions. It may be possible to investigate the characteristics of good and poor performances on the basis of the segmental inertia force contributions. In the standing long jump, for example, an inefficient action would be shown if two segmental forces opposed each other by lying on opposite sides of the line $F_z/W=1$. Such a counteraction of effects is unlikely in a well co-ordinated movement.

7.5 Standing Long Jump - Analysis of the Double Peak

a) The Nature of the Phenomenon

The double peak form of the final part of the force curve is an interesting feature of the measured vertical thrusts in both the standing long jump and the standing vertical jump. The two peaks are well marked in good actions and, in the case of one Olympic jumper, Adamson and Whitney (1) have even observed a triple peak in the vertical jump. In a number of studies they have found multiple peaking to be allied to a large impulse at take-off, while less effective performances produce a barely detectable double-peak. In view of this association between peaking and skilled performance, some discussion of the standing long jump is presented here.

The force platform measurements do not, of themselves, reveal the reason for double peaking. Direct observation suggests that the effect is caused by arm swing or plantar flexion in the final thrust before take-off, but little solid evidence can be obtained merely by viewing the film. The segmental accelerations causing the force variations cannot be detected by eye.

The double peak in the vertical jump was investigated in a more systematic way by Anthony et al(2)in whose study the subject was allowed first to jump in an unimpeded fashion and then performed a second jump with his arms held at

his sides. In the second case double peaking did not appear and it was suggested that the phenomenon must therefore be an arm swing effect. Without repeating such tests, including a film analysis, a full discussion of this work cannot be offered. However, it is suggested that locking of the arms does more than merely prevent the arm swing action. The whole dynamic balance of body motion during the jumping action may be upset by restriction of the arm movement. Thus, it is probable that the thrust action of the legs and the angulation of the trunk are basically different in the two cases.

An alternative approach to the analysis of the double peak may in principle be made by subdivision of the total vertical thrust as described in Section 7.4. This analysis of the unrestricted jumping action gives the contribution of each segment and should reveal those which produce peaking effects. Unfortunately, as Chapter 5 has shown, the problems of smoothing lead to a computed force curve which exhibits no double peaking. The finer points of the filmed motion have inevitably been eliminated with the removal of noise in the displacement data and the double peak appears as a single maximum. Figure 7.6 shows the discrepancy between the computed force and a typical measured vertical thrust in the standing long jump. The data are taken from the full record given in Figure 5.16, Chapter 5.

b) Discrepancies between Measured and Computed Force Values

We now consider this discrepancy in detail in order to assess what variations in the original displacement data could give rise to a double-peak force curve after double-differentiation. For the region of the force curve to be examined (Figure 7.6), the measured curve shows an approximate sine wave discrepancy superimposed on the computed function. Consideration of the equations of motion allows back-integration to the body mass centre displacements corresponding to the measured and computed forces. The difference between the latter constitutes the displacement discrepancy of Figure 7.6.

FIGURE 7.6

DISCREPANCIES BETWEEN COMPUTED AND MEASURED FORCES

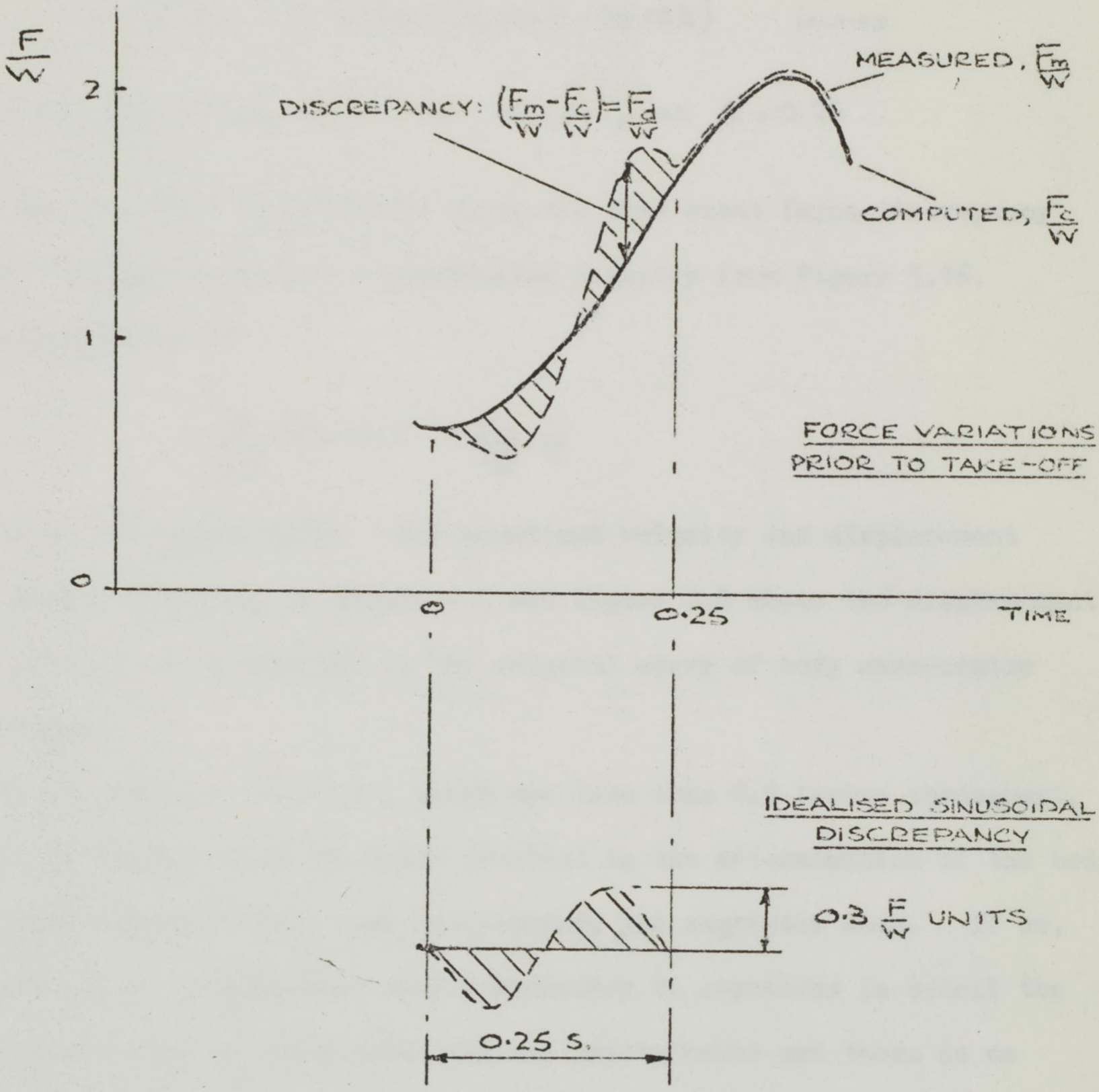

DISCREPANCY ANALYSIS:-

DISPLACEMENTS Z_m, Z_c CORRESPOND TO MEASURED AND COMPUTED FORCES F_m, F_c

THUS, $\left(\frac{F_m}{W} - 1\right)g = \frac{d^2 Z_m}{dt^2}$ AND $\left(\frac{F_c}{W} - 1\right)g = \frac{d^2 Z_c}{dt^2}$

GIVE:- $\left(\frac{F_m}{W} - \frac{F_c}{W}\right)g = \frac{d^2(Z_m - Z_c)}{dt^2} = \frac{F_d}{W}$

FOR THE SINUSOIDAL APPROXIMATION:-

$$\frac{F_d}{W} = -0.3 \sin\left(\frac{2\pi}{0.25} t\right)$$

A first approximate analysis was carried out by representing the force discrepancy as a pure sinusoid. This approach gave the results:-

$$z_m - z_c = 0.184\left[\sin(25.12\,t) - 25.12\,t\right] \quad \text{inches}$$

$$\text{and } (z_m - z_c)_{max} = -1.16 \text{ inches, at } t = 0.25$$

A better result was obtained using the more exact force discrepancy curve of Figure 7.7, which is constructed directly from Figure 5.16. Double integration of

$$\frac{d^2}{dt^2}(z_m - z_c) = \frac{F_d}{W} \cdot g$$

was carried out numerically. The resultant velocity and displacement discrepancies are given in Figure 7.7 and Figure 7.8 shows the displacement values applied as corrections to the original curve of body mass-centre displacement.

The corrections $(z_m - z_c)$, which are less than 0.9 inches throughout, may well be smaller than the error involved in the determination of the body mass-centre ordinates from cine measurements and segmental data. If so, the precision in displacement values necessary to represent in detail the force fluctuations of the double-peak are unattainable and there is no prospect of using cine film to elucidate the double-peak phenomenon.

7.6 Standing Long Jump - The Differentiation Problem

Smoothing and differentiation of displacement data remains, despite the investigations of Chapter 5, a difficult and imprecise process. In the earlier discussion it was shown that 20-frame spacing of the standing long jump data (sampling frequency 11.2 per second) gave reasonably smooth results at the second derivative stage. At the same time the inherent smoothing appeared to remove details of the final force curve, giving rise to the discrepancy treated in the previous Section. Having produced a correction to the body mass-centre displacement curve (Figure 7.8), we are in possession of the fine detail of the displacement corresponding to a double-peak

FIGURE 7.7 FORCE-DISCREPANCY AND DERIVED CURVES

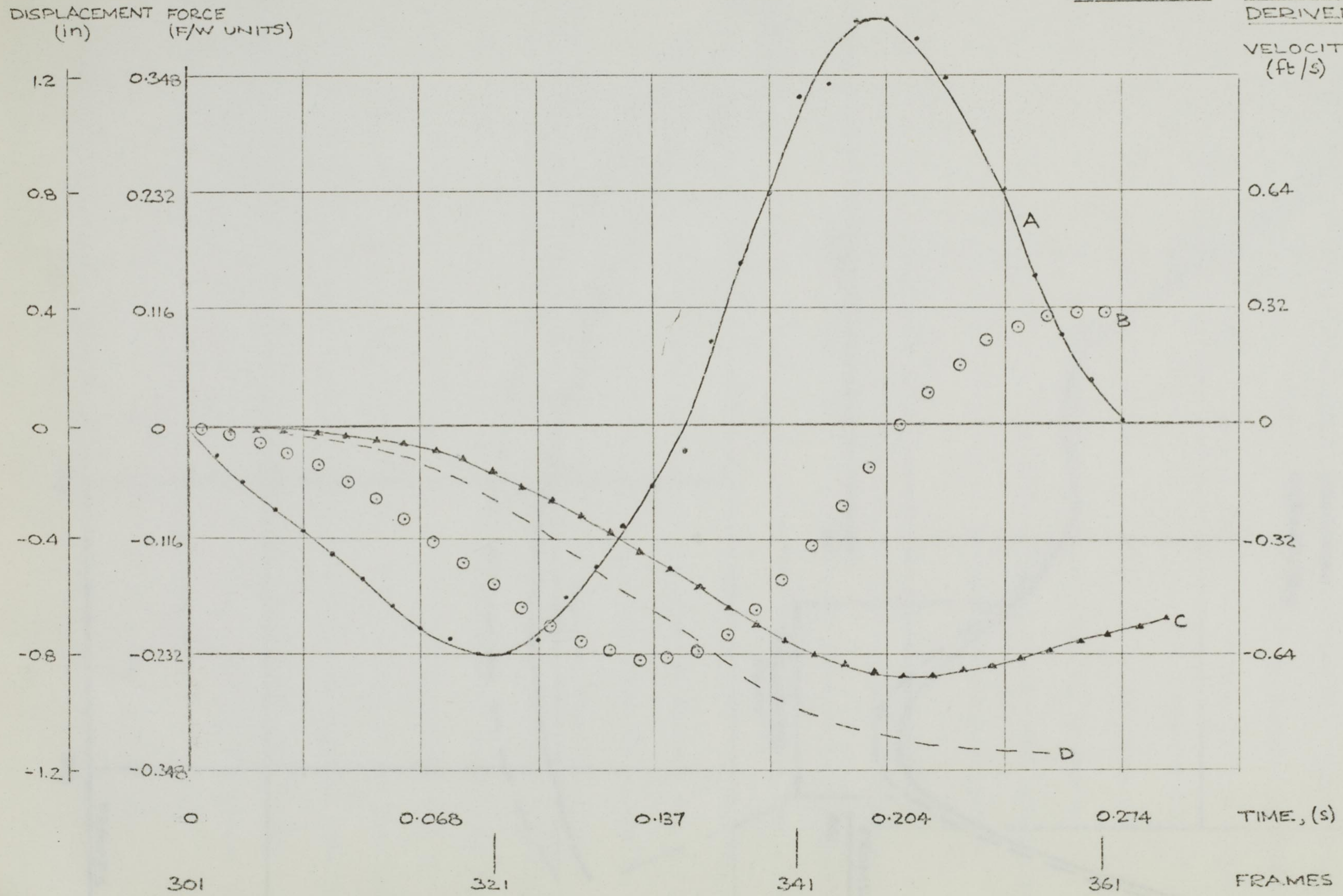

A - FORCE-DISCREPANCY

B - VELOCITY-DISCREPANCY (FIRST INTEGRAL OF A)

C - DISPLACEMENT CORRECTION TO BODY MASS-CENTRE TRAJECTORY (SECOND INTEGRAL OF A)

D - DISPLACEMENT CORRECTION FROM SINUSOIDAL APPROXIMAT

FIGURE 7.8

BODY MASS-CENTRE DISPLACEMENT AND DISCREPANCY CORRECTION

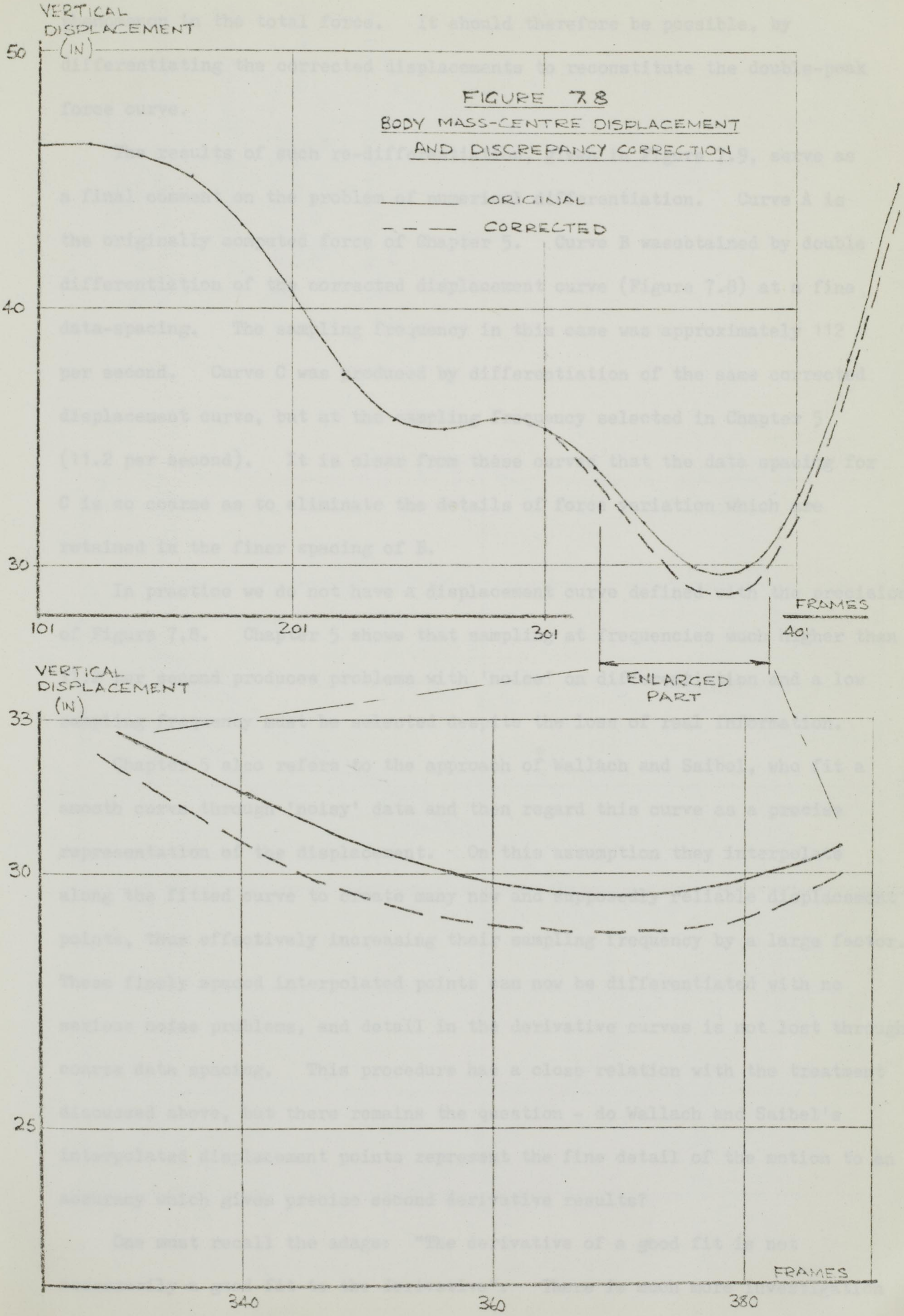

phenomenon in the total force. It should therefore be possible, by differentiating the corrected displacements to reconstitute the double-peak force curve.

The results of such re-differentiation, given in Figure 7.9, serve as a final comment on the problem of numerical differentiation. Curve A is the originally computed force of Chapter 5. Curve B wasobtained by double differentiation of the corrected displacement curve (Figure 7.8) at a fine data-spacing. The sampling frequency in this case was approximately 112 per second. Curve C was produced by differentiation of the same corrected displacement curve, but at the sampling frequency selected in Chapter 5 (11.2 per second). It is clear from these curves that the data spacing for C is so coarse as to eliminate the details of force variation which are retained in the finer spacing of B.

In practice we do not have a displacement curve defined with the precision of Figure 7.8. Chapter 5 shows that sampling at frequencies much higher than 11.2 per second produces problems with 'noise' on differentiation and a low sampling frequency must be selected despite the loss of real information.

Chapter 5 also refers to the approach of Wallach and Saibel, who fit a smooth curve through 'noisy' data and then regard this curve as a precise representation of the displacement. On this assumption they interpolate along the fitted curve to create many new and supposedly reliable displacement points, thus effectively increasing their sampling frequency by a large factor. These finely spaced interpolated points can now be differentiated with no serious noise problems, and detail in the derivative curves is not lost through coarse data spacing. This procedure has a close relation with the treatment discussed above, but there remains the question - do Wallach and Saibel's interpolated displacement points represent the fine detail of the motion to an accuracy which gives precise second derivative results?

One must recall the adage: "The derivative of a good fit is not necessarily a good fit to the derivative". There is much more investigation

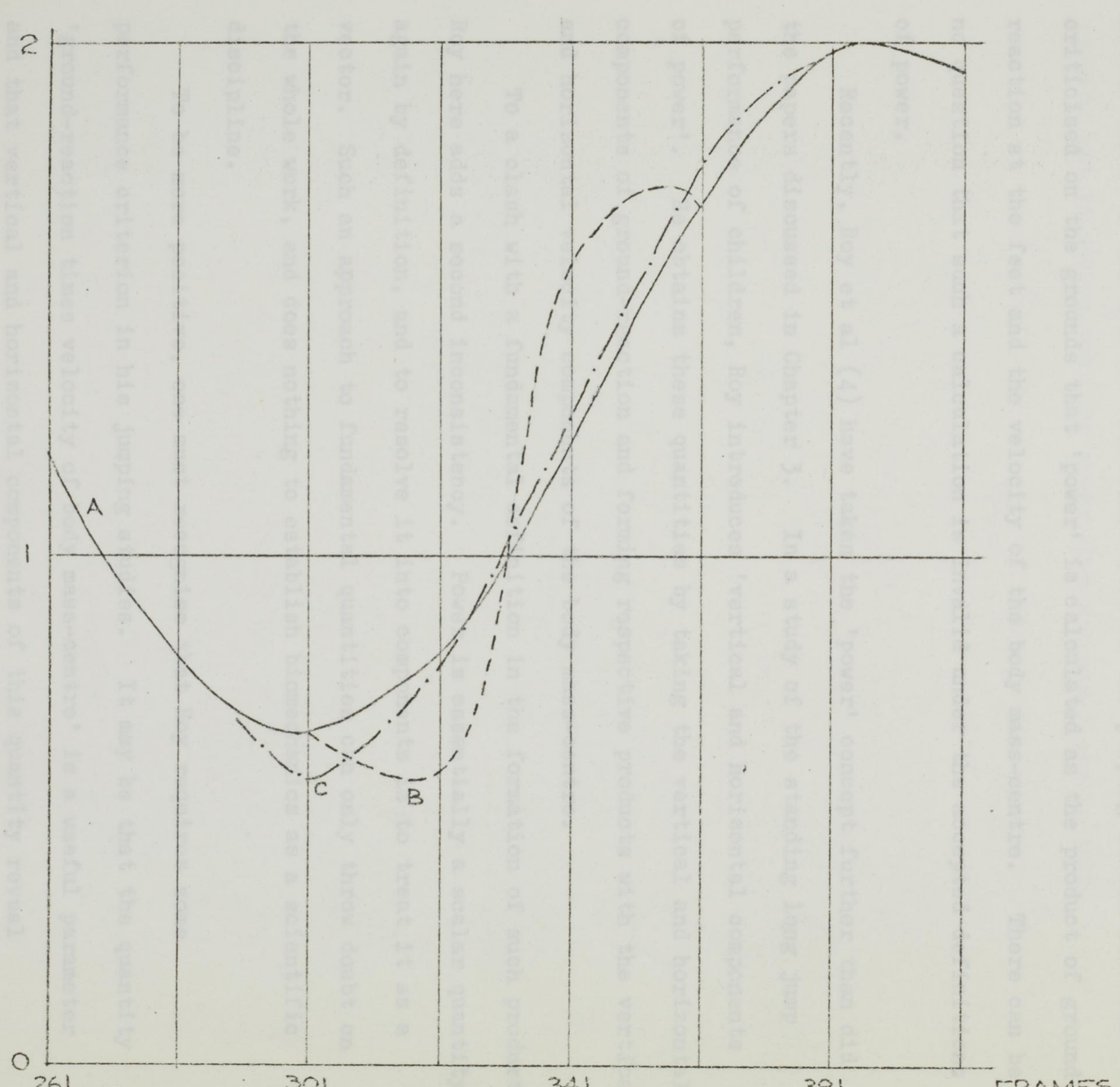

FIGURE 7.9
REDIFFERENTIATION OF
DISPLACEMENT DISCREPANCY

A - ORIGINAL COMPUTED FORCE

B - REDIFFERENTIATION OF
CORRECTED DISPLACEMENTS
AT $\nu_s = 11.2$ Hz

C - REDIFFERENTIATION
AT $\nu_s = 11.2$ Hz

to be carried out on numerical differentiation techniques. A refining process, such as Wallach and Saibel employ prior to differentiation, may remove 'noise' while retaining the fine detail of the real information. If this can be shown conclusively then many data handling problems in cine analysis will be solved.

7.7 Standing Long Jump - Power Calculations

In Chapter 3 the theoretical basis of the Power approach to explosive action has been discussed. Published work on the jumping action has been criticised on the grounds that 'power' is calculated as the product of ground reaction at the feet and the velocity of the body mass-centre. There can be no question that such a calculation is invalid under the accepted definitions of power.

Recently, Roy et al (4) have taken the 'power' concept further than did the papers discussed in Chapter 3. In a study of the standing long jump performance of children, Roy introduces 'vertical and horizontal components of power'. He obtains these quantities by taking the vertical and horizontal components of ground-reaction and forming respective products with the vertical and horizontal velocity components of the body mass-centre.

To a clash with a fundamental definition in the formation of such products, Roy here adds a second inconsistency. Power is essentially a scalar quantity, again by definition, and to resolve it into components is to treat it as a vector. Such an approach to fundamental quantities can only throw doubt on the whole work, and does nothing to establish biomechanics as a scientific discipline.

To be more positive, one must recognise that Roy requires some performance criterion in his jumping studies. It may be that the quantity 'ground-reaction times velocity of body mass-centre' is a useful parameter and that vertical and horizontal components of this quantity reveal characteristics of the jumping action related to good and poor performances. In this case there is every reason to study the behaviour of this force-

velocity product and, perhaps, to name it as a new biomechanical parameter.

If arguments here and in Chapter 3 seem too theoretical, the 'power' approach to trampolining should be considered. Here, the bed-reaction at the feet moves with a measurable velocity which is not that of the body mass-centre. The natural and correct expression of power supplied by the trampoline bed is the product of bed-reaction and velocity of its point of contact with the feet. The so-called 'power' statement of Roy and others may now be seen as misleading. One has only to envisage a progressively stiffer bed to deduce that the power from a rigid floor is zero.

7.8 References for Chapter 7

(1) Adamson, G.T.
Whitney, R.J.
Personal communication (1969)

(2) Anthony, B.L.
Garner, D.J.
Jones, M.G.
Course Study in Experimental Biomechanics
Department of Physical Education
University of Leeds (1967)

(3) Jones G.M.
Watt, D.G.D.
'Muscular Control of Landing from Unexpected Falls in Man'
J. Physiol. 219 3. 729-737 (1971)

(4) Roy, B.
Youm, Y.
Roberts, E.M.
'Kinematics and Kinetics of the Standing Long Jump in 7, 13, 16 year old Boys'
3rd International Seminar in Biomechanics, Rome (1971)

Chapter 8

Analysis of Some Muscle and Joint Forces in the Drop-Landing

8.1 Models of Muscle and Joint Action

Understanding of the action of human muscles and joints begins with anatomical study. The locations of muscles and their attachment to the skeleton are essential to the description of internal body actions. Anatomical texts provide a wealth of topographic material together with indications of the functions of particular muscles in flexion, extension or other motion at the joints. Information is also available concerning the mating contours of the joints and the forms of relative motion which they allow. Such detailed information of a qualititive kind has for decades been sufficient for the practice of surgery, physiotherapy and physical training.

Despite the descriptive detail of traditional anatomy, there is a notable dearth of mumerical data. Until recently there has been little call for dimensions associated with the musculo-skeletal system. Thus, in standard works it is rare to find figures for muscle and bone lengths, or radii of joint surfaces. Information on the variation of major skeletal measurements in the adult population is also difficult to obtain.

In the post-war years liaison between medicine and engineering has led to a more quantitive approach to the functioning of the body. The engineer asks not only which muscle is active during a joint flexion but also what tension that muscle is required to exert. In attempting to answer such a question he must be guided by the anatomist in obtaining skeletal and muscular dimensions necessary in the numerical work. The process represents an advance on purely descriptive anatomy but presents its own problems. The major difficulty lies in the setting up of a simple but realistic model of the joint and of the major muscles taking part in the action. If too complex a model is considered, the relevant equations become insoluble. On the other hand, sufficient detail must be incorporated to provide an acceptable anatomical description of the situation.

An experimental technique which sheds some light on the contribution of individual muscles in a body action is provided by electromyography. Using electrodes on the skin or inserted into the muscle, this technique gives an

indication of muscular tension during activity, and its use as a reliable method of force measurement has been advocated. The current view, however, seems to be that little reliance should be placed on numerical measures of tension from e.m.g. records. While restricted isometric tests have given repeatable relationships between static force and a function of the e.m.g., more general conditions of muscle contraction do not produce a simple response. In general, all that is certain is a rise in intensity of e.m.g. activity with an increase in tension.

No other method for direction estimation of muscle forces has been devised and indirect methods must therefore be called upon. In these methods the musculo-skeletal system is regarded as an engineering mechanism in which forces act according to the laws of statics or dynamics. It is usually necessary to consider a simplified system, because complete anatomical detail cannot be represented in a mechanical model. The number of unknown forces which can be determined is governed by the number of working equations applicable to the situation. Analysis in terms of all the active muscles will generally lead to an indeterminate problem with too many unknowns. Thus, the action of only a few major muscle groups can be considered. Further simplification must be introduced in representing the lines of action of these muscle groups. A straight line joining the origin and insertion seems reasonable, but in many instances the muscle attachments are spread over a wide area. Wrapping of muscles around each other and around bony protuberances adds further difficulty.

Models of muscle action which are capable of analysis may seem at first unacceptable to the anatomist. Major muscles are represented essentially by taut wires stretched between assumed points of attachment, and lesser muscles are omitted altogether. Nevertheless, there is no alternative to such an idealised treatment if numerical work is to be carried out. Admittedly, the accuracy of calculated forces cannot be great, but an indication of the order of magnitude of a force action is useful, provided that the underlying assumptions are fully understood.

8.2 Previous Estimates of Forces in the Lower Limbs

a) Anatomical Dimensions

The action of the lower limbs in support and locomotion has been studied by many workers. Until recently the problem has been regarded as one in statics, inertia effects of moving segments being ignored. Attempts to establish the positions of muscle origins and insertions, bone lengths and the centres of rotation of joints have been made with the aid of X-ray pictures. Inman (7) describes particularly detailed techniques in which wires were inserted into and wrapped round the leg muscles of cadavers. The muscles, having been partly cut out for the purpose, were then reinserted and X-ray photographs showed clearly the wires delineating important muscles. Inman also soaked muscles in a radio-opaque solution and obtained well-defined muscle locations by this means.

Williams and Svensson (16) drew on Inman's data for the treatment of hip-joint forces and added to it by making measurements on a skeleton. They used taut wires to estimate the lines of action of the ilio-psoas, rectus femoris and ilio-femoral ligament.

Both the X-ray and dry skeleton methods have been used by several workers and some additional data has been obtained by dissection. Morrison (9), for example, describes measurements on a cadaveric knee joint.

Tabulated data giving important dimensions relating to muscle and joint action are very much needed. Although measurement techniques are described in the literature, the numerical data obtained is seldom quoted, and study of subject differences has not been attempted.

b) Forces in Static Situations and and in Walking

Sokoloff (13), and Williams and Svensson give useful summary tables of several estimates of joint forces in the lower limbs. The usual aim of these analyses was the assessment of bone-to-bone forces at joints, with muscle forces as a secondary interest. Sokoloff's sources are quoted by him as Furmaier (4), Kummer (8), Williams and Lissner (15) and Groh and

Weinmann (5) but specific force estimates are not ascribed to their authors. The values are summarised in Table 8.1. The estimates of Paul (10), Morrison (9) and Rydell (12) are the only ones not based on a static analysis and should therefore be given more weight. Rydell's figure comes from experimental measurements with strain gauges implanted in a hip replacement. Paul and Morrison undertook detailed analyses of normal walking, combining cine analysis and force platform data with anatomical measurements to provide the first comprehensive dynamic treatment of muscle and joint actions.

Williams and Svensson's main contribution was to emphasise the three-dimensional nature of the hip-joint problem, although they deal only with a static case. Unfortunately, they do not record their anatomical data on muscle lines of action and moment arms, but, in a review of their analysis, the author (14) was able to deduce approximate values for the original dimensions. In this review it was also shown that variations of $\pm \frac{1}{4}$ in. in the five important dimensions could result in a hip-joint force estimate of 9.7 W ,whereas substitution of the original dimensions gave only 5.7 W (W = body weight). The supposed $\frac{1}{4}$ in. variations are not unreasonable, in view of the difficulty of establishing lines of action and attachment points of complicated muscle groups. The large difference between the resulting estimates of hip-joint force underlines the need for caution in accepting calculated values and, at the same time, shows that percentage errors in such calculations will be difficult to assess.

c) Forces in athletic activities

The study of muscle and joint forces in athletic activities has received little attention. Plagenhoef (11) gives an impressive range of values for total joint moments in many sports situations but does not use the data to investigate internal details of muscle and joint action. Even for the gentle activities of Table 8.1 above, some of the forces are surprisingly large, and it is to be expected that vigorous athletic movement will produce much higher loadings. The later parts of this Chapter are devoted to calculation of

internal actions at the knee and ankle joints for the drop-landing described in Chapter 4. This activity involves fairly large external forces at the feet and forms a useful starting point for the investigation of forces generated in athletic situations.

d) Strength of Tendons and Ligaments

Tendons transmit muscular tensions to their points of attachment on the bone, and ligaments tie two bony elements together. Both types of tissue ".....consist of collageneous, elastic and reticular fibres and varying amounts of an amorphous ground substance. Since elastic fibres contain the low modulus material elastin, the high modulus effects of tendons and ligaments are due to the collagenous material present." (Haut and Little(6)).

Some information is available concerning the behaviour under load of these connective tissues. Abrahams (1) has described their tensile behaviour in terms of the state of the collagenous fibres which, in the unstressed state, appear as long wavy ribbons running through the tissue. The tensile stress-strain curve is concave upwards and Abrahams explains its form as follows:-

Strain, %	Effect on collagen fibres
0 - 1.5	Fibres begin to straighten their wavy pattern ('Ductile' behaviour)
1.5 - 3	Fibres become fully oriented and begin to assume most of the load (Increasing stiffness)
3 - 5	Entire response due to fibres in pure tension (Near-linear relationship)

Haut and Little have shown a similar type of behaviour for canine ligament under varying rates of strain, from 1.7 to 36.8 % per minute. There is an increasing resistance to extension with higher strain rates and an indication of the effects is given below:-

Strain rate, %/min	Stress, kg/mm^2	Strain, %
1.7	50	8
36.8	50	3

Clearly the response of collagen fibre to dynamic loading is significantly different from its behaviour in static tensile tests. Unfortunately,

the tests were not continued to rupture, and it can only be conjectured that the ultimate tensile strength under static loading may be appreciably lower than the loads which can be carried under dynamic conditions.

As to ultimate strength, Burry (2) and Elliott (3) report static tensile tests on many types of tendon and give the range of ultimate tensile stress as 5 - 10 kg/mm^2. Burry speaks of the Achilles tendon as the strongest in the human body and gives an average rupture load of about 1000 lbf, implying that its cross-sectional area is about 65 mm^2.

The patellar tendon, sometimes more precisely described as a ligament, has a cross-sectional area approximately equal to that of the Achilles tendon. Measurements by the author on a fresh cadaveric adult specimen gave a value of 85 mm^2. On Burry's and Elliott's tensile stress figures the range of tensile loads at failure is 935 to 1700 lbf.

Table 8.1

JOINT	POSITION	WORKER	FORCE (Units of body wt)
Hip	standing on one leg	Williams & Svensson	6.0
"	" "	Blount	3.4
"	" "	Backman	2.9
"	" "	Inman	2.4 - 2.6
"	" "	Rydell	2.5
"	normal walking	Paul	5.8
"	" "	Rydell	2.5
"	" "	Sokoloff	2.2
Knee	normal walking (femoro-tibial)	Morrison	3.03
"	" "	Sokoloff	5.3
"	Normal walking (patello-femoral)	"	3.6
"	deep squat (femoro-tibial)	"	10.6
"	deep squat (patello-femoral)	"	6.5
Ankle	standing on two feet	"	0.84
"	normal walking	"	1.9
"	squat	"	1.0

8.3 Force and Moment Equations

Analysis of ankle and knee joint actions during the drop-landing may reasonably be written as a plane motion problem. Figure 8.1 illustrates the force systems involved and the necessary anatomical dimensions required in setting up the equations.

Muscle actions have been reduced to a few major effects. At the ankle forcible dorsiflexion is resisted by tension in the Achilles tendon. The main muscles acting at this insertion are Soleum and Gastrocnemius, the former acting across the ankle alone while the latter passes also across the knee joint. Even in this simple representation it will be impossible to solve the three equations of motion to obtain both the Soleus and Gastrocnemius forces. For a solution some assumption must be made concerning the relative tensions in the two muscles.

Electromyography on the downward jump indicated that Gastrocnemius was strongly operative while Soleus appeared to have little activity; but even if much reliance were placed on e.m.g , the relative magnitudes of the muscle forces could not be assessed with confidence. Thus, two separate calculations were made on the assumptions:-

a) that Gastrocnemius provides the whole Achilles tendon force.

b) that Soleus and Gastrocnemius share the tension equally.

Such a procedure gives an indication of the possible effects of one-joint and two-joint muscles in the system.

The knee joint, unlike the ankle, cannot be regarded as a simple hinge. The combined rolling and sliding motion of the condyles has an important effect upon the geometry of the joint through the range of flexion. The patella and its tendon transmit the resultant tension of Quadriceps across the joint to the tibia in a wrapping action. The compressive force at the joint itself, carried over contact surfaces on the cartilages must, for analysis, be regarded as a single resultant force acting at a point of contact between the condyles. For further simplicity, frictional action

FIGURE 8.1 (a)

FORCE AND MOMENT EQUATIONS

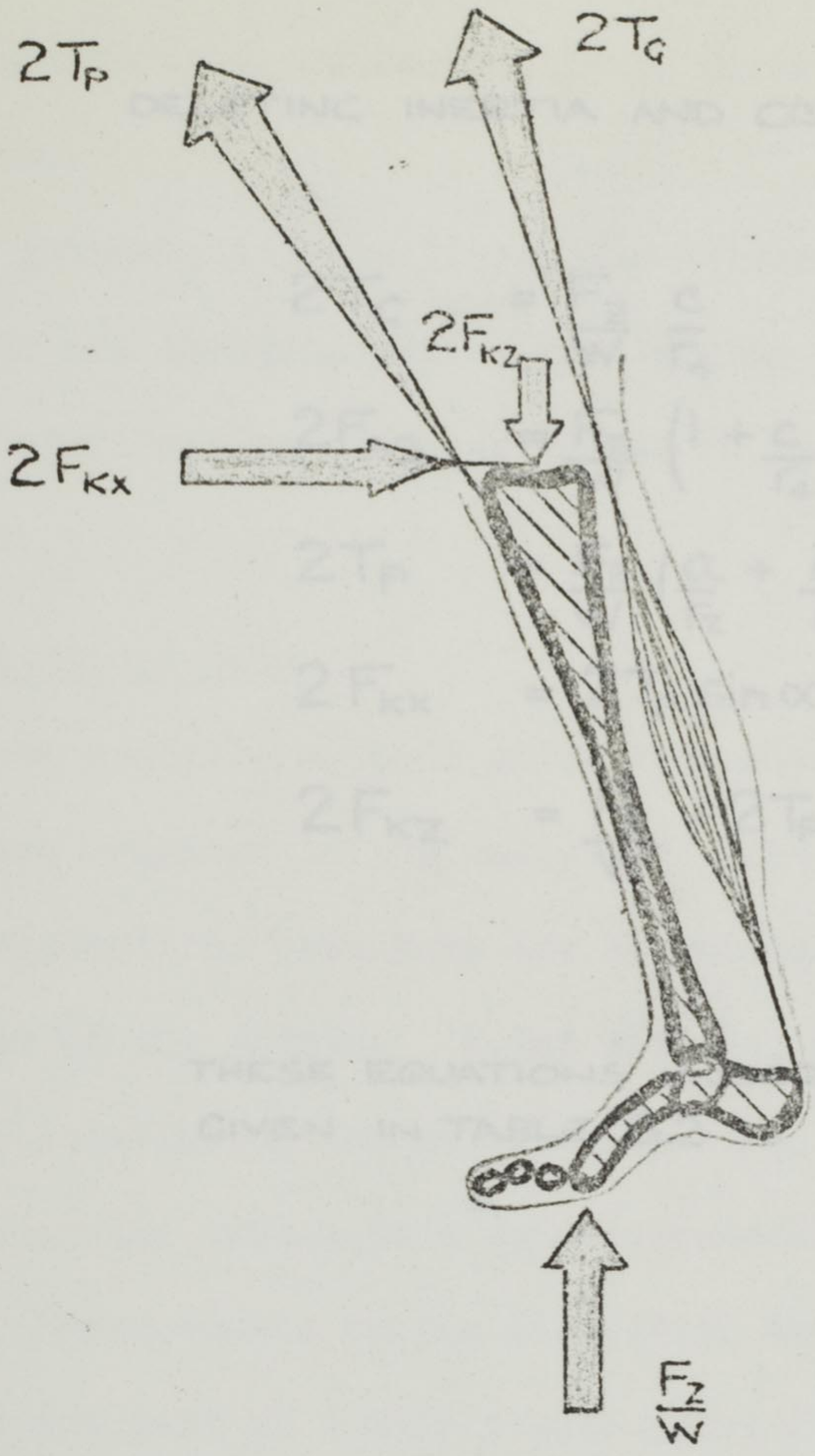

EXTERNAL, MUSCLE AND JOINT FORCES

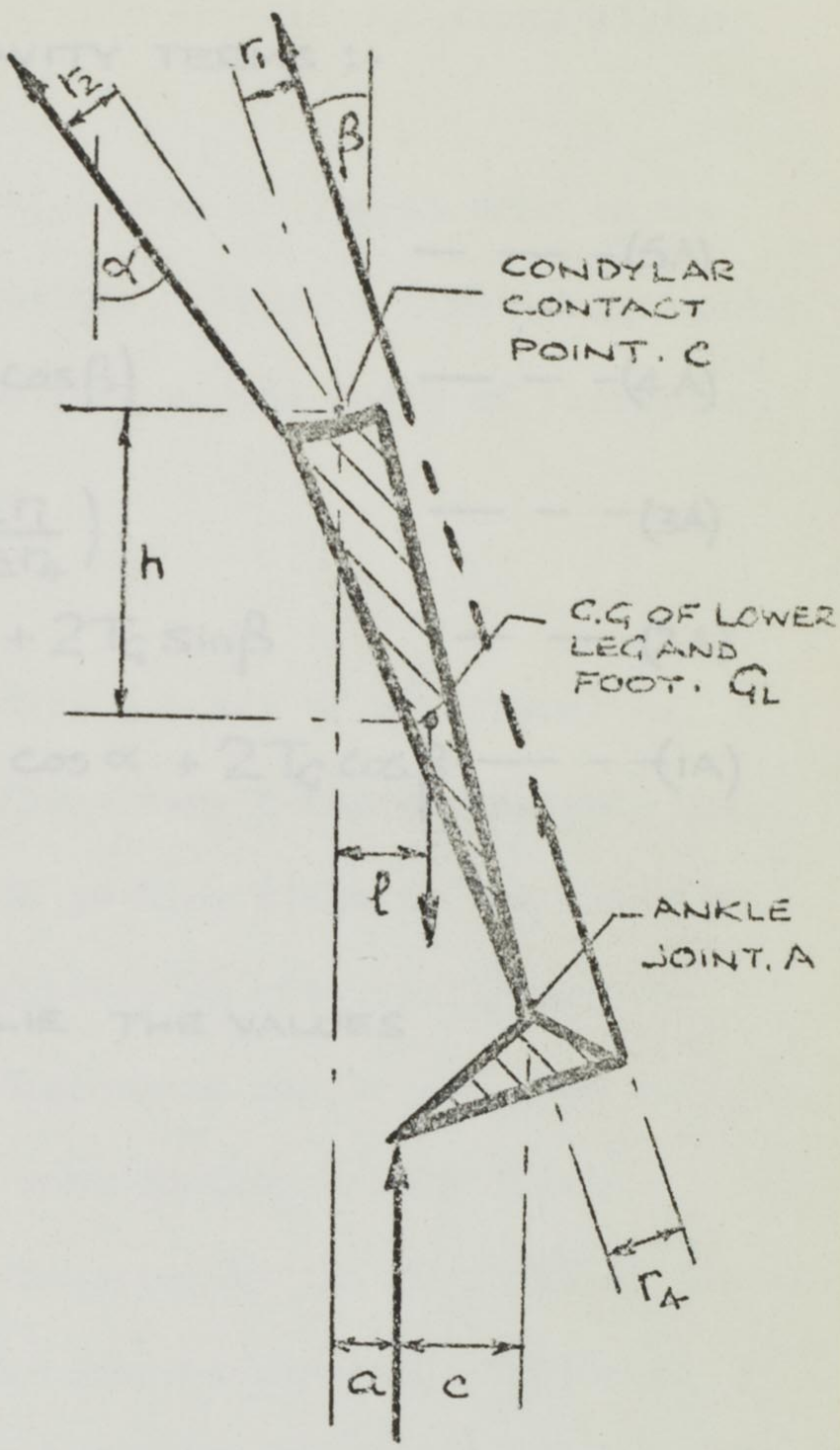

MOMENT ARMS

NOTES:-

INTERNAL FORCES SHOW ACTION OF BOTH LIMBS

BOTH LOWER LEGS AND FEET: MASS = $2m_L$, WEIGHT = $2W_L$, M.I. = I_{GL}

WHOLE-BODY : WEIGHT W

MASS OF FOOT ALONE CONSIDERED NEGLIGIBLE

MOMENT ARMS IN INCHES. OTHER UNITS lbf. slug. ft. s.

FOR LOWER LEGS AND FEET:-

$$\uparrow \quad \frac{F_z}{W} + 2T_p\cos\alpha + 2T_G\cos\beta - 2F_{KZ} = \frac{2m_L\ddot{z}}{W} + \frac{2W_L}{W} \quad ----(1)$$

$$\rightarrow \quad 2F_{KX} - 2T_p\sin\alpha - 2T_G\sin\beta = \frac{2m_L\ddot{x}}{W} \quad ----(2)$$

$$C) \quad \frac{F_z}{W}a - \frac{2W_L}{W}l + 2T_G r_1 - 2T_p r_2 = \left(\frac{2I_{GL}\ddot{\theta}}{W} + \frac{2m_L\ddot{x}h}{W} + \frac{2m_L\ddot{z}l}{W}\right) \quad -----(3)$$

FOR FEET ALONE:-

$$\uparrow \quad \frac{F_z}{W} + 2T_G\cos\beta = 2F_{AZ} \quad ----(4)$$

$$A) \quad \frac{F_z}{W}c = 2T_G r_4 \quad ----(5)$$

FIGURE 8.1 (b)

THE QUASI-STATIC MODEL

DELETING INERTIA AND GRAVITY TERMS :-

$$2T_G = \frac{F_z}{W}\frac{c}{r_4} \qquad \text{— — — (5A)}$$

$$2F_{AZ} = \frac{F_z}{W}\left(1 + \frac{c}{r_4}\cos\beta\right) \qquad \text{— — (4A)}$$

$$2T_P = \frac{F_z}{W}\left(\frac{a}{r_2} + \frac{cr_1}{r_2 r_4}\right) \qquad \text{— — (3A)}$$

$$2F_{KX} = 2T_P \sin\alpha + 2T_G \sin\beta \qquad \text{— — (2A)}$$

$$2F_{KZ} = \frac{F_z}{W} + 2T_P \cos\alpha + 2T_G \cos\beta \qquad \text{— — (1A)}$$

THESE EQUATIONS UNDERLIE THE VALUES GIVEN IN TABLE 8.2

at the point of contact is considered negligible. The outcome of these idealisations is a system soluble in terms of the dynamic equations at the knee joint.

In general, all the linear dimensions appearing as ,oment arms in the equations are changing during the landing action. Thus, a first requirement is the determination of these values as functions of the angle of flexion at the knee.

8.4 Anatomical Data

Three possible methods offer themselves as sources of anatomical dimensions required in the analysis. The first two, X-ray photographs and direct dissection, both have the advantage of getting close to the 'in vivo' operation of the joints. X-ray methods, however, do not usually produce clear delineation of the major muscles and dimensions can be obtained only by reducing the system to a two-dimensional construction on the drawing board. Measurements during dissection are hampered by the presence of tissue which is not part of a main muscle group and obscures important features.

The third technique for estimation of joint dimensions is a dry-bone rig. The major bones of the leg and foot, in a clean dry state, may easily be set and clamped in positions representing various degrees of joint flexion. Cords stretched between the estimated origins and insertions give the lines of action of muscles and allow measurement of moment arms. This latter method was adopted in the present studies.

Leg bones were obtained from excavations of mediaeval burials in York Minster. There were two reasons for going to such an unusual source. Firstly, medical skeletons for teaching purposes are often of rather small stature and unrepresentative of the normal adult male. Secondly, while a range of adult femurs and other bones may be available in a teaching hospital, matched sets of leg bones cannot easily be provided. The archaeological source was selected because complete skeletons were available and many possessed proportions comparable with the present day adult population.

FIGURE 8.2

DRY BONE RIG

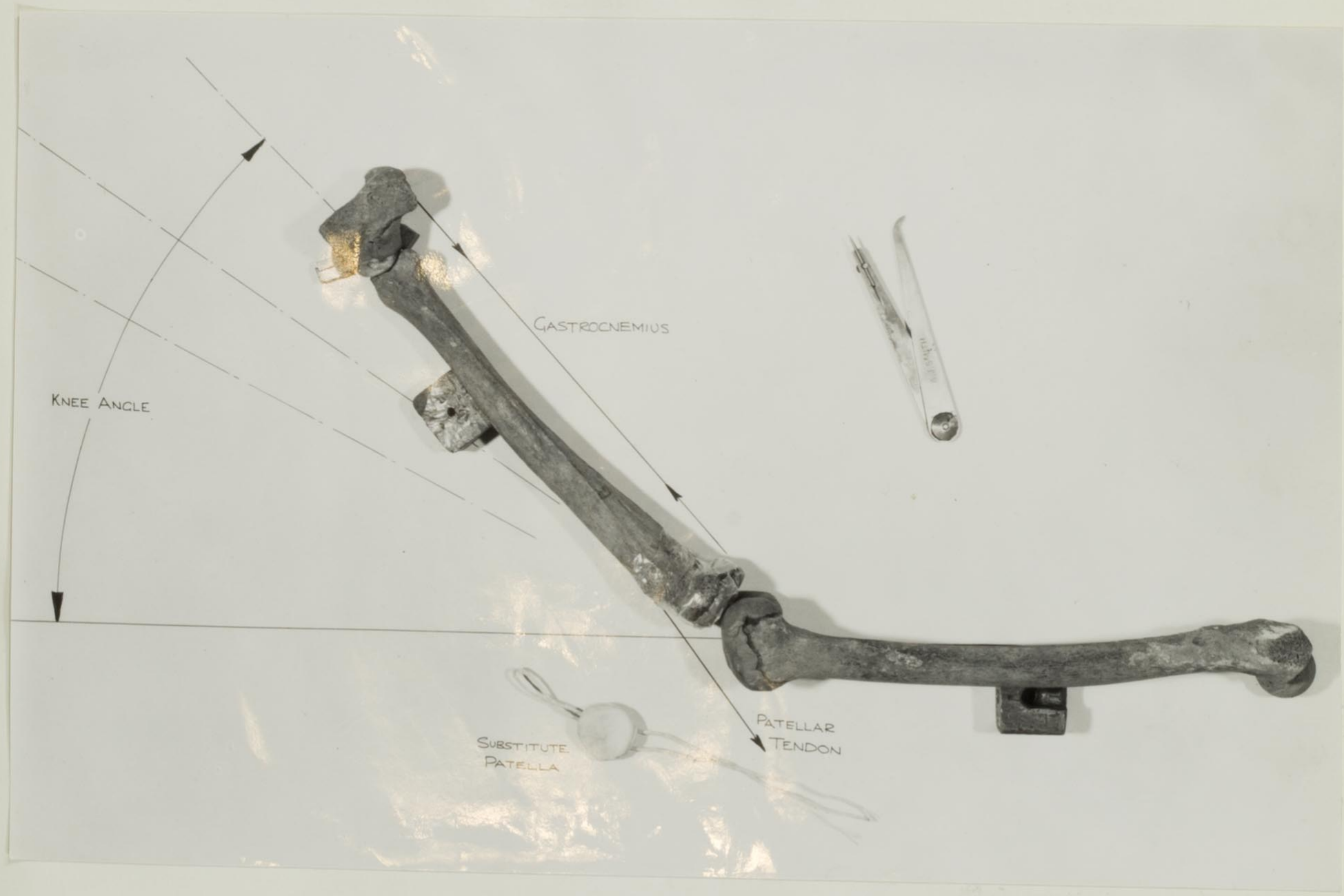

The dry-bone rig was set up on a horizontal surface and, at the outset, the cartilage surfaces at the joints were reconstituted. Dr. B.B. Seedhom assisted in this work and his detailed knowledge of knee-joint geometry was invaluable. The cartilaginous surfaces at the knee were reformed simply, but adequately, by moulding plasticine over the bone ends. The surfaces of the tibial condyles were covered with thin polythene sheet to prevent sticking. A substitute patella was moulded in a quick-setting resin with a cord cast into it to simulate the patellar tendon. The rig is illustrated in Figure 8.2.

Setting of the bones at various angles of knee flexion was carried out with particular attention to the point of contact between the femoral and tibial condyles. Moment arms at the knee were measured from this point with dividers, and similar dimensions were recorded at the ankle. The results of the dry bone measurements are summarised in Figures 8.3 and 8.4. In addition to direct measurement on the rig, bone contours and muscle lines were plotted on a large sheet of cartridge paper covering the working surface. Checking of some dimensions and angles was later carried out on the drawing board in the absence of the bones themselves. Cardboard formers representing the femur, tibia and foot were made to assist this graphical work. In the author's opinion, the simple methods employed in the bone rig and on the drawing board are quite adequate for the estimations of anatomical dimensions. Bearing in mind the simplifications imposed by the model of Figure 8.1, high accuracy in the measuring techniques is not warranted. Confidence in the results is better based on the fact that the curves of Figures 8.3 and 8.4 are fairly well defined by the experimental points.

8.5 Calculation of Muscle and Joint Forces

a) Initial quasi-static analysis

The lower limb positions were taken frame-by-frame from the drop-landing film (Chapter 4). Moment arms and muscle lines of action were read from Figures 8.3 and 8.4 at the appropriate knee angles, and the vertical forces

FIGURE 8.3

MEASUREMENT OF MOMENT ARMS

ON DRY-BONE RIG

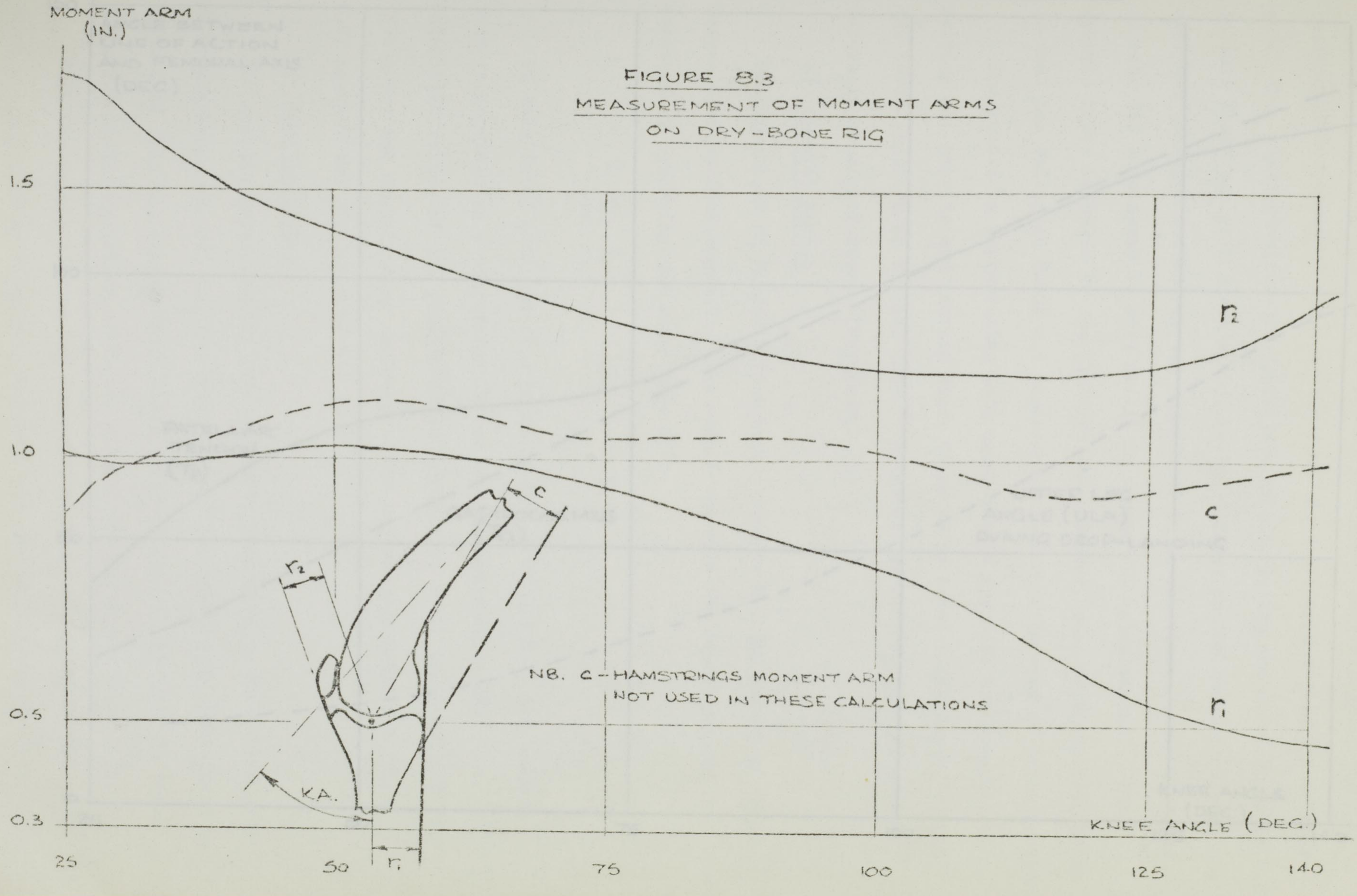

FIGURE 8.4

DIRECTIONS OF T_p AND T_g FROM DRY-BONE RIG

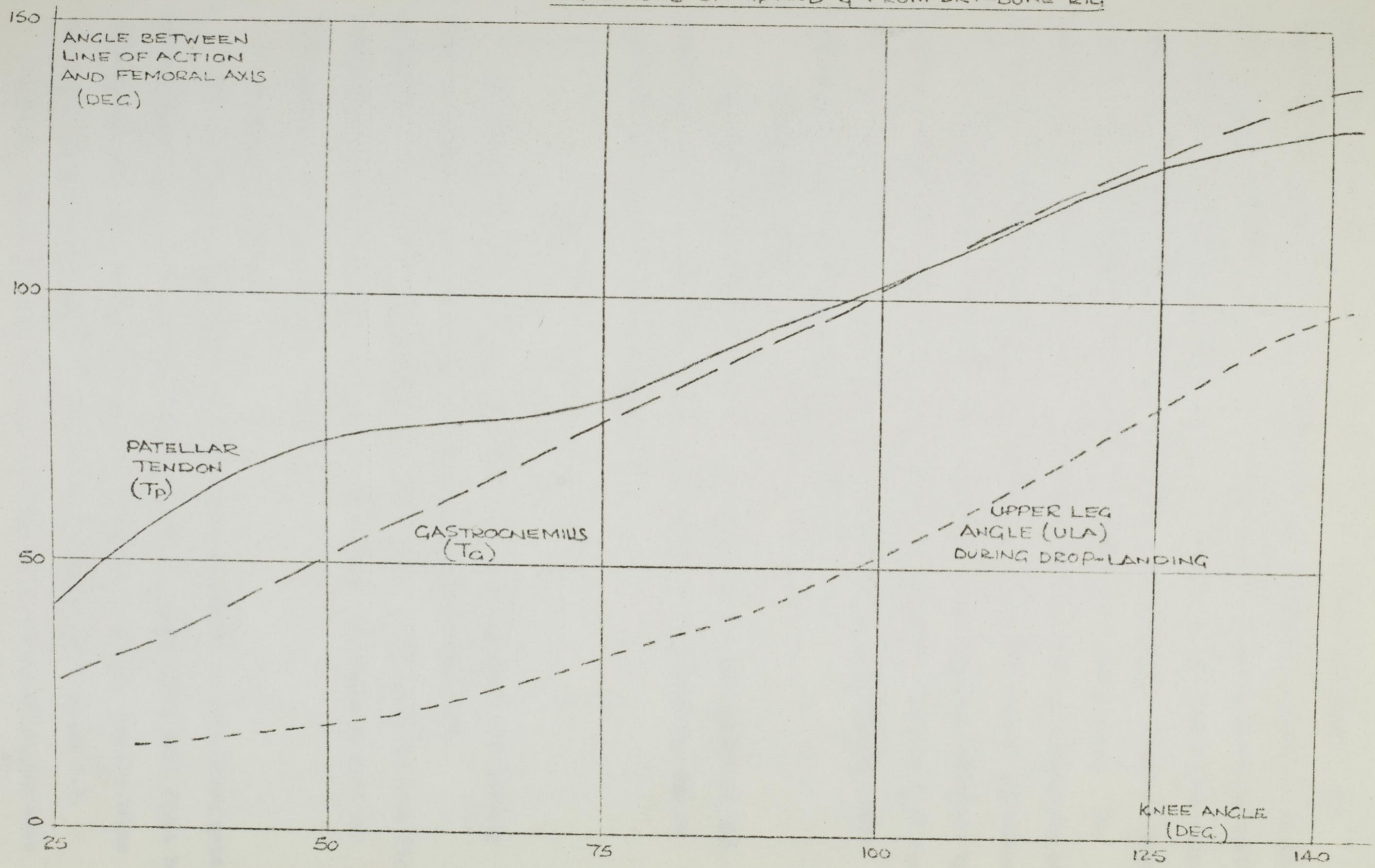

acting at the feet were taken from the force platform readings. The horizontal component of force at the foot was considered negligible in this activity. Extracts from the first tabular calculation are given in Table 8.2 In this first analysis gravity and inertia effects on the lower limb segments were not included and Soleus was considered to be inactive. Each of these effects was considered in more detail in subsequent calculations. The dynamic force measured by the platform was, however, used as a starting point so that the values in Table 8.2 represent a quasi-static view of the situation.

The equations representing this quasi-static approach are obtained by setting all gravity and inertia force terms to zero and inserting F_z/W from the force platform as initial data. Solution for T_p , T_g and the joint forces is straightforward. (Figure 8.1 (b))

b) Gravity Forces

The equations of Figure 8.1 contain a term in W_1, the weight of the lower-leg-plus-foot segment. Its significance in the equations may be assessed by comparing the magnitudes of :-

$$2\,\frac{W_L}{W}\cdot\frac{l}{r_2} \qquad \text{and} \qquad 2T_p$$

In this form, obtained from equation (3) of Figure 8.1, the gravity term is regarded as a correction factor on the muscle force 2Tp. Calculated values of the gravity force were fairly small compared with 2Tp throughout the drop-landing analysis. The values vary between 0.23 and 0.77 against the 2Tp range of 5.4 to 32.9.

c) Inertia Forces

The inertia terms require more elaborate treatment in that three sets of acceleration values, two translational and one rotational, must first be calculated from the displacement data. The effects of the inertia terms appearing in the equations of Figure 8.1 are summarised in Table 8.3.

Both the muscle tension and the vertical force component at the knee joint are modified by these computations, but the corrections are not serious.

TABLE 8.2 MUSCLE AND JOINT FORCES IN THE QUASI-STATIC MODEL

FRAME	KNEE ANGLE	GROUND FORCE F_z/W	$\frac{a}{r_2}$	$\frac{cr_1}{r_4 r_2}$	α	β	$2T_G$	$2T_P$	F_{AZ}	F_{KZ}	F_{KX}	LLA
1	33.6	9.0	0.63	1.19	40	19	17.1	16.3	12.6	18.8	8.0	18.3
2	42.4	3.0	1.67	1.37	49	25	6.2	9.1	4.3	7.3	4.7	24.6
3	54.7	2.8	2.58	1.78	53	35	7.0	12.2	4.3	7.9	6.9	33.5
4	60.2	4.0	3.63	1.55	53	37	8.4	20.7	5.4	11.6	10.8	36.4
5	71.4	5.3	4.53	1.68	49	42	12.2	32.9	7.2	18.0	16.5	38.0
6	90.3	4.0	4.92	1.80	51	48	10.2	27.0	5.4	13.9	14.3	46.7
7	101.0	1.8	5.73	1.46	51	49	3.8	12.9	2.2	6.3	6.4	47.6
8	109.8	1.0	5.73	1.22	49	49	2.0	7.0	1.2	3.5	3.4	46.2
9	114.9	0.8	5.73	1.07	49	49	1.5	5.4	0.9	2.7	2.6	45.1
10	119.4	1.0	6.00	0.94	48	49	1.8	6.9	1.1	3.4	3.3	43.8
11	124.5	1.8	5.75	0.87	45	46	3.4	11.9	2.1	6.3	5.5	45.7
12	124.9	1.8	6.33	0.82	45	46	3.2	12.9	2.0	6.8	5.7	43.6
13	128.4	2.3	6.68	0.73	42	44	3.7	17.0	2.5	8.8	6.5	43.0
14	130.2	2.3	6.68	0.67	41	44	3.7	16.9	2.5	8.9	6.8	42.2
15	134.1	2.4	6.40	0.68	39	42	4.1	17.0	2.7	9.3	7.2	41.5
16	137.0	2.5	6.40	0.64	35	40	4.0	17.6	2.8	10.0	6.3	41.7
17	141.0	2.7	6.15	0.50	33	39	3.9	18.0	2.9	10.4	6.1	42.5
18	144.0	3.0	5.62	0.55	31	38	5.0	18.5	3.5	11.4	6.3	43.0
19	149.1	3.2	5.42	0.53	29	37	5.3	19.0	3.8	12.1	6.2	46.8
20	149.8	3.3	5.42	0.47	27	36	5.4	19.4	3.9	12.5	6.0	46.2

- FORCES IN BODY-WEIGHT UNI
- RELEVANT EQUATIONS IN FIGURE 8.1 (b)

TABLE 8.3 EFFECT OF INERTIA FORCES

FRAME	(1) $\frac{2m_L\ddot{x}h}{W}$	(2) $\frac{2m_L\ddot{z}\ell}{W}$	(3) (1) + (2)	(4) $\frac{2I_{GL}\ddot{\theta}}{W}$	(5) (3) + (4) INERTIA COUPLE	ORIGINAL $2T_p$ (TABLE 8.2)	NEW $2T_p$	(6) $\frac{2m_L\ddot{z}}{W}$	ORIGINAL F_{kz} (TABLE 8.2)	NEW F_{kz}
1	+0.18	+2.54	2.72	−0.26	2.46	16.3	14.8	0.91	18.8	17.8
2	−1.56	+3.36	1.80	−0.37	1.43	9.1	8.1	0.91	7.3	6.5
3	−6.72	+4.64	−2.08	−0.52	−2.60	12.2	14.1	0.93	7.9	8.1
4	−7.65	+5.83	−1.82	−0.70	−2.52	20.7	22.6	1.06	11.6	11.6
5	−5.42	+6.02	0.60	−0.97	−0.37	32.9	33.2	0.97	18.0	17.6
6	−2.59	+3.32	0.73	−1.41	−0.68	27.0	27.6	0.49	13.9	13.8
7	+2.44	−1.25	1.19	−1.41	−0.22	12.9	13.1	−0.18	6.3	6.4
8	+3.88	−3.38	0.50	0.07	0.57	7.0	6.5	−0.52	3.5	3.6
9	+3.48	−3.58	−0.10	0.35	0.25	5.4	5.2	−0.55	2.7	2.9
10	+2.72	−1.61	1.11	0.30	1.41	6.9	5.7	−0.26	3.4	3.1
11	+1.50	+0.13	1.63	0.12	1.75	11.9	10.4	0.02	6.3	5.8
12	+0.39	+0.82	1.21	0.04	1.25	12.9	11.9	0.13	6.8	6.1
13	+0.23	+0.84	1.07	0.04	1.11	17.0	16.1	0.13	8.8	8.4
14	+0.49	+0.50	0.99	0.06	1.05	16.9	16.0	0.08	8.9	8.5
15	+0.90	+0.22	1.12	0.15	1.27	17.0	16.0	0.03	9.3	8.9
16	+0.77	0	0.77	0.28	1.05	17.6	16.8	0	10.0	9.7
17	−1.05	−0.50	−1.55	0.42	−1.13	18.0	18.9	−0.08	10.4	10.8
18	−1.44	−0.85	−2.29	0.46	−1.83	18.5	19.9	−0.13	11.4	12.0
19	−0.36	−1.27	−2.63	0.46	−2.17	19.0	20.6	−0.20	12.1	12.9
20	0	−1.69	−1.69	0.46	−1.23	19.4	20.3	−0.26	12.5	13.0

NOTES:-

(i) COLUMNS (1), (2) AND (4) FORM THE R.H.S. OF EQUATION (3) IN FIGURE 8.1 (a).

(ii) NEW $2T_p$ = ORIGINAL $2T_p$ − $\frac{\text{INERTIA COUPL}}{r_2}$ USING EQUATIONS (3) AND (3A) OF FIGURE 8.1.

(iii) COLUMN (6) GIVES THE INERTI FORCE ON THE RHS. OF EQUATION (1), FIGURE 8.1(a).

(iv) NEW F_{kz} IS OBTAINED FROM THE LATTER EQUATION USING THE NEW $2T_p$ VALUES AND THE INERTIA FORCES OF COL(6

(v) ALL FORCES NONDIMENSIONAL IN THE FORM $\frac{F}{W}$. ALL COUPLES AND MOMENTS IN THE FORM:- NONDIMENSIONAL FORCE × MOMENT ARM IN INCHES.

d) Contribution of Soleus

Until now the Achilles tendon tension has been ascribed entirely to Gastrocnemius. In the absence of more precise information on load-sharing between muscles, the effect of Soleus on the Achilles tendon can only be surmised. Some indication of its influence is given by assuming equal load carrying by Soleus and Gastrocnemius. The subsequent calculations were carried out on the quasi-static model and the values are compared in Table 8.5 with the original results, which assumed Soleus inactive.

e) General Comments

The corrections to the quasi-static results caused by the introduction of gravity and inertia terms in the equations of motion are relatively small. An informative picture of the orders of magnitude of muscle and joint forces throughout the drop-landing is given by the straightforward quasi-static analysis. The laborious inertia force calculations leading to the full dynamic analysis do not seem warranted in the present study. However, it must be noted that the translational moment-of-momentum terms (Columns 1 and 2 of Table 8.3) tend to cancel each other when their magnitudes are high. Had they been additive during frames 2, 3 and 4 their net effect on the later entries would have been appreciable. Omission of inertia forces has therefore not been justified as a general rule by the results of the drop-landing analysis.

The force calculations are summarised graphically in Figures 8.5 and 8.6.

As in the earlier force estimates (Chapters 4 and 5) it is clear that manual calculation, especially when inertia forces appear, is prohibitively tedious and the possibility of errors due to fatigue increases rapidly. A computer programme for internal force calculations is required and the basis is laid in the fundamental equations (Figure 8.1) and the anatomical data (Figures 8.3 and 8.4). Morrison's (5) work on the knee joint was computer based but the model had a rather simpler form than that employed in the drop-landing. In Morrison's studies it was found that either the patellar

FIGURE 8.5 DROP-LANDING FORCES IN THE QUASI-STATIC MODEL

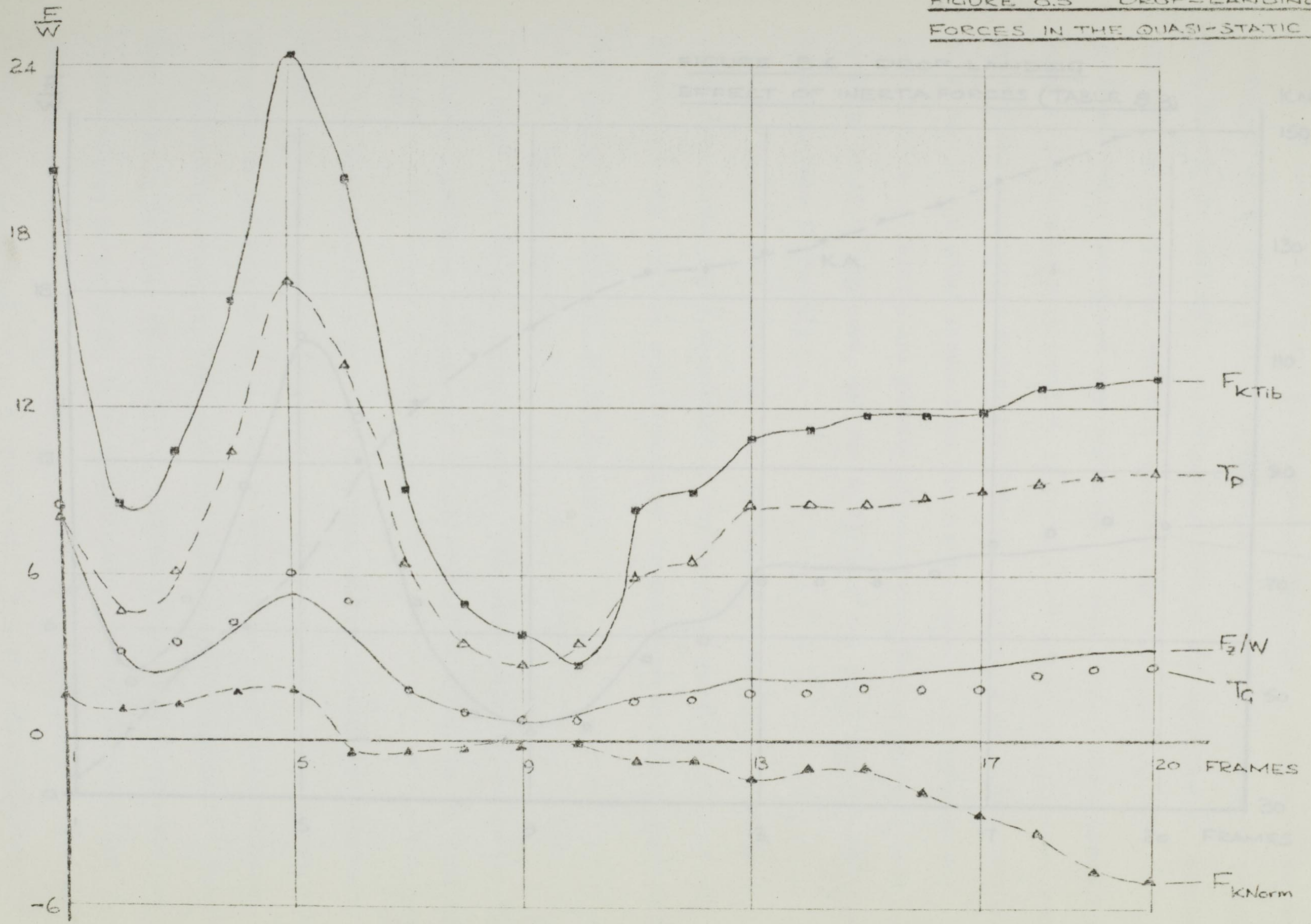

FIGURE 8.6 DROP-LANDING

EFFECT OF INERTIA FORCES (TABLE 8.3)

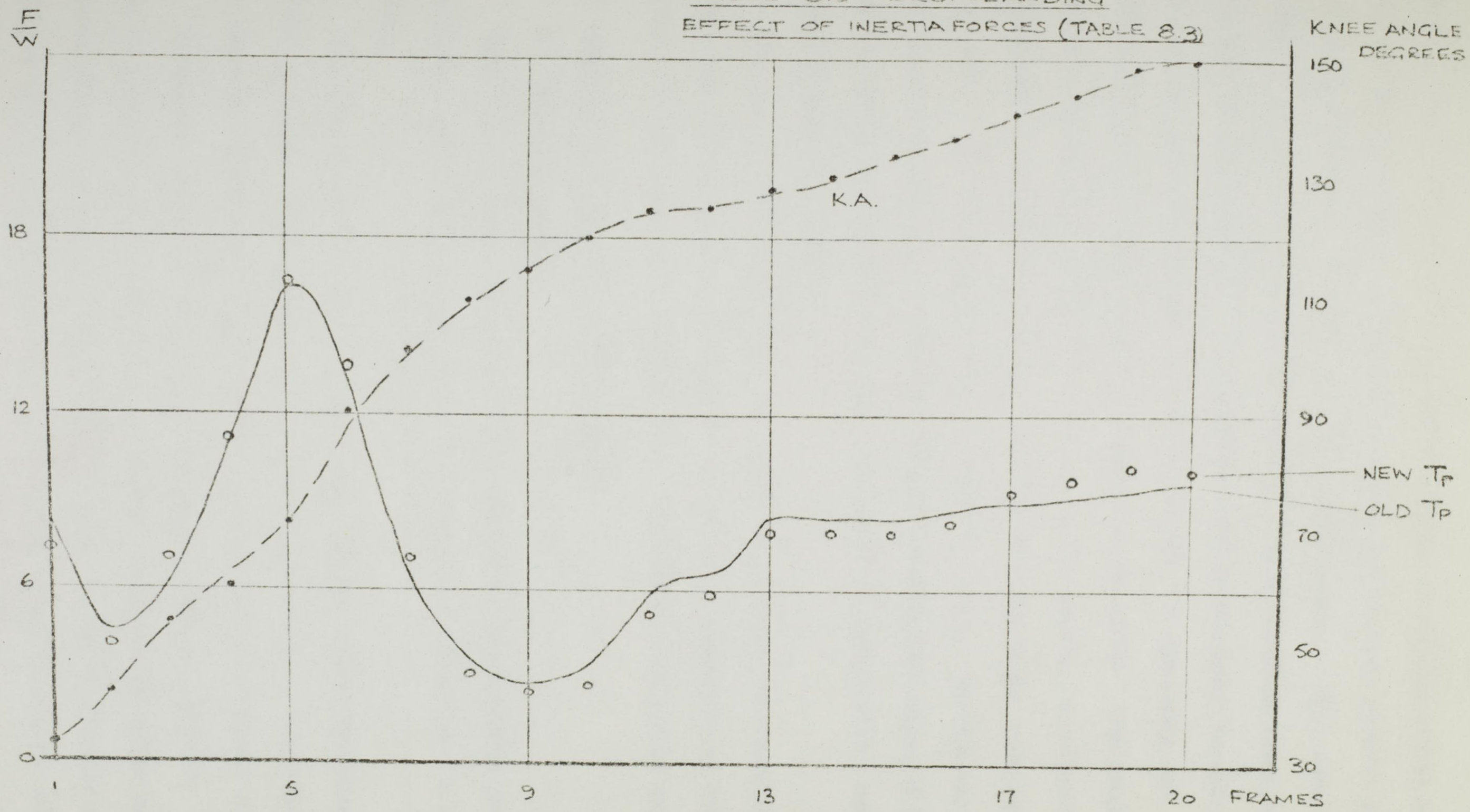

tendon or Gastrocnemius were in tension during the walking stride but not both at the same time. In the drop-landing model a more general representation is needed with Tp and T_Q acting simultaneously. This model may be useful in the study of a range of athletic activities where measurements of foot thrust are available. A programmed form of the model should include all the inertia effects, and will therefore call for smoothing and differentiation techniques examined earlier in this work. The programme would be particularly informative if inertia and gravity contributions were printed out as separate correction terms in addition to the main output of total muscle and joint forces from the dynamic model. In this way the significance of inertia and gravity effects for different types of body activity would be explored, and the validity of the quasi-static model could be tested more thoroughly.

The quasi-static model has been emphasised because its essential simplicity allows rapid assessment of the orders of magnitude of internal forces, and the physical significance of the equations is easily appreciated.

8.6 Assumptions Implicit in the Analysis

a) Inactive Muscles

Apart from Soleus, discussed above, some other major muscle groups in the lower limbs have been assumed to have negligible effect in the landing action.

The dorsiflexors of the foot have been omitted because the external effect of ground reaction is itself a strong dorsiflexor. Its moment about the ankle is unlikely to be assisted by internal action of flexor muscles.

Hamstring action has been neglected under a similar argument. The knee is being forcibly flexed due to external forces on the body, and the natural action in the limbs is to resist flexion by the Quadriceps and patellar tendon, not to aggravate the effect by adding Hamstring tension. Palpation of Hamstrings during a squat action reveals a slackness which supports this reasoning.

If it be argued that some stabilising tensions in these and other

muscles may be necessary, one should note that such additional forces in the system would, in general, add to the magnitudes of the internal forces already calculated.

b) Friction

The effect of frictional action in the joints has been ignored mainly for analytical simplicity, and it is reasonable to regard such effects as small compared with the force magnitudes appearing in the present analysis.

c) Ground reaction

The thrust of the ground on the feet has been assumed to be purely vertical. The drop-landing from a hanging position approximates to vertical motion of the body mass-centre and trials on the force platform showed very small horizontal components.

The point of application of the vertical thrust F_z was constructed on tracings from the cine frames by taking the mid-point of the contact line between the foot and the platform. More accurate experimental determination of the position does not appear possible, but during the calculations the effect of moving the point of contact across the contact area was examined. For a given limb position the moment arms a and c both vary, though their sum remains constant. A typical calculation (frame 7) showed that, with F_z acting at the point of contact nearest the heel, there was a reduction in T_G from 1.9 to 1.1 and an increase in Tp from 6.5 to 6.8. These variations are extreme, for it is reasonable to suppose that F_z acts somewhere in the central region of the contact area.

d) The Tibial Condyles

The line of action of Gastrocnemius was constructed tangentially to the rear radius of the tibial condyles. This construction determines the moment arm r_1 whose value has a direct influence on the value of Tp. An increase in r_1 from 0.8 to 1.2 causes Tp to increase from 6.5 to 8.2. It is not possible to give realistic anatomical variations in r_1 but it seems probable that the range here given is extreme.

In general, the comments under c) and d) above underline the fact that force estimates are subject to errors which may be fairly large but which themselves involve some uncertainty in their determination. The computed forces must be regarded as reasonable order-of-magnitude estimates showing the relative importance of the muscular and joint actions for a typical set of anatomical dimensions.

8.7 Interpretation of the Results

a) The Initial Impact

At frame 1 in the calculated results, the force platform reading of the high initial impact force has been taken as a starting point (Figure 7.1, Chapter 7). It was suggested there (Section 7.2) that the first contact of the toes on the platform acts upon the body more as a shock load at the end of a rigid bar than as a force causing response of the flexion properties of the joints and muscles. Probably the shock is dissipated in flexions and compressions within the joints of the foot and ankle. It is not possible to offer analysis of the foot actions in such a complex case, but downward jumping from a moderate height provides convincing sensations to the subject of the transmission of shock loads to the ankle and knee when landing stiffly.

In interpreting the results of Figures 8.5 and 8.6 therefore, the values at frames 1 and 2 should be given little credence. Estimates of joint force in such a situation would require a model of the elastic behaviour of bone and cartilage in the foot and leg, and a detailed knowledge of the loading applied to the system through the foot.

b) Maximum tendon forces (Frames 5-6)

These forces are the greatest calculated in the drop-landing analysis (ignoring the spurious results at frame 1). Appreciable joint flexions occur during the rise and decay of these forces and the values may be regarded as a good indication of the major internal actions in the limbs.

Maximum muscle tensions, Tp = 16.5 and T_G = 6.1 (body-weight units) are derived, and for a subject weighing 160 lbf the corresponding tensions

in the patellar and Achilles tendons are 2640 and 976 lbf. These forces are very large compared with the static tensile strength values of about 1000 lbf for the Achilles and patellar tendons (Section 8.2 d)). The present calculations appear to indicate serious damage or rupture, although the subject walked away from the drop-landing tests apparently unharmed.

It has been indicated in Section 8.2 d) that tendinous material at high rates of strain is much more resistant to extension ('stiffer') than under near-static loading. Damage to the tendinous tissue may be associated with over-extension of the fibrous structure and a consequent tearing of internal bonds. Thus increasingly 'stiff' response at high strain rates suggests that the tendon protects itself from overstrain by means of a velocity-dependent resistance to dynamic loading. In this way it may, during vigorous activity, be possible for tendons to transmit tensions which as static loads would cause damage.

The calculated tensions in the patellar tendon are influenced, in the model of Figure 8.1, by the presence or absence of Soleus action. If Soleus, acting only across the ankle joint, carries an appreciable part of the Achilles tendon load, then the tension transferred by the two-joint action of Gastrocnemius across the knee is reduced. The tension in the patellar tendon will also be a little lower in this case. However, the major effect is due to the thrust at the feet (equation (3) of Figure 8.1 (a)) and the overall effect of Soleus action is not great:-

Soleus action	Calculated patellar tendon tension at frame 5 (lbf)
Zero	2640
Equal load-sharing with Gastrocnemius	2277

Thus, the indications are that the Achilles and patellar tendons are very heavily loaded during the drop-landing, and it must be borne in mind that considerably more severe downward jumps are often performed, apparently without ill-effects.

c) Knee Joint Forces

The components F_{Kz} and F_{Kx} are referred to vertical and horizontal axes external to the body. More use may be made of these data if the forces are resolved into components along and normal to the tibial axis throughout the motion. The first of these new components may be considered an indication of the direct compressive force between the femoral and tibial condyles for there is no other means available in the joint to resist the thrust.

The second, normal to the tibial axis, approximates to a shearing action across the condylar surfaces. The structure of the joint suggests that an action of this kind will be resisted primarily by tension in the cruciate ligaments plus a lesser effect due to curvature of the mating surfaces of the joint.

Values for the tibial and normal components appear in Table 8.4. It will be seen that an enormous compressive force is calculated at frame 5. For a 160 lbf subject the force is 3904 lbf, which seems unbelievably high for a voluntary non-injurious activity.

Whatever may be the errors involved in the determination of such a force, it must be recognised that this value, and the other internal forces computed above, show clearly that the measured foot thrusts (F_z/W) are magnified to considerably higher forces within the muscles, tendons and joints. The oompressive forces at the tibial condyles calculated for the drop-landing (F_{KTib}) suggest strongly that such an impact situation may do more damage than the subject realises. The occurrence of torn cartilage in a hill-walker and a fast-bowler, mentioned in Chapter 1, are instances known personally to the author which show that repeated 'moderate' impacts probably cause irreparable damage. As in the drop-landing, the victim is unaware of anything more than a jolt at each impact, and neither he nor his medical adviser can assess the severity of the effects until it is too late, and the semilunar cartilages are damaged sufficiently to cause pain.

TABLE 8.4 TIBIAL AND NORMAL FORCES

FRAME	LLA	F_{KTib}	F_{KNorm}
1	18.3	20.3	1.7
2	24.6	8.6	1.2
3	33.5	10.4	1.4
4	36.4	15.8	1.8
5	38.0	24.4	1.9
6	46.7	20.0	-0.3
7	47.6	9.0	-0.3
8	46.2	4.9	-0.2
9	45.1	3.8	-0.1
10	43.8	2.7	0
11	45.7	8.3	-0.7
12	43.6	8.9	-0.6
13	43.0	10.9	-1.3
14	42.2	11.2	-0.9
15	41.5	11.7	-0.8
16	41.7	11.7	-1.9
17	42.5	11.8	-2.5
18	43.0	12.7	-3.2
19	46.8	12.8	-4.6
20	46.2	13.0	-4.9

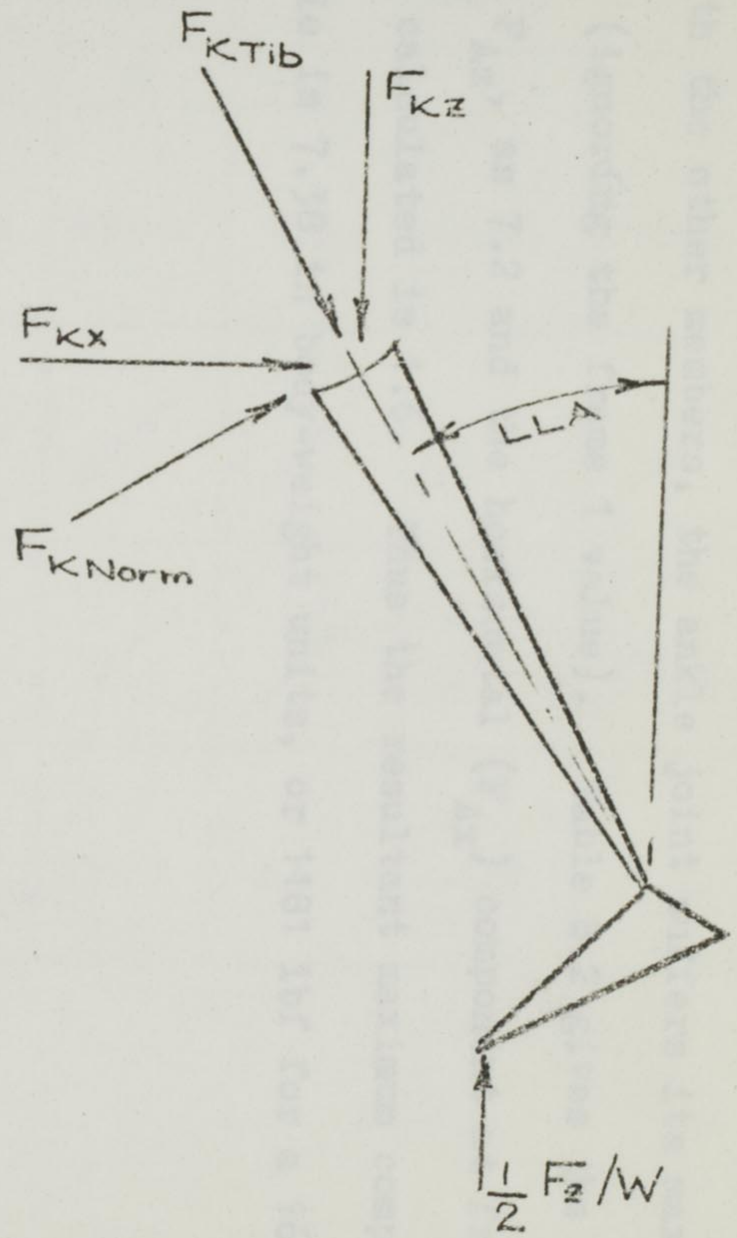

d) Ankle Joint Forces

As with the other members, the ankle joint suffers its maximum loading at frame 5 (ignoring the frame 1 value). Table 8.2 gives the vertical component, F_{Az}, as 7.2 and the horizontal (F_{Ax}) component at frame 5, separately calculated is 1.6. Thus the resultant maximum compressive load at the ankle is 7.38 in body-weight units, or 1181 lbf for a 160 lbf subject.

SECTION 8.5 e) TABLE 8.5. SUMMARY OF INTERNAL FORCES AT FRAME 5

COMPUTATION	T_G		T_P		F_A		F_{KTib}		F_{KNorm}		F_{Kz}	
	A	B	A	B	A	B	A	B	A	B	A	B
SOLEUS INACTIVE												
QUASI-STATIC MODEL	6.1	976	16.5	2640	7.4	1181	24.4	3904	1.9	304	18.0	2880
GRAVITY FORCE CORRECTION ON T_P	/	/	0.62	99	/	/	/	/	/	/	/	/
INERTIA FORCES INCORPORATED	/	/	16.6	2656	/	/	/	/	/	/	17.6	2816
SOLEUS ACTIVE												
QUASI-STATIC MODEL	3.1	488	14.2	2277	7.4	1181	17.0	2742	2.9	467	11.6	1859

A - BODY-WEIGHT UNITS
B - FORCE IN lbf FOR 160 lbf SUBJECT

FORCES ARE IN GENERAL MAXIMUM VALUES BUT MAX. F_{KNorm} IS -784 lbf AT FRAME 20 (DEEP-SQUAT)

8.6 References for Chapter 8

1. Abrahams, M. 'Mechanical behaviour of tendon in vitro, a preliminary report' Med. & Biol.Eng. 5. 433-443 (1967)

2. Burry, H.C. 'The Pathology of the Painful Heal' B.J. Sports Med. 6 1. 9-11 (1971)

3. Elliott, D.H. 'Structure and Function of Mammalian Tendon' Biol. Rev. 40 392 (1965)

4. Furmaier, ' 'Beitrag zur Mechanik der Patella' Arch. Orthop. Unfallchir 46 78-90 (1953)

5. Groh, Weinmann, 'Uber die am Kniegelenk auftretenden Krafte' Z. Orthop. 96 527-530 (1962)

6. Haut, R.C. Little, R.W. 'Rheological Properties of Canine Anterior Cruciate Ligaments' J. Biomech. 2 289-298 (1969)

7. Inman, V.T. 'Functional Aspects of the Abductor Muscles of the Hip' J. Bone & Jt.Surg. 29 607 (1947)

8. Kummer, 'Gait and Posture Under Normal Conditions' Clin. Orthop. 25 32-41 (1962)

9. Morrison, J.B. 'The Forces Transmitted by the Human Knee Joint during Activity' Ph.D Thesis. Univ. Strathclyde (1967)

10. Paul, J.P. 'Bioengineering studies of the forces transmitted by joints (ii) in 'Biomechanics and Related Engineering Topics' (ed. Kenedi) Pergamon Press (1965)

11. Plagenhoef, S. 'Patterns of Human Motion' Prentice Hall (1971)

12. Rydell, N. 'Forces in the hip-joint' as ref. 10 (1965)

13. Sokoloff, L. 'The Biology of Degenerative Joint Disease' Univ. Chicago Press (1969)

14. Smith, A.J. 'Estimation of Forces at the Hip and Knee Joints' Unpublished survey, Univ. Leeds (1970)

15. Williams, M. Lissner, H.R. 'Biomechanics of Human Motion' W.B. Saunders (1962)

16. Williams, J.F. Svensson, N.L. 'A force analysis of the hip joint' Bio-med.Eng. 3 8. 365 ff (1968)

Chapter 9

Summary and Conclusions

9.1 Body Moments of Inertia (chapter 2)

a) M.I. Factors

The discussion presented in Chapter 2 proposes the non-dimensional Moment of Inertia Factor as a basis for the study of the inertia properties of the human body. Three systematic methods for computation of Y-axis moments of inertia are developed. The column-total procedure is the most obvious, but the other two, based on the shift equations for a change in configuration, have certain merits. Direct use of the shift equations provides configuration-dependent functions expressing continuous change of body moment of inertia during a complex body movement. As an alternative, the Δk Tables, generated from the shift equations, offer some saving in numerical work and rough computations may quickly be made from the tables. Each of the three methods requires the shifts Δk of the segments from the reference (standing) position and it has been found that drawing-board construction at one-quarter full-size on the mean-man model will give the Δk values rapidly and with sufficient accuracy. A valuable adjunct to this work is a permanent drawing of a quarter-full-size model comprehensively labelled with the mean-man segmental masses, lengths and mass-centres in both normal and nondimensional units.

b) Model Comparisons and Improvement

The suggestion that moment of inertia be plotted against MH^2 appears fruitful, and the graphs of this form given in Chapter 2 highlight the behaviour of these mechanical quantities for both experimental and model determinations. Such plots also show up the effect of a model correction procedure in a qualitative fashion.

A quantitative assessment of improvements to model M.I. predictions has been based on the distribution of errors between the Santschi experimental data (66 subjects) and the values from a modified segmental model. Hanavan's scheme for 'tailor-made' segmental models, requiring a large computational programme, has been compared in Chapter 2 with my suggestion

for model correction on the basis of the single parameter Lz/H. Satisfactory improvements in the overall pattern of M.I. values are achieved by the Lz/H correction, and, as far as it has been investigated, this simple procedure seems to achieve results comparable with those of Hanavan.

c) Extension of M.I. Studies

Future work in this field is required along three main lines:-

1. Computation of moments of inertia for the X and Z axes.
2. Experimental determination of moment of inertia for subject groups of markedly different body build and the distribution pattern of these data on the I vs. MH^2 plot.
3. Further investigation of the Lz/H correction procedure for body configurations not studied in the present work.

9.2 Numerical Computation (Chapters 5 and 6)

a) Fourier and differentiation methods

Fourier analysis of displacement data has been found useful in the determination of the noise and information content of cine readings. An interesting feature of the frequency structure was the upper limit of the cut-off frequency at about 5 Hz with a corresponding sampling frequency around 10 Hz. This sampling frequency is close to the value determined independently by trial-and-error smoothing-differentiation procedures using a range of data spacing. By the latter method the 20-frame spacing at 224 frames per second (sampling frequency 11.2 Hz) was found to produce second derivative results which were acceptably smooth and agreed well with measured force values.

These results lead to the surprising conclusion that film taken at only 11 frames per second could have recorded the motion adequately, and that more detailed information recorded at higher frame rates is so inextricably mixed with noise that it will be lost in the essential smoothing processes applied during computation.

b) Digital filtering and its application

Many questions remain unanswered in the field of numerical differentiation, and it is probable that the most effective approach to the data processing problem will incorporate frequency analysis, not only of the displacement data but also of derived velocities and accelerations. It has been indicated in Chapter 5 that the three-point moving average procedure virtually removes the upper half of the frequency range of the original data. In communication engineering it is customary to speak of 'digital filtering' when data are put through a computational procedure. The effect is analogous to the feeding of an electrical signal through an electronic filter. Changes, particularly in the frequency structure of the signal or data, will occur. Numerical data passing through a smoothing, differentiation or other computational procedure will therefore undergo predictable changes in their frequency spectrum once the 'filtering' characteristics of the computation have been determined. It will be particularly valuable to the present work if the action of the five-point and nine-point second-derivative techniques as digital filters can be established.

c) Computer programme development

The force analysis programme of Chapter 6 requires further development to handle the X and Z translational components and the equation for plane rotational motion. The latter, developed in Chapter 3, calls for programming of body moment of inertia and its rate-of-change, and it is necessary here to bring in a general treatment of moment of inertia, such as the shift equations of Chapter 2. The rotational-motion section will demand a considerable period of programming and testing. It is possible that some terms, particularly those expressing moments of momentum relative to the mass-centre, may be negligible in practical application of the rotational-motion equation. If so, the programme will be considerably reduced and simple approximate methods may be adequate for manual calculation of body-rotation effects. It should be emphasised that the rotational

equations apply to both free aerial motions and to situations in which there is contact with external agencies.

The programme may be further refined by the incorporation of a Fourier section at the beginning, so that 'noise' is determined by a frequency analysis, and appropriate removal of higher-frequency terms is carried cut within the programme. The Fourier programme provided by Andrew (Chapter 5) was allied in his work to a study of best-fit procedures, and it is possible to select by such methods a curve fitting the displacement data according to a predetermined best-fit criterion. The production of a fitted curve may be of value in some applications of cine analysis.

It is clear that the computational aspects of the present work provide much scope for development and the value of the programme will be further enhanced if graphical output facilities can be included.

9.3 Force Calculations (Chapters 5 and 7)

a) Comparison with force platform measurements

In this work the force platform has been mainly used as a check on the forces calculated from cine analysis. Although smoothing erases some of the finer fluctuations in the force history obtained from cine calculations, general agreement with the force platform results is encouraging. It is disappointing that the double-peak effect cannot be generated by the cine analysis as it stands. However, there seems considerable promise in the curve-fitting and interpolation procedure used by Wallach and Saibel (Chapter 5) If the fine detail of the created points can be relied upon, differentiation can go ahead at a fine data-spacing and in the absence of serious noise. The discussion of differentiation at the double-peak in Chapter 7 shows that fine data-spacing (that is, a high sampling frequency) with little or no noise can reproduce the double-peak phenomenon to a high accuracy. The question to be settled is to what extent Wallach and Saibel's interpolation fitting can be relied upon to represent the 'true' data when second derivatives are to be computed. Here again an intriguing

problem in numerical analysis presents itself.

b) Study of skilled movement

The subdivision of total force into segmental contributions (Chapter 7) is proposed as a technique which may throw light on the pattern of co-ordinated human action. Apart from cine analysis of this kind there seems to be no other way in which the combination of limb and trunk motions into a skilled co-ordinated performance may be studied in detail. Certainly the filming process has the immense advantage of being remote from the performer and, further, it requires little prior preparation. It is hoped that the segmental subdivision method presented here will be developed as a useful technique in the study of skilled action and of learning processes in which the limb movements are gradually brought into proper co-ordination for the most effective result. It is clear, from the progressively improved drop-landings recorded in Chapter 7, that such a process of skilled adaptation is recorded by the force platform. It is reasonable to suppose that cine analysis of the landing actions would throw more light on the way in which the body can reduce the intensity of impact by well-timed limb and trunk movements.

9.4 Muscle and Joint Forces (Chapter 8)

a) The model and its shortcomings

The model of muscle and joint action in the leg which was employed in Chapter 8 has, not unexpectedly, been criticised for its simplicity. Colleagues in the medical world point out that Gastrocnemius and Soleus are not straight tension members attached at their extremes to the skeleton but that there is a complicated overlapping and wrapping of muscles. One answer to such comments is that no model incorporating the detailed geometry of the muscles and bones in the leg has been proposed and that solution for the forces in such a system would be impossible. In Chapter 8 it is made clear that, even with the simplified model used in the present studies, some assumption must be made concerning the presence or absence of Soleus

action. If we are to obtain any numerical estimates of muscle and joint forces the model must make considerable, but, it is hoped, reasonable simplifications while still retaining the essential features of the internal actions.

Because these simplifications are somewhat subjective, it is impossible to make quantitative statements about the degree of error involved in the model. I have endeavoured to indicate in Chapter 8 the effects of several types of variation which influence the final values of muscle and joint force but the variations are themselves chosen on a partly subjective basis.

A feature of the force calculations is the separate treatment of gravity and inertia effects which, in the drop-landing calculations, have only a small influence on the results. In this case it is clear that the 'quasi-static' model, omitting inertia and gravity effects, gives an adequate description of the behaviour of the limbs and provides a set of simple equations for muscle and joint action.

b) The calculated values

Table 8.5 of Chapter 8 summarises the maximum muscle and joint forces computed for the drop-landing. The most significant values are those of Tp (2640 lbf), F_{KTib} (3904 lbf) and F_{KNorm} (467 lbf). The first value appears to indicate a serious overload on the patellar tendon, according to approximate tensile strength figures. Even if the tendon is able to withstand higher loads under dynamic conditions the conclusion must be drawn that downward jumping on to a hard surface is not a particularly healthy pastime.

This conclusion is supported by the large compressive load between the tibial and femoral condyles expressed by F_{KTib}. A load of nearly 4000 lbf on the semilunar cartilages must be regarded as undesirable although its physiological effects cannot properly be assessed without the construction of a knee-joint simulation rig.

F_{KNorm} represents 'shearing' across the condyles and it can be assumed

that the cruciate ligaments carry the major part of this force. This normal component reaches a maximum in the deep-squat position, in contrast to the other forces which have their highest values at frame 5. The high stressing of the cruciates in the deep-squat confirms recent warnings that squat exercises in athletics, particularly with heavy weights on the shoulders, are liable to produce permanent over extension of the cruciates and a slack knee joint structure.

c) Future Work

The procedures and model data of Chapter 8 may be applied to many types of physical activity. An obvious extension would be the study of drop-landings from several heights and of other forms of downward jump. The take-off action in jumping is also of interest, and it should be possible to build up an overall picture of joint and muscle forces and to assess what forms of activity lead to unpleasantly high loads.

A second, useful piece of work would be the provision of anatomical dimensions, such as the moment arms in the present model, for a range of subjects. This kind of survey can only be performed on cadaveric specimens but it is important that some knowledge of subject differences be built up so that future models and calculations may be more realistic.

9.5 Biomechanical principles (Chapters 3 and 7)

Biomechanics is at a formative stage in which workers with backgrounds in various disciplines are coming together to contribute their knowledge. Successful fusion of the many approaches to the study of human activity will take time, but courses and conferences on biomechanics are already setting the standards for future development.

My criticisms of some published material in Chapters 3 and 7 are not intended as personal attacks on the authors concerned. It is difficult to put forward in print a strong criticism without appearing offensive, but I feel that the points on which I have taken issue are important. Students and other workers are naturally prepared to accept published work in

accredited journals as a reliable basis for their reading in biomechanics. They should not find incorrect and unjustified statements on mechanical principles such as those cited earlier on Work, Energy and Power. I find it disturbing that publications which, for lack of any other material, are effectively laying the foundations of biomechanical study, should contain confusing misapplications of mechanical ideas. It cannot be too strongly underlined, for instance, that no work is done by a force acting at a fixed point of application, and that energy and power are scalar quantities for which resolution in 'horizontal and vertical components' has no meaning. These are not subtle, advanced concepts about which experts may hold differing shades of opinion, but basic definitions which must be properly used if biomechanics is not to become a jumble of bad methods trying to produce good results.

It has also been my experience in personal discussion that incompletely understood principles are sometimes stoutly defended by their protagonists. While the concepts discussed are straightforward, it is possible to regard them a little too lightly, as matters which were mastered at school and are now second nature. In dealing with human motion we have to recognise that the body is a non-rigid system and is capable of internal energy production. These two features can cause difficulties if one is not prepared to think beyond particle and rigid-body mechanics to more general ideas.

I have ventured to be dogmatic in these remarks because statements on mechanical principles constitute the only section of the present work for which consideration of errors should be unnecessary. Unfortunately, some 'noise' seems to have crept into even this system, and it can only be hoped that newcomers to biomechanics will be able to apply some judicious filtering.